On the cover:

Seed dormancy and germination of *Convolvulus persicus* L., an endemic species of the Caspian Sea and the Black Sea, are reported by Bahadornejad Velashedi et al. (pp. 44–53).

ACTA BOTANICA CROATICA

An international journal of botany
issued by:
the Department of Biology,
Faculty of Science, University of Zagreb, Croatia

Vol. 84 (1)

Zagreb, April 2025

ACTA BOTANICA CROATICA

The journal originally entitled *Acta Botanica Instituti Botanici Regalis Universitatis Zagrebensis* was founded in 1925. In 1957 its name was changed to Acta Botanica Croatica. In 1998, it became an entirely English-language journal.

The journal covers field (terrestrial and aquatic) and experimental research on plants and algae; including plant viruses and bacteria; from the subcellular level to ecosystems. Manuscripts focusing upon the lowland and karstic areas of southern Europe, karstic waters, other types of fresh water, and the Adriatic (Mediterranean) Sea are particularly welcome. More detailed information is available on the link

http://www.abc.botanic.hr/index.php/abc/about

The following points make Acta Botanica Croatica an attractive publishing medium: 1) article submission and publishing are free of charge, 2) manuscripts subject to international review, 3) covered by major abstracting and indexing services.

Impact Factor calculated by Journal Citation Reports:
1.1 (2023)
5-year Impact Factor: 1.2

Acta Botanica Croatica is a member of CrossCheck by iThenticate. iThenticate is a plagiarism screening service that verifies the originality of content submitted before publication. The iThenticate software checks submissions against millions of published research papers, documents on the web, and other relevant sources. Authors and researchers can also use the iThenticate system to screen their work before submission by visiting research.ithenticate.com.

Acta Bot. Croat. 84 (1), 1–11, 2025
DOI: 10.37427/botcro-2025-001

CODEN: ABCRA 25
ISSN 0365-0588
eISSN 1847-8476

Leaf phenotypic plasticity of European ash (*Fraxinus excelsior*) at its northern range in Dinaric Alps

Antonio Vidaković, Sandi Matijašević, Katarina Tumpa, Igor Poljak*

University of Zagreb, Faculty of Forestry and Wood Technology, Department of Forest Genetics, Dendrology and Botany, Svetošimunska cesta 23, HR-10000 Zagreb, Croatia

Abstract – The Dinaric Alps have been recognised on numerous occasions as a biodiversity hotspot. They host a variety of species with great importance in sustainable forestry operations and nature conservation. One such species is the European ash (*Fraxinus excelsior* L., Oleaceae), a broad-leaved, wind-pollinated and wind-dispersed forest tree. In this paper, we aimed to determine the morphological variability of the European ash populations of the northern Dinaric Alps. For this purpose, leaf samples from 10 individuals in seven populations were collected. Morphometric analysis of intra- and interpopulation variability was conducted using 19 morphological leaf traits. We determined great variability of trees within, and small variability among populations. The variables that best discriminated studied populations were those relating to leaflet shape. Based on these variables, populations were grouped into two clusters. The first cluster encompassed individuals with acute leaflets, found in drier and rockier habitats, whereas the second cluster, defined by more rounded leaflets, was found in mesophilous and nutrient-rich habitats. However, this research revealed no influence of geographical or bioclimatic distances on morphological variability, which indicates that the rockiness and soil are most likely two predominant factors in shaping the phenotypic plasticity of European ash populations. These results are of great significance in the planning of future forest breeding programs, as populations from drier habitats are likely to persist and spread due to their adaptation to water scarcity, which will become more pronounced in the future.

Keywords: compound leaf, *Fraxinus excelsior*, morphometric analysis, plant morphology, plant variation, population variability

Introduction

Located along the eastern Adriatic coast, the Dinaric Alps are one of the most extensive mountainous areas of Europe. This area is known for its extremely high biodiversity and is one of the most floristically diversified regions, on both a European and a global scale (Mutke et al. 2010). In regards to vegetation, the dominant forest community in this region is *Omphalodo-Fagetum* (Tregubov 1957 corr. Puncer 1980) Marinček et al. 1993, with silver fir (*Abies alba* Mill.) and European beech (*Fagus sylvatica* L.) as the dominant tree species, with admixtures of other ecologically and economically important species like sycamore (*Acer pseudoplatanus* L.), wych elm (*Ulmus glabra* Huds.), small-leaved lime (*Tilia cordata* Mill.), and European ash (*Fraxinus excelsior* L.) (Boncina 2011). In the context of progressing climate change and intensive dieback caused by the pathogen fungus *Hymenoscyphus fraxineus* (T. Kowalski) Baral, Queloz et Hosoya, the European ash stood out as a species to which attention should be paid in order to conserve its natural populations across Europe and maintain sustainable forest management.

European or common ash is a deciduous, trioecious, and anemophilous tree species, belonging to the Oleaceae family (Pliûra and Heuertz 2003). It is a fast-growing species, reaching a mature height of up to 40 m. Its specific epithet, *excelsior* (lat. *excelsus* = noble, tall), refers to the tall growth of the European ash (Šugar 1990), likely in comparison to a related European species, the manna ash (*Fraxinus ornus* L.). The European ash is a highly economically significant tree species in forestry, due to its high-quality timber (Herman 1971). As such, it has been used for centuries, particularly in carpentry and wheelwrighting, as well as in the production of looms, handles, agricultural tools, sporting goods, boats, airplanes, train carriages etc.

The natural range of the European ash covers most of Europe, with the exception of the most northern and southern

* Corresponding author e-mail: ipoljak@sumfak.unizg.hr

parts of the continent (Herman 1971, Pliûra and Heuertz 2003). The northern limits stretch across southern Norway, Sweden and Finland, whereas in southern Europe, the species can be found in mountainous regions of the Pyrenees, the Apennines, the Alps and the mountains of the Balkan Peninsula. Further east, the species stretches across the northern parts of Asia Minor and the Caucasus, where it encompasses the mountainous southern edge of the Caspian Sea.

The European ash requires moist and rich soils and tolerates soil pH-values as low as 4.5, but prefers pH values above 5.5 (Beck et al. 2016). The species exhibits intermediate properties between a pioneer species and a permanent forest component. It is a species of mixed deciduous forests, in which it occupies moist soils, in plant communities well-adapted to long periods of snow cover or those found in conditions of high air humidity (Herman 1971, Vukelić 2012, Beck et al. 2016). As a young seedling and sapling, it can tolerate shade, but will require full sunlight as a mature tree to fully develop (Pliûra and Heuertz 2003). In northern and western parts of its range, the European ash grows in lowland forests, on cool and moist soils of valleys and plains, where it demonstrates great tolerance to seasonal water-logging. It is not, however, tolerant of prolonged flooding, thus not growing on highly compacted soils of flood-plain forests. The European ash is somewhat opportunistic, and will form near to pure stands in favourable conditions, especially after major disturbances. The species tolerates various altitudes, temperatures and moisture availability, which appear to be the limiting factors to its distribution. In southern part of its range, it grows predominantly in higher altitudes; up to 2200 m a.s.l. (Herman 1971, Beck et al. 2016).

As an economically and ecologically significant species, the European ash has been the subject of much scientific research. The majority of investigations, however, focused on its genetic diversity across the species' range (Heuertz et al. 2004a,b, Sutherland et al. 2010, Tollefsrud et al. 2016, Belton et al. 2022), as well as on the aftermath of the ash dieback disease (Pautasso et al. 2013, Coker et al. 2018). On the other hand, the morphological diversity of the species is largely overlooked. This lack of research into the morphological differences between the numerous populations across Europe is abated only slightly by research into the interspecies hybrids (Fernández-Manjarrés et al. 2006, Gerard et al. 2006) between the European ash and the narrow-leaved ash (*Fraxinus angustifolia* Vahl), which are morphologically ambiguous. As a result, the morphological traits, and potential differences among the populations of European ash morphology need to be further investigated, which could benefit the distinction of hybrids as well.

In this research, therefore, we analysed the morphological traits and diversity of seven populations of European ash in the northern Dinaric Alps. This region is thought to have served as a refugium during the last glaciation for many species, including *F. excelsior* (Heuertz et al. 2004a). Refugium populations in general may accumulate higher genetic, and therefore morphological, diversity, due to their persistence and stability over glacial cycles (Hewitt 1996), which prompted us to investigate the morphological diversity of *F. excelsior* in one of its refugial areas. In the Dinaric Alps, the European ash is predominantly found in humid ditches and dales, where organic matter accumulates and thus creates unfavourable conditions for the dominant species, which is the beech (Vukelić 2012). It is, however, also found on skeletal, shallow soils on limestone, where the overall conditions are warmer and drier (Herman 1971). Furthermore, the pioneering character of the species comes to the foreground in these habitats, with ash trees occupying and quickly overshadowing other species in small openings and forest edges, following any disturbance. Due to these varying conditions within each population, the selected populations represent and interesting sample of the broader Dinaric range of the European ash, where expected morphological differences between the populations are likely under the influence of the environment.

The aims of this study were: (1) to describe variation of leaf dimension and shape parameters for European ash populations in the northern Dinaric Alps; and (2) to verify whether leaf dimensions and shape of these populations change with geographical or environmental distances among populations.

Material and methods

Plant material

Samples for the morphometric analyses were collected in seven European ash populations of the northern Dinaric Alps (Fig. 1, On-line Suppl. Tab. 1): P1-Žumberak, P2-Crni Lug, P3-Delnice, P4-Vrbovsko, P5-Brinje, P6-Prozor, P7-Perušić.

A total of 70 trees were sampled, with 20 leaves being collected from every tree. Sampling was conducted in late summer, once the leaves were fully developed. Furthermore, only the optimally developed leaves of short shoots were collected, i.e., those from well-sunlit parts of the crown, with no visible defects or pest and pathogen damage. Once collected, the leaves were immediately placed in cardboard folders and transported back to the Herbarium of the Department for Forest Genetics, Dendrology and Botany, at the Faculty of Forestry and Wood Technology. Finally, leaves were herbarized between sheets of newsprint.

Morphometric analysis

Once fully dried, leaves were scanned, using an A3-format scanner (MICROTEK ScanMaker 9800XL), at a resolution of 600 dpi (.TIF). Image files created in this way were further analysed in the software package WinFolia PRO (Winfolia TM 2001). Using the Interactive Measurement option, the length of rachis (RL) and leaf petiole (PL) were measured on each leaf. Afterwards, on each leaf a top leaflet and one lateral leaflet in the middle part of the leaf were selected and measured using the Leaf Morphology option. In total, eight traits were measured on both the lateral and

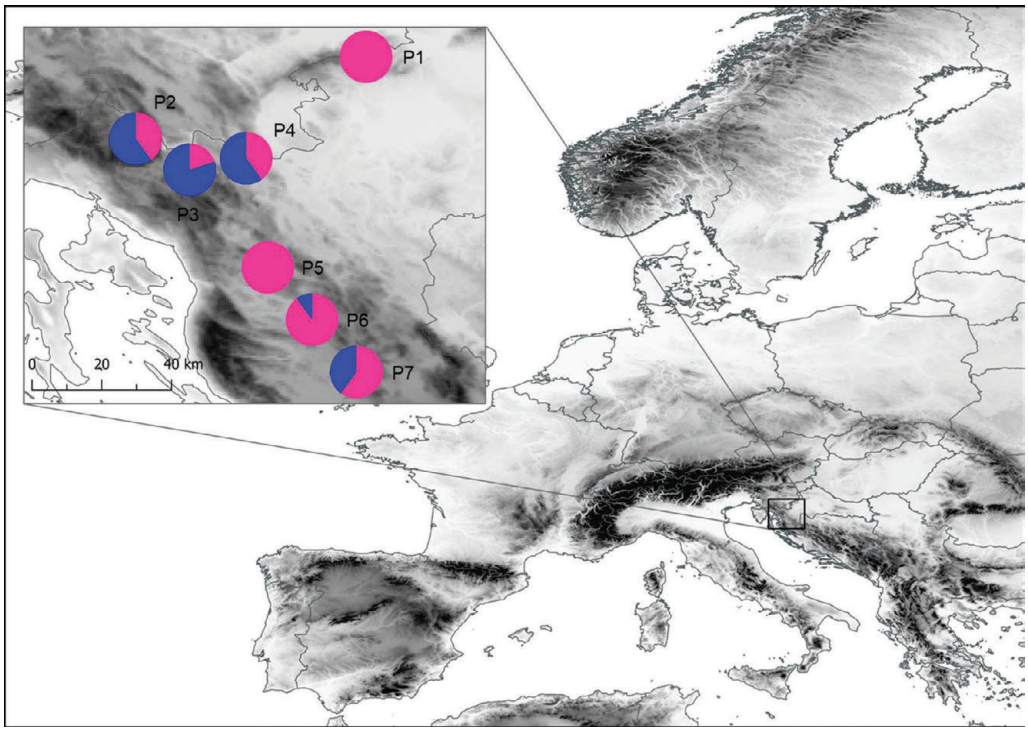

Fig. 1. Results of the K-means clustering method based on 19 leaf phenotypic traits and locations of the seven sampled *Fraxinus excelsior* populations. The proportions of the membership of each population in each of the defined clusters are colour-coded: cluster A–pink, cluster B–blue. Abbreviations of populations: P1 – Žumberak, P2 – Crni Lug, P3 – Delnice, P4 – Vrbovsko, P5 – Brinje, P6 – Prozor, P7 – Perušić.

terminal leaflets, separately, with "LL" de-nominating traits referring to lateral, and "TL" to terminal leaflets: leaflet area (LA); leaflet length (LL); maximum leaflet width (MLW); leaflet length, measured from its base to the point of maximum width (PMLW); leaflet width at 50% of its length (LW1); leaflet width at 90% of its length (LW2); angle enclosed by the main leaflet vein and point on its edge, at 10% of its length (LA1); and angle enclosed by the main leaflet vein and point on its edge, at 25% of its length (LA2). Additionally, petiolule length of the terminal leaflet (TL-PL) was measured.

Population diversity and structure

Arithmetic mean, standard deviation, and coefficient of variation were calculated for the particular trait for each population in order to determine the range of their variation. Pearson correlation coefficients were calculated among all leaf traits including all trees using the CORR procedure in R Version 3.2.2 (R Core Team 2016).

To detect the level of inter- and intrapopulation variability, hierarchical analysis of variance was used. The analysed factors were populations and trees within populations ("tree" factor nested inside the "population" factor). In addition, statistically significant differences in all pairs of populations were identified using Fisher's LSD multiple comparison test, at $P \leq 0.05$. Hierarchical analysis of variance was carried out using the STATISTICA software package version 13 (Statistica, ver. 13 2018).

To analyse structure of the studied populations, two multivariate statistical methods were performed. The K-means method was applied to detect phenotypic structure and define the number of K-groups that best explained the morphological variation of European ash populations. If the proportion of a specific population was equal to or higher than 0.7, that population was assumed to belong to one cluster, and if it was lower than 0.7, that population was considered to be of mixed origin (Poljak et al. 2018). Furthermore, discriminant analysis was performed to evaluate the utility and importance of the measured leaf traits by determining which were most useful in maximally discriminating the populations. In addition, a canonical discriminant analysis was performed based on the leaf traits that best discriminated the studied populations, as determined by stepwise discriminant analysis. Finally, the squared Mahalanobis distances between class means, canonical variables, and eigenvalues were calculated, and the first two canonical variables were plotted. The above multivariate statistical analyses were conducted using the "MorphoTools" R scripts in R Version 3.2.2 (R Core Team 2016) following the manual of Koutecký (2015).

Environmental variability and relationship between morphological variability, environment and geography

To test correlations among morphometric, geographic and environmental data three different matrices were calculated. Data of the bioclimatic conditions for the period from 1970 to 2000, in the area of the studied populations,

were obtained from the WorldClim 2 database with a spatial resolution close to a square kilometre (Fick and Hijmans 2017). Firstly, using Spearman´s rank correlation coefficients, highly correlated bioclimatic variables were discarded. In total, six bioclimatic variables were selected and included in the analysis: BIO1 (annual mean temperature), BIO3 (isothermality), BIO11 (mean temperature of coldest quarter), BIO12 (annual precipitation), BIO18 (precipitation of warmest quarter), BIO19 (precipitation of coldest quarter). In addition, altitude values retrieved from GPS data recorded during fieldwork were used to calculate the environmental distance matrix, as well. Finally, environmental differences were calculated as the Euclidian distance between the population means for the first three principal components of the principal component (PC) analysis. Squared Mahalanobis distances among the populations were computed to obtain a matrix of morphometric distances among the studied populations. Geographic distances were calculated from the latitude and longitude of the site of sample collection. Finally, to assess isolation by distance (IBD) and isolation by environment (IBE), response matrix (morphological differences) was compared to the two predictor matrices (environmental differences and geographic distance) using simple Mantel tests (Mantel 1967). The significance level was assessed after 10,000 permutations, as implemented in NTSYS-pc Version 2.21L (Rohlf 2009).

Results

Descriptive statistics

The results of the descriptive statistical analysis are shown in Tab. 1, on the individual population level (N = 200), as well as for the overall sample (N = 1400). Rachis length (RL) had a mean value of 13.99 cm and was relatively variable, with coefficient of variation on the overall sample of 27.15%, with the range between 18.24% (population P2) to 36.15% (population P5). Petiole length (PL) demonstrated a slightly less variable character, with mean length of 6.81 cm and overall CV value of 19.85%. Furthermore, it was also defined by a similarly broad range of variability among the populations, from 11.75% (population P6) to 27.60% (population P7).

The average area of the lateral leaflet (LL-LA) for all seven observed populations was 16.61 cm^2, and its length (LL-LL) was 8.88 cm. Furthermore, the average maximum lateral leaflet width (LL-MLW) was 2.83 cm. Coefficients of variations for the lateral leaflet area (LL-LA) were within the range from 30.39% (population P5) to 41.71% (population P7). As the most variable traits, width of the lateral leaflet at 90% of leaflet length (LL-LW2) and leaflet area (LL-LA) stood out, with the respective coefficients of variation of 44.92% and 37.02%. On the other hand, the least variable trait was the angle enclosed by the main vein and the line

Tab. 1. Descriptive statistical parameters for studied leaf morphometric traits. Descriptive parameters: M–arithmetic mean; SD–standard deviation CV–coefficient of variation (%). Acronyms of populations: P1 – Žumberak, P2 – Crni Lug, P3 – Delnice, P4 – Vrbovsko, P5 – Brinje, P6 – Prozor, P7 – Perušić. TL – terminal leaflet, LL – lateral leaflet. Morphometric traits: LA – leaflet area (cm^2), LL – leaflet length (cm), MLW – maximum leaflet width (cm), PMLW – leaflet length, measured from its base to the point of maximum width (cm), LW1 – leaflet width at 50% of its length (cm), LW2 – leaflet width at 90% of its length (cm), LA1 – angle enclosed by the main leaflet vein and point on its edge, at 10% of its length (°), LA2 – angle enclosed by the main leaflet vein and point on its edge, at 25% of its length (°), PL – petiole length (cm), RL – rachis length (cm).

Trait	Descriptive parameters	Total	P1	P2	P3	P4	P5	P6	P7
TL-LA	M	13.89	11.87	14.41	14.70	16.94	13.71	10.70	14.31
	SD	5.33	3.79	5.74	5.01	5.46	5.15	3.56	5.58
	CV	38.33	31.91	39.79	34.06	32.21	37.56	33.29	39.02
TL-LL	M	8.40	7.85	8.45	8.36	8.91	9.17	7.73	8.19
	SD	1.49	1.55	1.29	1.52	1.30	1.69	1.10	1.38
	CV	17.78	19.73	15.30	18.16	14.56	18.44	14.24	16.88
TL-MLW	M	2.82	2.67	2.84	3.01	3.24	2.58	2.37	2.94
	SD	0.66	0.45	0.66	0.60	0.68	0.52	0.53	0.71
	CV	23.49	16.86	23.21	20.06	21.12	20.31	22.43	23.98
TL-PMLW	M	4.31	4.16	4.44	4.25	4.49	4.64	3.97	4.22
	SD	0.81	0.84	0.75	0.77	0.73	0.98	0.62	0.79
	CV	18.85	20.13	16.84	18.01	16.20	21.23	15.71	18.81
TL-LW1	M	2.72	2.56	2.74	2.91	3.14	2.46	2.30	2.83
	SD	0.65	0.43	0.66	0.59	0.67	0.49	0.51	0.69
	CV	23.78	16.67	24.11	20.35	21.36	19.89	22.22	24.30
TL-LW2	M	0.51	0.51	0.47	0.48	0.51	0.46	0.47	0.64
	SD	0.28	0.30	0.20	0.20	0.25	0.28	0.19	0.42
	CV	55.12	59.28	43.06	41.06	49.69	61.08	40.21	65.50
TL-LA1	M	21.40	17.29	24.65	24.92	26.07	18.63	17.84	19.46
	SD	5.48	3.33	4.36	3.40	5.84	3.56	3.61	4.27
	CV	25.61	19.24	17.70	13.64	22.39	19.10	20.24	21.93

Tab. 1. continued

Trait	Descriptive parameters	Total	P1	P2	P3	P4	P5	P6	P7
TL-LA2	M	22.04	20.56	22.18	24.27	24.65	19.27	19.32	23.53
	SD	4.06	2.74	3.01	3.37	4.63	2.93	2.87	4.00
	CV	18.43	13.34	13.57	13.88	18.77	15.23	14.86	17.01
TL-PL	M	1.22	0.78	1.26	1.41	1.75	1.07	0.93	1.26
	SD	0.53	0.40	0.39	0.40	0.53	0.41	0.26	0.57
	CV	43.59	51.32	31.01	28.17	30.52	38.13	28.36	45.39
LL-LA	M	16.61	15.54	18.79	17.54	18.95	15.46	14.31	15.68
	SD	6.15	4.76	7.09	6.93	6.09	4.70	4.79	6.54
	CV	37.02	30.67	37.74	39.50	32.14	30.39	33.49	41.71
LL-LL	M	8.88	8.66	9.12	8.78	9.26	9.51	8.31	8.53
	SD	1.66	1.71	1.52	1.99	1.64	1.49	1.26	1.63
	CV	18.74	19.71	16.70	22.70	17.71	15.73	15.16	19.11
LL-MLW	M	2.83	2.77	3.02	3.02	3.13	2.54	2.55	2.79
	SD	0.63	0.46	0.62	0.65	0.62	0.46	0.55	0.72
	CV	22.14	16.64	20.63	21.41	19.69	18.06	21.66	25.74
LL-PMLW	M	3.44	3.61	3.45	3.28	3.59	3.73	3.10	3.34
	SD	0.84	0.76	0.78	0.86	0.82	0.97	0.67	0.79
	CV	24.28	21.16	22.69	26.29	22.87	25.98	21.63	23.62
LL-LW1	M	2.64	2.63	2.81	2.79	2.91	2.34	2.37	2.63
	SD	0.61	0.44	0.60	0.60	0.60	0.48	0.54	0.72
	CV	23.03	16.71	21.45	21.50	20.61	20.55	22.79	27.40
LL-LW2	M	0.55	0.57	0.57	0.53	0.58	0.49	0.55	0.56
	SD	0.25	0.22	0.25	0.21	0.28	0.23	0.25	0.27
	CV	44.92	38.58	43.67	40.05	48.38	47.65	45.40	47.93
LL-LA1	M	37.43	31.79	43.40	42.80	39.60	32.29	38.08	34.03
	SD	7.30	5.69	5.02	6.33	7.11	5.13	4.78	6.12
	CV	19.52	17.90	11.56	14.79	17.97	15.90	12.55	18.00
LL-LA2	M	29.04	28.18	30.36	31.54	30.45	24.74	28.77	29.24
	SD	4.52	3.36	3.35	4.74	4.90	3.13	3.94	4.45
	CV	15.56	11.93	11.05	15.03	16.09	12.65	13.68	15.23
RL	M	13.99	14.95	16.36	14.60	14.57	11.34	14.04	12.09
	SD	3.80	3.68	2.98	2.85	3.74	4.10	3.26	3.39
	CV	27.15	24.61	18.24	19.49	25.68	36.15	23.20	28.04
PL	M	6.81	6.98	6.97	7.12	6.16	7.18	6.88	6.39
	SD	1.35	1.81	0.96	1.15	1.03	1.27	0.81	1.76
	CV	19.85	25.96	13.83	16.18	16.66	17.70	11.75	27.60

defined by the leaflet basis and point on the edge of the leaflet located at 25% of the total leaflet's length (LL-LA2) (CV = 15.56%).

Population P4 was defined by, on average, the largest lateral leaflet area (LL-LA), the highest value of the maximum lateral leaflet width (LL-MLW), the widest lateral leaflet at 50% (LL-LW1) and 90% (LL-LW2) of the leaflet's width. The longest and the narrowest lateral leaflets, with the largest distance between the leaflet basis and the point of maximum lateral leaflet width (LL-PMLW), was observed in population P5. The lateral leaflets in population P6 had the lowest mean value of LL-LA and LL-LL, as well as the smallest LL-PMLW value. The largest mean angle value of LL-LA1, was found in population P2, whereas the lowest value of LL-LA1 was noted for population P1. The most variable traits overall, LL-LW2 and LL-LA, demonstrated highest CV values in populations P4 and P7, respectively, whereas the lowest variability for those two traits was noted in populations P1 (CV = 38.58%) and P5 (CV = 30.39%), respectively. On the other hand, the least variable traits were LL-LA2 and LL-LA1, with the lowest CV values noted for population P2, 11.05% and 11.56%, respectively.

Overall, terminal leaflets had somewhat smaller leaflet areas, as well as shorter lengths, than lateral leaflets. The average terminal leaflet area for the seven observed populations was 13.89 cm^2, length 8.40 cm, and width 2.82 cm. The angles of LA1 and LA2 demonstrated similar mean values, 21.40° and 22.04° respectively, but differed in the coefficients of variability, with 25.61% noted for LA1 and 18.43% for LA2. The terminal petiolule length was 1.22 cm, which also had the second highest CV value (CV = 43.59%), after trait LW2 (CV=55.12%).

Population P4 stood out for having the highest values for six of the nine measured traits: TL-LA, TL-MLW, TL-LW1, TL-LA1, TL-LA2, TL-PL. Additionally, the remaining maximum values were noted in populations P5 (TL-LL, TL-PMLW) and P7 (TL-LW2). On the other hand, the minimum values were found predominantly in population P6 (TL-LA, TL-LL, TL-MLW, TL-PMLW, TL-LW1), as well as in populations P1 (TL-LA1, TL-PL) and P5 (TL-LW2, TL-LA2). Populations P2, P3 and P7 were of predominantly intermediate values. When the variability of measured traits is considered, the most variable traits were TL-LW2 and TL-PL, with coefficient of variability values of 65.50% (population P7) and 51.32% (population P1), respectively. The least variable traits were TL-LA1 (CV = 13.64%) and TL-LA2 (CV = 13.34%), in populations P3 and P1, respectively. Generally speaking, population P1 stood out as the population with the highest CV values for only two traits (TL-LL, TL-PL), but the lowest values for four traits (TL-LA, TL-MLW, TL-LW1, TL-LA2).

Correlations

A total of 119 statistically significant correlations were noted between the tested pairs of morphological traits (Online Suppl. Tab. 2). Out of the total 119 correlations, only seven were negative. Furthermore, 30 positive correlations had r-values greater than 0.7, whereas none of the negative correlations demonstrated r-values greater than –0.7.

When lateral leaflet traits are considered, the majority of the trait pairs correlated significantly among themselves, with the exception of the following pairs: LW2 and LL; LA1 and LA, LA1 and LW2; LA1 and LW2 and LA2 and LA. Furthermore, the rachis length (RL) correlated only with the following lateral leaflet traits: LA, MLW, LW1, LW2 and LA1, whereas the petiole length (PL) correlated exclusively with LL of lateral leaflet. This is somewhat expected, as longer petiole automatically means longer leaf, i.e., larger leaflets.

When terminal leaflet traits are considered, the majority too demonstrated significant correlations among themselves. There was, however, no significant correlation between the terminal leaflet traits and traits of the petiole (PL) and rachis (RL). In addition, no significant correlations were noted for the following pairs: LL and LW2, LA1 and LA2; PWLW and LA1 and LA2; and LW2 and LA1.

The correlations between traits of the terminal and the lateral leaflets were also analysed and revealed a large number of significant correlations, with MLW and LW1 standing out by correlating to all other traits. On the other hand, LL did not correlate with LW2, LA1, LA2 or PL. Overall, lateral leaflets demonstrated a far greater number of significant correlations than the terminal leaflets.

Analysis of variance

Statistically significant differences between the observed populations of the European ash were confirmed for 12 out of the 19 analysed traits (Tab. 2). Generally speaking, populations can be best distinguished using the morphometric traits of the terminal leaflets. For the total of seven out of nine traits measured on the terminal leaflets, as well as for

Tab. 2. Results of the hierarchical analysis of variance. LA – leaflet area, LL – leaflet length, MLW–maximum leaflet width, PMLW – leaflet length, measured from its base to the point of maximum width, LW1 – leaflet width at 50% of its length, LW2 – leaflet width at 90% of its length, LA1 – angle enclosed by the main leaflet vein and point on its edge, at 10% of its length, LA2 – angle enclosed by the main leaflet vein and point on its edge, at 25% of its length, PL – petiole length, RL – rachis length.

Trait	Components of the variance	F	P-Value	Percent of variability
TL-LA	Among populations	3.36	0.0061	10.2
	Within populations	19.61	0.0000	43.3
	Error			46.6
TL-LL	Among populations	2.31	0.0444	6.9
	Within populations	27.07	0.0000	52.7
	Error			40.4
TL-MLW	Among populations	4.50	0.0007	15.0
	Within populations	21.77	0.0000	43.3
	Error			41.7
TL-PMLW	Among populations	1.52	0.1861	2.6
	Within populations	20.96	0.0000	48.7
	Error			48.8
TL-LW1	Among populations	4.59	0.0006	15.3
	Within populations	21.86	0.0000	43.2
	Error			41.5
TL-LW2	Among populations	2.06	0.0701	2.5
	Within populations	6.23	0.0000	20.2
	Error			77.3

Tab. 2. continued

Trait	Components of the variance	F	P-Value	Percent of variability
TL-LA1	Among populations	13.74	0.0000	41.7
	Within populations	27.36	0.0000	33.1
	Error			25.2
TL-LA2	Among populations	6.04	0.0000	25.4
	Within populations	44.87	0.0000	51.3
	Error			23.4
TL-PL	Among populations	13.91	0.0000	32.7
	Within populations	13.18	0.0000	25.5
	Error			41.8
LL-LA	Among populations	1.70	0.1352	3.6
	Within populations	20.98	0.0000	48.2
	Error			48.2
LL-LL	Among populations	1.19	0.3231	1.0
	Within populations	23.63	0.0000	52.5
	Error			46.4
LL-MLW	Among populations	3.13	0.0095	9.3
	Within populations	17.78	0.0000	41.4
	Error			49.3
LL-PMLW	Among populations	1.62	0.1551	2.6
	Within populations	14.10	0.0000	38.6
	Error			58.9
LL-LW1	Among populations	2.77	0.0188	7.9
	Within populations	17.95	0.0000	42.3
	Error			49.8
LL-LW2	Among populations	0.44	0.8475	0.0
	Within populations	10.74	0.0000	31.5
	Error			68.5
LL-LA1	Among populations	11.91	0.0000	37.6
	Within populations	23.43	0.0000	33.0
	Error			29.4
LL-LA2	Among populations	5.67	0.0001	19.1
	Within populations	19.34	0.0000	38.7
	Error			42.2
RL	Among populations	4.14	0.0015	15.3
	Within populations	25.66	0.0000	46.8
	Error			37.9
PL	Among populations	1.41	0.2231	2.3
	Within populations	26.01	0.0000	54.3
	Error			43.4

four out of eight traits of lateral leaflets, the analysed populations were statistically different. Statistically significant differences were also found for RL, whilst trait PL did not differentiate any of the populations. Furthermore, results of the analysis of variance demonstrated that trees within populations were significantly different, when all measured traits are considered.

In most of the cases, intrapopulation variability was greater than the interpopulation variability. As an exception, traits TT-LA1, LL-LA1 and TL-PL were defined by having greater interpopulation variability. Furthermore, most of the results indicated that leaf variability within each tree was equal to or slightly lower than the variability of individual trees within a population. In just six instances, leaf variability within each tree (the error component) had a higher share of the total variability, when compared to the variability of trees within populations.

The results of Fisher's LSD test are shown in On-line Suppl. Tab. 3. The number of differing traits among populations varies from one to 10. The most similar populations were P1 and P6, and P3 and P4, which differed only in one trait, LL-LA10 and TL-PL, respectively. On the other hand, pairs of populations with the most differences were P3 and P5, and P4 and P5, each counting 10 differing traits, followed by nine differing traits in pairs of P6 and P2, P3 and P4.

K-means and discriminant analysis

K-means clustering method (Fig. 1) inferred the population structure of the seven populations based on eight morphological leaf traits. Two clusters were clearly visible, mainly corresponding to geographical regions. The first cluster, cluster A, encompassed four populations, marked pink. The three populations were marked blue and formed the second, well-defined cluster, cluster B. Cluster A (pink) was defined by populations P1 (proportion of membership: 1.0), P5 (proportion of membership: 1.0), and P6 (proportion of membership: 0.9). In addition, the population P7 demonstrated a mixed but overwhelmingly cluster A origin. Population P3 demonstrated origin assigned to cluster A (proportion of membership: 0.8), whereas populations P2 and P4 showed a partial cluster affiliation belonging to cluster A (proportion of membership: 0.4) and cluster B (proportion of membership: 0.6).

Five out of eight selected traits have shown to be significant in discriminating the observed European ash populations. The greatest discriminating power was noted for three terminal leaflet traits TL-LA1, TL-LA2 and TL-PL, with partial Wilks' lambda values of 0.56 (On-line Suppl. Tab. 4). Other significant traits, in descending order of significance, were LL-LA1 and RL. For eight variables and seven groups defined in the canonical analysis, six canonical variates were defined. The first canonical variate (CV1) demonstrated eigenvalue greater than 1 and explained 73.5% of total variability (Fig. 2).

Along the same CV, when the studied individuals and populations were considered in two-dimensional morphospace, although with some overlap, a clear separation of individuals from the central part (P2, P3 and P4) and the northern (P1) and southern (P5, P6 and P7) parts of the studied area was visible. The classification accuracy for all of the populations was 77.1%. The highest classification accuracy, i.e., 100% of correctly classified individuals, was noted for the population P1, whereas the accuracy for the individuals of the populations P3 and P4 amounted to only 50%.

Environmental variability and relationship between morphological variability, environment and geography

Principal component (PC) analysis, based on the environmental data, showed that the first two principal components had eigenvalues greater than 1 and together explained 83.4% of the total variability (On-line Suppl. Tab. 5). The first principal component explained 54.1% of the total variability. The variables displaying the highest negative correlations with the first principal component (–0.7) were altitude and BIO18, while the variables displaying the highest positive correlations (0.7) with the same principal component were

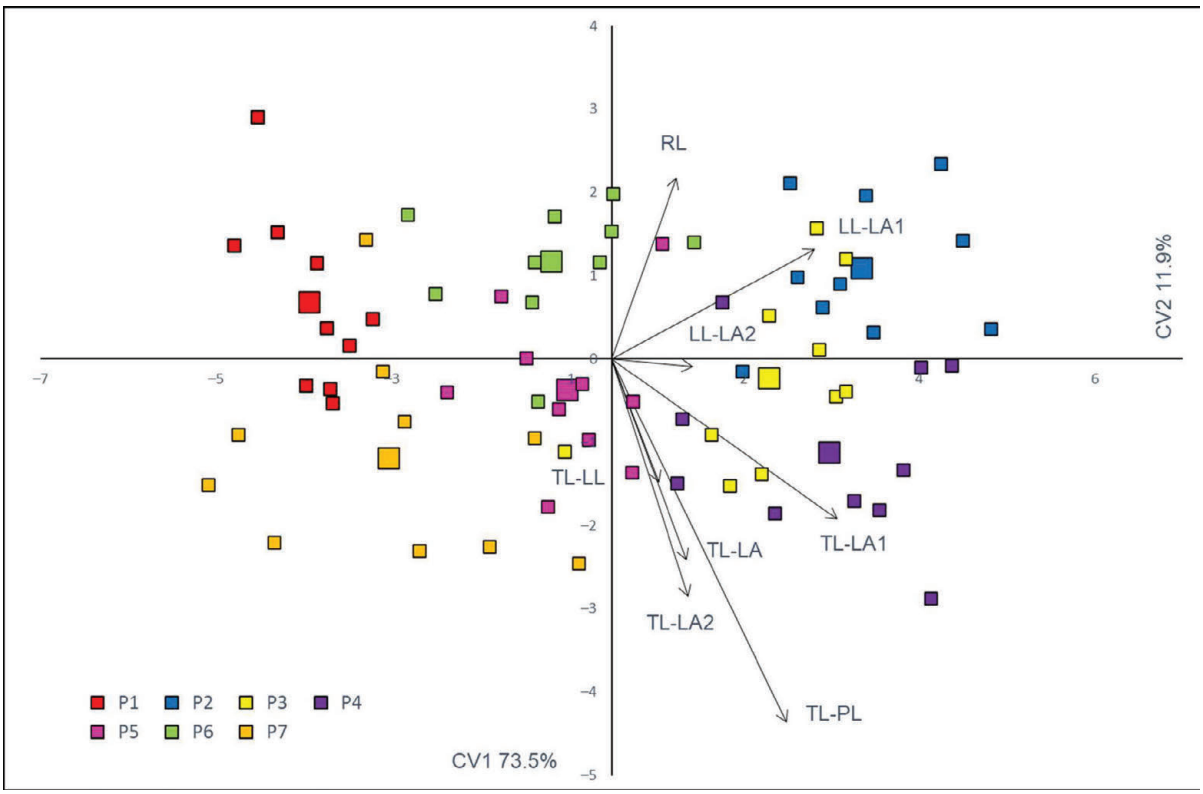

Fig. 2. The first two canonical variates of the canonical discriminant analysis (CV1 and CV2) of seven *Fraxinus excelsior* populations based on eight morphological traits. Each individual tree is indicated by a small sign, while the population barycenters are represented by larger ones. Acronyms of populations: P1 – Žumberak, P2 – Crni Lug, P3 – Delnice, P4 – Vrbovsko, P5 – Brinje, P6 – Prozor, P7 – Perušić. TL – terminal leaflet, LL – lateral leaflet. Morphometric traits: LA – leaflet area, LL – leaflet length, LA1 – angle enclosed by the main leaflet vein and point on its edge, at 10% of its length, LA2 – angle enclosed by the main leaflet vein and point on its edge, at 25% of its length, PL – petiole length, RL – rachis length.

BIO1 and BIO11. The second principal component explained 29.3% of the total variability. The variables that showed the highest correlations with the second PC axis were BIO19 and BIO3. The biplot of the principal component analysis based on seven environmental variables is shown in On-line Suppl. Fig. 1. A clear separation of populations along the first PC axis according to the geographical principle was observed, with populations P1-P3 grouped on the left, and populations P4-P7 on the right side of the diagram. Populations on the left side of the biplot are characterized by higher altitudes, higher annual precipitation (BIO12) and precipitation during the warmest quarter (BIO18). On the other hand, populations on the right side are characterized with lower altitudes, with higher annual mean temperature (BIO1) and the mean temperature of the coldest quarter (BIO11). Along the second PC axis separation of P1 of other studied populations is clearly visible.

In order to determine whether the observed morphological variability was caused by geographical (IBD) or environmental distances (IBE) between the studied populations, the Mantel test was performed. Our results showed that population-level pairwise morphological distances were not related to the geographic distances between populations ($r = 0.487$, $P = 0.066$), nor to environmental distances ($r = 0.326$, $P = 0.149$).

Discussion

The results of the leaf morphometric analysis revealed that both the average terminal and lateral leaflet lengths, of 8.4 cm and 8.9 cm respectively, were within the previously reported intervals of 3-12 cm (Herman 1971, Beck et al. 2016). Furthermore, average widths of the lateral (2.8 cm) and terminal (2.8 cm) leaflets were also within the reported interval of 0.8-3 cm (Beck et al. 2016) but were somewhat shorter than values reported by Idžojtić (2009). Petiole length (6.8 cm), on the other hand, demonstrated value on the shorter side of the interval reported by Idžojtić (2009), 5-10 cm. When the whole leaf is observed, the measured mean length (29.2 cm) was within the reported intervals of 20-40 cm (Herman 1971, Idžojtić 2009, Beck et al. 2016). The two most variable traits for the leaflets were those pertaining to leaflet size (LA and LW2). Significant variability of leaflet area in compound leaves has been previously reported (Wang et al. 2022) and could be explained by the general plasticity of leaves as the main photosynthetic organs of the plant (Henry et al. 2020).

Our research showed larger and longer lateral than terminal leaflets, while their width was almost identical, which indicates that leaflet position within the leaf can influence its morphology. According to Chitwood et al. (2012), variability of leaflet shape and size can be influenced by multiple factors, including the heteroblasty, the proximal-distal and left-right axes of leaves, sun and shade conditions and developmental stage. In case of *Fraxinus excelsior*, the proximal-distal axis of each leaf influences the leaflet shape and developmental stage. Namely, *F. excelsior* leaves develop basipetally, that is, the terminal leaflet is developmentally older than the proximal pairs of lateral leaflets (Moline and Bostrack 1972, Chitwood et al. 2012), causing the differences in leaflets' shape and symmetry. Generally, terminal, i.e., older leaflets show greater variability, previously reported for *Sorbus domestica* L. (Poljak et al. 2015) and various *Solanum* L. section *Lycopersicon* species (Chitwood et al. 2012).

The results confirmed significant correlations between the vast majorities of the studied morphological traits. Although both terminal and lateral leaflets showed a moderate to high degree of correlation within and between each other, only the lateral leaflet showed correlation with the length of the rachis and petiole. Interdependence of compound leaf morphological traits has been previously recorded for a number of *Pistacia* L. species (Kafkas et al. 2002, Karimi et al. 2009), as well as *Juglans regia* L. (Kabiri et al. 2018) and *Robinia pseudoacacia* L. (Guo et al. 2022). Although the mentioned studies did not include lateral leaflet, and generally covered fewer leaflet traits, a positive correlation between the length and width of the terminal leaflet was detected. However, in contrast to Kafkas et al. (2002), we did not discover a correlation between petiole length and terminal leaflet length.

Conducted research revealed variability that was high within, and somewhat lower among populations. On the interpopulation level, significant differences were observed for 12 of the studied morphological traits, while seven traits did not show significant differentiation on the intrapopulation level, and have accounted for a very small percentage of total variability. Significantly lower intrapopulation variability could be attributed to lower genetic diversity of *F. excelsior* among populations in central Europe, confirmed in the study by Heuertz et al. (2004b) and Ballian et al. (2008). According to Hamrick and Godt (1996), such a pattern of genetic diversity is typical for outcrossing, woody plants, as they tend to be more genetically diverse and have less genetic differentiation among their populations. A similar pattern of morphological variability has also been described for narrow-leaved ash (*Fraxinus angustifolia* Vahl) populations in Slovenia (Jarni et al. 2011).

For several traits in this research, significant differentiation between the European ash populations was observed, particularly for the traits relating to leaflet base shape, for both the lateral and terminal leaflets. In addition, terminal leaflet petiole length showed great differentiating power as well. These differences can most likely be ascribed to phenotypic plasticity, which is the result of conditions in the microhabitats the observed populations are found in. Namely, multivariate analyses have shown that the ash populations could be separated into two groups, depending on the microhabitat conditions they grow in. The first group encompasses individuals from the central part of the researched area, the populations P2-P4, whereas the second group included the northernmost population P1 and populations P5-P7, found in the southern part of the researched area. The first group of populations grows on nutrient-rich and less dry habitats, whereas the second group inhabits skeletal and, generally

speaking, drier terrains. In the conditions of extensive gene flow, phenotypic plasticity enables individuals to express different and locally adapted phenotypes formed under the influence of contrasting habitat and environmental conditions (Stotz et al. 2021). In the case of the drier habitats, populations were characterized by more acute and somewhat narrower leaflets, when compared to the more humid habitats, in which leaflets demonstrated rounder base and larger area generally. Leaf and leaflet growth were proved to be significantly affected by water stress in *R. pseudoacacia* as well (Zhang et al. 2012). This difference in shape between the populations of contrasting habitats, indicates that leaf shape is under the influence of microhabitat conditions, with smaller leaf area likely being the result of lower water availability. This has previously been shown to be the case for numerous plant species, on the global level (Peppe et al. 2011). On the other hand, the influence of altitude and bioclimatic variables on leaflet morphology can be almost completely excluded, as no statistically significant correlation between the ecological and morphological distances between the populations was detected.

Furthermore, no IBD pattern for the European ash populations of the Dinaric Alps was established. IBD, or isolation by distance, is a model of genetic differentiation between populations, in which genetic differences increase with geographic scale (Morente-López et al. 2018). The lack of IBD in this research is visible in the grouping of the P1 from the northernmost part of the researched area with southern populations of P5-P7. This was further confirmed by the Fisher LSD tests. Namely, geographically close populations, e.g., P4 and P5, differed by 10 analysed traits, unlike the two most distant populations, P1 and P7, which only had two traits that differed. Nevertheless, IBD is a well-documented pattern of differentiation, noted in both plant (Twyford et al. 2020) and animal species (Bayne 2017), as well as on the level of whole landscapes (van Strien et al. 2014).

Conclusions

Significant differences between studied European ash populations were found for 12 out of 19 traits. In general, the traits related to shape of the leaflet base have shown to be more significant in describing differences between populations and also had the lowest coefficient of variation. On the other hand, the traits related to the size of the leaflets had a high degree of variability and, using them, the populations did not, in most cases, statistically differ. The high between-tree variation within the populations, and relatively low among-population variation, found in our research can be explained by effective gene flow. Nevertheless, when the traits with the highest discriminatory power between the populations are considered, the results of the multivariate statistical methods revealed two groups of populations defined by the common microsite conditions the researched populations are found in. These differences can most likely be ascribed to phenotypic plasticity, which caused leaflets on the drier and skeletal habitats to be smaller and acute, whereas those individuals from mesophilous and nutrient-rich habitats had somewhat larger and rounder leaflets. Furthermore, no statistically significant influence of the altitude and bioclimate variables on leaf variability was established. Overall, the results of this investigation provide additional insight into the variability of the species, which can be useful in creating guidelines for conservation, breeding, and afforestation programs, which is needed for sustainable forest management in the area.

References

Ballian, D., Monteleone, I., Ferrazzini, D., Kajba, D., Belletti, P., 2008: Genetic characterization of common ash (*Fraxinus excelsior* L.) populations in Bosnia and Herzegovina. Periodicum Biologorum 110(4), 323–328.

Bayne, B. L., 2017: Biology of oysters. Elsevier, Amsterdam.

Beck, P. S. A., Caudullo, G., Tinner, W., de Rigo, D., 2016: *Fraxinus excelsior* in Europe: distribution, habitat, usage and threats. In: San-Miguel-Ayanz, J., de Rigo, D., Caudullo, G., Houston Durrant, T., Mauri, A. (eds.), European Atlas of Forest Tree Species, e0181c0+. Publications Office of the European Union, Luxembourg.

Belton, S., Fox, E., Kelleher, C. T., 2022: Characterising the molecular diversity of ash (*Fraxinus excelsior* L.) at its western marginal range in Europe — phylogeographic insights and implications for conservation in Ireland. Tree Genetics and Genomes 18, 36. https://doi.org/10.1007/s11295-022-01567-6.

Boncina, A., 2011: History, current status and future prospects of uneven-aged forest management in the Dinaric region: an overview. Forestry 84(5), 467–478. https://doi.org/10.1093/forestry/cpr023.

Chitwood, D. H., Headland, L. R., Kumar, R., Pengz, J., Maloof, J. N., Sinha, N. R., 2012: The development trajectory of leaflet morphology in wild tomato species. Plant Physiology 158(3), 1230–1240. https://doi.org/10.1104/pp.111.192518.

Coker, T. L. R., Rozsypálek, J., Edwards, A., Harwood, T. P., Butfoy, L., Buggs, R. J. A., 2018: Estimating mortality rates of European ash (*Fraxinus excelsior*) under the ash dieback (*Hymenoscyphus fraxineus*) epidemic. Plants People Planet 1(1), 48–58. https://doi.org/10.1002/ppp3.11.

Fernández-Manjarrés, J. F., Gerard, P. R., Dufour, J., Raquin, C., Frascaria-Lacoste, N., 2006: Differential patterns of morphological and molecular hybridization between *Fraxinus excelsior* L. and *Fraxinus angustifolia* Vahl (Oleaceae) in eastern and western France. Molecular Ecology 15(11), 3245–3257. https://doi.org/10.1111/j.1365-294X.2006.02975.x.

Fick, S. E., Hijmans, R. J., 2017: WorldClim 2: New 1km spatial resolution climate surfaces for global land areas. International Journal of Climatology 37(12), 4302–4315. https://doi.org/10.1002/joc.5086.

Gerard, P. R., Fernandez-Manjarres, J. F., Frascaria-Lacoste, N., 2006: Temporal cline in a hybrid zone population between *Fraxinus excelsior* L. and *Fraxinus angustifolia* Vahl. Molecular Ecology 15(12), 3655–3667. https://doi.org/10.1111/j.1365-294X.2006.03032.x.

Guo, Q., Liu, J., Li, J., Cao, S., Zhang, Z., Zhang, J., Zhang, Y., Deng, Y., Niu, D., Su, L., Li, X., Dong, L., Sun, Y., Li, Y., 2022: Genetic diversity and core collection extraction of *Robinia pseudoacacia* L. germplasm resources based on phenotype, physiology, and genotyping markers. Industrial Crops and Products 178, 114627. https://doi.org/10.1016/j.indcrop.2022.114627.

Hamrick, J. L., Godt, M. J. W., 1996: Effects of life history traits on genetic diversity in plant species. Philosophical Transactions: Biological Sciences 351(1345), 1291–1298.

Henry, R. J., Furtado, A., Rangan, P., 2020: Pathways of photosynthesis in non-leaf tissues. Biology 9(12), 438. https://doi.org/10.3390/biology9120438.

Herman, J., 1971: Šumarska dendrologija (Dendrology in forestry). Stanbiro, Zagreb.

Heuertz, M., Fineschi, S., Anzidei, M., Pastorelli, R., Salvini, D., Paule, L., Frascaria-Lacoste, N., Hardy, O. J., Vekemans, X., Vendramin, G. G., 2004a: Chloroplast DNA variation and postglacial recolonization of common ash (*Fraxinus excelsior* L.) in Europe. Molecular Ecology 13(11), 3437–3452. https://doi.org/10.1111/j.1365-294X.2004.02333.x.

Heuertz, M., Hausman, J.-F., Hardy, O. J., Vendramin, G. G., Frascaria-Lacoste, N., Vekemans, X., 2004b: Nuclear microsatellites reveal contrasting patterns of genetic structure between western and south eastern European populations of the common ash (*Fraxinus excelsior* L.). Evolution 58(5), 976–988. https://doi.org/10.1111/j.0014-3820.2004.tb00432.x.

Hewitt, G., 1996: Some genetic consequences of ice ages, and their role in divergence and speciation. Biological Journal of the Linnean Society 58(3), 247–276. https://doi.org/10.1006/bijl.1996.0035.

Idžojtić, M., 2009: Dendrologija – list [Dendrology – leaf]. Sveučilište u Zagrebu, Zagreb.

Jarni, K., Westergren, M., Kraigher, H., Brus, R., 2011: Morphological variability of *Fraxinus angustifolia* Vahl in the northwestrn Balkans. Acta Societatis Botanicorum Poloniae 80(3), 245–252. https://doi.org/10.5586/asbp.2011.014.

Kabiri, G., Bouda, S., Elhansali, M., Haddioui, A., 2018: Morphological and pomological variability analysis of walnut (*Juglans regia* L.) genetic resources from the middle and high Atlas of Morocco. Atlas Journal of Biology 2018, 575–582. https://doi.org/10.5147/ajb.v0i0.179.

Kafkas, S., Kafkas, E., Perl-Treves, R., 2002: Morphological diversity and a germplasm survey of three wild *Pistacia* species in Turkey. Genetic Resources and Crop Evolution 49(3), 261–270. https://doi.org/10.1023/A:1015563412096.

Karimi, H. R., Zamani, Z., Ebadi, A., Fatahi, M., 2009: Morphological diversity of *Pistacia* species in Iran. Genetic Resources and Crop Evolution 56(4), 561–571. https://doi.org/10.1007/s10722-008-9386-y.

Koutecký, P., 2015: MorphoTools: A set of R functions for morphometric analysis. Plant Systematics and Evolution 301(4), 1115–1121. https://doi.org/10.1007/s00606-014-1153-2.

Mantel, N., 1967: The detection of disease clustering and a generalized regression approach. Cancer Research 27(2), 209–220.

Moline, H. E., Bostrack, J. M., 1972: Abscission of leaves and leaflets in *Acer negundo* and *Fraxinus americana*. American Journal of Botany 59(1), 83–88.

Morente-López, J., García, C., Lara-Romero, C., García-Fernández, A., Draper, D., Iriondo, J. M., 2018: Geography and environment shape landscape genetics of Mediterranean Alpine species *Silene ciliata* Poiret. (Caryophyllaceae). Frontiers in Plant Science 9, 1968. https://doi.org/10.3389/fpls.2018.01698.

Mutke, J., Kreft, H., Kier, G., Barthlott, W., 2010: European plant diversity in the global context. In: Settele, J., Penev, L., Georgiev, T., Grabaum, R., Grobelnik, V., Hammen, V., Klotz, S. (eds.), Atlas of biodiversity risk, 4-5. Pensoft Publishers, Sofia.

Pautasso, M., Aas, G., Queloz, V., Holdenrieder, O., 2013: European ash (*Fraxinus excelsior*) dieback – A conservation biology challange. Biological Conservation 158(12), 37–49. https://doi.org/10.1016/j.biocon.2012.08.026.

Peppe, D. J., Royer, D. L., Cariglino, B., Oliver, S. Y., Nweman, S., Leight, E., Enikolopov, G., Fernandez-Burgos, M., Herrera, F., Adams, J. M., Correa, E., Currano, E. D., Erickson, M., Hinojosa, L. F., Hoganson, J. W., Iglesias, A., Jaramillo, C. A., Johnson, K. R., Jordan, G. J., Kraft, N. J. B., Lovelock, E. C., Luska, C. H., Niinemets, Ü., Peñuelas, J., Rapson, G., Wing, S. L., Wright, I. J., 2011: Sensitivity of leaf size and shape to climate: global patterns and paleoclimatic applications. New Phytologist 190(3), 724–739. https://doi.org/10.1111/j. 1469-8137.2010.03615.x.

Pliûra, A., Heuertz, M., 2003: Common ash (*Fraxinus excelsior*). EUFORGEN Technical Guidelines for Genetic Conservation and Use. International Plant Genetic Resources Institute, Maccarese.

Poljak, I., Idžojtić, M., Šapić, I., Korijan, P., Vukelić, J., 2018: Diversity and structure of Croatian continental and Alpine-Dinaric populations of grey alder (*Alnus incana* (L.) Moench subsp. *incana*): Isolation by distance and environment explains phenotypic divergence. Šumarski List 142(1-2), 19–32. https://doi.org/10.31298/sl.142.1-2.2.

Poljak, I., Kajba, D., Ljubić, I., Idžojtić, M., 2015: Morphological variability of leaves of *Sorbus domestica* L. in Croatia. Acta Societatis Botanicorum Poloniae 84(2), 249–259. https://doi.org/10.5586/asbp.2015.023.

R Core Team, 2016: A Language and Environment for Statistical Computing; R Foundation for Statistical Computing: Vienna. Retrieved September 15, 2023 from http://www.R-project.org

Rohlf, F. J. 2009: NTSYS-pc: Numerical Taxonomy and Multivariate Analysis System, version 2.2; Applied Biostatistics Inc., New York.

Statistica (Data Analysis Software System), 2018: TIBCO Software Inc., Palo Alto. Retrieved November 15, 2023 from http://www.statsoft.com

Stotz, G. C., Salgado-Luarte, C., Escobedo, V. M., Valladares, F., Gianoli, E., 2021: Global trends in phenotypic plasticity of plants. Ecology Letters 24(10), 2267–2281. https://doi.org/10.1111/ele.13827.

Sutherland, B. G., Belaj, A., Nier, S., Cottrell, J. E., Vaughan, P. S., Hubert, J., Russell, K., 2010: Molecular biodiversity and population structure in common ash (*Fraxinus excelsior* L.) in Britain: Implications for conservation. Molecular Ecology 19(11), 2196–2211. https://doi.org/10.1111/j.1365-294X.2009.04376.x.

Šugar, I., 1990: Latinsko-hrvatski i hrvatsko-latinski botanički leksikon [Latin-Croatian and Croatian-Latin botanical glossary]. Globus i JAZU, Zagreb.

Tollefsrud, M. M., Myking, T., Sønstebø, J. H., Lygis, V., Hietala, A. M., Heuertz, M., 2016: Genetic structure in the northern range margins of common ash *Fraxinus excelsior* L. PLoS One 11(12), e0167104. https://doi.org/10.1371/journal.pone.0167104.

Twyford, A. D., Wong, E. L. Y., Friedman, J., 2020: Multi-level patterns of genetic structure and isolation by distance in the widespread plant *Mimulus guttatus*. Heredity 125, 227–239. https://doi.org/10.1038/s41437-020-0335-7.

van Strien, M. J., Holderegger, R., van Heck, H. J., 2014: Isolation-by-distance in landscapes: considerations for landscape genetics. Heredity 114(1), 27–37. https://doi.org/10.1038/hdy.2014.62.

Vukelić, J., 2012: Šumska vegetacija Hrvatske [Forest vegetation in Croatia]. Sveučilište u Zagrebu, Zagreb.

Wang, G. Y., Chen, B. H., Huang, Y.-C., Jin, G.-Z., Liu, Z.-L., 2022: Effects of growing position on leaflet trait variations and its correlations in *Fraxinus mandshurica*. Chinese Journal of Plant Ecology 46(6), 712–721. https://doi.org/10.17521/cjpe.2021.0421.

WinFolia TM, 2001: Version PRO 2005b. Regent Instruments Inc., Quebec City.

Zhang, Y., Equiza, M. A., Zheng, Q., Tyree, M. T., 2012: Factors controlling plasticity of leaf morphology in *Robinia pseudoacacia* L. II: the impact of water stress on leaf morphology of seedlings grown in a controlled environment chamber. Annals of Forest Science 69(1), 39–47. https://doi.org/10.1007/s13595-011-0134-7

Acta Bot. Croat. 84 (1), 12–21, 2025
DOI: 10.37427/botcro-2025-011

CODEN: ABCRA 25
ISSN 0365-0588
eISSN 1847-8476

The anatomy, micromorphology, and essential oils of the Turkish endemic and endangered species *Alchemilla orduensis*

Öznur Ergen Akçin[1]*, Tuğba Özbucak[1], Şükran Öztürk[2], Hüseyin Ümit Uzunömeroğlu[3]

[1] Ordu University, Faculty of Science and Art, Department of Molecular Biology and Genetics, 52200 Ordu, Türkiye

[2] Ordu University, Ulubey Vocational School, Department of Veterinary Health and Laboratory, Program, 52200 Ordu, Türkiye

[3] Ordu University, Education Faculty, 52200 Ordu, Türkiye

Abstract – In this study, the anatomical and micromorphological characteristics of the vegetative organs and the essential oil constituents of the aerial and underground parts of the local and endangered endemic species *A. orduensis* Pawł. were evaluated. For anatomical study, sections of root, rhizome, stem, leaves and petiole were excised and stained with safranin/fast green mixture. Leaf and petiole structures were examined micromorphologically. Essential oil contents were determined by headspace solid-phase microextraction coupled with gas chromatography-mass spectrometry (HS-SPME/GC-MS) analysis. The results showed that rectangular meristematic cells were present in the root. The leaf is of the bifacial and amphistomatic type. Stomata cells are of the anomocytic type. The stomatal index for the upper surface of the leaves is 0.04, while the stomatal index for the lower surface is 0.17. Druse crystals were found in the rhizome, stem and leaves. Among the various compounds identified, the most abundant groups in the aboveground parts are alcohols (39.81%) and ketones (14.99%) with 1-Octen-3-ol, 1-octan-3-one and borane- methyl sulfide complex as the main compounds. Terpenes (23.44%) and alcohols (11.82%), in which myrtenolis was the main compound, were most abundant in the underground parts.

Keywords: *Alchemilla*, anatomy, endemic species, essential oils, micromorphology

Introduction

The genus *Alchemilla* L. (Rosaceae) is represented by 82 species in Türkiye, and among them 36 species are considered to be endemic. The endemism rate of the genus is 33.8% (Pawlowski and Walters 1972, Ozhatay et al. 2011).

Alchemilla species are very rich in tannin, salicylic acid, essential oil, phytosterol and vitamin C. The genus is medically important because of its active substances. It is consumed both as a medicinal plant and as an herbal tea. *Alchemilla* species are used as a wound healing agent, sedatives, diuretics, and cough suppressants (Baytop 1999, Shrivastava 2011, Polat et al. 2015). Some *Alchemilla* species have antioxidant, anti-inflammatory, antiproliferative, weakening and anti-aging effects (Benaiges et al. 1998, Oktyabrsky et al. 2009, Said et al. 2011). *Alchemilla caucasica* Buser has significant antiulcer activity. This effect is due to flavonoids (Shrivastava et al. 2007, Falchero et al. 2010, Karaoglan et al. 2020). *Alchemilla orduensis* Pawł. is a narrow endemic in Ordu, Giresun and Trabzon provinces in the eastern Black Sea region of Türkiye. It is listed as an Endangered (EN) species in the Red Book of Plants of Türkiye (Ekim et al. 2000).

Alchemilla orduensis is known as "Ordukeltatı" in Anatolia (Ayaz 2012). The species has an erect and dense patent and erecto-patent stem and petioles. Leaves are green and reniform. The leaves have 5-9 subtriangular lobes and 5-14 teeth. Flowers are 3-5 mm wide. Sepals and epicalyx lobes sparsely hairy and sparsely ciliate. Sepals are ovate and the epicalyx is thinner than the sepals. *A. orduensis* is distributed at altitudes between 1400-1600 m a.s.l. It grows in an area including lake shores, wetlands, marshes, and rocky habitats (Kalheber 1994, Ozbucak et al. 2022). The species shows morphological similarities to closely related species such as *A. erzincanensis* Pawł. These morphological similarities cause confusion regarding the taxonomic rank.

Chemotaxonomic characteristics can be used to classify genera and species when morphological and anatomical

* Corresponding author e-mail: oakcin@gmail.com

data are limited. Many studies have shown that essential oils can be used for chemotaxonomic purposes (Hegnauer 1986, Setyawan 2002, Tundis et al. 2014). Several different compounds have been used as taxonomic markers in the Rosaceae family, such as cyanogenic glycosides, flavonoids, tannins, sorbitol, and essential oils (Wallaart 1980, Okuda et al. 1992, Morgan et al. 1994). Essential oils are important compounds found in such plant structures as roots, leaves, bark, flowers, fruits, and seeds. Essential oils generally contain compounds such as terpenes (monoterpenes and sesquiterpenes), aldehydes, alcohols, phenols, and terpenoids (Mohamed et al. 2010, Tongnuanchan and Benjakul 2014). *Alchemilla* species are known to be rich in phenolic compounds such as flavonoids and tannins (Shrivastava et al. 2007, Falchero et al. 2010, Kaya et al. 2012, Ilgun et al. 2014) but there are not many studies on the essential oils. The presence of phenolic compounds has been determined in *A. orduensis* species (Kaya et al. 2012)

Ozbucak et al. (2022) investigated the micromorphology and some ecological characteristics of the flowers and fruits of the *A. orduensis* species, but investigations of the vegetative organs are lacking. Therefore, the aim of this study was to examine the anatomical and micromorphological characteristics as well as the essential oil composition of the vegetative organs of this endangered endemic species.

Material and methods

The *A. orduensis* species was collected from Ordu Province (A6: Aybastı, Perşembe plateau, meander) in Türkiye in 2017 (40. 416583 N, 37. 233919 E, *sensu* WGS84) (Fig. 1).

The plant samples were determined according to the Flora of Turkey (Pawlowski and Walters 1972). Plant materials are kept at the Faculty of Arts and Sciences of Ordu University, Türkiye. Cross and surface sections of the root, stem, leaves, rhizome, and petiole were excised by hand, and then covered with glycerin-gelatin (Vardar 1987) and stained with a safranin/fast green (1/9) mixture (Bozdağ et al. 2016). Photographs were taken using a Nikon FDX-35 microscope and all measurements and observations were made using imaging software (NIS-Elements, Version 3.00 SP5). For each parameter, measurements were made on twenty plant individuals. Stoma index and stoma ratio were calculated on the leaf surface of the plant (Meidner and Mansfield 1968). For scanning electron microscopy (SEM), the leaf samples were coated with 12.5-15 nm gold, and electron microscopy (Hitachi-SU 1510) shots were taken with a voltage of 10-15 kilovolts. Surface shapes were determined according to Stearn (1985).

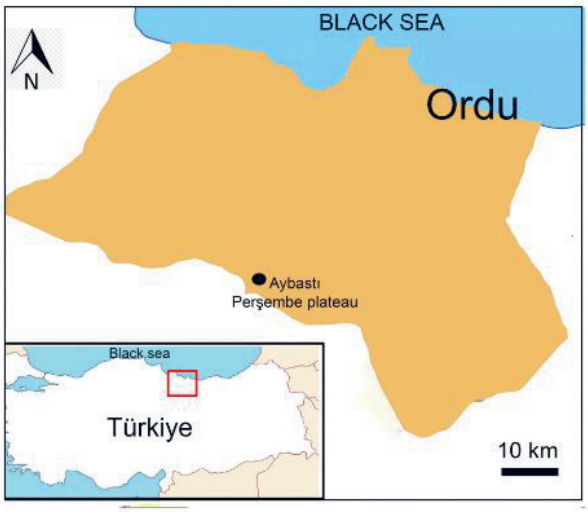

Fig. 1. Geographic distribution area of *Alchemilla orduensis* Pawł. in Ordu province in Türkiye. The plants were collected from Perşembe Plateau.

The essential oil composition of both the aboveground parts (leaves, flowers, and stems) and underground parts (rhizomes and roots) of *A. orduensis* was determined during the flowering period, which is more suitable for essential oil production. The analysis was conducted using headspace solid phase microextraction (SPME, Supelco, Germany) followed by gas chromatography mass spectrometry (GC-MS). The above and below ground parts of 3-4 fresh plants were cut and homogenized. Half grams of the sample (approximately one third of the vial volume) was weighed into a 15 mL vial closed with a PTFE /Silicone septa cap. The sample was placed on a heating block at 60 °C under magnetic stirring. After equilibration for 15 min, a Carboxen/polydimethylsiloxane manual SPME fibre was inserted into the vial and maintained in the headspace for 30 min at 60 °C to extract volatile compounds from the sample. This analysis was performed using a Restek Rxi-5ms (30 m, 0.25 mm ID, 0.25 μm) column integrated into the Shimadzu QP 2010 Ultra GC-MS instrument. Helium was used as the carrier gas at a flow rate of 1.44 mL min^{-1}; the column temperature program of GC was initially set at 40 °C for 2 min and gradually increased to 250 °C at 4 °C per min, then kept there for 5 min.

The essential components of the samples were determined by comparing data concerning their mass spectral libraries (NIST11-FFNSC) and LRI (Linear Retention Indices) generated using alkane standards. Relative quantitation of these compounds was also accomplished by evaluating the relative percentage for each peak (peak area/total ion chromatogram (TIC) area) (Tab. 2) (Mazı et al. 2019).

Results

Anatomical and micromorphological properties

The anatomical structures of the leaves and petiole of the above-ground part of the species were studied (Tab. 1, Fig. 2).

The leaves of the species are of the palmate type. The leaves have 5-9 lobes, and each lobe has 5-14 teeth. The number of lobes increases with the size of the leaves. The leaf of the species is bifacial. The upper epidermis cells of the leaf are larger than the lower epidermis cells. The mesophyll layer consists of two-layered palisade parenchyma

Tab. 1. Results of anatomical measurements (N = 20) of the aboveground (stem, petiole and leaf), and underground (root and rhizome) parts of the endangered endemic species *Alchemilla orduensis*. Mean ± standard deviation (SD) is shown.

		Width/Diameter (µm) Mean ± SD	Length (µm) Mean ± SD			Width/Diameter (µm) Mean ± SD	Length (µm) Mean ± SD
Root	Periderm	29.03 ± 4.64	11.48 ± 2.81	Leaf	Upper epidermis	18.69 ± 3.98	20.09 ± 3.42
	Epidermis	32.72 ± 4.56	23.36 ± 5.43		Lower epidermis	13.62 ± 3.82	14.25 ± 1.40
	Cortex parenchyma	33.27 ± 7.62	–		Collenchyma	23.92 ± 3.15	–
	Endoderma	9.86 ± 6.58	2.20 ± 1.53		Cortex parenchyma	36.70 ± 6.31	–
	Pericycle	14.77 ± 8.55	4.34 ± 1.89		Bundle sheath	12.94 ± 1.88	6.83 ± 1.85
	Phloem	10.45 ± 7.03	2.01 ± 1.73		Phloem	10.05 ± 2.1	–
	Cambium	8.95 ± 1.5	–		Xylem	12.05 ± 1.55	–
	Xylem	7.08 ± 1.44	–		Palisade parenchyma	7.73 ± 1.26	18.24 ± 2.68
					Spongy parenchyma	15.42 ± 3.44	–
Stem	Epidermis	22.36 ± 5.14	17.60 ± 3.03	Rhizome	Epidermis	36.30 ± 5.25	26.25 ± 5.19
	Collenchyma	27.74 ± 4.93	–		Cortex parenchyma	46.72 ± 11.70	–
	Cortex parenchyma	60.18 ± 13.67	–		Xylem	23.73 ± 3.21	–
	Endoderma	14.45 ± 3.01	10.18 ± 1.71		Pith paranchyma	70.35 ± 14.55	–
	Phloem	21.58 ± 4.35	12.96 ± 2.11		Starch	9.85 ± 2.03	–
	Cambium	13.90 ± 2.68	10.1 ± 2.52		Druz	38.34 ± 9.48	–
	Xylem	15.17 ± 2.89	–	Petiole	Epidermis	16.32 ± 2.46	15.27 ± 3.20
	Pith paranchyma	61.04 ± 12.13	–		Collenchyma	22.17 ± 3.18	–
	Druz	37.39 ± 6.07	–		Cortex parenchyma	57.38 ± 15.14	–
					Phloem	13.80 ± 2.84	–
					Xylem	22.36 ± 3.63	–

and three-layered spongy parenchyma. There are many middle vascular bundles and small vascular bundles between them. There are evident bundle sheath cells around the small vascular bundles. Collenchyma cells are located under the epidermis layer in the middle vascular bundles (Tab. 1., Fig. 2A-2H and Fig. 3A-3E).

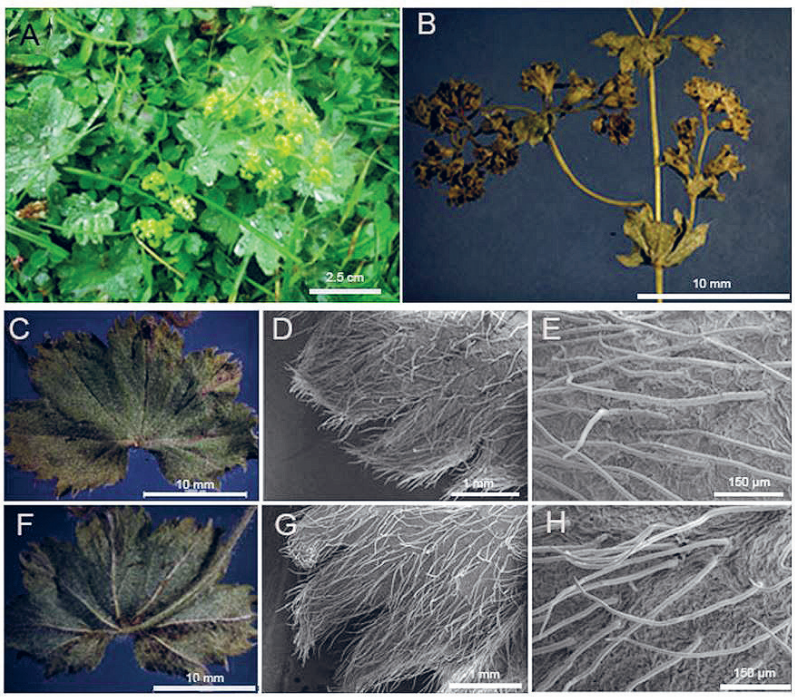

Fig. 2. General appearance of *Alchemilla orduensis* and light and scanning electron microscope (SEM) micrographs of the upper and lower leaf surfaces. A – general appearance of the species in its habitat. B – aboveground part of the plant. C – detailed view of upper surface of the leaf. D, E – SEM micrographs of the upper surface of the leaf and detail of the eglandular hairs. F – detailed view of the lower surface of the leaf. G, H – SEM micrographs of the lower surface of the leaf and detail of eglandular hairs. vb – vascular bundle (photo: H. U. Uzunömeroglu).

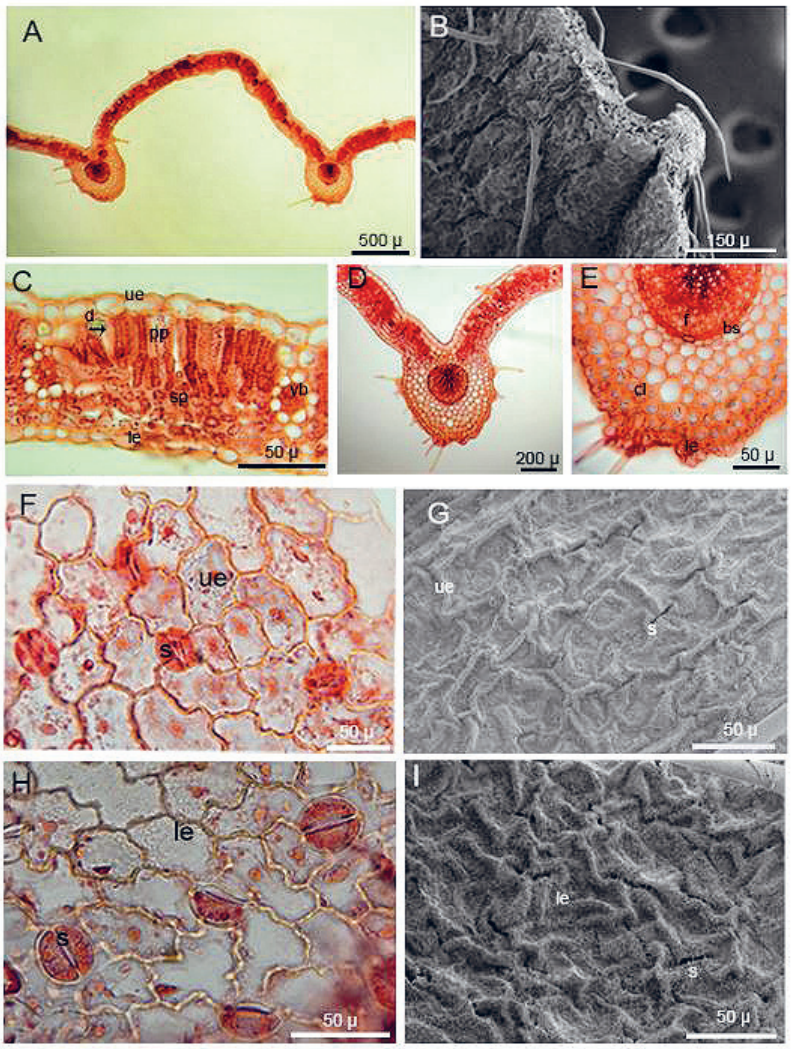

Fig. 3. Light microscope and SEM micrographs of the leaf of *Alchemilla orduensis*. A – cross section of leaf. B – SEM micrographs of cross section of leaf and view of eglandular hairs. C – detailed view of cross section of bifacial leaf lamina and vascular bundles, black arrow indicates druse crystal. D, E – middle vascular bundle region of leaf and detailed view of collenchyma cells and vascular bundle. F – surface section of upper surface of leaf and view of anomocytic type stomata and epidermis cells. G – SEM micrograph of stomata and epidermis cells on the upper leaf surface H – surface section of lower surface of leaf and view of anomocytic type stomata and epidermis cells. I – SEM micrograph of stomata and epidermis cells on the lower leaf surface. d – druse crystal, le – lower epidermis, s – stomata, sp – spongy parenchyma, pp – palisade parenchyma, ue – upper epidermis, vb – vascular bundle.

The upper epidermal cells are rectangular with smooth and curved anticlinal cell walls, while the lower epidermal cells have undulated and curved anticlinal cell walls. The epidermal cell walls are prominent and raised, and stomata cells of the anomocytic type are present on both the upper and lower surfaces of the leaf. The sizes of stomata on the upper surface measure 22.969 ± 1.841 × 25.192 ± 2.860 µm, while those on the lower surface measure 23.597 ± 1.875 × 29.290 ± 2.680 µm. The lower surface of the leaves has more stomata cells. The stomatal index for the upper surface of the leaves is 0.04, while that for the lower surface is 0.17. The leaves have both eglandular and glandular hairs, with the eglandular hairs being usually very long. The density of hairs is greater on the margins of the leaf. Glandular hairs typically consist of a base cell and a secretory cell. The stomata and epidermal cells are nearly level with each other on the upper surface, while on the lower surface, the stomata are situated deeper than the epidermal cells (Tab. 1, Fig. 3F-3I).

Petiole is triangular. There are single-layered epidermis cells in the outermost part of the petiole. Numerous glandular and eglandular hairs were found on the petiole. There are 1-2 layers of collenchyma cells under the epidermis layer. Multilayered parenchyma cells follow the collenchyma layer. There are three vascular bundles in the petioles. One of these vascular bundles is large and two are smaller. Vascular bundles are of the concentric type (Tab. 1, Fig. 4A-4E).

The underground parts of the species have roots and rhizomes. The outermost part of the root of species has an epiderma layer. In some areas, a periderma formation is observed. (Fig. 5A-5D). There are oval or round shaped parenchymatic cells in the cortex layer. The endoderma layer consists of multicellular and rectangular meristematic cells. There is a one layered pericycle layer under the endo-

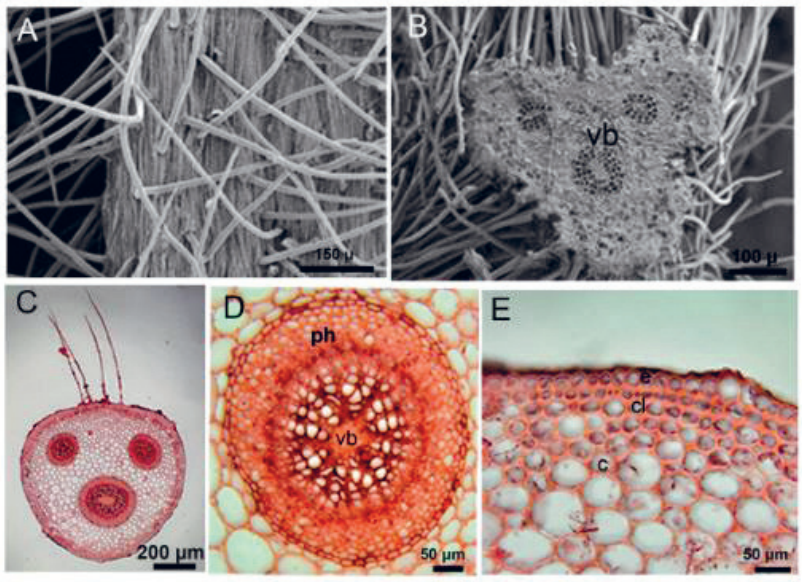

Fig. 4. Light microscope and SEM micrographs of the petiole of *Alchemilla orduensis*. A – SEM micrograph of hairs on the surface of the petiole. B – SEM micrograph of three vascular bundles in petiole cross-section. C – images of three vascular bundles, one large and two small, in petiole cross-section. D – detailed view of the large concentric vascular bundle. E – appearance of single-row epidermis, 1-2 row collenchyma and multi-row parenchyma cells. c – cortex, cl – collenchyma, e – epidermis, ph – phloem, vb – vascular bundle.

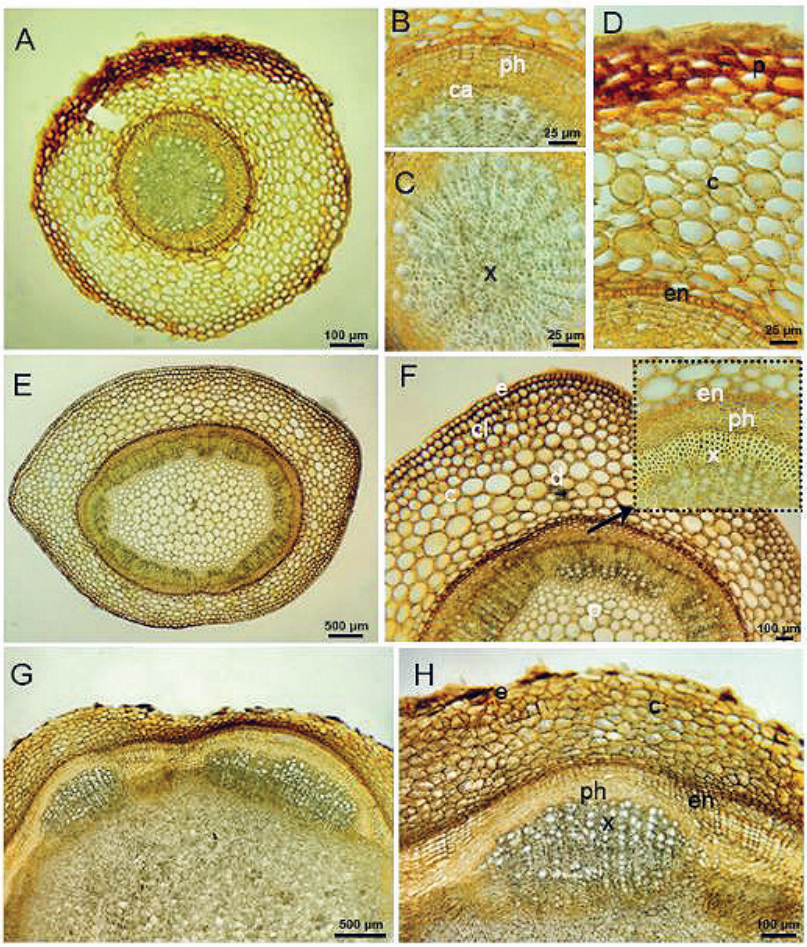

Fig. 5. Micrographs of cross section of root, stem and rhizome of *Alchemilla orduensis*. A – micrograph of cross section of root. B – detailed view of phloem and cambium in the root. C – xylem cells filling most of the central cylinder of the root. D – view of multilayered endodermis in the root. E – micrograph of cross section of stem. F – detailed view of the epidermis, cortex and central cylinder in the stem, arrow points to the endodermis, phloem and xylem. G, H – micrographs of cross section of rhizome. H – detailed view of epidermis, parenchyma cells and open colleteral vascular bundle. c – cortex, ca – cambiyum, cl – collenchyma, e – epidermis, en – endodermis, d – druse, p – pith, ph – phloem, x – xylem.

derma. The cambium layer is clearly visible. Phloem is 5-6 layered. Secondary xylem covers a large area in the root. The pith rays contain 1-2 rows of ray parenchyma cells. The center of the root is filled with tetrarch shaped primary xylem elements.

Tab. 2. Essential oil composition of aboveground (stem, petiole and leaf) and underground (root and rhizome) parts of *Alchemilla orduensis* species identified by GC-MS. GC-MS – gas chromatography-mass spectrometry, RI – retention index, CAS number – chemical abstracts service number.

RI	Compounds	Aboveground (%Area)	Underground (%Area)	Cas No:
662	2-Methylbutan-1-al	0.4		96-17-3
677	1-Penten-3-one	1.8		1629-58-9
680	1-Penten-3-ol	2.73	0.95	616-25-1
697	Pentan-3-one	5.14	0.84	96-22-0
729	Isoamyl alcohol		0.79	123-51-3
769	(Z)-2-Penten-1-ol	3.02		1576-95-0
850	(E)-2-Hexen-1-al	2.61		6728-26-3
853	(Z)-3-Hexen-1-ol	3.6	2.46	928-96-1
867	n-Hexanol	2.17	1.39	111-27-3
915	Amyl acetate	1.51		628-63-7
967	Isoamyl-Propionate	1.11		105-68-0
978	1-Octen-3-ol	29.36	4.82	3391-86-4
986	Octan-3-one	9.85	7.35	106-68-3
991	Myrcene	0.92	1.06	123-35-3
995	-6-Methylhept-5-en-2-ol		2.22	1569-60-4
1006	1-Octanal	1.12	0.95	124-13-0
1008	(Z)-3-Hexenyl acetate	2.75		3681-71-8
1012	Hexyl ethanoate	0.91		142-92-7
1029	Heptyl formate		3.84	112-23-2
1030	2-Ethyl-hexan-1-ol	0.73	1.01	104-76-7
1040	Benzyl alcohol		0.64	100-51-6
1045	2-Phenylacetaldehyde	0.96		122-78-1
1080	trans-Linalooloxide	1.13		34995-77-2
1101	Linalool	2.68	2.18	78-70-6
1107	1-Nonanal	1.96		124-19-6
1141	trans-Pinocarveol		1.83	1674-08-4
1165	Isoborneol		0.6	124-76-5
1198	α-Terpineol	1.23	3.39	98-55-5
1202	Myrtenol		20.38	515-00-4
1208	1-Decanal	0.98	0.73	112-31-2
1450	Geranylacetone	0.83	1.25	3796-70-1
1653	Methyl dihydrojasmonate		0.9	2630-39-9
1855	6-Acetyl-1,1,2,4,4,7-hexa-methyltetralin		1.81	21145-77-7

There is a single layer of epidermis in the outermost part of the aboveground stem of the species (Fig. 5E-5F). There are 1-2 layered collenchyma cells under the epidermis. There are 9-10 rows of parenchyma cells in the cortex. The starch sheath is arranged in a single layer and is distinguishable. Vascular bundles are numerous and arranged in a ring. The vascular bundles have an evident cambium layer located between the phloem and the xylem. The pith region of the stem is filled with parenchyma cells. Druse crystals were found in groups or individually in both the cortex and pith regions of the stem (Fig. 5E-5F).

The underground stem of the species is a rhizome. Although there are epidermis cells in the outermost part, periderma formation is also observed in places. In the rhizome structure, a multi-layered meristematic endodermis is seen. Open collateral vascular bundles are present. The pith region of the rhizome is filled with parenchymatic cells. The parenchymatic cells contain a large number of starch grains and druse crystals (Fig. 5G-5H).

Essential oil composition

The HS-SPME/GC-MS analysis revealed the presence of 33 essential components, in total, in *A. orduensis*. The aboveground and underground parts contained 24 and 22 components, respectively. The most common compounds in the aboveground part were octen-3-ol (29.36%), octan-3-one (9.85%), borane-methyl sulfide complex (6%), and penton-3-one (5.14%). High amounts of myrtenol (20.38%), octan-3-one (7.35%), and methane nitroso- (7.17%) were detected in the underground parts of the plant (Tab. 2).

The aboveground part contained mainly alcohols (39.81%) and ketones (14.99%), while the underground part contained terpenes (23.44%) and alcohols (11.82%) (Tab. 3).

Tab. 3. Chemical groups to which the essential oils of aboveground (stem, petiole and leaf) and underground (root and rhizome) parts of *Alchemilla orduensis* belong, along with their respective percentages.

	Aboveground (%)	Underground (%)
Aldehydes	11.63	4.14
Alcohols	39.81	11.82
Terpenes	5.96	29.44
Acids		1.81
Esters	6.28	4.74
Ketones	14.99	8.19
Miscellaneous	11.27	24.05
Unidentified	9.77	15.67

Discussion

In this study, the anatomical and micromorphological characteristics and the essential oil composition of the local and endangered endemic species *A. orduensis* were determined. The leaves of the species were found to have 5-9 lobes, with each lobe having 5-14 teeth. The number of lobes was

observed to increase with the size and position of the leaves. It is worth noting that Renda et al. (2017) reported differences in the number of leaf lobes among *Alchemilla* species.

The roots of *A. orduensis* species exhibit a single-layered epidermis and exodermis layer. In the cortex, there is a multilayered endodermis composed of prominent, rectangular cells. According to Zhu et al. (2015), the formation of a cork layer and a multilayered endodermis was also observed in *A. japonica* Nakai et Hara. The multilayered endodermis is formed through the meristematic characterization and division of endodermis cells. The *Cyperus papyrus* L. (Cyperaecae) also exhibits a multilinear endodermis structure. These structures have been referred to as meristematic endodermis-derived structures by researchers (Menezes et al. 2005). The root's pith region is composed of tetrarch primary xylem elements. In *A. japonica*, the pith region is filled with primary xylem elements.

The rhizome-shaped underground stem of the species is composed of an outermost layer of single-layered epidermis cells, multilayered parenchyma cells, and an endodermis layer. Boruz (2010) reported that the rhizome of *A. connives* Buser and *A. crinita* Buser species have a multilayered endodermis layer. In *A. orduensis*, the endodermis was determined to have 8-12 layers. In *A. connives*, the endodermis layer has 8-10 layers, and in *A. crinita*, it has 7-8 layers. The rhizome of *A. orduensis* contains parenchymatic cells with abundant starch and druse crystals, either individually or in groups. According to Ilgun et al. (2016), the presence and arrangement of these crystals are crucial in distinguishing the species. In the present case, the stem pith is filled with parenchymatic cells and lacks ventilation cavities. According to Zhu et al. (2015), *A. japonica* and *A. connives* species have ventilation cavities, while *A. glaucescens* Wallr. does not have any ventilation cavities in the pith region of the stem (Boruz 2011).

The petiole of *A. orduensis* contains three vascular bundles, one large and two small. According to Grytsyk et al. (2019), the presence of vascular bundles in the petiole of *Alchemilla* species in Ukraine varies among species. Faghır et al. (2016) stated that petiole and leaf anatomical features have limited taxonomic value in *Alchemilla* species. The leaves of *A. orduensis* are bifacial, which is a common characteristic of leaves in the Rosaceae family (Watson and Dallwitz 1991). Studies on various *Alchemilla* species have shown that the leaves are of the bifacial type, although differences in the number of palisade and spongy parenchyma layers have been observed (Zhu et al. 2015, Ilgun et al. 2016, Jimenez-Noriega et al. 2017). The stomata in the studied species are anomocytic. Our results are consistent with previous studies on the stomata of *Alchemilla* species (Zhu et al. 2015, Ilgun et al. 2016).

Alchemilla orduensis has eglandular and glandular hairs on the petiole, stem, and leaves. According to Zhu et al. (2015), *A. japonica* has both simple and branched eglandular hairs and multicellular glandular hairs. Faghır et al. (2016) conducted a study on the petioles of 24 *Alchemilla* species and concluded that eglandular hairs are of taxonomic significance for these species. *A. orduensis* has a palisade parenchyma consisting of two layers and a spongy parenchyma consisting of two to three layers, as well as single druse crystals. In *A. procumbens*, it has been reported that the palisade parenchyma consists of one to two layers and druse crystals are present in the mesophyll (Jimenez-Noriega et al. 2017). The presence of druse crystals, either in clusters or individually, on leaves and stems has been shown in *A. mollis* (Buser) Rothm (Ilgun et al. 2016). According to Zhu et al. (2015), the presence of clustered calcium oxalate crystals in *A. japonica* is a distinctive character.

In this study, 33 different compounds were identified in the aboveground and underground parts of the species *A. orduensis*. The most abundant groups vary in the aboveground and underground parts. The major groups were found to be alcohols (39.81%) and ketones (14.99%) in the aboveground and terpenes (23.44%) and alcohols (11.82%) in the underground. Alcohol and aldehydes were reported as the most abundant essential oil groups in aboveground parts of the species *A. alpina* and *A. xanthochlora* Rothm (Falchero et al. 2008, 2009). In *A. persica,* the main classes were alkanes and diterpenes (Afshar et al. 2015). *Alchemilla faeroensis* (Lange) Buser., *A. alpina* L., and *A. vulgaris* have been reported to contain triterpenes such as oleanolic acid, ursolic acid and euscophic acid (Olafsdottir et al. 2001, Fai and Tao 2009). The major constituents were (Z)-3-hexen-1-ol (11.20%), linalool (10.36%) and 1-octen-3-ol (8.98%) in aboveground parts of *A. xanthochlora* species and α-terpineol (12.55%), linalool (11.03%) and (Z)-3-hexen-1-ol (10.23%) in the aboveground parts of *A. alpina* (Falchero et al. 2008, 2009). These components were not found in *A. persica* Rothm. (Afshar et al. 2015). Essential oils were analyzed in the flowers and leaves of *A. flabellata* Bus., *A. phegophila* Juz. and *A. subrenata* Bus. The highest essential oil content was found in the flowers of *A. flabellata* (16884.6 mg kg^{-1}) and the lowest essential oil content was found in the leaves of *A. phegophila* (4895.5 mg kg^{-1}) (Dubel et al. 2022). 1-Octen-3-ol (29.36%), and octan-3-one (9.85%) are the most common compounds in the aboveground of *A. orduensis*. According to Falchero et al. (2008, 2009) and Dubel et al. (2022), αterpinol, linalool, (Z)-3-hexen-1-ol, 1-nonanal and 1-octen-3-ol compounds, which were found in other *Alchemilla* species, these were also determined in our study. The ratios of essential oil components in plants belonging to the same genus are thought to be affected by the localities at which the plants were collected and by climatic factors. Myrtenol (20.38%) is the major constituent in the underground pars of *A. orduensis*. It is a monoterpene compound with various therapeutic properties (Clarke 2008). This substance has a membrane stabilizing effect. Thus, it helps the formation and protection of cell and organelle membranes (Dragomanova et al. 2018). Myrtenol was found in the aboveground parts of the species *A. xanthochlora* and *A. persica* (Falchero et al. 2009, Afshar et al. 2015). It was reported that this compound was

not found in *A. alpina* species (Falchero et al. 2008). Octan-3-one is a compound found in both above and below ground parts of the *A. orduensis* species. It is used as an olfactory and gustatory component and has insect attractant properties (Muto et al. 2022, Reshna et al. 2022). Linalool and α-terpineol are monoterpene tertiary alcohols commonly found in *A. orduensis* and other *Alchemilla* species. They are the main floral fragrances in nature and are widely used in perfumery (Falchero et al. 2008, 2009, Dubel et al. 2022). α-terpineol has various biological applications, including use as an antioxidant, anticancer agent, and antiulcer agent. It is also of interest for its insecticidal properties (Khaleel et al. 2018).

Conclusion

This study determined the anatomical and micromorphological characteristics as well as the essential oil content of the Turkish narrow endemic species *A. orduensis*. Anatomical and micromorphological features are crucial in distinguishing *Alchemilla* species. Anatomically, important characters include the presence and arrangement of crystals, the shape of vascular bundles, and the presence of hairs in leaves and petiole. Micromorphologically, the epidermis and stomatal characteristics were also considered.

The *A. orduensis* species has been found to have an important medicinal potential, with 33 different compounds present in its underground and above-ground parts combined. The most common compounds are 1-Octen-3-ol in the above-ground parts and myrtenolis in the underground parts. Volatile compounds in plants vary depending on the species or ecological factors. Therefore, it is important to determine the essential oil profile of the endemic and endangered species *A. orduensis* collected from a special location.

Acknowledgments

This study was funded by Ordu University Research Council (Project no: A-1832).

Author contribution statement

Ö.E.A. – methodology, funding, writing and review, T.Ö – writing, review and editing, Ş.Ö. – anatomical studies, writing, H.Ü.U. – collection and chemical analysis of plants.

References

Afshar, F. H., Maggi, F, Ferrari, S, Peron, G, Dall'Acqua, S., 2015: Secondary Metabolites of *Alchemilla persica* Growing in Iran (East Azarbaijan). Natural product communications 10(10), 1705–1708. http://dx.doi.org/10.1177/1934578X1501001018

Ayaz, S., 2012: *Alchemilla*. In: Güner, A., Aslan, S., Ekim, T., Vural, M., Babaç M. T. (eds.), Türkiye Bitkileri Listesi (Damarlı Bitkiler) (A Check List of the Flora of Turkey (Vascular Plants)), 791–794. Nezahat Gökyiğit Botanik Bahçesi ve Flora Araştırmaları Derneği Yayını, İstanbul.

Baytop, T., 1999: Türkiye'de bitkiler ile tedavi (Treatment with herbs in Türkiye). Nobel Tıp Publication, Istanbul.

Benaiges, A., Marcet, P., Armengol, R., Betes, C., Girones, E., 1998: Study of refirming of a plant complex. International Journal Cosmetic Science 20(4), 223–230. https://doi.org/10.1046/j.1467-2494.1998.176608.x

Boruz, V., 2010: The stem anatomy of *Alchemilla connivens* and *Alchemilla crinita* species. Analele Universitatii din Craiova, seria Biologie, Horticultură, Tehnologia Prelucrării Produselor Agricole, Ingineria Mediului 15(1), 76–81.

Boruz, V., 2011: Morpho-anatomical considerations on the leaf from *Alchemilla glaucescens* species. Analele Universitatii din Craiova, seria Agricultura – Montanologie – Cadastru 41(2), 42–46.

Bozdağ, B., Kocabaş, O., Akyol, Y., Özdemir, C., 2016: Bitki Anatomisi çalışmalarında el kesitleri için yeni boyama yöntemi (A new painting method for hand sections in plant anatomy studies). Marmara Pharmaceutical Journal 20(2), 184–190. https://doi.org/10.12991/mpj.20162044231

Clarke, S., 2008: Families of compounds that occur in essential oils, In: Clarke, S. (ed.), Essential chemistry for aromatherapy, 41–77. (2nd ed.). Churchill Livingstone, Edinburgh.

Dragomanova, S., Tancheva, L. P., Georgieva, M., 2018: A review: Biological activity of myrtenal and some myrtenal-containing medicinal plant essential oils. Scripta Scientifica Pharmaceutica 5, 22–33.

Dubel, N., Grytsyk, L., Kovaleva, A., Grytsyk, A., Koshovyi, O., 2022: Research in components of essential oils from flowers and leaves of the genus *Alchemilla* L. species. ScienceRise: Pharmaceutical Science 3(37), 34–39. https://doi.org/10.15587/2519-4852.2022.259059

Ekim, T., Koyuncu, M., Vural, M., Duman, H. Aytaç, Z., Adıgüzel, N., 2000: Türkiye bitkiler kırmızı kitabı (Red data book of Turkish plants). Türkiye Tabiatını Koruma Derneği, Ankara.

Faghır, M. F., Mehrmanesh, A., Attar, F., 2016: Leaf and petiole anatomical characters of the genus *Alchemilla* (Rosaceae) in Iran and their use in numerical analysis. Journal of Taxonomy and Biosistematics 8(28), 1–20. https://doi.org/10.22108/tbj.2016.20983

Fai, M. Y., Tao, C. C., 2009: A review of precence of oleanolic acid in natural products. Natura Proda Medica 2, 271.

Falchero, L., Coppa, M., Esposti, S., Tava, A., 2008: Essential oil composition of *Alchemilla alpina* L. em. Buser from western alpine pastures. Journal of Essential Oil Research 20(6), 542–545. https://doi.org/10.1080/10412905.2008.9700084

Falchero, L., Coppa, M., Fossi, A., Lombardi, G., Ramella, D., Tava, A., 2009: Essential oil composition of lady's mantle (*Alchemilla xanthochlora* Rothm.) growing wild in Alpine pastures. Natural Product Research 23(15), 1367–1372. https://doi.org/10.1080/14786410802361438

Falchero, L., Lombardi, G., Gorlier, A., Lonati, M., Odoardi, M., Cavallero A., 2010: Variation in fatty acid composition of milk and cheese from cows grazed on two alpine pastures. Dairly Sciense Technology 90(6), 657–672. https://doi.org/10.1051/dst/2010035

Grytsyk, L. M., Tuchak, N. I., Grytsyk, A. R., Melnyk, M. V., Shumska, N. V., 2019: Морфолого-анатомічне дослідження видів приворотня, Що зростають в західному регіоні (Morpho anatomical investigation of *Alchemilla* L. species of western region of Ukraine). Farmatsevtychnyi Zhurnal 1, 78–91.

Hegnauer, R., 1986: Phytochemistry and plant taxonomy-an essay on the chemotaxonomy of higher plants. Phytochemistry 25, 1519–1535. https://doi.org 10.1016/S0031-9422(00)81204-2

Ilgun, S., Baldemir, A., Koşar, M., 2014: *Alchemilla* L. türlerinin kimyasal bileşikleri ve biyolojik aktiviteleri (Chemical com-

pounds and biological activities of *Alchemilla* L. species). Hacettepe University Journal of the Faculty of Pharmacy 34(1), 17–30.

Ilgun, S., Baldemır, A., Sam, N., Delımustafaoglu, F.G., Kosar, M., 2016: Phytochemıcal and morpho-anatomical properties of *Alchemılla mollıs* (Buser) Rothm. growing in Turkey. Bangladesh Journal Botany 45(3), 685–692.

Jimenez-Noriega, P. M. S., Terrazas, T., Lopez-Mata, L., Sanchez-Gonzales, A., Vıbrans, H., 2017: Anatomical variation of five plant species along an elevation gradient in Mexico City basin within the Trans-Mexican Volcanic Belt, Mexico. Journal of Mountain Science 14(11), 2182–2199. https://doi.org/10.1007/s11629-017-4442-8

Kalheber, H., 1994: The Genus *Alchemilla* L. (Rosaceae) in the Turkish Vilayet Rize (Northeastern Anatolia) with some remarks on the distribution of the genus in other parts of Northern Anatolia. Sendtnera 2, 389–430.

Karaoglan, E. S., Bayir, Y., Albayrak, A., Toktay, E., Özgen, U., Kazaz, C., Kahramanlar, A., Cadirci, E., 2020: Isolation of major compounds and gastroprotective activity of *Alchemilla caucasica* on ındomethacin ınduced gastric ulcers in rats. Eurasian Journal Medicine 52(3), 249–253. https://doi.org/10.5152/eurasianjmed.2020.19243

Kaya, B., Menemen, Y., Saltan, F.Z., 2012: Flavonoids in the endemic species of *Alchemilla* L., (Section *Alchemilla* L. Subsection *Calycanthum* Rothm. Ser. *Elatae* Rothm.) from North-East Black Sea Region in Turkey. Pakistan Journal of Botany 44(2), 595–597.

Khaleel, C., Tabanca, N., Buchbauer, G., 2018: α-terpineol, a natural monoterpene: a review of its biological properties. Open Chemistry 6, 349–361. https://doi.org/10.1515/chem-2018-0040

Mazı, B. G., Koç Güler, S., Bostan, S. Z., 2019: Post-harvest ripening of kiwifruit: changes in volatile compound profile. In: Kalıpcı, E. (ed.), Proceedings of the Third International Conference on Agriculture, Food, Veterinary and Pharmacy Sciences, 1574–1582. Academy Global Conferences & Journals, Nevşehir.

Meidner, H., Mansfield, T. A., 1968: Physiology of stomata. McGraw Hill, London.

Menezes, N. L., Silva, D. C., Arruda, R. C. O., Melode-Pınna, G. F., Cardoso, V. A., Castro, N. M., Scatena, V. L., Scremın-Dıas, E., 2005: Meristematic activity of the endodermis and the pericycle in the primary thickening in monocotyledons: considerations on the "PTM". Anais da Academia Brasileira de Ciências 77(2), 259–274. https://doi.org/10.1590/s0001-37652005000200006

Mohamed, A. A., El-Emary, G. A., Ali, H. F., 2010: Influence of some citrus essential oils on cell viability, glutathione-s-transferase and lipid peroxidation in Ehrlich ascites Carcinoma cells. Journal of American Science 6(10), 820–826.

Morgan, D. R., Soltis, D. E., Robertson, K. R., 1994: Systematic and evolutionary implications of rbcL sequence variation in Rosaceae. American Journal of Botany 81(7), 890–903. https://doi.org/10.1002/j.1537-2197.1994.tb15570.x

Muto, Y., Sakuno, E., Ishihara, A., Osaki-Oka, K., 2022: Antimicrobial activity of octan-3-one released from spent mushroom substrate of shiitake (Lentinula edodes) and its inhibitory effects on plant diseases. Journal of General Plant Pathology 89(2), 122–131. https://doi.org/10.1007/s10327-022-01110-4

Oktyabrsky, O., Vysochina G., Muzyka N., Samoilova Z., Kukushkina T., Smirnova G., 2009: Assessment of anti-oxidant activity of plant extracts using microbial test systems. Journal Applied Microbiology 106(4), 1175–1183. https://doi.org/10.1111/j.1365-2672.2008.04083

Okuda, T., Yoshida, T., Hatano, T., Iwasaki, M., Kubo, M., Orime, T., Naruhashi, N., 1992: Hydrolysable tannins as chemotaxonomic markers in the Rosaceae. Phytochemistry, 31(9), 3091–3096. https://doi.org/10.1016/0031-9422(92)83451-4

Olafsdottir, S. E., Omarsdottir, S., Jaroszewski, W. J., 2001: Constituents of three ıcelandic *Alchemilla* species. Biochemical Systematics and Ecology 29(9), 959–962. https://doi.org/10.1016/S0305-1978(01)00038-2

Ozbucak, T., Ergen Akçin, Ö., Öztürk, Ş., Uzunömeroğlu, H. Ü., 2022: Lokal endemik tür *Alchemilla orduensis* B. Pawl üzerine eko-biyolojik bir çalışma (An eco-biological study on the localy endemic species *Alchemilla orduensis* B. Pawl). Kahramanmaraş Sütçü İmam Üniversitesi Tarım ve Doğa Dergisi 25(2), 342–351.

Ozhatay, F. N., Kültür, S., Gurdal, M. B., 2011: Check-list of additional taxa to the supplement Flora of Turkey V, Turkish Journal of Botany 35, 589–624. https://doi.org/10.3906/bot-1101–20

Pawlowski, B., Walters, S. M., 1972: *Alchemilla* ın: Davis, P. H (ed.), Flora of Turkey and the East Aegean Islands, vol. 4, 80–104. Edinburgh University Press, Edinburgh.

Polat, R., Cakılcioglu, U., Kaltalioglu, K., Ulusan, M. D., Türkmen, Z., 2015: An ethno botanical study on medicinal plants in Espiye and its surrounding (Giresun-Turkey). Journal of Ethnopaharmacology163, 1–11. https://doi.org/10.1016/j.jep.2015.01.008

Renda, G., Tevek, F., Korkmaz, B., Yaylı, N., 2017: Comparison of the *Alchemilla* L. samples from Turkish Herbal Market with the European Pharmacopoeia 8.0. Fabad Journal of Pharmaceutical Sciences 42(3), 167–177.

Reshna, K. R., Gopi, S., Preetha, B., 2022: Flavors and fragrances in food processing. In: Gopi, S., Preetha, B. (eds.), Preparation and characterization methods. ıntroduction to flavor and fragrance in food processing, 1-19. ACS Symposium Series, Washington.

Said, O., Saad, B., Fulder, S., Khalil, K., Kassis, E., 2011: Weight loss in animals and humans treated with "weighlevel" a combination of four medicinal plants used in traditional arabic and ıslamic medicine. Evidence-Based Complementary and Alternative Medicine, Ecam 874538. https://doi.org/10.1093/ecam/nen067:ecAM

Setyawan, A. D., 2002: Chemotaxonomic studies on the genus *Amomum* based on chemical components of volatile oils. Hayati 9(3), 71–79.

Shrivastava, R. 2011: Clinical evidence to demonstrate that simultaneous growth of epithelial and fibroblast cells is essential for deep wound healing. Diabetes Research and Clinical Practice, 92(1), 92–99. https://doi.org/10.1016/j.diabres.2010.12.021

Shrivastava, R., Cucuat, N., John, W. G., 2007: Effects of *Alchemilla vulgaris* and glycerine on epithelial and myofibroblast cell growth and cutaneous lesion healing in rats. Phytotherapy Research 21(4), 369–373. https://doi.org/10.1002/ptr.2060

Stearn, W. T., 1985: Botanical Latin. Redwood Burn Limited, London.

Tongnuanchan, P., Benjakul, S., 2014: Essential oils: extraction, bioactivities, and their uses for food preservation. Journal of Food Science 79(3), 1231–1244. https://doi.org/10.1111/1750-3841.12492

Tundis, R., Peruzzi, L., Menichini, F., 2014: Phytochemical and biological studies of *Stachys* species in relation to chemotaxonomy: A review. Phytochemistry 102, 7–39.

Vardar, Y., 1987: Botanikte preparasyon teknigi (Preparation technique in botany). Ege University Press, İzmir.

Wallaart, R. A., 1980: Distribution of sorbitol in Rosaceae. Phytochemistry 19(12), 2603–2610. https://doi.org/10.1016/S0031-9422(00)83927-8

Watson, L., Dallwitz, M. J., 1991: The families of angiosperm: automated descriptions, with interactive identification and information retrieval. Australian Systematic Botany 4(4), 681–695. https://doi.org/10.1071/SB9910681

Zhu, Y., Zhang, N., Li, P., 2015: Pharmacognostical identification of *Alchemilla japonica* Nakai et Hara. Journal of Pharmacy & Pharmacognosy Research 3(3), 59–68.

Acta Bot. Croat. 84 (1), 22–26, 2025
DOI: 10.37427/botcro-2025-002

CODEN: ABCRA 25
ISSN 0365-0588
eISSN 1847-8476

Rapid spread of the Mediterranean glycophyte *Catapodium rigidum* in Hungary

Norbert Bauer[1]*, János Csiky[2], Attila Mesterházy[3], Mátyás Wolf[4], Dávid Schmidt[5]

[1] Hungarian Natural History Museum, Department of Botany, Könyves K. krt. 40, H-1089 Budapest, Hungary

[2] University of Pécs, Department of Ecology, Ifjúság u. 6, H-7624 Pécs, Hungary

[3] Hunyadi utca 55, H-9500 Celldömölk, Hungary

[4] Árvácska utca 38, H-7451 Kaposvár, Hungary

[5] Sopron University, Institute of Environmental Protection and Nature Conservation, Bajcsy-Zsilinszky u. 4, H-9400 Sopron, Hungary

Abstract – This paper discusses the spread of the Mediterranean plant *Catapodium rigidum* (L.) C.E. Hubb. in Hungary, which is found in the transition zone between the sub-Mediterranean and continental climatic zones of Central Europe. This alien species has been found at 12 new localities in Hungary in recent years. Some of these stands are located along main roads, while others are found in urban weed vegetation. The species was most likely introduced by increasing road traffic and tourism. Our preliminary findings suggest that the spread of the species is not concentrated along main roads due to its salt sensitivity. Instead, it is more likely to be found in xerothermic weed vegetation in urban areas where salting and winter de-icing are not applied.

Keywords: agochory, anthropochory, global warming, *Poaceae*, urban flora, weed species

Introduction

Catapodium rigidum (L.) C.E. Hubb. (*Desmazeria rigida* (L.) Tutin), fern grass or rigid-fescue (Poaceae family), is one of the most common synanthropic weed species in the Mediterranean region. It occurs in dry stony grasslands, particularly in ruderal places along roadsides, and municipal areas (Coste 1906, Fiori 1923, Jávorka 1925, Horvat et al. 1974). A recent study by Jasprica et al. (2017) found that this species is one of the most widespread weed species in railway stations in the North-Western Balkans. *Catapodium rigidum* s. str. has a Mediterranean-Atlantic distribution (Rikli 1943–1948, Meusel et al. 1965, Tutin et al. 1980). However, fern grass has been known to occur adventitiously in areas far from its original range, such as Asia, North and South America, Southern Africa, Australia (Clark 1974, Bhat et al. 2021, GBIF 2023). The species is considered indigenous to a small part of Switzerland (between Sézegnin and Soral), but introduced occurrences have also been long known in several large towns and cities, at railway stations, along railway lines, and in several cities in Germany (Hegi 1935, Buttler et al. 2018). Very few occurrences have been reported in Central Europe, east of Germany. Its casual occurrence was reported for the first time from Graz, Austria (Melzer 1954). The first report of this species in the Czech flora was almost 50 years ago by Dostál (1989), but there have been no confirmations. In 2009, Stöhr et al. reported a second observation of fern grass in Austria, in the surroundings of Salzburg (the community of Lamprechtshausen).

Old data (published or herbarium) reported occasional introductions of many Mediterranean species in Hungary. An accelerated spread of such plants has been observed recently (see Schmidt et al. 2016, Kun et al. 2023). However, in the BP herbarium specimens of *C. rigidum* originated from 19th century and the plants were grown from seeds in the botanical garden. Neither Borbás (1891) nor Filarszky (1894) mentioned it in their related papers. The species was first observed in Hungary by Solymosi (2008) along the main road near Becsehely (Zala County, Western Hungary). A decade later, Schmidt (2019) reported a finding of the species on the Szombathely bypass (Vas County, Western Hungary). In recent years, the species has been found in many

* Corresponding author e-mail: bauer.norbert@nhmus.hu

locations, particularly in the western part of the country (Transdanubia). While the manuscript of this study was being written, Rigó et al. (2023) reported the species from the capital (Budapest) in a single locality. The aim of our study is to provide a comprehensive summary of the current distribution of *C. rigidum* in Hungary, based on both published and unpublished data.

Material and methods

All authors conducted independent fieldwork, examining roadside vegetation and urban areas in various regions of the country. We recorded the geographic coordinates of the occurrences using GPS devices. A list of the sites is provided, along with the observation dates, geographical coordinates, grid numbers in the Central European Flora Mapping System (Niklfeld 1971), estimated number of individuals, and occurrence conditions. The specimens collected from the new sites in Hungary have been deposited in the BP and JPU Herbaria (Thiers 2024).

Results

The oldest specimens of *Catapodium rigidum* collected in Hungary were obtained from plants grown from seeds sown in a botanical garden (leg. Fekete, 30.10.1903, *culta in h. bot. Budapest* BP 313807, 408777). Recent spontaneous occurrences are summarised in Tab. 1.

The distribution pattern of the species in Hungary (Fig. 1) indicates a spread in Western and Southern Transdanubia. The species was predominantly found in high-traffic locations, such as main roads and popular tourist areas.

Tab. 1. Introduced occurrences of *Catapodium rigidum* found in Hungary until the end of 2023. CEU = grid number of the Central European Flora Mapping System (Niklfeld 1971).

CEU	Settlement	Locality	Coordinate	Habitat	Number of individuals	Date	Observer / Collector	Herbarium specimen
9566.2 / 9566.4	Becsehely	main road 7	–	road bank	no data	2007	P. Solymosi	–
8765.4	Szombathely	main road 86 (E65)	N 47.221971 E 16.658571	road bank	appr. 200	2017, 2019- onwards	D. Schmidt	–
8965.2	Egyházasrádóc	main road 86 (E65)	N 47.104442 E 16,637393	monodominant along road bank	1000	22.06.2022.	N. Bauer	HNHM-TRA 00129733, HNHM-TRA 00129734
8965.4	Körmend	main road 86 (E65)	N 47,025314 E 16, 365181	asphalt road edge	< 20	26.06.2022.	A. Mesterházy	–
9975.1	Pécs	Tettye, Zöldfa street	N 46.081557 E 18.232826	along the pavement and the asphalt road	10–20	25.05.2023.	M. Wolf	–
8765.4	Szombathely	main road 86 (E65)	N 47.221971 E 16.658571	smaller stand on road bank	100	28.05.2023.	D. Schmidt	HNHM-TRA 00702573
8480.1	Budapest	III. District, Gyűrű street	N 47.598549 E 19.060334	small trampled lawn patch and crevices of pavement	~400	31.05.2023.	A. Rigó	–
9975.1	Pécs	Tímár street (in the city centre)	N 46.074521 E 18.233905	in a one-way street with limited traffic, at the foot of the buildings	10-20	16.06.2023.	J. Csiky	JPU
9364.4	Rédics	main road 86 (E65)	N 46.618997 E 16.465032	massive population along road bank	1000	17.06.2023.	D. Schmidt	HNHM-TRA 00702574
9172.4	Balatonszemes	pedestrian section at yacht harbor	N 46.812442 E 17.770822	under the strip of shrubs at the edge of the sidewalk, few	< 20	18.06.2023.	N. Bauer & A. Hüvös-Récsi	HNHM-TRA 00702591
9270.3	Balatonmáriafürdő	interior area, Keszeg street	N 46.703155 E 17.375309	sidewalk edge, car driveway	10–20	30.06.2023.	D. Schmidt	–
9270.4	Balatonfenyves	interior area, at the crossing of Kölcsey street and the railway	N 46.712215 E 17.478821	asphalt road edge	< 20	02.07.2023.	N. Bauer	HNHM-TRA 00702590

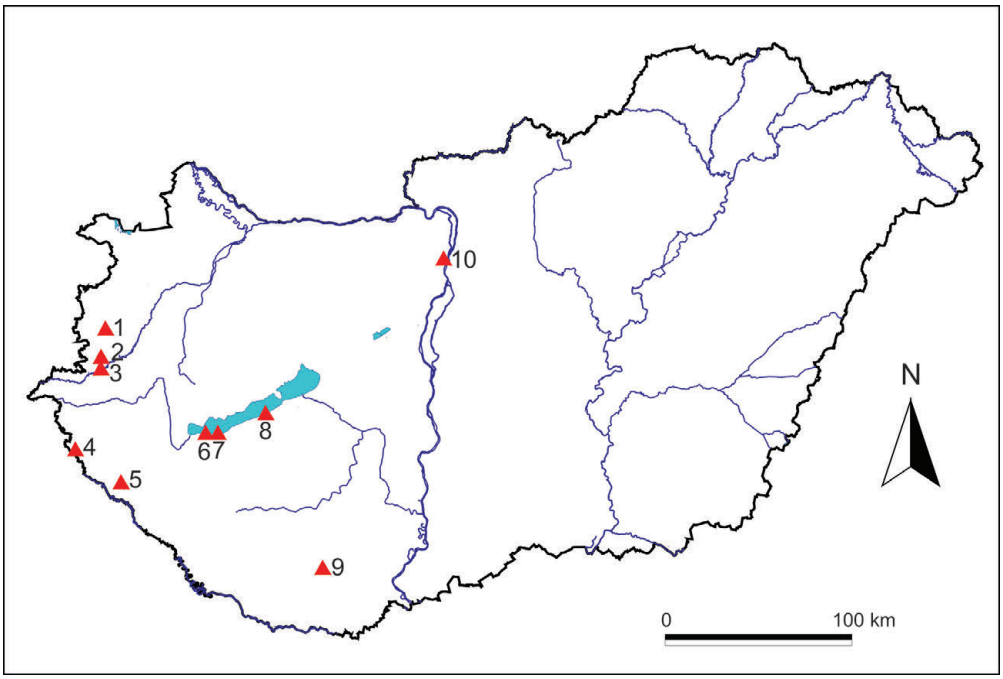

Fig. 1. Current known occurrences of *Catapodium rigidum* in Hungary (December 2023). The red triangle shows the places where *Catapodium rigidum* was found: 1 – Szombathely, 2 – Egyházasrádóc, 3 – Körmend, 4 – Rédics, 5 – Becsehely, 6 – Balatonmáriafürdő, 7 – Balatonfenyves, 8 – Balatonszemes, 9 – Pécs, 10 – Budapest.

Discussion

Our presumption is that the presence of the fern grass in Hungary can be attributed to human activities, particularly international transport and tourism. The type of dispersal can be classified as anthropochory and agochory, as described by van der Maarel (2005) and Schulze et al. (2005). Where heavy traffic occurs on main roads (roadsides, roundabouts, pavements), the vector could be mainly motor vehicles carrying propagules on pieces of gravel. However, small populations found at sites where waste accumulates (e.g. Balatonszemes harbour; Pécs, at the base of buildings in a one-way street) suggest that lesser amounts of propagules may have been transported by human clothing and tools. The current new occurrences may be the result of independent introductions.

Although mentioned as a synanthropic species by Hegi (1935), its recent distribution in Europe (Fig. 2. GBIF) is rather dispersed and scattered outside of its original climatic requirements, specifically outside of the regions with oceanic and Mediterranean climates.

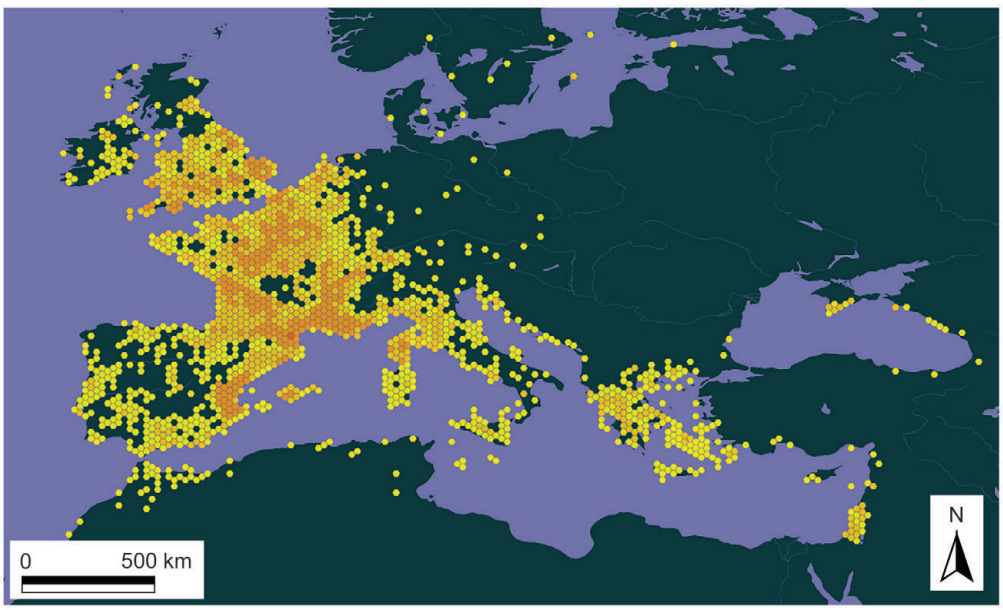

Fig. 2. Distribution of *Catapodium rigidum* in Europe based on GBIF data (2 October 2023). The dots show the reported occurrences of *C. rigidum*, the shades of yellow (from light to dark) reflect the amount of data detected.

Its natural distribution limit is almost identical to the January 0 C° isotherm (Michael 2021, p. 52.). Previous occurrences of this species in Central Europe were sporadic, and for a long time, its presence was not confirmed in Austria and in the Czech Republic (Melzer 1954, Dostál 1989, Stöhr et al. 2009, Pyšek et al. 2012). The establishment of the species in continental areas has been restricted, due to the limiting effect of winter frost (see Manley 1958, Grimm et al. 2008). However, according to the current climate change trends in the Pannonian region (Bartholy et al. 2014), the species is predicted to become established in Central Europe and other areas with a humid continental climate (Beck et al. 2018).

Currently, there are limited and conflicting data regarding the survival of plants in the stands. In the city of Szombathely, it was first discovered in 2017, disappeared for a year, and then reappeared in 2019, remaining present ever since. This observation suggests that if the habitat is suitable self-sustaining populations may develop. Mild winters do not appear to be a limiting factor if there are no periods of heavy frost. However, not all of the stands known for more than two years can be confirmed in the coming year. For instance, one of the most abundant populations found in 2022 (Egyházasrádóc village) was not observed on the roadside during the same period the following year. Given that the winter between the two field surveys of the site was the second mildest in the last 100 years (Szolnoki-Tótiván 2023), it is necessary to consider other limiting factors that may affect the survival of the introduced plants. Occasional mass emergence may occur due to extensive propagule introduction after winter. However, despite significant mass seed dispersal, germination in the following early spring may not be possible due to the high osmotic stress on roadside verges (Davison 1971). According to the Ellenberg-type indicator values database (Tichý et al. 2023), the species is presumably a glycophyte (salt-sensitive), so the use of salt to de-ice main roads is likely to reduce its long-term viability. The experimental confirmation by Talbi Zribi et al. (2018) also supports the strong salt sensitivity of *C. rigidum* when planted for forage in arid areas. Additionally, its long-term survival on main road verges may be reduced because *C. rigidum* is an annual C3 species. Its phenology is characterised by early spring germination, when the effect of winter salting is still strong and the leaching effect of precipitation is still weak. It is uncertain whether a population, even a relatively large one, can be considered self-sustaining in the future. However, due to the ever-increasing flow of traffic from the Mediterranean, the frequent introduction of its propagules is almost inevitable. It is possible that urban weed vegetation not subject to salting and de-icing will be more likely to have persistent, established populations, even if these are smaller. The aforementioned increases in the chance of establishment are already assumed for many species with similar climatic requirements and have shown recent area expansion (Bátori et al. 2012, Schmidt et al. 2016, Bauer 2018, Mesterházy et al. 2021, Bauer and Verloove 2023, Kun et al. 2023). It is expected that *C. rigidum* will continue to occur and spread in temperate continental areas of Central Europe, particularly along busy roads and in towns, with an increasing number of observations in the coming years.

Acknowledgments

We thank everyone who helped us, Annamária Hüvös-Récsi, Zoltán Kenyeres, Attila Rigó, Tamás Wirth in the fieldwork and/or with their remarks. The authors would like to express their gratitude to the two anonymous reviewers for their remarks.

Author contribution statement

N.B., D.S. and J.Cs. compiled a significant part of the manuscript, all the authors together wrote the conclusions.

References

Bartholy, J., Pongrácz, R., Pieczka, I. 2014: How the climate will change in this century? Hungarian Geographical Bulletin 63(1), 55–67. https://doi.org/10.15201/hungeobull.63.1.5

Bátori, Z., Erdős, L., Somlyay, L., 2012: *Euphorbia prostrata* (Euphorbiaceae), a new alien in the Carpathian Basin. Acta Botanica Hungarica 54(3–4), 235–243. https://doi.org/10.1556/ABot.54.2012.3-4.2

Bauer, N., 2018: Distribution of *Medicago orbicularis* (Fabaceae) in Hungary. Studia Botanica Hungarica 49(2), 49–60. https://doi.org/10.17110/StudBot.2018.49.2.49

Bauer, N., Verloove, F., 2023: The accelerated spread of a neophyte introduced to Europe long ago. First occurrence of *Sporobolus indicus* (Poaceae) in Hungary. Acta Botanica Croatica 82(1), 20–26. https://doi.org/10.37427/botcro-2022-024

Beck, H. E., Zimmermann, N. E., McVicar, T. R., Vergopolan, N., Berg, A., Wood, E. F., 2018: "Present and future Köppen-Geiger climate classification maps at 1-km resolution". Scientific Data 5: 180214. https://doi.org/10.1038/sdata.2018.214

Bhat, M. A., Shakoor, S. A., Chowdhary, P., Badgal, P., Mir, B. A., Soodan, A. S., 2021: Taxonomic description and annotation of *Catapodium rigidum* (L.) C.E. Hubbard (Poaceae: Pooideae, Poeae, Parapholiinae) from Kashmir Himalayas, India. Vegetos 34 (3), 692–699. https://doi.org/10.1007/s42535-021-00223-z

Borbás, V., 1891: A növények vándorlása s Budapest flórájának vendégei (The migration of plants and alien plants of Budapest). Pótfüzetek a Természettudományi Közlönyhöz 13(1) (Supplementum), 1–18.

Buttler, K. P., Thieme, M. et al. 2018: Florenliste von Deutschland – Gefäßpflanzen. Version 10. (August 2018) Frankfurt am Main. https://doi.org/10.11585 /buttler_et_al_florenliste_v10 Retrieved October 3, 2023 from https://publikationen.ub.uni-frankfurt.de/frontdoor/index/index/docId/52612

Clark, S. C., 1974: Biological Flora of British Isles *Catapodium rigidum* (L.) C. E. Hubbard. Journal of Ecology 62(3), 937–958. https://doi.org/10.2307/2258963

Coste, H., 1906: Flore descriptive et illustrée de la France de la Corse et des contrées limitrophes. Tome 3. Paul Elinsieck, Paris.

Davison, A. W., 1971: The effects of de-icing salt on roadside verges. I. Soil and plant analysis. Journal of Applied Ecology 8(2), 555–561. https://doi.org/10.2307/2402891

Dostál, J., 1989: Nová květena ČSSR (New flora of the CSSR). Academia, Praha.

Filarszky, N., 1894: Adatok Budapest flórájához (Data for the flora of Budapest). Pótfüzetek a Természettudományi Közlönyhöz 29–30 (Supplementum), 117–121.

Fiori, A., 1923: Nuova flora analitica d'Italia. Vol. I. M. Ricci, Firenze.

GBIF, 2023: Global Biodiversity Information Facility. Species: *Catapodium rigidum* (L.) C.E. Hubb. Retrieved October 2, 2023 from https://www.gbif.orgbifg/species/2705228

Grimm, N. B., Faeth, S. H., Golubiewski, N. E., Redman, C. L., Wu, J., Bai, X., Briggs, J. M., 2008: Global change and the ecology of cities. Science 319(5864), 756–760. https://doi.org/10.1126/science.1150195

Hegi, G., 1935: Illustrierte Flora von Mittel-Europa. Band I. 2. Auflage. J. F. Lehmans Verlag, München.

Horvat, I., Glavač, V., Ellenberg, H., 1974: Vegetation Südosteuropas. Gustav Fischer Verlag, Stuttgart.

Jasprica, N., Milović, M., Dolina, K., Lasić, A., 2017: Analyses of the flora of railway stations in the Mediterranean and sub-Mediterranean areas of Croatia and Bosnia and Herzegovina. Natura Croatica 26(2), 271–303. https://doi.org/10.20302/NC.2017.26.21

Jávorka, S., 1925: Magyar Flóra. Flora Hungarica. Studium, Budapest.

Kun, A., Exner, T., Bauer, N., 2023: A *Torilis nodosa* új behurcolásai és terjedése Magyarországon. (New occurrences and spread of the adventive species *Torilis nodosa* in Hungary). Kitaibelia 28 (1), 26–31. https://doi.org/10.17542/kit.28.030

Manley, G., 1958: On the frequency of snowfall in metropolitan England. Quarterly Journal of the Royal Meteorological Society 84(1), 70–72. https://doi.org/10.1002/qj.49708435910

Melzer, H., 1954: Zur Adventivflora der Steiermark I. Mitteilungen des Naturwissenschaftlichen Vereines Steiermark 84, 103–120.

Mesterházy, A., Wirth, T., Schmidt, D., Csiky, J. 2021: A *Vulpia ciliata* morfológiája és magyarországi terjedésének sikere a vasúthálózat mentén (Spreading along the railways: morphology and invasion success of *Vulpia ciliata* in Hungary). Kitaibelia 26(2), 145–156. https://doi.org/10.17542/kit.26.145

Meusel, H., Jäger, E. J., Weinert, E. (eds.), 1965: Vergleichende Chorologie der Zentraleuropäischen Flora. Band I. Gustav Fischer Verlag, Jena.

Michael, T. (ed.), 2021: Diercke International Atlas. Westermann, Braunschweig (Brunswick).

Niklfeld, H., 1971: Bericht über die Kartierung der Flora Mitteleuropas. Taxon 20(4), 545–571. http://dx.doi.org/10.2307/1218258

Pyšek, P., Danihelka, J., Sádlo, J., Chrtek, J., Chytrý, M., Jarošík, V., Kaplan, Z., Krahulec, F., Moravcová, L., Pergl, J., Štajerová, K., Tichý, L., 2012: Catalogue of alien plants of the Czech Republic (2nd edition): Checklist update, taxonomic diversity and invasion patterns. Preslia 84, 155–255.

Rigó, A., Malatinszky, Á., Barina, Z., 2023: Inventory of the urban flora of Budapest (Hungary) hightlighting new and noteworthy floristic records. Biodiversity Data Journal 11(2), e110450. https://doi.org/10.3897/BDJ.11e110450

Rikli, M., 1943, 1946, 1948: Das Pflanzenkleid der Mittelmeerländer. 1–3. Band. Verlag Hans Huber, Bern.

Schmidt, D., 2019: Vonalas létesítmények mentén terjedő növények Vas megyében (Plants spreading along the linear facilities in Vas County). Vasi Szemle 73(2), 160–174.

Schmidt, D., Dítě, Z., Horváth, A., Szűcs, P., 2016: Coastal newcomer on motorways: the invasion of *Plantago coronopus* in Hungary. Studia Botanica Hungarica 47(2), 319–334. https://doi.org/10.17110/StudBot.2016.47.2.319

Schulze, E-D., Beck, E., Müller-Hohenstein, K., 2005: Plant Ecology. Springer, Berlin, Heidelberg.

Solymosi, P., 2008: Két új termofil pázsitfűfaj jelent meg Magyarországon (Two new thermophilic grass species appeared in Hungary). Növényvédelem 44(3), 141–142.

Stöhr, O., Pilsl, P., Essl, F., Wittmann, H., Hohla, M., 2009: Beiträge zur Flora von Österreich, III. Linzer biologische Beiträge 41(2), 1677–1755. https://doi.org/10.5281/zenodo.5279728

Szolnoki-Tótiván, B., 2023: 2022/2023 telének időjárása (Weather in winter 2022/2023). Időjárás 68(2), 96–101.

Talbi Zribi, O., Slama, I., Trabelsi, N., Hamdi, A., Abdelly, C., 2018: Combined effects of salinity and phosphorus availability on growth, gas exchange, and nutrient status of *Catapodium rigidum*. Arid Land Research and Management 32(3), 277–290. https://doi.org/10.1080/15324982.2018.1427640

Tichý, L., Axmanová, I., Dengler, J., Guarino, R., Jansen, F., Midolo, G., Nobis, M. P., van Meerbeek, K., Aćić, S., Attorre, F., Bergmeier, E., Biurrun, I., Bonari, G., Bruelheide, H., Campos, J. A., Čarni, A., Chiarucci, A., Ćuk, M., Ćušterevska, M., Didukh, Y., Dítě, D., Dítě, Z., Dziuba, T., Fanelli, G., Fernández-Pascual, E., Garbolino, E., Gavilán, R. G., Gégout, J.-C., Graf, U., Güler, B., Hájek, M., Hennekens, S. M., Jandt, U., Jašková, A., Jiménez-Alfaro, B., Julve, P., Kambach, S., Karger, D. N., Karrer, G., Kavgacı, A., Knollová, I., Kuzemko, A., Küzmič, F., Landucci, F., Lengyel, A., Lenoir, J., Marcenò, C., Moeslund, J. E., Novák, P., Pérez-Haase, A., Peterka, T., Pielech, R., Pignatti, A., Rašomavičius, V., Rūsiņa, S., Saatkamp, A., Šilc, U., Škvorc, Ž., Theurillat, J.-P., Wohlgemuth, T., Chytrý, M., 2023: Ellenberg-type indicator values for European vascular plant species. Journal of Vegetation Science 34(1), e13168. https://doi.org/10.1111/jvs.13168

Tutin, T. G., Heywood, V. H., Burges, N. A., Moore, D. M., Valentine, D. H., Walters, S. M., Webb, D. A. (eds.), 1980: Flora Europaea. Vol. 5. Cambridge University Press, Cambridge.

Thiers, B. M., 2024: Index Herbariorum: A global directory of public herbaria and associated staff. New York Botanical Garden's Virtual Herbarium. Retreived April 4, 2024 from https://sweetgum.nybg.org/science/ih/

van der Maarel, E. (ed.), 2005: Vegetation Ecology. Blackwell Publishing, Malden-Oxford-Carlton.

Acta Bot. Croat. 84 (1), 27–32, 2025
DOI: 10.37427/botcro-2025-009

CODEN: ABCRA 25
ISSN 0365-0588
eISSN 1847-8476

Additional data on the ongoing naturalization of the non-native woody plant *Duranta erecta* (Verbenaceae) in Sicily, Italy

Salvatore Pasta[1], Pietro Lo Cascio[2], Emilio Badalamenti[3,4]*

[1] Institute of Biosciences and BioResources (IBBR), National Research Council (CNR), Unit of Palermo, via Ugo La Malfa 153, 90146 Palermo, Italy

[2] Associazione Nesos, Corso Vittorio Emanuele II 24, 98055 Lipari (ME), Italy

[3] University of Palermo, Department of Agricultural, Food and Forest Sciences, Viale delle Scienze, 90128 Palermo, Italy

[4] NBFC, National Biodiversity Future Center, 90133 Palermo, Italy

Abstract – We recorded the occurrence of *Duranta erecta* L. in the Aeolian Islands (Sicily, Italy), where it currently behaves as a casual alien. At the global scale, however, this woody species has shown highly invasive behaviour in different island ecosystems. On the basis of this evidence, we have investigated which ecological and biological traits may have allowed its establishment and spread, and could trigger its further expansion in the Aeolian Islands in the near future. Several factors seem to have favoured its success on a global scale, such as the wide edaphic and climatic range, the tolerance to anthropogenic disturbance, and the production of toxic metabolites that protect it from herbivore browsing and from competition with other plants. The study of the organisms that perform pollination and seed dispersal is probably the key to understanding the local naturalization of this plant, introduced about three centuries ago in Europe and the Mediterranean, and is here discussed in detail for the first time.

Keywords: alien woody plants, early detection, golden dewdrop, hedge plant, invasion biology

Introduction

The management of invasive plants is quite difficult, especially in the case of widespread species. Indeed, early detection and prompt actions are considered to be the most effective tools for the control of invasive species and for limiting their negative impacts on native species and ecosystems (Regulation EU 1143/2014, https://eur-lex.europa.eu/legal-content/EN/TXT/PDF/?uri=CELEX:32014R1143). In the framework of field observations and literature search aimed at updating the vascular flora of the Aeolian Islands (Sicily, Italy), we report here the record of *Duranta erecta* L., a new alien plant species occurring in the archipelago. *D. erecta* is a spreading, sometimes climbing, evergreen shrub; on nutrient-rich and deeper soils, it can reach the size of a small tree (up to 7 m tall) (Arengo 2015). Naturally, it mostly occurs in dry coastal areas (yearly annual precipitation between 800 and 1800 mm: Arengo 2015) from sea level up to more than 1600 m a.s.l. (populations growing at 3500 m a.s.l. occur on some of the Caribbean Islands). Notwithstanding its tropical origins, *D. erecta* proved to be a hardy plant, being able to withstand even short frost events (Arengo 2015). Moderately shade-intolerant, *D. erecta* does not compete well with taller woody plants and, consequently, is usually not found in dense plant communities. Within its natural distribution range, it commonly grows in well-lit areas, mostly on rocky or sandy soils, and prefers low and discontinuous herb- and grass-rich plant communities and thickets (PIER 2013). Under moister conditions, it may also occur in inland areas prone to anthropogenic disturbance (e.g., roadsides: Adams 1972).

The karyological studies on *D. erecta* pointed out a high variability throughout the native distribution range (from 2n = 16 to 2n = 36, Munir 1995). Hence, the extremely wide climatic and edaphic amplitude of the golden dewdrop; and its remarkable adaptability to man-made habitats may depend on the varied response to disturbance of different populations bearing different genetic traits. The ecological plasticity of this plant is paralleled by the high variability of many of its morphological traits, encompassing the growth form (shrub, liana or small tree), the habit (erect *vs*. prostrate), the

* Corresponding author e-mail: emilio.badalamenti@unipa.it

leaf margin shape (entire *vs*. dentate), the leaf size (large or small). These features, together with the presence of axillary thorns (on mature individuals only), explain the plethora of specific epithets given to the very same species during the last 250 years (see http://www.theplantlist.org/tpl/record/kew-65221); the most commonly featured synonyms are *Duranta repens* L., *D. ellisia* Jacq., and *D. plumieri* Jacq. Reported to be native to the Americas, *D. erecta* grows along the Pacific rims of central and southern America (from Texas, Arizona and California south to Peru) as well as along the Atlantic coast from Florida, Louisiana to Puerto Rico south to Brazil and Argentina (POWO 2024). The secondary range encompasses many tropical and subtropical countries in South America, Africa and East Asia (POWO 2024). Due to the wide spectrum of traditional usages within its native range and its widespread cultivation outside it, dozens of vernacular names have been given to *D. erecta* across Asia (India, Indonesia, China, etc.), south and central America, W-Africa and the Pacific islands (Missouri Botanic Garden 2018, Srivastava and Shanker 2022).

Although frequently cultivated in Mediterranean Europe, and being generically reported for Türkiye (Uludağ et al. 2017), no record of naturalization has been hitherto reported (Raab-Straube von 2022+). Hence, this paper also aims to provide an updated picture of knowledge on the ecology and distribution of this species on a global scale as well as to give some clues to interpreting the meaning of the new record within the peculiar biogeographical context of the Aeolian Islands.

Material and methods

We made an in-depth bibliographic search on the two most popular databases of scientific literature, namely Scopus (https://www.scopus.com/search/form.uri?display=basic#basic) and Web of Science (https://www.webofscience.com/wos/woscc/basic-search) to find out additional information on *Duranta erecta*. To this aim, we cross-checked papers and reports using the above-reported binomial epithets and the keywords "allelopathy", "chemical compounds", "climate", "cultivation", "dispersal", "distribution range", "ecological amplitude", "genetics", "introduction", "invasiveness", "metabolites", "pollination", "niche", "soil", "substrate", "typification" and "vegetation".

In the meantime, we carried out regular field surveys across the whole Aeolian Archipelago between 1994 and 2024.

Results

In November 2019, a few decimetres tall individual of an unknown woody species was observed growing on the inner edge of a sidewalk at the limit of a building in the centre of the town of Lipari (the largest island of the Aeolian archipelago), at about 20 m a.s.l. A more accurate observation allowed us to classify the plant as *Duranta erecta* (Verbenaceae J.St.-Hil.), a small shrub native to the Americas and also known by the English names of golden dewdrop, pigeon berry, and skyflower. The putative parents grew about 20 meters off, *i.e.*, on the terrace of an apartment located just above the sidewalk. Probably, some berries fell from the terrace through the gutter, from which rainwater drains to just where the individual grows. Within the last four years, the plant probably enjoyed additional water coming from the gutter: in fact, it was able to grow steadily (it now exceeds 2 metres, see Fig. 1) and two years ago it began to bloom and regularly fructify.

Fig. 1. The self-sown individual of *Duranta erecta* found growing wild in the centre of Lipari (Aeolian Islands, Sicily, Italy). It is more than two meters high and has started fruiting (see the small picture taken from the same plant, up on the left) (photo: Pietro Lo Cascio).

D. erecta was introduced in the private garden of one of the authors (PLC) in at least the 1970s. However, no bibliographic information is available about an earlier introduction of this species on Lipari Island, where it was first observed under cultivation only recently by Domina and Mazzola (2008). This individual can be considered fully established but the species should be considered as a casual alien plant, due to the uniqueness of the finding and the current lack of self-sustaining populations.

The golden dewdrop is not featured in the list of the alien plants naturalized in Sicily (Raimondo et al. 2005a,b). Despite having been reported as spontaneously occurring

in the urban areas of Palermo (Domina et al. 2019), *D. erecta* is not featured either in the Euro+Med PlantBase (Raab-Straube 2022+) or in the last inventory of the Italian non-native flora (Galasso et al. 2024). Hence, our data represents the first clear indication of its ongoing naturalisation both at the national and the Euro-Mediterranean scale, and the first concerning Mediterranean small islands. Moreover, this paper provides a detailed picture of its spatio-temporal invasion process at the global scale, as well as the future implications of a likely further spread in the Mediterranean.

Discussion

Introduction history: from the global scale to Sicily

Duranta erecta was introduced far from its native range very early, probably many centuries ago, *i.e.*, long before being described by botanists, when the Europeans learnt from native Americans about its properties. This may explain the remarkably wide spectrum of medicinal "traditional" uses of this plant in countries like Nigeria, India, China, and the Philippines (see Srivastava and Shanker 2022 and references therein).

A second impetus to the spread of the species on a global scale was given by its massive use as a popular hedge plant. In fact, from the 18th century, its showy flowers and fruit made it one of the most commonly cultivated ornamental plants in tropical and subtropical gardens worldwide, not only in most of the islands and archipelagos of the Pacific and Indian Ocean but even in the Mediterranean Basin (Missouri Botanical Garden 2018).

During his stay in Leiden, Linnaeus (1753, p. 637) probably based his description of *Duranta erecta* on the original drawings of Charles Plumier (who was cited in the protologue), a French botanist who probably was the first to observe the plant growing in the wild during one of his three voyages to the Caribbean islands between 1689 and 1697 (Moroni et al. 2018). We can therefore assume that the golden dewdrop was imported into Europe shortly after, perhaps by Plumier himself, who described this species using the polynomial epithet "*Castorea racemosa*, *flore caeruleo*, *fructu amaro*" (Plumier 1703, p. 30). His choice to dedicate the species to the Italian botanist Castore Durante (1529-1590) was followed by Linneus (1753), who decided to assign it within the genus *Duranta*.

A careful search for mentions of *D. erecta* (and of its synonyms) in Europe led to a reference by Sims (1815), who clearly stated that Philip Miller cultivated it in London even before 1739. As far as Italy is concerned, the oldest record is featured in the catalogue of plants cultivated at the Royal Botanical Garden of Mantua (Anonymous 1785). In the first half of the nineteenth century, the species was also cultivated in the botanical gardens of Bologna and Ferrara, as mentioned in the letters by the Italian botanist Antonio Bertoloni (Buldrini et al. 2017).

As for Sicily, it can be assumed that *D. erecta* was first introduced in Palermo during the last decade of the 18th century. In fact, it did not appear in either the Ucria (1789) or the Tineo (1790) checklists of cultivated plants, while, just a few years later, it was listed among the plants cultivated at the Botanical Garden of Palermo in the lists of Tineo (1799, 1802). Since then, *D. erecta* has been massively used in Sicily: in fact, it is featured among the forty most frequent ornamental non-native plant species occurring in the island's historic gardens (Bazan et al. 2005).

Why the Aeolian Islands?

The synergic effect of mild winters, abundant overnight dew accumulation during the dry season, and good soil quality make Mediterranean volcanic islands an ideal place for alien plant cultivation, frequently followed by fast naturalisation events and unwanted spread (Pretto et al. 2012, Blackburn et al. 2016, Celesti-Grapow et al. 2016, Pasta et al. 2017, Guarino et al. 2021, Minissale et al. 2023). Not surprisingly, the Aeolian archipelago has long been the perfect scenario for the introduction and establishment of many ornamental non-native plants (Domina and Mazzola 2008, Di Gristina et al. 2021, Barone et al. 2023). In fact, these islands were home to the first or the only Italian or Sicilian naturalization cases of plants coming from all over the world: for instance, *Curio talinoides* (DC.) P.V. Heath, first reported on Vulcano under the name *Kleinia mandraliscae* by Tineo (1855), and escaped from private gardens in the 19th century (Pasta 2003), *Arctotheca calendula* (L.) Levyns (Madon 1994) and *Pelargonium graveolens* (Thunb.) L'Hér. (Di Gristina et al. 2021) from S-Africa, *Paraserianthes lophanta* (Willd.) I.C. Nielsen (Domina and Spallino 2007) and *Cotula australis* (Sieber ex Spreng.) Hook. f. (Guarino et al. 2018) from S-Australia, *Salvia leucantha* Cav. (Pasta et al. 2008) from central America and *Passiflora incarnata* L. from N-America (Di Gristina et al. 2021).

Why *Duranta erecta* is a successful invader worldwide?

Duranta erecta may behave as an invasive, prolific, fast-growing plant spread by birds from man-made habitats to natural areas. In such cases, conservation practitioners may have serious problems in keeping it under control. For instance, it has been identified as an invasive alien species in most of the Pacific islands and archipelagos like Tonga, Fiji, Hawai'i, French Polynesia, Micronesia (PIER 2013), in South Africa (Foxcroft et al. 2008), SE Australia (Mulvaney 1991), Mayotte Islands in the Indian Ocean (IUCN-France 2013), and Taiwan (Wu et al. 2004). In many other areas where it was introduced a long time ago, like E and SE Africa (Witt and Luke 2017), Mauritius, India, Indonesia, China and Japan, it is fully naturalized but not invasive (Missouri Botanical Garden 2018). However, as a consequence of its wide cultivation and favourable biological traits, *D. erecta* was listed in the most comprehensive and recent checklist of invasive trees and shrubs at the global scale (Rejmánek and Richardson 2013).

How concrete is the risk of *Duranta erecta* expansion over the Mediterranean Basin?

On the one hand, when selecting exotic ornamental plants, horticulturists are used to prefer species characterized by a broad climatic and edaphic amplitude, *i.e.*, capable

of growing in environmental conditions that are as diverse as possible. On the other hand, invasion biologists are increasingly aware of the strong correspondence between these traits and those increasing the likelihood that "candidate invasive plants" will become successfully established in the introduced range, as well as showing a fast spread and invasive behaviour (Pasta 2022). This evidence makes it hard to manage non-native ornamental plants, which account for a major portion of the global naturalized plant database (van Kleunen et al. 2018). As for *D. erecta,* another favourable trait may be related to its chemical weapons. In fact, *D. erecta* produces several allelopathic compounds (Tur et al. 2010) and has even been used against mosquitos (Dacko et al. 2020). These toxic substances represent a very effective defence against herbivores, that mainly work outside its native distribution range, according to the novel weapons hypothesis (Callaway and Ridenour 2004). In fact, the leaves and the unripe (yellow-orange) berries are toxic, and are confirmed to have killed children in the past (Wheeler 1895) and domestic animals more recently (Thompson 2007).

During the last decade, numerous exotic ornamental plants of tropical and subtropical origin, introduced several centuries ago in the Mediterranean, have been the protagonists of apparently sudden cases of naturalization in Sicily (e.g., Pasta et al. 2014, Speciale et al. 2015, Badalamenti 2021, Collesano et al. 2021). In most cases, their success probably depended on their entry as a functional element in the trophic networks of the recipient ecosystems. In fact, these species have managed to create stable interactions with other organisms that allow them to carry out two crucial phases such as pollination and seed dispersal. Hence, the study of the organisms that perform pollination and seed dispersal will probably provide the key to understanding the local naturalization of *D. erecta*. As far as we know, in its home range pollination is performed by hummingbirds (Byragi Reddy and Subba Reddi 1996). Nonetheless, as the blooming period of this species is almost all year long, different groups of insects such as butterflies and moths, bees and wasps (Byragi Reddy and Subba Reddi 1996) may be effective as well.

Based on literature data, the berries may be dispersed by pigeons and songbirds (Missouri Botanical Garden 2018). During the last two years, one of the authors (PLC) repeatedly observed blackbirds (*Turdus merula* Linnaeus 1758) feeding on the fruits. Hence, given the presence of birds that could facilitate its seed dispersal, the possible spread of the golden dewdrop requires careful monitoring.

Acknowledgments

This work was supported by the National Biodiversity Future Centre Project (NBFC), identification code CN00000033, CUP B73C22000790001 (Spoke 3-Biodiversity), financed under the National Recovery and Resilience Plan (NRRP).

References

Adams, C. D., 1972: Flowering plants of Jamaica. University of the West Indies, Mona, Jamaica, 848 pp.

Anonymous, 1785: Catalogus plantarum H.[orti] R.[egii] B.[otanici] M.[antuani]. Nella stamperia di Giuseppe Braglia, Mantova.

Arengo, E., 2015: *Duranta erecta* (golden dewdrop). CABI Compendium. https://doi.org/10.1079/cabicompendium.20192

Badalamenti, E., 2021: First record of *Heptapleurum arboricola* Hayata (Araliaceae) as a casual non-native woody plant in the Mediterranean area. BioInvasions Records 10(4), 805–815. https://doi.org/10.3391/bir.2021.10.4.05

Barone, G., Bajona, E., Bartolucci, F., Cancellieri, L., Caruso, G., Conti, F., Domina, G., Fascetti, S., Franzoni, J., Laface, V. L. A., Pinzani, L., Rosati, L., Scoppola, A., Stinca, A., Tilia, A., Crisafulli, A., 2023: Contribution to the floristic knowledge of Lipari and Panarea Islands (Sicilia, Italy). Italian Botanist 16, 59–71. https://doi.org/10.3897/italianbotanist.16.113415

Bazan, G., Geraci, A., Raimondo, F. M., 2005: La componente floristica dei giardini storici siciliani. Quaderni di Botanica Ambientale e Applicata 16, 93–126.

Blackburn, T. M., Delean, S., Pyšek, P., Cassey, P., 2016: The island biogeography of alien species. Global Ecology and Biogeography 25(7), 859–868. https://doi.org/10.1111/geb.12339

Buldrini, F., Mazzanti, M. B., Lim, G. M., Bosi, G., 2017: Le lettere di Antonio Bertoloni e altri botanici del territorio emiliano-romagnolo custodite nell'Autografoteca dell'Orto Botanico di Modena. Atti della Società dei Naturalisti e Matematici di Modena 148, 171–206.

Byragi Reddy, T., Subba Reddi, C., 1996: Pollination ecology of *Duranta repens* (Verbenaceae). Journal of the Bombay Natural History Society 93, 193–201.

Callaway, R. M., Ridenour, W. M., 2004: Novel weapons: invasive success and the evolution of increased competitive ability. Frontiers in Ecology and the Environment 2(8), 436–443. https://doi.org/10.1890/1540-9295(2004)002[0436:NWISAT]2.0.CO;2

Celesti-Grapow, L., Bassi, L., Brundu, G., Camarda, I., Carli, E., D'Auria, G., Del Guacchio, E., Domina, G., Ferretti, G., Foggi, B., Lazzaro, L., Mazzola, P., Peccenini, S., Pretto, F., Stinca, A., Blasi, C., 2016: Plant invasions in small Mediterranean islands: an overview. Plant Biosystems 150(5), 1119–1133. https://doi.org/10.1080/11263504.2016.1218974

Collesano, G., Fiorello, A., Pasta, S., 2021. *Strelitzia nicolaii* Regel & Körn. (Musaceae), a casual alien plant new to Europe and the Mediterranean basin. Webbia 76(1), 135–140. https://doi.org/10.36253/jopt-10183

Dacko, N. M., Reyna Nava, M., Vitek, C., Debboun, M., 2020: Chapter 7. Mosquito Surveillance. In: Debboun, M., Reyna Nava, M., Rueda, L. M., (eds.), Mosquitoes, communities, and public health in Texas, 221–247. Academic Press, San Diego (California). https://doi.org/10.1016/B978-0-12-814545-6.00007-9

Di Gristina, E., Domina, G., Barone, G., 2021: The alien vascular flora of Stromboli and Vulcano (Aeolian Islands, Italy). Italian Botanist 12, 63–75. https://doi.org/10.3897/italianbotanist.12.74033

Domina, G., Di Gristina, E., Scafidi, F., Calvo, R., Venturella, G., Gargano, M. L., 2019: The urban vascular flora of Palermo (Sicily, Italy). Plant Biosystems, 154(5), 627–634. https://doi.org/10.1080/11263504.2019.1651787

Domina, G., Mazzola, P., 2008: Flora ornamentale delle isole circumsiciliane. Quaderni di Botanica Ambientale e Applicata 19, 107–119.

Domina, G., Spallino, R. E., 2007: *Paraserianthes lophantha* (Mimosaceae) nell'isola di Pantelleria e nell'arcipelago delle isole

Eolie. Quaderni di Botanica Ambientale e Applicata 18, 303–304.

Foxcroft, L. C., Richardson, D. M., Wilson, J. R., 2008: Ornamental plants as invasive aliens: problems and solutions in Kruger National Park, South Africa. Environmental Management 41, 32–51. https://doi.org/10.1007/s00267-007-9027-9

Galasso, G., Conti, F., Peruzzi, L., Alessandrini, A., Ardenghi, N. M. G., Bacchetta, G., Banfi, E., Barberis, G., Bernardo, L., Bouvet, D., Bovio, M., Castello, M., Cecchi, L., Del Guacchio, E., Domina, G., Fascetti, S., Gallo, L., Guarino, R., Gubellini, L., Guiggi, A., Hofmann, N., Iberite, M., Jiménez-Mejías, P., Longo, D., Marchetti, D., Martini, F., Masin, R. R., Medagli, P., Musarella, C. M., Peccenini, S., Podda, L., Prosser, F., Roma-Marzio, F., Rosati, L., Santangelo, A., Scoppola, A., Selvaggi, A., Selvi, F., Soldano, A., Stinca, A., Wagensommer, R. P., Wilhalm, T., Bartolucci, F., 2024: A second update to the checklist of the vascular flora alien to Italy. Plant Biosystems, https://doi.org/10.1080/11263504.2024.2320129

Guarino, R., Chytrý, M., Attorre, F., Landucci, F., Marcenò, C., 2021: Alien plant invasions in Mediterranean habitats: an assessment for Sicily. Biological Invasions 23, 3091–3107. https://doi.org/10.1007/s10530-021-02561-0

Guarino, R., Lo Cascio, P., Mustica, C., Pasta, S., 2018: A new naturalized alien plant in Sicily: *Cotula australis* (Sieber ex Spreng.) Hook. f. (Asteraceae) on the acropolis of Lipari (Aeolian Islands). Naturalista siciliano 42(1), 125–135.

IUCN-France, 2013: Les espéces envahissantes en outre-mer. Comité Français de l'Union Internationale pour la Conservation de la Nature. Retrieved June 3, 2024 from https://especes-envahissantes-outremer.fr

Linnaeus, C., 1753: Species Plantarum, vol. 2. Holmiae [Stockholm]: impensis Laurentii Salvii. https://doi.org/10.5962/bhl.title.669

Madon, O., 1994: Un taxon nouveau pour l'Italie: *Arctotheca calendula*. Flora Mediterranea 4, 201–202.

Minissale, P., Cambria, S., Montoleone, E., Tavilla, G., Giusso del Galdo, G., Sciandrello, S., Badalamenti, E., La Mantia, T., 2023: The alien vascular flora of the Pantelleria Island National Park (Sicily Channel, Italy): new insights into the distribution of some potentially invasive species. BioInvasions Records 12(4), 861–885. https://doi.org/10.3391/bir.2023.12.4.01

Missouri Botanical Garden, 2018: Tropicos database. St. Louis, Missouri (USA), Missouri Botanical Garden. Retrieved March 10, 2024 from http://www.tropicos.org/

Moroni, P., Salomon, L., O'Leary, N., 2018: A framework for untangling Linnaean names based on Plumier's Nova plantarum americanarum genera: revised typification of *Duranta erecta*. Taxon 67(6), 1202–1208. https://doi.org/10.12705/676.19

Mulvaney, M. J., 1991: Far from the garden path: an identikit picture of woody ornamental plants invading South-Eastern Australian Bushland. PhD Thesis. Research School of Pacific Studies, Australian National University, Canberra. https://doi.org/10.25911/5d74e8610f1fb

Munir, A. A., 1995: A taxonomic revision of the genus *Duranta* L. (Verbenaceae) in Australia. Journal of the Adelaide Botanic Gardens 16, 1–16. https://www.jstor.org/stable/23874197

Pasta, S., 2003: Note su *Kleinia mandraliscae* Tin. (Asteraceae), pianta succulenta descritta come endemica delle Isole Eolie (Tirreno meridionale, Italia). Webbia 58(2), 451–457. https://doi.org/10.1080/00837792.2003.10670758

Pasta, S., 2022: Never underestimate Sicilians: some case histories dealing with narrow native ranges, deliberate introduction, claimed extinction and predictable plant invasion worldwide. Flora Mediterranea 32, 403–420. https://doi.org/10.7320/FlMedit32.403

Pasta, S., Ardenghi, N. M. G., Badalamenti, E., La Mantia, T., Livreri Console, S., Parolo, G., 2017: The alien vascular flora of Linosa (Pelagie Islands, Strait of Sicily): update and management proposals. Willdenowia 47(2), 135–144. https://doi.org/10.3372/wi.47.47205

Pasta, S., La Mantia, T., Badalamenti, E., 2014: A casual alien new to Mediterranean Europe: *Ceiba speciosa* (Malvaceae) in the suburban area of Palermo (NW Sicily, Italy). Anales del Jardín Botánico de Madrid 71(2): e010. https://doi.org/10.3989/ajbm.2387

Pasta, S., Lo Cascio, P., Allegrino, G., Viegi, L., 2008: Una xenofita naturalizzata nuova per la flora siciliana: *Salvia leucantha* Cav. a Lipari (Isole Eolie, Tirreno Meridionale). Naturalista siciliano 32(3–4), 479–481.

PIER (Pacific Islands Ecosystems at Risk), 2013: *Duranta erecta* L., Verbenaceae. 2013. Honolulu, USA: HEAR, University of Hawaii. Retrieved March 10, 2024 from http://www.hear.org/pier/species/duranta_erecta.htm

Plumier, C., 1703: Nova plantarum americanarum genera. […]. Parisiis, apud Iohannem Boudot, Regis et Regiæ Scientiarum Academiæ Typographus. https://doi.org/10.5962/bhl.title.59135

POWO, 2024: Plants of the World Online. Facilitated by the Royal Botanic Gardens, Kew. Published on the Internet. Retrieved March 10, 2024 from http://www.plantsoftheworldonline.org/

Pretto, F., Celesti-Grapow, L., Carli, E., Brundu, G., Blasi, C., 2012: Determinants of non-native plant species richness and composition across small Mediterranean islands. Biological Invasions 14, 2559-2572. https://doi.org/10.1007/s10530-012-0252-7

Raab-Straube, E. von 2022+: Verbenaceae. In: Euro+Med PlantBase - the information resource for Euro-Mediterranean plant diversity. Retrieved March 10, 2024 from https://europlusmed.org/

Raimondo, F. M., Domina, G., Spadaro, V., Aquila, G., 2005a: Prospetto delle piante avventizie e spontaneizzate in Sicilia. Quaderni di Botanica Ambientale e Applicata 15(2004), 153–164.

Raimondo, F. M., Domina, G., Spadaro, V., Aquila, G., 2005b: Aggiunte al "Prospetto delle piante avventizie e spontaneizzate della Sicilia". Quaderni di Botanica Ambientale e Applicata 16, 219–220.

Rejmánek, M., Richardson, D. M., 2013: Trees and shrubs as invasive alien species – 2013 update of the global database. Diversity and Distributions 19(8), 1093–1094. https://doi.org/10.1111/ddi.12075

Sims, J., 1815: Plate nº 1759. *Duranta Ellisia*. Pricly Duranta. Curtis's Botanical Magazine, vol. XLII.

Speciale, M., Cerasa, G., Lo Verde, G., 2015: First record in Europe of seedlings of *Ficus macrophylla* f. *columnaris* (Moraceae) and of its pollinating wasp *Pleistodontes* cf. *imperialis* (Chalcidoidea Agaonidae). Naturalista Siciliano 39(2), 399–406.

Srivastava, M., Shanker, K., 2022: *Duranta erecta* Linn.: a critical review on phytochemistry, traditional uses, pharmacology, and toxicity from phytopharmaceutical perspective. Journal of Ethnopharmacology 293, 115274. https://doi.org/10.1016/j.jep.2022.115274

Thompson, N., 2007: Poisonous plants in Australia: enabling consumers to buy safe plants. WWF-Australia: 10.

Tineo, G., 1790: Index Plantarum Horti Botanici Academiæ Regiæ Panormitanæ. Una cum Nominibus pharmaceuticis, atque vernaculis in usum Medicæ Juventutis Anno MDCCXC. Nomina vernacula ex operibus Cl. Cupani excerpta, & a nobis usque nunc detecta exhibentur. Panormi.

Tineo, G., 1799: Synopsis plantarum Horti Botanici Academiae Regiae Panormitanae anno MDCCXCIX.. Academia Regia Panormitana, Panormi.

Tineo, G., 1802: Synopsis plantarum Horti Botanici Academiae Regiae Panormitanae anno MDCCCII.. Academia Regia Panormitana, Panormi.

Tineo, V., 1855: Nuova specie di *Kleinia*. Annali di Agricoltura Siciliana 3, 315–317.

Tur, C. M., Borella, J., Hernandez Pastorini, L., 2010: Alelopatia de extratos aquosos de *Duranta repens* sobre a germinação e o crescimento inicial de *Lactuca sativa* e *Lycopersicum esculentum*. Biotemas 23(2), 13–22. https://doi.org/10.5007/2175-7925.2010v23n2p13

Ucria (da), B., 1789: Hortus Regius Panormitanus aere vulgaris anno MDCCLXXX noviter extructus septoque ex indigenis, exoticisque plerisque complectens plantas; accurante p. f. Bernardino ab Ucria S. Francisci RR. Provinciae Vallis Mazariensis [...]. Typis Regiis, Panormi.

Uludağ, A., Aksoy, N., Yazlık, A., Arslan, Z. F., Yazmış, E., Üremiş, I., Cossu, T. A., Groom, Q., Pergl, J., Pyšek, P., Brundu, G., 2017: Alien flora of Turkey: checklist, taxonomic composition and ecological attributes. NeoBiota 35, 61–85. https://doi.org/10.3897/neobiota.35.12460

van Kleunen, M., Essl, F., Pergl, J., Brundu, G., Carboni, M., Dullinger, S., Early, R., González-Moreno, P., Groom, Q. J., Hulme, P. E., Kueffer, C., Kühn, I., Máguas, C., Maurel, N., Novoa, A., Parepa, M., Pyšek, P., Seebens, H., Tanner, R., Touza, J., Verbrugge, L., Weber, E., Dawson, W., Kreft, H., Weigelt, P., Winter, M., Klonner, G., Talluto, M. V., Dehnen-Schmutz, K., 2018: The changing role of ornamental horticulture in alien plant invasions. Biological Reviews 93(3), 1421–1437. https://doi.org/10.1111/brv.12402

Wheeler J. A., 1895. A fatal case of poisoning, presumably by berries of *Duranta plumieri*. The Australasian Medical Gazette XIV, 338–339.

Witt, A., Luke, Q., 2017: Guide to the naturalized and invasive plants of Eastern Africa. CABI, Wallingford, UK. Retrieved March 10, 2024 from https://www.cabidigitallibrary.org/doi/epdf/10.1079/9781786392145.0000

Wu, S. H., Hsieh, C. F., Rejmánek, M., 2004: Catalouge of the Naturalized Flora of Taiwan. Taiwania 49(1), 16–31. https://doi.org/10.6165/tai.2004.49(1).16

Acta Bot. Croat. 84 (1), 33–43, 2025
DOI: 10.37427/botcro-2025-014

CODEN: ABCRA 25
ISSN 0365-0588
eISSN 1847-8476

Seed morphological diversity of Egyptian *Allium* L. (Amaryllidaceae) and its taxonomic significance

Iman H. Nour[1]*, Ahmed K. Osman[2], Rim S. Hamdy[3], Ibrahim A. El Garf[3]

[1] Alexandria University, Faculty of Science, Botany and Microbiology Department, 21511 Alexandria, Egypt

[2] South Valley University, Faculty of Science, Botany and Microbiology Department, 83523 Qena, Egypt

[3] Cairo University, Faculty of Science, Botany and Microbiology Department, 12613 Cairo, Egypt

Abstract – *Allium* L. (Amaryllidaceae, Allioideae, Allieae) has disputed generic delimitation and species boundaries, compounded by the proliferation of the species' synonyms. This study provides for the first time a comprehensive description of the seed morphology of native, endemic, and near-endemic species in Egypt and addresses the significance of seed traits for infrageneric classification. Twenty-two *Allium* taxa belonging to four subgenera and six sections were investigated using fresh or dry materials from their mature seeds. Thirty-eight quantitative and qualitative traits of the seeds' dorsal and ventral sides were investigated using stereomicroscopy and scanning electron microscopy (SEM). Statistical and multivariate analyses were performed. This work provides the first description of the seeds of 13 *Allium* taxa, including *A. artemisietorum* Eig & Feinbrun, *A. barthianum* Asch. & Schweinf., *A. blomfieldianum* Asch. & Schweinf., *A. crameri* Asch. & Boiss., *A. desertorum* Forssk., *A. erdelii* Zucc., *A. mareoticum* Bornm. & Gauba, *A. papillare* Boiss., *A. roseum* subsp. *tourneuxii* Boiss., *A. sativum* L., *A. sinaiticum* Boiss., *A. spathaceum* Steud. ex A.Rich., and *A. trifoliatum* Cirillo. This study reports for the first time a comparative investigation of dorsal seed surface traits against ventral traits, revealing conspicuous differences for most species and highlighting the most informative diagnostic seed traits for distinguishing taxa. *Allium* subg. *Allium* L. has a broader range of variation than any of the other subgenera.

Keywords: *Allium*, endemic and near-endemic, macro- and micromorphology, multivariate analysis, scanning electron microscope, seed, taxonomy.

Introduction

Allium L. (Amaryllidaceae, Allioideae, Allieae) has a disputed generic delimitation and species boundaries, which is compounded by the proliferation of its synonyms (Choi et al. 2012, Nour et al. 2022). It is one of the most taxonomically complex and species-rich genera, with approximately 1063 species (Sennikov and Lazkov 2023). Members of the genus exhibit high morphological diversity in their floral parts (Friesen et al. 2006). *Allium* is a bulbous plant with a short rhizome, membranous tunics, and linear leaves. Its inflorescence is a multiflowered umbel, and the floral parts are strongly withered once the capsules have matured. Capsules are trigonous and typically contain ovate to drop-shaped seeds; however, the shape of the seeds varies greatly depending on the characteristics of the capsule (Fritsch 2001). The genus is dispersed across Africa; southwestern, middle, and central Asia; Europe; and North and South America (Friesen et al. 2006, Khassanov 2018). *Allium* was classified into 15 subgenera and 67 sections using the internal transcribed spacer region (ITS) (Friesen et al. 2006). *Allium* species have a high rate of endemism, particularly with respect to the Mediterranean area, which is regarded as the main *Allium* diversity center (Brullo et al. 2019). Bedair et al. (2023) reported that *A. barthianum* Asch. & Schweinf., *A. blomfieldianum* Asch. & Schweinf., *A. mareoticum* Bornm. & Gauba and *A. trifoliatum* Cirillo are Mediterranean endemic species; these species are included in this study.

In the Flora of Egypt, El Garf (2000) recognized 20 *Allium* species, and Boulos (2009) recorded 29 *Allium* taxa (21 wild, four cultivated species, and four subspecies).

* Corresponding author e-mail: Iman.nour@alexu.edu.eg

According to the classification of Friesen et al. (2006), those taxa occupied four subgenera and six sections: *Allium* subg. *Allium* L. (*Allium* sect. *Allium* L. and *A.* sect. *Codonoprasum* Rchb.), *A.* subg. *Amerallium* Traub. (*A.* sect. *Briseis* (Salisb.) Stearn. and *A.* sect. *Molium* G.Don ex Koch.), *A.* subg. *Cepa* Radic (*A.* sect. *Cepa* L.), and *A.* subg. *Melanocrommyum* Webb et Berth. (*A.* sect. *Melanocrommyum*). *Allium crameri* Asch. & Boiss. and *A. mareoticum* are endemic to Egypt (Abdelaal et al. 2018), while *A. barthianum* and *A. blomfieldianum* are near-endemic (Bedair et al. 2023). A restricted distribution was observed for *A. artemisietorum* Eig & Feinbrun, *A. desertorum* Forssk., and *A. papillare* Boiss. (from Egypt to Jordan), *A. erdelii* Zucc. (from Northeast Libya to Syria), *A. sinaiticum* Boiss. (from Sinai, Egypt, to Northwest Saudi Arabia), and *A. spathaceum* Steud. ex A.Rich. (from East Sudan to North Somalia) (POWO 2021). Although *A. spathaceum* was recorded in the Egyptian Flora as a rare species collected earlier from Gebel Elba, in the southeastern corner of Egypt, it was included in this study (Täckholm 1974).

The taxonomic significance of the quantitative and qualitative traits of *Allium* seeds has been studied. Some studies focused on a particular region, including those in Europe. Cesmedziev and Terzijski (1997) investigated the spermoderm structures of 18 Bulgarian species of *A.* subg. *Codonoprasum*. Eight *Allium* species, following five subgenera and five sections, were examined in Poland by Bednorz et al. (2011), revealing the presence of unusually raised anticlinal walls. Moreover, sixty-two *Allium* taxa from Türkiye were classified into four subgenera, and nine sections were examined to determine the taxonomic relevance of the epidermal cell shape; sculpturing of periclinal walls; and position, shape, and undulation type of anticlinal walls (Celep et al. 2012).

Several studies were carried out on the Asian *Allium*; Lin and Tan (2017) investigated 38 species belonging to seven subgenera and 19 sections from Xinjiang, China. Baasanmunkh et al. (2020) also described 48 species from Uzbekistan, Kyrgyzstan, and Mongolia, representing seven subgenera and 24 sections. There were differences in seed size and shape, the arrangement of epidermal cells, and the different anticlinal and periclinal wall traits between the species and sections. These differences were shown in both studies. The Iranian *Allium* was examined based on 20 species classified into four subgenera and 11 sections studied by Neshati and Fritsch (2009). Veiskarami et al. (2018) investigated 23 species from two subgenera that compose the *A. ampeloprasum* L. alliance. Khorasani et al. (2020) examined thirteen species and five sections. The authors found that the most influential traits were seed shape, periclinal wall sculpture, anticlinal wall undulations, and type of verruca.

Other publications address the testa ultrastructure of 88 taxa belonging to 15 sections in *A.* subg. *Melanocrommyum* was investigated by Fritsch et al. (2006). Yusupov et al. (2022) studied 95 worldwide species belonging to 14 subgenera and 58 sections. The latter reported that the description of the periclinal wall shape and the anticlinal wall curvature could indicate the evolutionary state of a species. A new technique called unsupervised machine learning was implemented to analyze the seed coat patterns of approximately 100 species of *Allium* that have been previously described (Ariunzaya et al. 2022). The authors classified the studied taxa according to their anticlinal wall pattern: irregularly curved, irregularly curved to nearly straight, straight, S-type, U-type, U- to Ω-type, and Ω-type. The periclinal walls were also divided into five types: granule, small verrucae, large verrucae, marginal verrucae, and verrucate verrucae. Some phylogenetic studies of *Allium* correlate the morphological characteristics of seeds with the evolutionary status of each species (Choi et al. 2012, Yusupov et al. 2022).

The present study provided a detailed seed morphological description of 22 *Allium* taxa – using stereomicroscopy and scanning electron microscopy (SEM) – to provide information on the native, endemic, and near-endemic species in Egypt and address the significance of seed traits for infrageneric classification. This work provides the first description of the seeds of 13 *Allium* taxa, including *A. artemisietorum*, *A. barthianum*, *A. blomfieldianum*, *A. crameri, A. desertorum*, *A. erdelii*, *A. mareoticum*, *A. papillare*, *A. roseum* subsp. *tourneuxii* Boiss., *A. sativum* L., *A. sinaiticum*, *A. spathaceum*, and *A. trifoliatum*. Additionally, this study reports for the first time a comparative investigation of dorsal seed surface traits against ventral traits, revealing conspicuous differences for most species and highlighting the most informative diagnostic seed traits for distinguishing taxa.

Material and methods

Plant material

Twenty-two *Allium* species were investigated using fresh or dried materials from their mature seeds. The voucher specimens were deposited in two herbaria: the Cairo University Herbarium (CAI), located at the Botany Department, Faculty of Science, Cairo University, Egypt; the Agricultural Research Center Herbarium (CAIM), located at the Flora and Phytotaxonomy Research Department, Horticultural Research Institute, Cairo, Egypt; and the South Valley University Herbarium, Qena, Egypt (On-line Suppl. Tab. 1). The studied taxa were identified according to Boulos (2009). The nomenclature and synonyms used were revised according to the International Plant Names Index (IPNI 2022).

Seed macro- and micromorphology

Seeds were washed with 70% ethyl alcohol to remove dust or any attached floral parts. For the macromorphological study, the seeds were examined using an Olympus stereomicroscope supported with a 1 cm ocular micrometer and photographed to measure the following seed size parameters: length, width, length/width (L/W) ratio, area, and seed shape.

The dorsal and ventral sides of the seeds were mounted on a copper stub with double-sided tape for micromorphology. The samples were then gold-coated in a fine-coat JEOL JFC-1100E (Japan) ion sputtering device for five minutes. The seeds were investigated using a JEOL JSM-IT200 SEM (Tokyo, Japan) at the Faculty of Science, Shatebi Building, Alexandria University, Alexandria, Egypt. Thirty-seven quantitative and qualitative traits were investigated. Diagnostic quantitative characteristics were evaluated using ImageJ (1.51j8). The number of epidermal cells was counted at a magnification of 700 ×, equivalent to a field view area of 182.9 × 137.1 µm. The terminology used comes from Barthlott et al. (1981) and Yusupov et al. (2022).

Data analysis

The quantitative data were analyzed using Minitab Ltd. version 19.1 (64-bit). Descriptive statistics were calculated for each variable on both seed surfaces. Different comparisons were conducted using one-way analysis of variance (ANOVA). The P values were considered significant at < 0.05. A post hoc analysis of twenty-two taxa was conducted for each variable using Tukey's test for pairwise mean comparisons. The results are represented as letters, where means that do not share similar letters are significantly different. Furthermore, a post hoc analysis of the interaction between the seed dorsal and ventral surfaces was performed for each taxon via Tukey's test for pairwise mean comparisons. A P value of a trait less than 0.05 is represented by an asterisk (*) to indicate a significant difference between the two surfaces.

A principal component analysis (PCA) was conducted based on 26 quantitative traits for the studied taxa without any predefined groups. The eigenvalues and percent variances of 21 principal components and the character loadings of the first two axes were analyzed according to the seed morphometric characteristics. In addition, a discriminant analysis was performed to indicate the most discriminant traits for separating sections of *Allium*. Multivariate analysis was performed using Past software version 4.03 (Hammer et al. 2001).

Results

The descriptive morphometric measurements of *Allium* taxa seed traits for dorsal and ventral seed surfaces are illustrated in On-line Suppl. Tab. 2. The quantitative macromorphological characteristics of the examined seeds are summarized in On-line Suppl. Tab. 3, and the micromorphological characteristics of the seed coat are exemplified in On-line Suppl. Tab. 4. The qualitative seed morphological characteristics of the studied *Allium* taxa are described in On-line Suppl. Tab. 5. The scanning electron micrographs of the investigated samples, illustrating the whole seeds and the detailed features of testa cells, are also exemplified in Figs. 1–5.

The seeds of the examined taxa were dull, shiny, or glossy black. The seed length varied from 1.54 mm (*A. blomfieldianum*) (Fig. 2: 5A, 5D) to 3.70 mm (*A. crameri*) (Fig. 2: 7A, 7D). The narrowest seeds (0.88 mm) were observed in *A. artemisietorum* (Fig. 1: 2A, 2D), and the widest seeds (2.55 mm) were observed in *A. cepa* (Fig. 2: 6A, 6D).

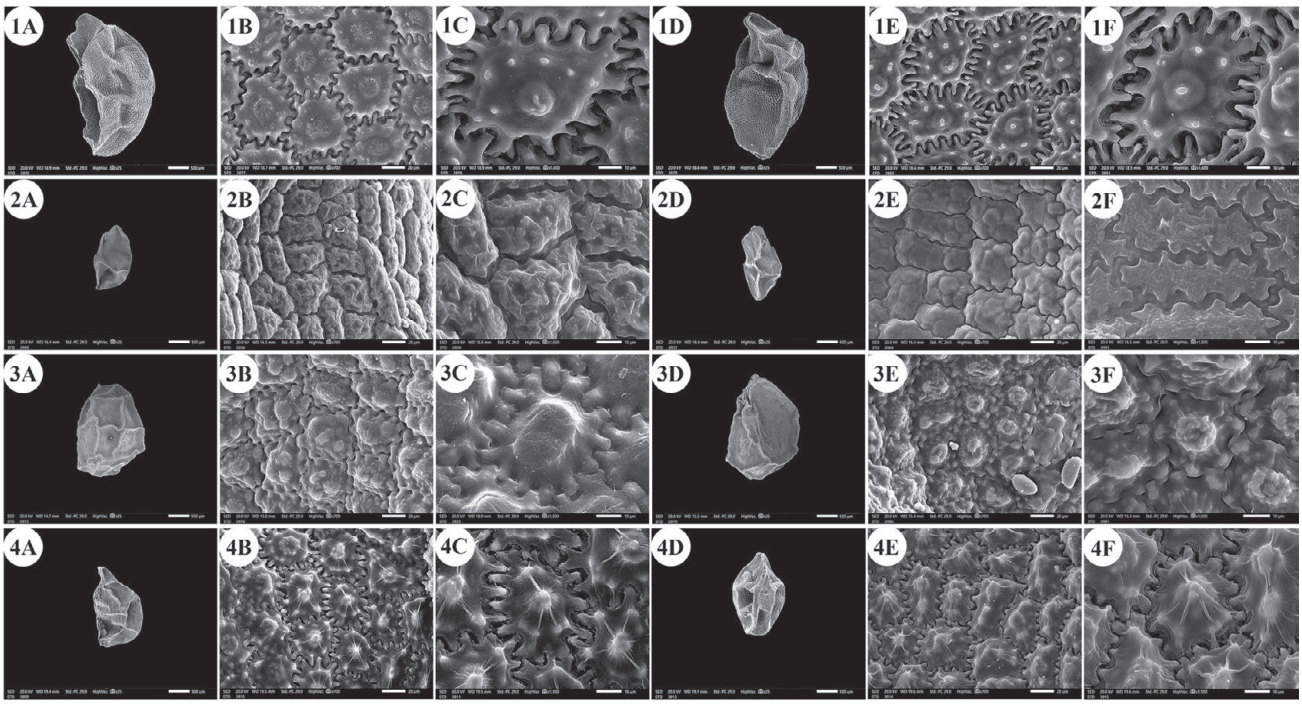

Fig. 1. Scanning electron micrographs of *Allium* seeds. A–C: dorsal surface, D–F: ventral surface. 1 – *A. ampeloprasum*, 2 – *A. artemisietorum*, 3 – *A. aschersonianum*, 4 – *A. barthianum*. Scale bars: A, D = 500 µm; B, E = 20 µm; C, F = 10 µm.

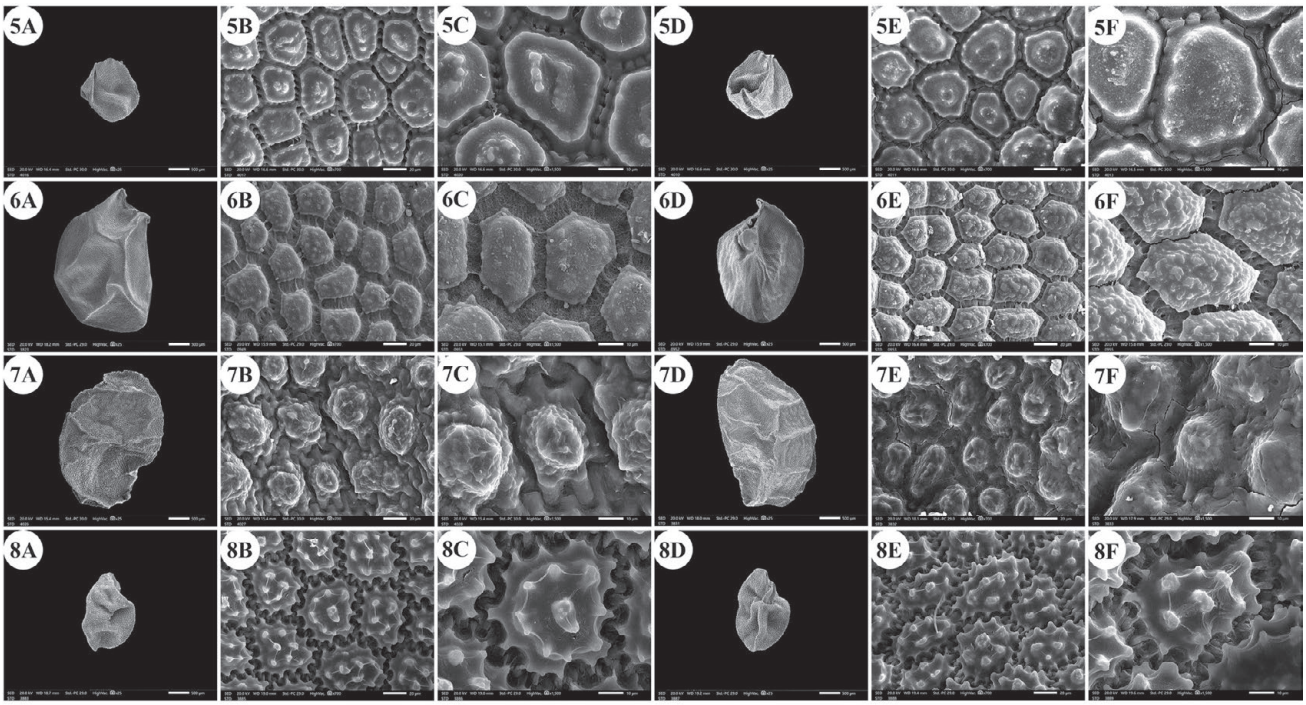

Fig. 2. Scanning electron micrographs of *Allium* seeds. A–C: dorsal surface, D–F: ventral surface. 5 – *A. blomfieldianum*, 6 – *A. cepa*, 7 – *A. crameri*, 8 – *A. curtum*. Scale bars: A, D = 500 µm; B, E = 20 µm; C, F = 10 µm.

The seed length/width ratio ranged from 1.01 in *A. blomfieldianum* to 2.40 in *A. sinaiticum* (Fig. 5: 19A, 19D). The smallest seed area (1.045 mm^2) was recorded for *A. artemisietorum*, and the highest (7.148 mm^2) was recorded for *A. crameri* (On-line Suppl. Tab. 3). The seeds were widely elliptical, elliptical, widely ovate, ovate, while some taxa had mixed shapes, widely elliptical and elliptical (On-line Suppl. Tab. 5).

The number of epidermal cells per unit area ranged from 12 to 48 cells in *A. neapolitanum* Cirillo and *A. pallens* L. (Fig. 4: 13E, 14B). Notably, the epidermal cell count at the dorsal surface was greater than that at the ventral surface (On-line Suppl. Tab. 2). The minimum epidermal cell length was recorded for *A. spathaceum* (18.54 µm) (Fig. 5: 20E, 20F), and the maximum length was 99.97 µm for *A. crameri* (Fig. 2: 7E, 7F). The lowest epidermal cell width was 21.22

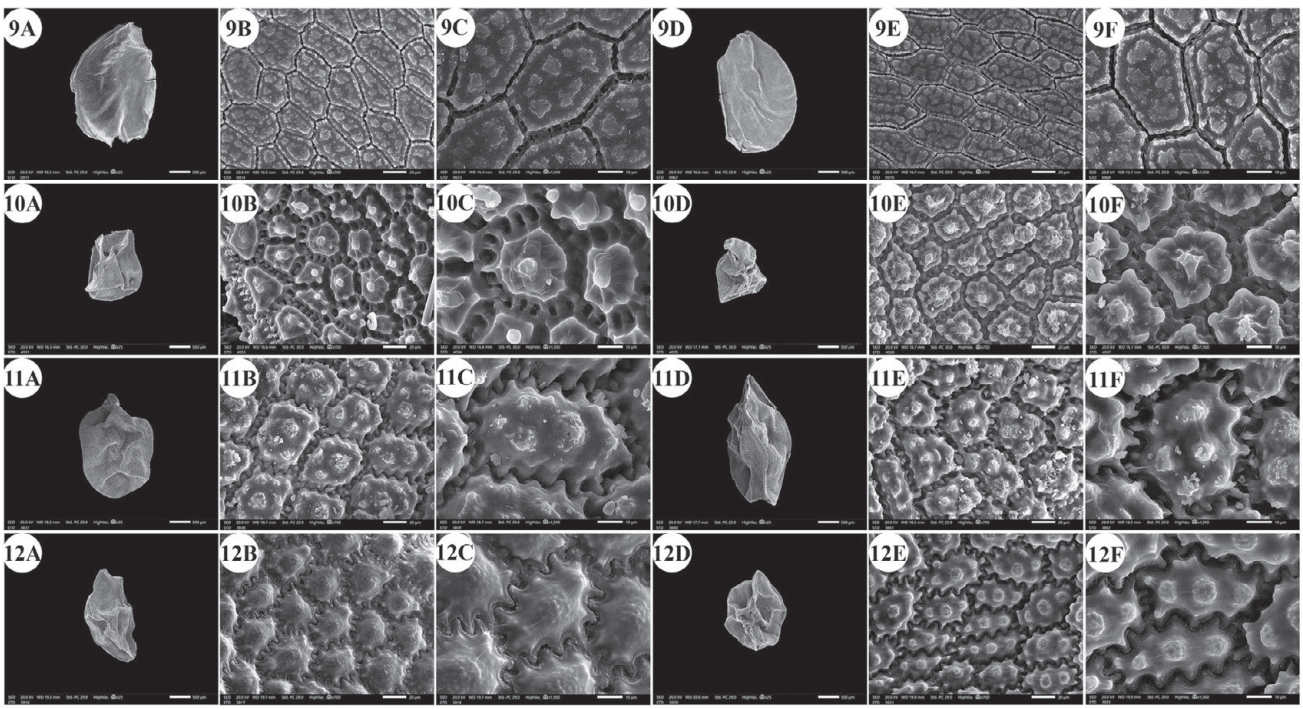

Fig. 3. Scanning electron micrographs of *Allium* seeds. A–C: dorsal surface, D–F: ventral surface. 9 – *A. desertorum*, 10 – *A. erdelii*, 11 – *A. kurrat*, 12 – *A. mareoticum*. Scale bars: A, D = 500 µm; B, E = 20 µm; C, F = 10 µm.

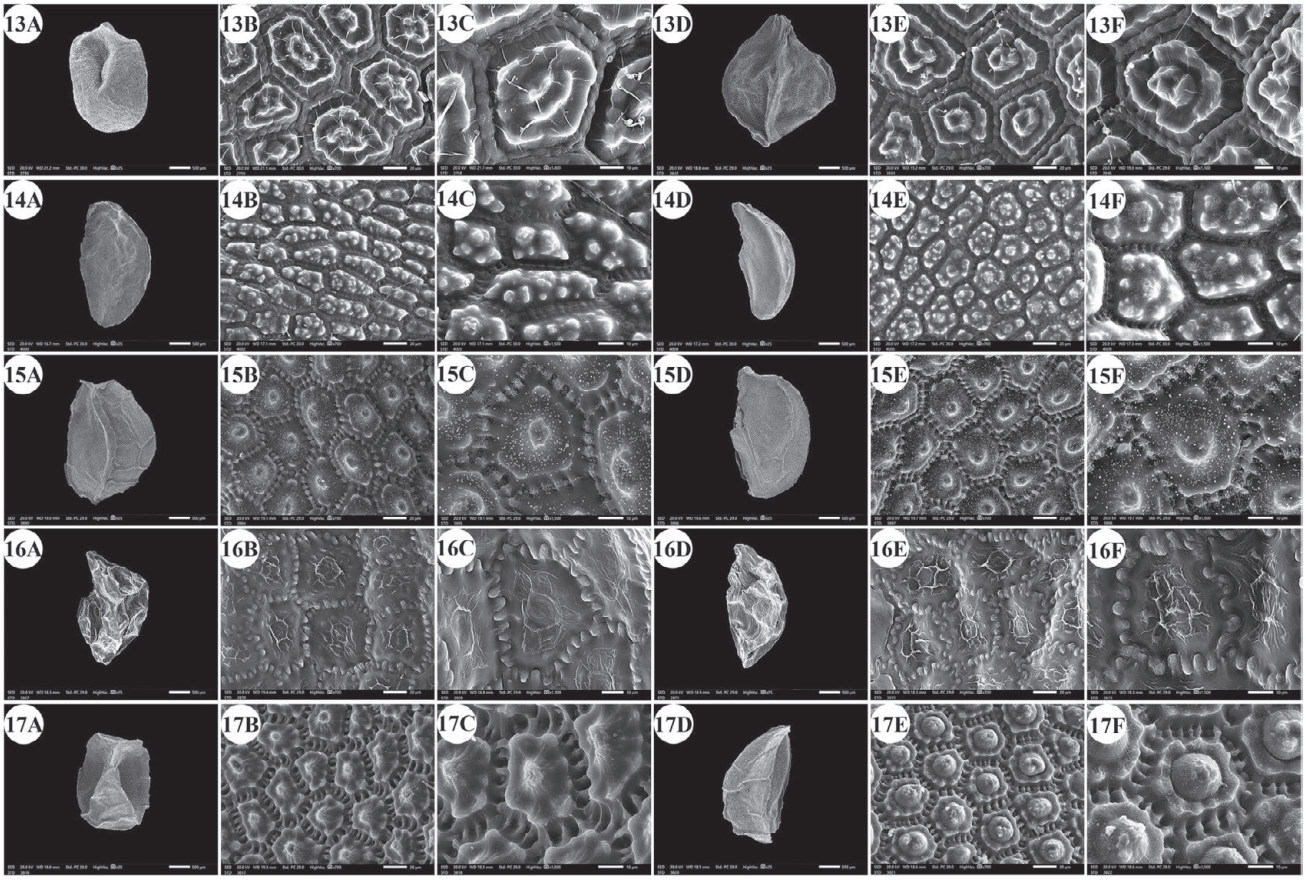

Fig. 4. Scanning electron micrographs of *Allium* seeds. A–C: dorsal surface, D–F: ventral surface. 13 – *A. neapolitanum*, 14 – *A. pallens*, 15 – *A. papillare*, 16 – *A. porrum*, 17 – *A. roseum* subsp. *tourneuxii*. Scale bars: A, D = 500 μm; B, E = 20 μm; C, F = 10 μm.

μm in *A. desertorum* (Fig. 3: 9E, 9F), and the greatest width was 97.18 μm in *A. neapolitanum* (Fig. 4: 13B, 13C). However, the epidermal cell length/width ratio varies within species, where the cell length is sometimes greater than the cell width and sometimes otherwise. This ratio ranges from 0.31 (as in *A. spathaceum*; Fig. 5: 20E, 20F) to 2.42 (as in *A. cepa*; Fig. 2: 6B, 6C). Its area ranged from 582.90 μm^2 in *A. pallens* (Fig. 4: 13B, 13C) to 5785.0 μm^2 in *A. crameri* (Fig. 2: 7E, 7F). The epidermal cell shape varied from orbicular to widely elliptic, elliptic, oblong, or polygonal with 4 to 8 edges. The cells may be arranged in a jigsaw-like pattern or side-by-side. The epidermal cells may be close to each other with no intercellular space, as in *A. neapolitanum* and *A. spathaceum* (Fig. 4: 13B and Fig. 5: 20E, respectively), or distant where the intercellular space length may reach up to 13.45 μm, as in *A. cepa* (Fig. 2: 6B, On-line Suppl. Tab. 4).

The anticlinal wall (AW) may be straight, irregularly curved, or undulating with various forms of undulation elements, such as S-type, U-type, or Ω-type (Omega-type) (On-line Suppl. Tab. 5). The count of undulation elements per cell varied from 8 (*A. crameri*) (Fig. 2: 7B, 7C) to 33 (as in *A. pallens*; Fig. 4: 13B, 13C). The length of the undulation elements fluctuates from 1.29 μm (as in *A. artemisietorum*; Fig. 1: 2B, 2C) to 14.35 μm (as in *A. crameri*) (Fig. 2: 7B, 7C), and the width ranges from 1.99 μm (as in *A. trifoliatum*; Fig. 5: 22E, 22F) to 11.20 μm (as in *A. crameri*; Fig. 2: 7B, 7C). The L/W ratio of the undulation elements ranged from 0.40 (as in *A. spathaceum*; Fig. 5: 20B, 20C) to 2.60 (as in *A. barthianum*; Fig. 1: 4B, 4C). The distance between each of the two undulation elements varied from 0.58 μm in *A. spathaceum* (Fig. 5: 20E, 20F) to 17.58 μm in *A. crameri* (Fig. 2: 7E, 7F) (On-line Suppl. Tab. 4). The cell boundaries were channeled in most taxa or raised in *A. neapolitanum* (Fig. 4: 13C, 13F) and *A. papillare* (Fig. 4: 15C, 15F). The relief of the intercellular space or cell boundary was scabrate (*A. artemisietorum*; Fig. 1: 2C, 2F), *A. erdelii*, *A. porrum* L., *A. roseum* subsp. *tourneuxii*, *A. pallens*, *A. papillare*, *A. spathaceum*, and members of *A.* subg. *Melanocrommyum*), striate (*A. neapolitanum*; Fig. 4: 13C, 13F), reticulate with a broad mesh of connecting threads (*A. cepa*; Fig. 2: 6C, 6F, and *A. sativum*; Fig. 5: 18C, 18F), or with a narrow mesh of thin connecting threads in the remaining species. The curvature of the periclinal wall is generally convex, except for that of *A. desertorum,* which was flat (Fig. 3: 9C, 9F), and that of *A. porrum*, which was flat and concave toward the center (Fig. 4: 16C, 16F). All the studied taxa had verrucate periclinal walls, while verrucae were absent for *A. artemisietorum* (Fig. 1: 2C, 2F), *A. papillare* (Fig. 4: 15C, 15F), and *A. porrum* (Fig. 4: 16C, 16F). *Allium artemisietorum* and *A. papillare* have densely granulated periclinal walls (On-line Suppl. Tab. 5).

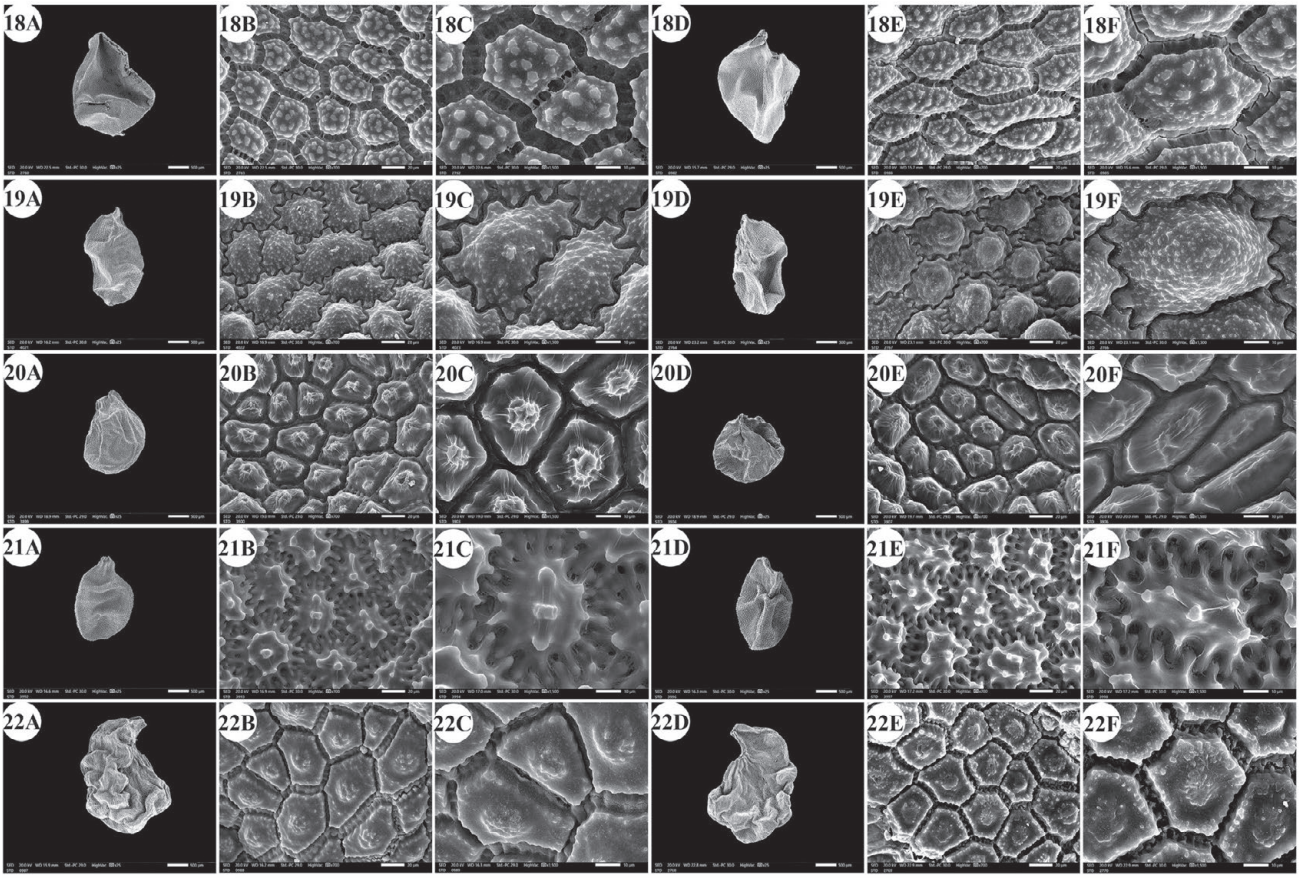

Fig. 5. Scanning electron micrographs of *Allium* seeds. A–C: dorsal surface, D–F: ventral surface. 18 – *A. sativum*, 19 – *A. sinaiticum*, 20 – *A. spathaceum*, 21 – *A. sphaerocephalon*, 22 – *A. trifoliatum*. Scale bars: A, D = 500 μm; B, E = 20 μm; C, F = 10 μm.

Data analysis

One-way ANOVA, which was utilized to test the variation between the dorsal and ventral seed surfaces, revealed a significant difference in the epidermal cell count for most taxa except *A.* subg. *Cepa* (*A. cepa*) and *A.* subg. *Melanocrommyum* (*A. aschersonianum* Barbey and *A. crameri*) showed a non-significant difference between the surfaces. The distance between two undulation elements showed non-significant variation for both surfaces of the studied taxa, except for *A. artemisietorum* and *A. roseum* subsp. *tourneuxii*. The highest number of traits showing significant differences between the two surfaces was recorded in *A. erdelii*; these traits included epidermal cell count per unit area, epidermal cell length, width, the L/W ratio, undulation element width, and the L/W ratio. In contrast, *A. cepa* demonstrated insignificant variation between the two surfaces except in the epidermal cell area (On-line Suppl. Tab. 4).

One-way ANOVA was used to assess the significant differences in the variation among taxa. For *A.* sect. *Allium*, the studied traits were significant for each pair of taxa; however, the epidermal cell L/W ratio (dorsal surface) was insignificant for all taxa. The two species of *A.* sect. *Codonoprasum* are very different in terms of the number of epidermal cells per unit area, the length of epidermal cells (dorsal surface), the number of undulation elements per cell, the width of undulation elements, and the L/W ratio of undulation elements. There were also non-significant differences in the following traits among the members of *A.* sect. *Molium*: epidermal cell length, epidermal cell width (ventral surface), epidermal cell L/W ratio, epidermal cell area (ventral surface), undulation element length, and distance between two undulation elements (ventral surface). The other traits exhibited significant variation between each pair of species. The two species comprising *A.* sect. *Melanocrommyum* were significantly different in the following traits: seed length and area, undulation element length (dorsal surface), undulation element width, undulation element L/W ratio (ventral surface), and the distance between two undulation elements (dorsal surface) (On-line Suppl. Tab. 4).

PCA explained 99.96% of the total variation in the first two components (Fig. 6, On-line Suppl. Tab. 6).

The first component exhibited 87.90% of the total variation. This component separates some species of *A.* sect. *Allium* (*A. ampeloprasum*, *A. curtum* Boiss. & Gaill., *A. kurrat* Schweinf. ex K.Krause, *A. porrum*, *A. sinaiticum*, and *A. sphaerocephalon* L.); *A. crameri* of *A.* sect. *Melanocrommym*; and *A.* sect. *Molium* (*A. blomfieldianum* and *A. neapolitanum*) in the right side from the other taxa of *A.* sect. *Allium* (*A. artemisietorum*, *A. barthianum*, *A. mareoticum*, and *A. sativum*); *A.* sect. *Briseis* (*A. spathaceum*); *A.* sect. *Cepa* (*A. cepa*); *A.* sect. *Codonoprasum* (*A. desertorum* and *A. pallens*); *A. aschersonianum* of *A.* sect. *Melanocrommym*; and *A. erdelii*, *A. papillare*, *A. roseum* subsp. *tourneuxii*; and *A. trifoliatum* of *A.* sect. *Molium*. Species on the right side were

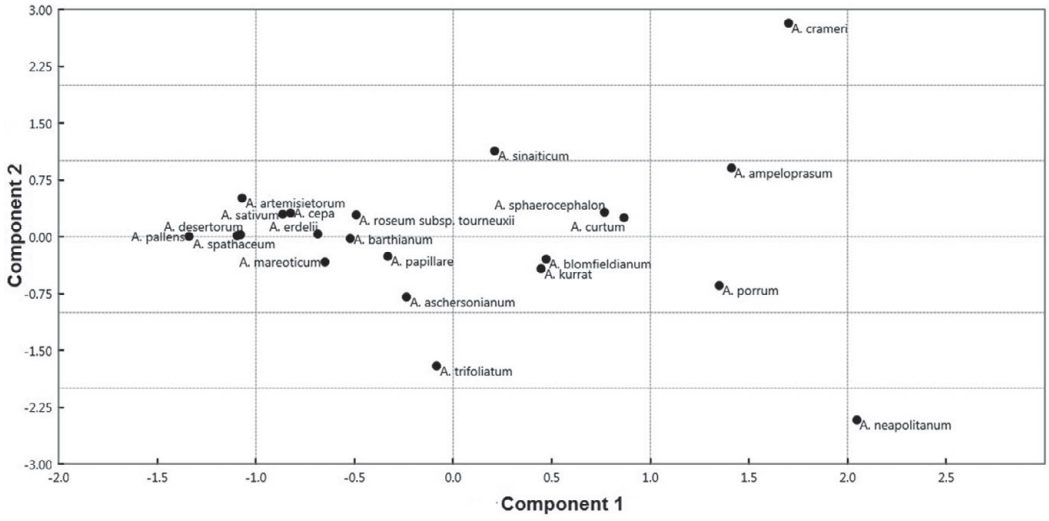

Fig. 6. Scatterplot of the first two axes from principal component analysis (PCA) of the 22 *Allium* taxa based on analyzed seed morphological traits.

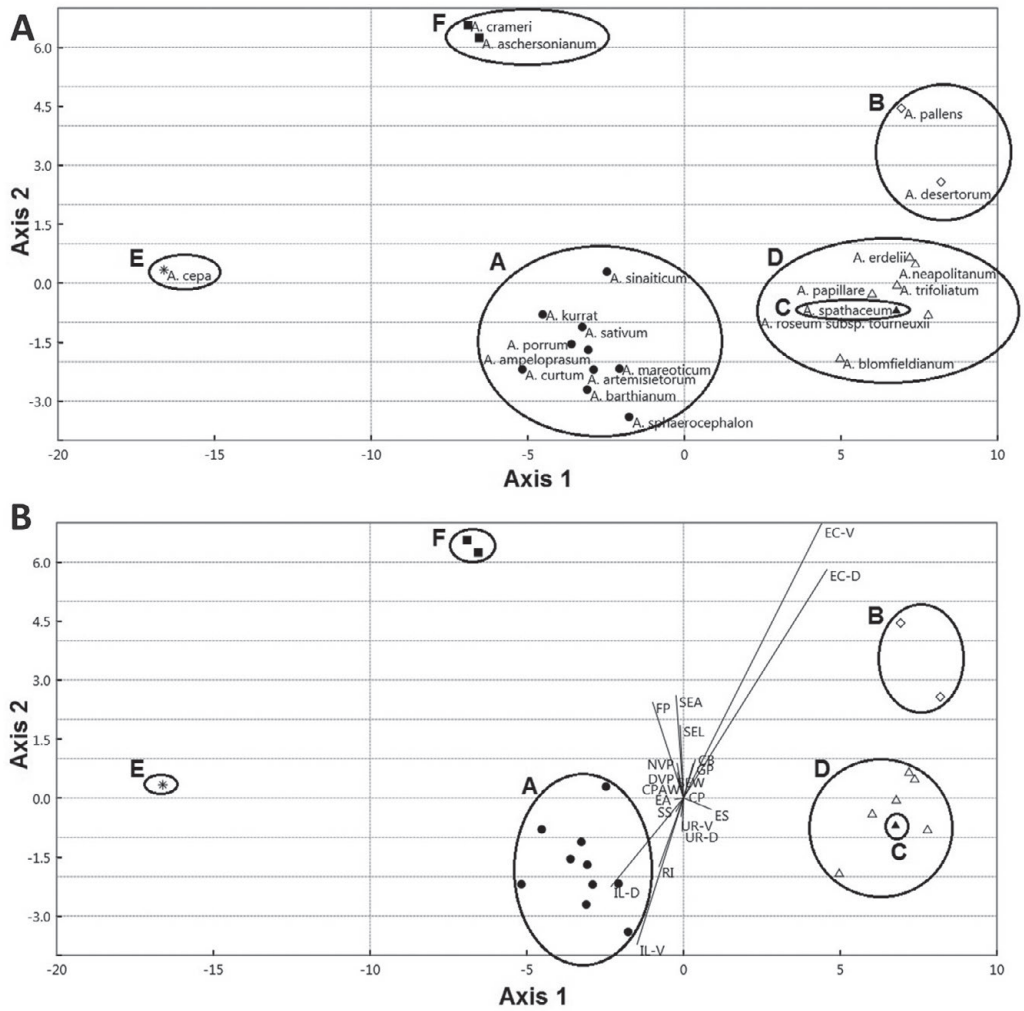

Fig. 7. Scatterplot (A) and biplot (B) of the first two axes from Discriminant Analysis for the sectional classification of *Allium*. A – *A.* sect. *Allium*, B – *A.* sect. *Codonoprasum*, C – *A.* sect. *Briseis*, D – *A.* sect. *Molium*, E – *A.* sect. *Cepa*, F – *A.* sect. *Melanocrommyum*. Abbreviations: SEL – seed length, SEW – seed width, SEA – seed area, EC-D – epidermal cell count/unit area (dorsal), EC-V – epidermal cell count/unit area (ventral), IL-D – intercellular space length (dorsal), IL-V – intercellular space length (ventral), UR-D – undulation element L/W ratio (dorsal), UR-V – undulation element L/W ratio (ventral), SS – seed shape, ES – epidermal cell shape, EA – epidermal cell arrangement, CPAW – curvature pattern of the anticlinal wall, CB – cell boundary, RI – relief of intercellular space (cell boundary), CP – curvature of the periclinal wall (PW), FP – fine relief of the PW, DVP – diameter of verrucae on PW, NVP – number of verruca on PW, GP – P/A of granules on PW.

characterized by larger epidermal cell area ranging from 2013.37 to 3821.03 mm^2, whereas the left side taxa have smaller values ranging from 880.10 to 1557.04 mm^2. The contribution of the individual measured traits to the first and second components are illustrated in On-line Suppl. Tab. 7. The discriminant analysis results showed that six sections of *Allium* were successfully identified. Twenty seed traits represent the most important variables in discriminating the studied taxa (Fig. 7A and 7B). These characteristics are used to perform an artificial key for 22 *Allium* taxa.

Artificial key of *Allium* taxa based on the most significant seed quantitative traits and qualitative macro- and micromorphological traits

1. a. The epidermal cell arrangement is a jigsaw-like pattern **2**

b. The epidermal cell arrangement is a side-by-side pattern **12**

2. a. The undulation pattern of the anticlinal wall is Ω-type **3**

b. The undulation pattern of the anticlinal wall is otherwise **5**

3. a. The seed length is 3.4–3.7 mm, and the seed area is 6.08–7.14 mm^2..... ***A. crameri***

b. The seed length is 1.95–2.76 mm, and the seed area is 1.81–4.81 mm^2 ..... **4**

4. a. The intercellular space length is 0.23–0.93 µm, and the periclinal wall is sparsely granulated ..... ***A. aschersonianum***

b. The intercellular space length is 2.04–5.99 µm, and the periclinal wall has no granules ..... ***A. curtum***

5. a. The undulation pattern of the anticlinal wall is S-type undulation ..... ***A. artemisietorum***

b. The undulation pattern of the anticlinal wall is U-type undulation **6**

6. a. Polygonal epidermal cells, and the curvature of the periclinal wall is flat and centrally concave without verrucae ..... ***A. porrum***

b. Orbicular, widely elliptic, or elliptic epidermal cells, and the curvature of the periclinal wall is convex with verrucae **7**

7. a. Ovate seed shape, the seed length is 3.4–3.58 mm, the seed width is 1.99–2.3 mm, and the seed area is 4.84–5.63 mm^2 ..... ***A. ampeloprasum***

b. Widely elliptic or elliptic seed shape: the seed length is 1.7–3.0 mm, the seed width is 0.88–1.83 mm, and the seed area is 1.10–3.58 mm^2 ..... **8**

8. a. The seed length is 2.49–3.0 mm, the seed width is 1.55–1.83 mm, and the seed area is 3.16–3.58 mm^2..... ***A. kurrat***

b. The seed length is 1.76–2.10 mm, the seed width is 0.88–1.44 mm, and the seed area is 1.10–2.32 mm^2..... **9**

9. a. The epidermal cell count per unit area is 30–31 cells ..... ***A. mareoticum***

b. The epidermal cell count per unit area is 17–27 cells **10**

10. a. The number of periclinal wall verrucae is ≤ 15 ..... ***A. sphaerocephalon***

b. The number of periclinal wall verrucae is > 15 ..... **11**

11. a. The intercellular space length is 3.4–8.92 µm, and the undulation element L/W ratio is 1.1–2.60 ..... ***A. barthianum***

b. The intercellular space length is 1.24–2.05 µm, and the undulation element L/W ratio is 0.8–0.99 ..... ***A. sinaiticum***

12. a. The anticlinal wall is straight to irregularly curved **13**

b. The anticlinal wall is undulated **15**

13. a. The relief of the intercellular space is a narrow mesh of thin connecting threads, the epidermal cell count per unit area is 33–35 cells, the intercellular space length is 1.75–2.78 µm, and the periclinal wall is non-granulated ..... ***A. desertorum***

b. The relief of the intercellular space is reticulate with a broad mesh of connecting threads, the epidermal cell count per unit area is 21–28 cells, the intercellular space length is 5.94–13.4 µm, and the periclinal wall is granulated **14**

14. a. The seed area is 4.2–6.09 mm^2..... ***A. cepa***

b. The seed area is 3.2–3.3 mm^2..... ***A. sativum***

15. a. The undulation pattern of the anticlinal wall is U-type **16**

b. The undulation pattern of the anticlinal wall is S-type **18**

16. a. Raised cell boundary, and the periclinal wall is without verrucae ..... ***A. papillare***

b. Channeled cell boundary, and verrucate periclinal wall **17**

17. a. The seed length is 1.56–1.64 mm, the seed area is 1.25–1.75 mm^2, the epidermal cell count per unit area is 32–35 cells, and the periclinal wall has one large central dome ..... ***A. erdelii***

b. The seed length is 2.24–2.45 mm, the seed area is 2.62–3.37 mm^2, the epidermal cell count per unit area is 23–24 cells, and the periclinal wall has one small central dome ..... ***A. roseum* subsp. *tourneuxii***

18 a. The epidermal cells are close to each other (intercellular space is absent) **19**

b. The epidermal cells are distant from each other (intercellular space is present) **20**

19. a. Raised striate relief of cell boundary, the seed length is 2.61–3.16 mm, seed width is 1.77–2.54 mm, seed area is 3.84–5.36 mm^2, and the epidermal cell count per unit area is 12–14 cells ..... ***A. neapolitanum***

b. Channeled scabrate relief of cell boundary, the seed length is 1.84–1.99 mm, seed width is 1.42–1.48 mm, seed

area is 2.08–2.15 mm^2, and the epidermal cell count per unit area is 33–34 cells ..... ***A. spathaceum***

20. a. The seed length is 1.54–1.77 mm, and the seed area is 1.48–2.03 mm^2..... ***A. blomfieldianum***

b. The seed length is 2.56–3.16 mm, and the seed area is 2.72–4.14 mm^2..... **21**

21. a. Ovate seed shape, the epidermal cell count per unit area is 43–44 cells, the undulation element L/W ratio is 0.72–0.95, and the periclinal wall has many small domes ... . ***A. pallens***

b. Elliptic seed shape, the epidermal cell count per unit area is 27–28 cells, the undulation element L/W ratio is 1.23–1.47, and the periclinal wall has one small central dome ..... ***A. trifoliatum***

Discussion

A high degree of seed morphological diversity has been observed in the genus *Allium*, as scanning electron microscopy (SEM) can clearly illustrate the details of the seed testa (Neshati and Fritsch 2009, Bednorz et al. 2011, Celep et al. 2012, Veiskarami et al. 2018, Baasanmunkh et al. 2020, Khorasani et al. 2020, Yusupov et al. 2022). Yusupov et al. (2022) noted that Kruse (1988) reported the inter- and intraspecific variation of *Allium*, indicating that some seed testa traits are section- and species specific. Our results follow the latter seed morphological studies, indicating the most informative diagnostic traits for distinguishing *Allium* taxa at the species level. Discriminant analysis is a very informative method for evaluating the utility and importance of the studied morphological traits by determining which traits were most useful for maximizing differentiation between the studied groups (Temunović et al. 2024). These traits are summarized as seed length, width, area, and shape, epidermal cell count/unit area, intercellular space length, undulation element L/W ratio, epidermal cell shape and arrangement, curvature pattern of the anticlinal wall, cell boundary, relief of intercellular space, curvature and fine relief of the periclinal wall, diameter and number of verrucae on PW, and the presence/absence of granules on the periclinal wall.

Fritsch et al. (2006) recognized that S-like, U-like, and Ω-like are the most common anticlinal wall undulation modes and, the present study revealed the same types of undulations. A limited amount of variation in the different parts of a single seed surface was observed also by Fritsch et al. (2006); this variation was restricted to the presence or absence of granules on the periclinal wall of epidermal cells and their size. This study reported for the first time a detailed comparative investigation of the quantitative traits of dorsal and ventral seed surfaces. The variation between the dorsal and ventral seed surfaces exhibited a conspicuous difference for 19 out of 22 species in terms of epidermal cell count/unit area. Additionally, there was significant variation in undulation element width (seven species); the epidermal cell L/W ratio; the area; the count of undulation elements per cell (six species); undulation element length and the undulation element L/W ratio (five species); epidermal cell length, width, and intercellular space length (four species); and the distance between two undulation elements (two species).

Fritsch (2001) described the seed sizes of the different subgenera but reported numerous exceptions: *A.* subg. *Allium* is roughly light-grained; *A.* subg. *Melanocrommyum* is heavy-grained, whereas *A.* subg. *Amerallium* ranges from small to large-grained. In the present study, the seed size of *A.* subg. *Allium* is 1.61–3.59 × 0.89–2.30 mm, *A.* subg. *Amerallium* is 1.54–3.47 × 1.21–2.55 mm, *A.* subg. *Cepa* is 2.54–3.26 × 1.98–2.55 mm, and *A.* subg. *Melanocrommyum* is 1.95–3.70 × 1.34–2.40 mm.

Our observations revealed that the epidermal cell shape was not different in *A.* subg. *Amerallium* to that in other subgenera. This study agrees with the findings of Yusupov et al. (2022): the seeds are broad to narrowly ovoid, and the anticlinal wall undulation type is mostly straight to arched. Species of *A.* sect. *Molium*, on the other hand, are arched to the S-type. Yusupov et al. (2022) mentioned that Kruse (1988) described *A.* sect. *Molium* as having wide, depressed channel-like anticlinal walls and prominent verrucose structures on their periclinal walls. However, the present study revealed that two out of five species had raised walls: *A. neapolitanum* and *A. papillare*. Celep et al. (2012) measured the seed size of *A.* subg. *Amerallium* to be in the range of 2.5–3.90 × 1.0–1.86 mm, and the seed L/W is 2.10–2.64. Our results differ slightly for the seed minimum length, which is 1.54–3.47 × 1.21–2.54 mm, 1.01–1.99. The smallest seed length in the subgenus was detected for *A. blomfieldianum* (1.54–1.77 × 1.21–1.59 mm), and the widest seed was *A. neapolitanum* (2.61–3.16 × 1.77–2.54 mm). They also reported that Meikle (1985) performed similar measurements for *A. neapolitanum*. The latter researchers also reported that *A.* sect. *Molium* shares a polyhedral cell with a striate or rugulate intercellular region covered by many small verrucae coalescing to a marginal ledge and with mostly one verruca in the center of the periclinal wall. This finding is compatible with our description, as the relief of the cell boundary was striate in *A. neapolitanum*, scabrate in *A. erdelii* and *A. papillare*, or had a narrow mesh of thin connecting threads in *A. blomfieldianum* and *A. trifoliatum*.

According to Fritsch et al. (2006), the epidermal cells of *A.* subg. *Melanocrommyum* demonstrated less variation than the other subgenera. The latter authors reported similar results for members of *A.* sect. *Melanocrommyum* because they had anticlinal walls that were Ω-like undulations and convex periclinal walls with verrucate sculptures. Some species have agranulous periclinal walls, while others, such as *A. aschersonianum*, do not have any granules. In addition, Celep et al. (2012) revealed that periclinal walls contain several or more verrucae.

The multivariate analyses revealed that members of *A.* subg. *Allium* have a wide range of variation characterizing the subgenus. This finding is congruent with the finding of

Fritsch (2001) that *A*. subg. *Allium* is the most diverse and rich subgenus of the genus *Allium*. Minor dissimilarities in epidermal cell arrangement were observed between the members. Although the seed shape and the anticlinal and periclinal walls of the members of *A*. sect. *Allium* were variously undulated, these results are consistent with those of Neshati and Fritsch (2009), Veiskarami et al. (2018), and Baasanmunkh et al. (2020). Bednorz et al. (2011) revealed the presence of unusually raised anticlinal walls in some species of *A*. sect. *Allium*. In contrast, a channeled pattern was observed for the investigated members of *A*. sect. *Allium*.

Allium ampeloprasum is a polymorphic species complex sometimes treated as a wild leek without considering any subspecies, and sometimes as a cultivated leek with subspecies or varieties (Dey and Khaled 2013, Guenaoui et al. 2013). In the present study, *A. ampleoprasum* was treated as a wild accession, while *A. kurrat* and *A. porrum* were recorded as cultivated culinary species; this follows Boulos's (2009) work on the Egyptian flora. *Allium kurrat* and *A. porrum* have not been observed naturalizing in other habitats far from their cultivation fields (Mifsud and Mifsud 2018). *Allium ampeloprasum*, *A. kurrat*, and *A. porrum* exhibited significant differences between pairs of species in terms of seed length, L/W ratio, area, epidermal cell count per unit area, intercellular space length (dorsal surface), undulation element length and width, the L/W ratio, and the distance between two undulation elements (dorsal surface). Moreover, there were non-significant differences in the following traits: seed width, epidermal cell size parameters, intercellular space length (ventral surface), count of undulation elements per cell, and distance between two undulation elements (ventral surface). The epidermal cells of the three species exhibit a jigsaw-like arrangement, and the anticlinal walls exhibit a U-type undulation mode with channeled cell boundaries. *Allium ampeloprasum* and *A. kurrat* share many characteristics, but the latter species has more verrucae (>15) on the periclinal walls. *Allium porrum* was distinguished from the other two species by its variably polygonal epidermal cells with 5 to 7 edges; the periclinal wall is peripherally flat, centrally concave, and wrinkled but lacking verrucae. The description of *A. porrum* is well matched with that of Lin and Tan (2017).

Conclusions

The present study carried out a detailed seed macro- and micromorphological investigation of 22 *Allium* taxa, including 11 species that are described for the first time; six of them are endemic species: *A. barthianum*, *A. blomfieldianum*, *A. mareoticum*, *A. trifoliatum* (Mediterranean endemic species), *A. crameri* and *A. mareoticum* (endemic to Egypt). Our results highlighted the most informative diagnostic traits for distinguishing *Allium* taxa. These traits are summarized as seed length, width, area, and shape, epidermal cell count/unit area, intercellular space length, undulation element L/W ratio, epidermal cell shape and arrangement, curvature pattern of the anticlinal wall, cell boundary, relief of intercellular space, curvature and fine relief of the periclinal wall, diameter and number of verrucae on PW, and the presence/absence of granules on the periclinal wall. The count of undulation elements per cell, the undulation element length and width, the L/W ratio, and the distance between two adjacent undulation elements were measured for the first time in this study. This study reported for the first time a detailed comparative investigation of the quantitative traits of dorsal and ventral seed surfaces. Dorsal and ventral seed surface variations exhibited conspicuous differences in most species. Multivariate analysis revealed that members of *A*. subg. *Allium* have a wide range of variation characterizing the subgenus. *Allium* subg. *Allium* is the most diverse and rich subgenus of the genus. *Allium ampleoprasum* is treated as a wild accession, while *A. kurrat* and *A. porrum* are recorded as cultivated culinary species in the Egyptian flora because they have not been observed naturalizing in other habitats far from their cultivation fields. *Allium ampeloprasum*, *A. kurrat*, and *A. porrum* exhibited significant differences between pairs of species; as a result, they are treated herein as distinct species. Additional regional studies should be conducted on the seeds of native, endemic, and near-endemic *Allium* taxa for the better understanding of the variation within the genus. Finally, *Allium* merits being subjected to integrated investigations through different approaches to resolve the taxonomic problems of the genus.

References

Abdelaal, M., Fois, M., Fenu, G., Bacchetta, G., 2018: Critical checklist of the endemic vascular plants of Egypt. Phytotaxa 360(1), 19–34. https://doi.org/10.11646/phytotaxa.360.1.2

Ariunzaya, G., Baasanmunkh, S., Choi, H. J., Kavalan, J. C. L., Chung, S., 2022: A multi-considered seed coat pattern classification of *Allium* L. using unsupervised machine learning. Plants 11(22), 1–19. https://doi.org/10.3390/plants11223097

Baasanmunkh, S., Lee, J. K., Jang, J. E., Park, M. S., Friesen, N., Chung, S., Choi, H. J., 2020: Seed morphology of *Allium* L. (Amaryllidaceae) from central Asian countries and its taxonomic implications. Plants 9(9), 1–21. https://doi.org/10.3390/plants9091239

Barthlott, W., 1981: Epidermal and seed surface characters of plants: systematic applicability and some evolutionary aspects.: Nordic Journal of Botany 1(3), 345–355. https://doi.org/10.1111/j.1756-1051.1981.tb00704.x

Bedair, H., Shaltout, K., Halmy, M. W. A., 2023: A critical inventory of the Mediterranean endemics in the Egyptian flora. Biodiversity and Conservation 32(4), 1327–1351. https://doi.org/10.1007/s10531-023-02555-5

Bednorz, L., Krzymińska, A., Czarna, A., 2011: Seed morphology and testa sculptures of some *Allium* L. species (Alliaceae). Acta Agrobotanica 64 (2), 33–38.

Boulos, L., 2009: Flora of Egypt Checklist, Revised Annotated Edition. Al Hadara, Cairo.

Brullo, S., Brullo, C., Cambria, S., del Galdo, G. G., Salmeri, C., 2019: *Allium albanicum* (Amaryllidaceae), a new species from Balkans and its relationships with *A. meteoricum* Heldr. & Hausskn. ex Halácsy. PhytoKeys 119, 117–136. https://doi.org/10.3897/phytokeys.119.30790

Celep, F., Koyuncu, M., Fritsch, R. M., Kahraman, A., Dogan, M., 2012: Taxonomic importance of seed morphology in *Al-*

lium (Amaryllidaceae). Systematic Botany 37(4), 893–912. https://doi.org/10.1600/036364412X656563

Cesmedziev, I., Terzijski, D., 1997: A scanning electron microscopic study of the spermoderm in *Allium* subg. *Codonoprasum* (Alliaceae). Bocconea 5, 755–758.

Choi, H. J., Giussani, L. M., Jang, C. G., Oh, B. U., Cota-Sánchez, J. H., 2012: Systematics of disjunct northeastern Asian and northern north American *Allium* (Amaryllidaceae). Botany 90(6), 1–18. https://doi.org/10.1139/b2012-031

Dey, P., Khaled, K. L., 2013: An extensive review on *Allium ampeloprasum* a magical herb. International Journal of Science and Research 4(7), 371–377.

Friesen, N., Fritsch, R. M. R., Blattner, F. F. R., 2006: Phylogeny and new intrageneric classification of *Allium* (Alliaceae) based on nuclear ribosomal DNA ITS sequences. Aliso 22(1), 372–395. https://doi.org/10.5642/aliso.20062201.31

Fritsch, R. M., 2001: Taxonomy of the genus *Allium* L. Contribution from IPK Gatersleben. Herbertia 56(2), 19–50.

Fritsch, R. M., Kruse, J., Adler, K., Rutten, T., 2006: Testa sculptures in *Allium* L. subg. *Melanocrommyum* (Webb & Berth.) Rouy (Alliaceae). Feddes Repertorium 117(3–4), 250–263. https://doi.org/10.1002/fedr.200611094

El Garf, I. A., 2000: Alliaceae in the flora of Egypt 1. Systematic revision of the indigenous species of *Allium* L. Taeckholmia 20(2), 181–194.

Guenaoui, C., Mang, S., Figliuolo, G., Neffati, M., 2013: Diversity in *Allium ampeloprasum*: from small and wild to large and cultivated. Genetic Resources and Crop Evolution 60, 97–114. https://doi.org/10.1007/s10722-012-9819-5

Hammer, Ø., Harper, D. A. T., Ryan, P. D., 2001: Past: paleontological statistics software package for education and data analysis. Palaeontologia Electronica 4(1), 1–9.

IPNI, 2022: International Plant Names Index., The Royal Botanic Gardens, Kew, Harvard University Herbaria & Libraries and Australian National Botanic Gardens. Retrieved March 1, 2023 from http://www.ipni.org

Khassanov, F. O., 2018: Taxonomical and Ethnobotanical Aspects of *Allium* Species from Middle Asia with Particular Reference to Subgenus *Allium*. In: Shigyo, M., Khar, A., Abdelrahman, M. (eds.), The *Allium* genomes, 230. Springer, Switzerland.

Khorasani, M., Mehrvarz, S. S., Zarre, S., 2020: Seed morphology and testa ultrastructure in *Allium stipitatum* complex (Amaryllidaceae; Allioideae) and their systematic significance. Turkish Journal of Botany 44(6), 618–632. https://doi.org/10.3906/bot-2004-25

Kruse, J., 1988: Rasterelektronenmikroskopische untersuchungen an samen der gattung *Allium* L. III. Die Kulturpflanze 36(2), 355–368.

Lin, C.-Y., Tan, D.-Y., 2017: Seed testa micromorphology of thirty-eight species of *Allium* (Amaryllidaceae) from from central Asia, and its taxonomic implications. Nordic Journal of Botany 35, 189–200. https://doi.org/10.1111/njb.01259

Meikle, R. D., 1985: *Allium*. Flora of Cyprus, 1608–1628. vol. 2. Bentham-Moxon Trust and Royal Botanic Gardens, Kew.

Mifsud, S., Mifsud, O., 2018: A revision of *Allium* subsect. *Allium* (Amaryllidaceae) for the Maltese Islands. Flora Mediterranea 28, 27–51. https://doi.org/10.7320/FlMedit28.027

Neshati, F., Fritsch, R. M., 2009: Seed characters and testa sculptures of some Iranian *Allium* L. species (Alliaceae). Feddes Repertorium 120(5–6), 322–332. https://doi.org/10.1002/fedr.200911112

Nour, I. H., Hamdy, R. S., Osman, A. K., Badry, M. O., 2022: Palynological study of *Allium* L. (Amaryllidaceae) in the flora of Egypt. Palynology 46(3), 1–15. https://doi.org/10.1080/01916122.2022.2031329

POWO, 2021: Plants of the World Online. Facilitated by the Royal Botanic Gardens, Kew. Retrieved November 7, 2023 from http://www.plantsoftheworldonline.org

Sennikov, A. N., Lazkov, G. A., 2023: Taxonomic revision of the *Allium filidens* group (Amaryllidaceae) in Kyrgyzstan. Nordic Journal of Botany, e04050, 1–10. https://doi.org/10.1111/njb.04050

Täckholm, V., 1974: Students' Flora of Egypt. Second Edition. Cooperative Printing Company, Cairo.

Temunović, M., Šola, Z., Jakšić, V., Vidaković, A., Liber, Z., Poljak, I., Bogdanović, S., 2024: Clarifying genetic and taxonomic relationships among *Pistacia* taxa (Anacardiaceae) in Croatia. Acta Botanica Croatica 83(1), 1–13. https://doi.org/10.37427/botcro-2024-009

Veiskarami, G., Khodayari, H., Heubl, G., Zarre, S., 2018: Seed surface ultrastructure as an efficient tool for species delimitation in the *Allium ampeloprasum* L. alliance (Amaryllidaceae, Allioideae). Microscopy Research and Technique 81(11), 1275–1285. https://doi.org/10.1002/jemt.23134

Yusupov, Z., Ergashov, I., Volis, S., Makhmudjanov, D., Dekhkonov, D., Khassanov, F., Tojibaev, K., Deng, T., Sun, H., 2022: Seed macro- and micromorphology in *Allium* (Amaryllidaceae) and its phylogenetic significance. Annals of Botany 129(7), 869–911. https://doi.org/10.1093/aob/mcac067

Acta Bot. Croat. 84 (1), 44–53, 2025
DOI: 10.37427/botcro-2025-005

CODEN: ABCRA 25
ISSN 0365-0588
eISSN 1847-8476

Overcoming seed dormancy and improving germination of *Convolvulus persicus*, an endangered coastal plant in north of Iran

Razieh Bahadornejad Velashedi, Sedigheh Kelij*, Naser Jafari

University of Mazandaran, Department of plant sciences, 47416-13534 Babolsar, Iran

Abstract – *Convolvulus persicus* L. is an endemic endangered species distributed in the coastal regions of the Caspian Sea and the Black Sea that displays limited germination, potentially impacting its ability to regenerate. To gain an understanding of the dormancy status and germination needs of *C. persicus*, seed characteristics, seed coat permeability and different dormancy-breaking treatments were assessed. The results revealed that *C. persicus* seed coats are water-impermeable and that both cold and warm stratification were effective in breaking dormancy. Furthermore, GA_3 pretreatment with combination of either cold or warm stratification proved successful in releasing dormancy. However, the highest germination percentage and rate as well as seed vigour was achieved by mechanical scarification followed by H_2SO_4 application and warm stratification. Warm stratification was recognized to be more favourable for overcoming seed dormancy and promoting seedling survival than cold stratification. Notably, the influence of population type on germination capacity was found to be negligible. These findings may facilitate the conservation and collection management of this threatened plant species, which is currently underrepresented in *ex situ* conservation efforts.

Keywords: germination percentage, gibberellic acid, seed viability, stratification

Introduction

Climate changes and human activities such as deforestation, urbanization, industrial activities and agriculture often lead to the extinction of plant species that are unable to survive or reproduce in a degraded ecosystem. Particularly, species with narrow geographical ranges are at higher risk of extinction (Newbold et al. 2018). Among threatened species, a critical factor driving extinction is the failure to replenish populations with new individuals. Therefore, pinpointing the reasons for species' inability to regenerate is paramount for the protection and restoration of endangered species. Seed characteristics are directly related to the conservation and population growth of threatened plants (Cochrane et al. 2014). Successful preservation and the establishment of *ex situ* conservation of endangered plants primarily depends on successful germination and seedling establishment (Güleryüz et al. 2021). Understanding the specific requirements for successful germination is imperative for effectively conserving these plants (Cochrane et al. 2002).

Seed dormancy, which delays germination and inhibits seedling development, is an evolutionary adjustment that helps seed persistence through adverse conditions ensuring germination occurs when environmental situations become more favourable for seedling establishment (Kildisheva et al. 2020). However, during the dormancy period, seeds are often lost due to animal consumption, attack by microorganisms and environmental stresses, limiting the ability of plants to expand their population (Chen et al. 2022). Comprehending the seed dormancy type enables environmentalists to improve targeted strategies to break dormancy and stimulate germination. In accordance with the modified version of the classification of seed dormancy proposed by Baskin and Baskin (2004), seed dormancy can be categorized into five classes: morphological dormancy (MD), physiological dormancy (PD), morphophysiological dormancy (MPD), physical dormancy (PY) and combinational dormancy (PY + PD) (Baskin and Baskin 2004). Recently, Baskin and Baskin (2021) presented an expanded system for primary seed dormancy classification, which includes a greater diversity of subclasses, levels and types (Baskin and Baskin

* Corresponding author e-mail: s.kelij@umz.ac.ir

2021). The Convolvulaceae, which includes two subfamilies: Convolvuloideae and Hombertoideae, is known for seeds with physical dormancy. Physical dormancy occurs when seeds are unable to germinate due to physical barriers, often caused by a water-impermeable seed coat (Jayasuriya et al. 2009). Previous studies have identified physical dormancy in seeds of *Calystegia sepium* (L.) R. Br., *Calystegia soldanella* (L.) Roem. & Schult. and *Convolvulus arvensis* L. from the tribe Convolvuleae within the subfamily Convolvuloideae (Jayasuriya et al. 2008a). In view of these findings, as well as of the presence of a hard seed coat in *C. persicus*, it is likely that physical dormancy is present in the seeds of this species. Depending on the type of dormancy, some treatments such as seed coat scarification, cold and warm stratification and different chemical treatments can overcome dormancy barriers (Fernández and Tapias 2022).

Convolvulus persicus L. (Convolvulaceae) is an endemic endangered perennial species that grows in the coastal regions of the Caspian Sea and the Black Sea. It is threatened due to the restricted ranges and destruction of its environment by human actions and natural conditions. Plants inhabiting coastal dune ecosystems are exposed to harsh natural conditions, including soil salinity, salt spray, nutrient deficiency, sand burial, sea waves and flooding, strong winds and high light intensity (Hesp 1991). The plant produces ovate-elliptical and short petioled leaves and white, funnel-shaped and bisexual flowers (Strat and Holobiuc 2018). Previous studies have demonstrated that *C. persicus* produces few or no seedlings in its natural habitat on the southern coast of Caspian Sea in Iran and the Danube delta shore in Romania. In fact, *C. persicus* reproduces primarily through asexual reproduction via rhizome buds (Strat and Holobiuc 2018, Asheqian et al. 2021). Field surveys conducted on the Iranian coast of the Caspian Sea revealed a significantly low seed production percentage in *C. persicus* compared to its flower production percentage. Additionally, seed germination percentage across three populations of *C. persicus* along the southern coastline of the Caspian Sea was found to be poor (< 10%) (Asheqian et al. 2021). Collectively, a large number of unfertilized flowers, low seed production rate, low seed germination percentage, harsh coastal habitat conditions and human actions increase the extinction risk of *C. persicus*. Consequently, this species is categorized as critically endangered across various regions including Iran, Azerbaijan, Romania, Bulgaria, and Turkey (Holobiuc et al. 2015, Sayadi and Mehrabian 2017, Strat and Holobiuc 2018, Asheqian et al. 2021).

The primary objective of this study was to elucidate the dormancy status and germination requirements of *C. persicus*, thereby offering valuable insights for conservation and collection management efforts. To our knowledge, this research is the initial attempt to investigate the dormancy type and enhance the seed germination rate of *C. persicus* seeds. We hypothesized that the thick coat of *C. persicus* seeds is impermeable, which results in physical dormancy. Thus, application of various treatments that can lead to seed coat permeability, ultimately can lead to seed dormancy release. We put forward the hypothesis that germination capacity depends on seed traits, which are influenced by the climate conditions of plant communities. Therefore, we expected that seeds from different populations would exhibit varying seed qualities and germination percentage. To assess our hypothesis, our study focused on four key aspects: (1) evaluation of seed characteristics; (2) assessment if seed coat permeability; (3) investigation of the effects of temperature on fresh seed germination and (4) application of different dormancy release methods including scarification, sulphuric acid, cold and warm stratification and gibberellic acid.

Materials and methods

Seed collection

Seeds were obtained from two different localities (Goharbaran Sari, 36˚50.054' N, 53˚12.9681' E and Naftchal Babolsar, 36˚44.0311' N, 52˚47.6602' E) situated in the Mazandaran province of Iran in July 2022. Climatic factors for these areas are presented in Tab. 1, sourced from the Mazandaran meteorology general office. The collected seeds were stored in dark glass bottles at 5 °C for a duration of 6 months before utilization.

Tab. 1. Climatic factors of two different localities, Babolsar and Sari (average values for the 2020–2022 period) situated in the Mazandaran province of Iran.

Climatic factors	Babolsar	Sari
Mean annual precipitation (mm)	826.30	555.50
Mean annual maximum temperature (°C)	20.16	22.83
Mean minimum annual temperature (°C)	13.80	14.93
Mean relative humidity (%)	79.33	78.33
Annual evaporation (mm)	991.33	1213.06
Sunshine hours (h)	2003.67	2373.67
Wind speed (km h^{-1})	19.67	24

Determination of seed characteristics

Seed dimensions including width, length and thickness were determined by a Vernier calliper with an accuracy of 0.02 mm. Ten randomly selected seeds were weighed from each population using an electronic balance. Tetrazolium test was utilized for assessment seed viability by analysing the intensity of coloration in stain embryos. Colourless 2,3,5-triphenyl-2H-tetrazolium chloride (TTC) can penetrate intact membranes and change into red coloured formazan in living cells, a process catalysed by dehydrogenase enzymes concerned with aerobic respiration. In seeds, cells that are metabolically active will exhibit a pink or red staining pattern (Kittock and Law 1968). For tetrazolium testing, seeds were imbibed for 24 h in distilled water. Subsequently they were transferred to 1% (w/v) TTC solution and kept for 24 h at room temperature. Red colouring and uniformity of staining were used to determine seed viability as shown in Fig. 1 (ISTA 2003).

Germination test

To evaluate the germination potential of fresh seeds (within 14 days of seed collection), a preliminary germination test was performed for each population. Seeds were sterilized with sodium hypochlorite solution (1%) for 3 min and subsequently rinsed three times with sterilized water. Four replicates of 10 sterilized seeds were situated in 8 cm Petri plates on double filter paper and moistened with 3 mL of distilled water. Seeds were incubated at different temperatures: 10, 15, 20, 25, 30 and 40 °C for 4 weeks.

Water imbibition test

Seed imbibition mechanically scarified seeds and control seeds was compared to assess seed coat permeability. Each set contained three replicates of ten seeds. Seeds in each replicate were initially weighed and were placed onto moistened filter paper in Petri plates and kept under identical conditions. The seeds were removed, dried gently with a paper towel and reweighed after 2, 4, 6, 8, 10, 12, 24, 48, and 72 h. Percent increase of fresh mass was calculated using the equation:

$$\%Wr = [(Wf–Wi)/Wi] \times 100,$$

where Wr is percent increase in mass, Wi is initial fresh weight prior to imbibition and Wf is fresh mass following a specifc period of imbibition (Zhang et al. 2015).

Dormancy-breaking treatment

To disrupt the seed coat and break the seed dormancy, various physical and chemical treatments were applied (Kildisheva et al. 2020). For each treatment four replicates of ten seeds were considered.

Primary treatments:

- Scarification: seeds were mechanically scarified by sandpaper (N150) in two separated treatments for 3 min and 5 min.
- Sulfuric acid (H_2SO_4): seeds were soaked in 90% H_2SO_4 in two separate treatments for 5 and 15 min.
- Cold stratification: seeds were incubated at 4 °C in two separate treatments for 4 and 8 weeks.
- Warm stratification: seeds were incubated at a fixed temperature of 28 °C in two separated treatments for 4 and 8 weeks.
- Gibberellic acid (GA_3): seeds were soaked in 300 and 600 mg L^{-1} GA_3 for 48 h.

Combined treatments:

- Mechanical scarification (5 min) + 25% H_2SO_4 (15 min) + cold stratification (4 weeks).
- Mechanical scarification (5 min) + 25% H_2SO_4 (15 min) + warm stratification (4 weeks).
- GA_3 (300 and 600 mg L^{-1}) + cold stratification (4 weeks).
- GA_3 (300 and 600 mg L^{-1}) + warm stratification (4 weeks).

Control included sterilized and untreated seeds. Both control and treated seeds were placed in a growth chamber under controlled conditions (22–24 °C, 14 h light/10 h dark cycle).

Germination was monitored daily and the test concluded after 30 days. Germination was defined as radicle protrusion (> 2 mm). Percentage of germination, rate of germination and seed vigour were calculated using the following formulae:

$$GP(\%) = \frac{n}{N} \times 100$$

where GP is germination percentage; N is the total number of seeds and n is the number of germinated seeds.

$$GR = \sum \frac{ni}{Ti}$$

where GR is germination rate; ni is the number of germinated seeds after i days and Ti is the number of days from the beginning of the test.

$$SV = \frac{LS \times GP}{100}$$

where SV is seed vigour, LS is the mean of seedling length and GP is the germination percentage (Abdul-Baki and Anderson 1973).

Statistical analysis

Statistical analyses were conducted using the SPSS version 25.0 (IBM Corporation, Armonk, NY, USA). The normality of the variable distribution was assessed using the Kolmogorov-Smirnov test. To compare seed qualities between the two collection sites (Sari and Babolsar), an independent-sample t-test was employed. A one-way analysis of variance (ANOVA), followed by Duncan's multiple range test, was performed to test the differences of seed germination percentage at various temperatures, water uptake between control and scarified seeds of both sites. Furthermore, a one-way ANOVA was performed to determine whether various dormancy-breaking treatments significantly increased the final germination percentage (GP, %), germination rate (GR) and seed vigour (SV) relative to control seeds. Statistical significance was set at $P < 0.05$. All data were expressed as the means ± standard error (SE) of the four independent replicates except for the imbibition test which was conducted with three replicates.

Results

Seed characteristics

The seeds of *C. persicus* are enclosed within capsules that split open upon maturity. These seeds typically appear large, black and sometimes dark brown (Figs. 1A-D).

The length, width, thickness and weight of *C. persicus* seeds obtained from Sari were significantly higher than those from Babolsar ($P < 0.05$, Tab. 2). The viability of *C. persicus* seeds collected from two sites did not differ significantly (Tab. 2).

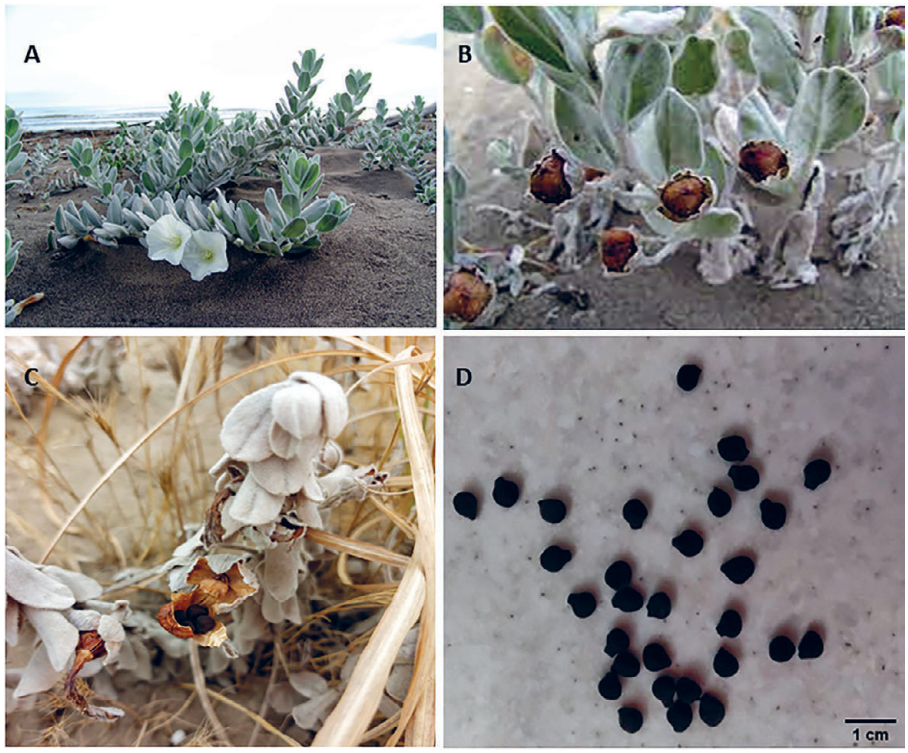

Fig. 1. *Convolvulus persicus* in the Mazandaran province of Iran: mature plants (A), fruits (B), capsule dehiscence (C) and seeds (D).

Tab. 2. Seed characteristics of *Convolvulus persicus* from two different localities in the Mazandaran province of Iran. Data represents the mean ± standard error (N = 4). Student's t-test was used to determine the significance between means (*) at P < 0.05, n.s. - not significant.

Seed characteristic	Babolsar	Sari	t-value	P-value
Seed length (mm)	6 ± 0.06	6.2 ± 0.04*	–3.47	0.03
Seed width (mm)	4.1 ± 0.03	4.3 ± 0.02*	–4.9	0.01
Seed thickness (mm)	3.14 ± 0.1	3.60 ± 0.09*	–4.7	0.006
Seed weight (mg)	50.68 ± 4.3	55.65 ± 4.3*	–2.5	0.04
Seed viability (%)	77 ± 6.7	82 ± 5.3 n.s.	–1.9	0.21

Germination test

Statistical analysis did not reveal significant differences in germination percentage at 15, 20, 25, 30 °C (P = 0.08). Seeds incubated at low and high temperatures (10 and 40 °C) did not germinate. In general, the germination percentage at different temperatures in both populations did not exceed 10% (Fig. 2).

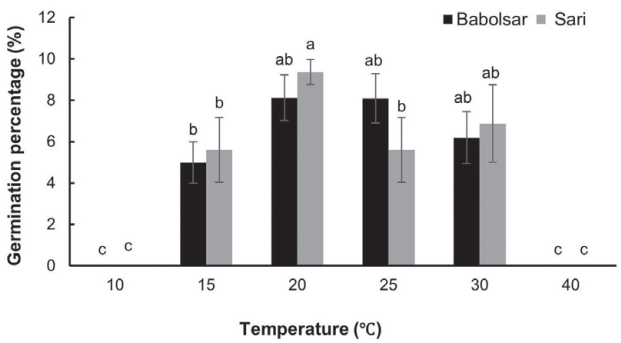

Fig. 2. Effect of temperature on seed germination of *Convolvulus persicus* from two localities in the Mazandaran province of Iran. Data represent the mean ± standard error (N = 4). Different letters indicate significant differences at P < 0.05 (one-way ANOVA with Duncan's post hoc test).

Water imbibition test

Significant differences were observed in water absorption rates between early and late hours of imbibition in intact and mechanically scarified seeds within both populations (P < 0.05, Fig. 3). Scarified seeds demonstrated a higher and faster rate of water absorption compared to the non-scarified seeds in both the Babolsar and Sari populations. Mechanical scarification resulted in a significant increase in water uptake compared to the control after 72 h. By the end of the 72-h observation period, scarified seeds showed water uptake of 62 ± 2.13% for Babolsar and 75 ± 2.66% for Sari, whereas non-scarified seeds showed an increase of only 24 ± 1.37% for Babolsar and 28 ± 1.74% for Sari (P < 0.05, Fig. 3).

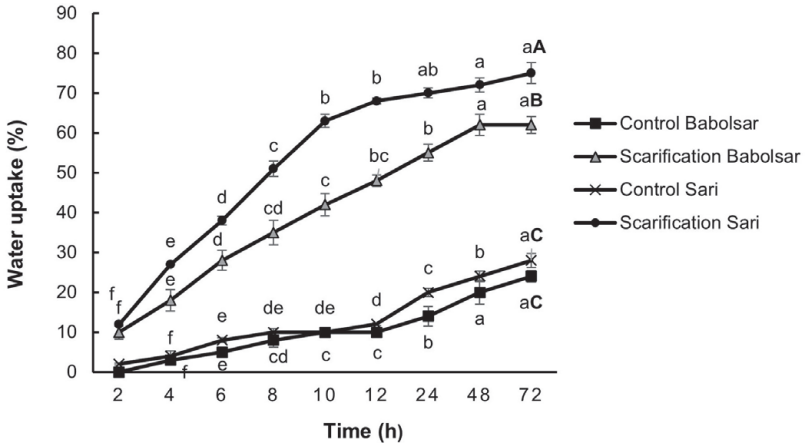

Fig. 3. Water uptake for control and scarified seeds of *Convolvulus persicus* from two localities in the Mazandaran province of Iran. Data represent the mean ± standard error (N = 3). Small letters indicate comparison of water uptake (%) in each time within a group and capital letters represent comparison water uptake (%) among groups after 72 h at $P < 0.05$ (one-way ANOVA with Duncan's post hoc test).

Dormancy-breaking treatments

Considering primary treatments ANOVA analysis showed that mechanical scarification for 3 min had no significant effect on germination percentage when compared to the control in both Babolsar and Sari populations (5% and 7.5%, respectively, $P > 0.05$). But application of mechanical scarification for 5 min exhibited a statistically significant impact on germination percentage of both Babolsar and Sari populations (27% and 22%, respectively, $P < 0.05$).

In seeds pretreated with 90% H_2SO_4 (for 5 and 15 min) the germination percentage did not significantly differ from that of the control and this result was identical in both populations ($P > 0.05$, Fig. 4).

The results showed that the germination percentage in seeds under GA_3 treatments was less or equal to control regardless of the concentration used and GA_3 did not improve seed germination percentage in either population, Babolsar or Sari ($P > 0.05$, Fig. 4).

In contrast, cold and warm stratification significantly ($P < 0.05$) increased germination percentage in both populations, with warm stratification showing higher efficacy than cold stratification. In Babolsar, germination percentage significantly increased under cold stratification from 5% to 20 ± 4% and 17.5 ± 4.7%, for 4 and 8 weeks, respectively. While under warm stratification it increased to 25% for both 4- and 8-weeks duration. The results of the cold and warm stratification treatments on seeds from Sari revealed that the germination percentage was enhanced from 10% to 20% and 22% by 4- and 8-week cold stratification, respectively and improved to 35% and 27% under 4- and 8-week warm stratification, respectively. Seeds of *C. persicus* collected from Sari had the highest germination percentage (35 ± 2.8%) under 4-week warm stratification ($P < 0.05$, Fig. 4).

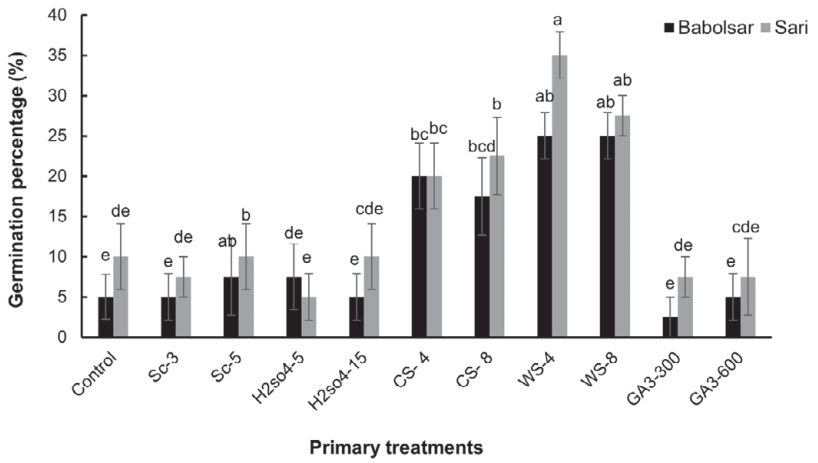

Fig. 4. The seed germination percentage of *Convolvulus persicus* under different physical and chemical treatments in two populations from Mazandaran province of Iran. Data represent the mean ± standard error (N = 4). Mean values with different letters differ significantly at $P < 0.05$ according to one-way ANOVA with Duncan's post hoc test. Sc – mechanical scarification (3 and 5 min), H_2SO_4 application of sulfuric acid (5 and 15 min), CS – cold stratification (4 °C, 4 and 8 weeks), WS – warm stratification (28 °C, 4 and 8 weeks), GA_3 – application of gibberellic acid (300 and 600 mg L^{-1}).

Following the assessment of scarification for 5 min and cold and warm stratification on seed dormancy release of *C. persicus*, combined treatments were administered involving scarification along with cold and warm stratification for 4 weeks. The result of one-way ANOVA revealed that mechanical scarification in combination with H_2SO_4 and cold stratification greatly improved the germination of *C. persicus* seeds by 71 ± 3.8% and 84 ± 3.1% ($P < 0.05$) in both populations, Babolsar and Sari, respectively. In addition, the mechanical scarification in combination with H_2SO_4 and warm stratification led to a substantial rise in germination percentage for Babolsar and Sari seeds, reaching 71 ± 3.1% and 81 ± 3.6%, respectively. However, no statistically significant difference was found in the germination percentage between the two mentioned treatments ($P > 0.05$, Fig. 5A).

The seed germination percentage of *C. persicus* under GA_3 in combination with cold stratification treatment increased significantly ($P < 0.05$) by 34 ± 5.9% and 40 ± 3.1% for 300 mg L^{-1} GA_3 and 43 ± 3.6% and 37 ± 8.8% for 600 mg L^{-1} GA_3, for Babolsar and Sari, respectively (Fig. 5A). Exposure to GA_3 in combination with warm stratification treatment also significantly ($P < 0.05$) improved the seed germination of *C. persicus* in both populations (Fig. 5A) in which the germination percentage of Babolsar treated seeds were 40 ± 5.9% and 37 ± 7.21% (for 300 and 600 mg L^{-1} GA_3, respectively) and for Sari treated seeds were 40 ± 5.9% and 50 ± 5.1%, (for 300 and 600 mg L^{-1} GA_3, respectively). However, the germination percentage of *C. persicus* seeds was unaffected by concentration of GA_3 and was not different ($P > 0.05$) for two concentrations (300 and 600 mg L^{-1}) of GA_3, Fig. 5A).

The highest germination rates were observed in seeds treated with mechanical scarification in combination with H_2SO_4 and warm stratification in the Sari population (2 ± 0.19, $P < 0.05$). However, seeds under the same combination of treatments in the Babolsar population exhibited a lower germination rate than the Sari population (1.5 ± 0.15, $P < 0.05$). The seed germination rates under combined treatment of scarification in combination with H_2SO_4 and cold stratification were not significantly different ($P > 0.05$) from the control in either population. Germination rate for seeds treated with GA_3 (both 300 and 600 mg L^{-1}) under cold stratification also did not significantly differ ($P > 0.05$) from the corresponding control in either population. On the other hand, in seeds treated with GA_3 (both 300 and 600 mg L^{-1}) under warm stratification, the seed germination rate was significantly ($P < 0.05$) enhanced in both populations (Fig. 5B).

Our experimental findings underscored the loss of vigour in control seeds, leading to their inability to thrive as young seedlings. Control seeds displayed a limited capacity for germination, as evidenced by the emergence of the radicle exceeding 2 mm in length. However, no subsequent stages of seedling development such as radicle elongation, hypocotyl arch emergence, appearance of folded cotyledons, and full emergence of open cotyledons were observed. Consequently, these control seeds did not progress to seedling

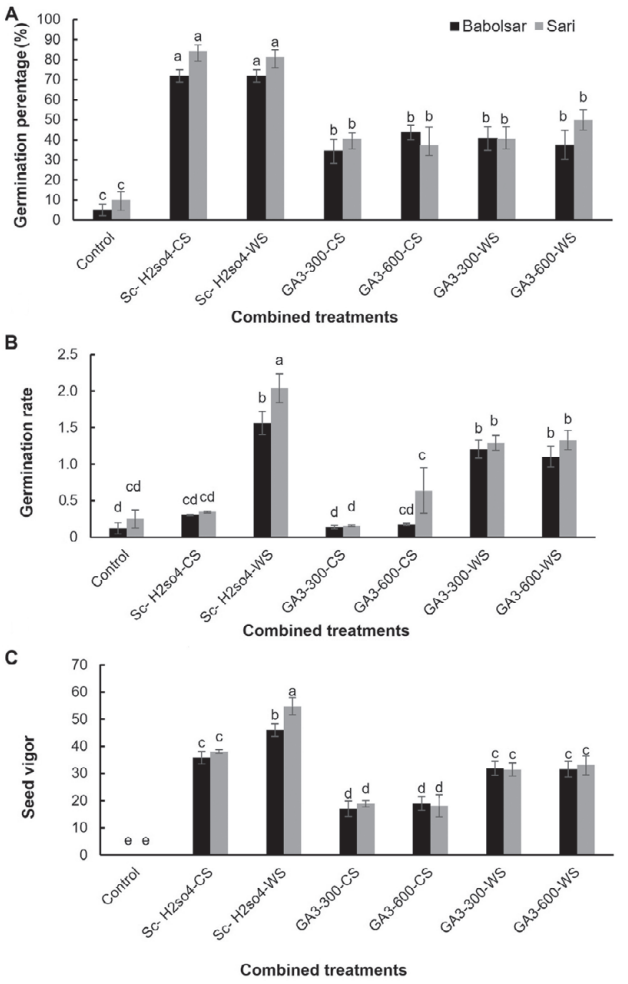

Fig. 5. Effects of combined physical and chemical treatments on seed germination percentage (A), germination rate (B) and seed vigour (C) of *Convolvulus persicus* in two populations from Mazandaran province of Iran. Data represent the mean ± standard error (N = 4). Mean values with different letters differ significantly at $P < 0.05$ according to one-way ANOVA with Duncan's post hoc test. Sc-H_2SO_4-CS – mechanical scarification in combination with sulphuric acid and cold stratification, Sc-H_2SO_4-WS – mechanical scarification + sulphuric acid + warm stratification, GA_3-300-CS – gibberellic acid (300 mg L^{-1}) + cold stratification, GA_3-600-CS – GA_3 (600 mg L^{-1}) + cold stratification, GA_3-300-WS – GA_3 (300 mg L^{-1}) + warm stratification, GA_3-600-WS – GA_3 (600 mg L^{-1}) + warm stratification.

maturity and displayed a seed vigour value of zero due to stunted radicle and hypocotyl growth. The seeds under primary treatments exhibited a low germination percentage and rate with a considerable portion failing to advance to the stage of mature seedlings. Consequently, we abstained from assessing their germination rate and seed vigour. In contrast, all seeds treated with combined treatments exhibited progressive growth through all stages of seedling development until reaching maturity (Fig. 6). Among the treated seeds, the highest seed vigour was found in the seeds treated with scarification in combination with H_2SO_4 and warm stratification, especially in the Sari population (54 ± 3.2, $P < 0.05$) while combined treatment with cold stratification gave significantly lower values (Fig. 5C). Seeds treated with

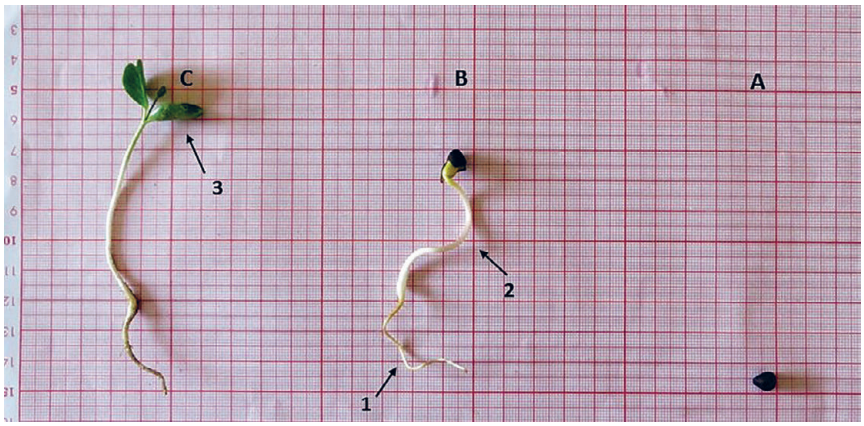

Fig. 6. Seed germination of *Convolvulus persicus* in the Mazandaran province of Iran: swollen seed (A), germinated seed is developing into mature seedling; 1 – radicle and 2 – hypocotyl (B) and mature seedling; 3 – cotyledon leaves (C).

GA_3 (both 300 and 600 mg L^{-1}) under cold stratification showed the lowest seed vigour (ranging from 17 to 19) compared to other treatments ($P < 0.05$, Fig. 5C).

Discussion

Worldwide, 50-90% of wild plants generate seeds that show some dormancy after maturity. The characteristics of seed dormancy depend on genetics, ecological conditions, growth pattern and geographical distribution (Baskin and Baskin 2014). The interruption of seed dormancy and improvement in germination percentage and rates are influenced by a combination of environmental conditions such as light, temperature, moisture content and hormonal balance. With an understanding the specific requirements of different plant species and implementing appropriate techniques such as scarification, stratification, light exposure, temperature control, and moisture management, seed dormancy can be interrupted and germination rates can be improved (Nautiyal et al. 2023). Our investigation was prompted by the Asheqian et al. (2021) report on poor germination of *C. persicus* seeds, which motivated us to explore the dormancy status and germination of this endangered and endemic species on the northern coasts of Iran. For reporting of dormancy type and dormancy release treatments, some information should be provided, such as seed qualities, imbibition testing and germination status (Kildisheva et al. 2020).

Our study of *C. persicus* seed characteristics showed that the seeds collected from Sari were greater in size and weight than the seeds collected from Babolsar. Our previous investigation into *C. persicus* revealed that the species exhibits more vegetative and reproductive growth in the Sari site than in Babolsar (Asheqian et al. 2021). This disparity can be attributed to the climatic factors present in Sari, such as higher temperatures and increased sunshine hours as shown in Tab. 1. Consequently, the larger seeds observed in Sari may be directly correlated to the prevailing climatic conditions in this particular location. The viability of Sari and Babolsar seeds did not significantly different and both of them were above 75%. In general, seed characteristics is ascertained by genetic potential and environmental factors, especially the nutrition of the mother plant throughout seed formation. It is known that, the seed size and viability have a meaningful impact on germination, seedling growth and establishment (Li et al. 2017). The size of a seed plays a vital role in the early phases of seedling growth, as larger seeds provide more nutrients for development. Additionally, the speed at which seeds germinate may be influenced by their size, with larger seeds typically holding more water. Also, the vitality of a seed is crucial for successful germination and the creation of normal seedlings. A strong germination rate is essential for the successful establishment and seedlings growth, impacting their capacity to contend and thrive in their environment (Tumpa et al. 2021). According to the viability test in our investigation, the regeneration of *C. persicus* does not seem to be limited by seed viability.

The next critical step in identifying seed dormancy is to assess seed germination across varying temperature conditions (Baskin and Baskin 1998). Seeds are typically considered nondormant if they exhibit a high germination percentage (over 75%). On the contrary, if seeds have low or no germination at diverse temperature levels, they are probably dormant (Erickson et al. 2016). Our investigation revealed that the germination percentage of *C. persicus* seed under alternating temperatures in both populations was notably low, not surpassing 10%. This observation strongly suggests the presence of dormancy in *C. persicus* seeds. To further explore this dormancy, we conducted imbibition testing to assess the water permeability of the seed coat. Seeds with impermeable coats are often physically dormant (Silveira 2013). The imbibition essay displayed that the percentage and speed of water absorption in the scarified seeds in both Sari and Babolsar populations were higher than in non-scarified seeds. This finding confirms that the *C. persicus* seed coat is impermeable. Several studies have reported a water-impermeable coat in Convolvulaceae that causes physical seed dormancy (Jayasuriya et al. 2008b, Baskin and Baskin 2014, Kildisheva et al. 2020). Thus, our findings are aligned with existing literature and underscore the importance of understanding seed coat properties in dormancy mechanisms.

After mechanical or chemical scarification, non-deep physically dormant seeds will immediately and extensively germinate (Nautiyal et al. 2023). However, our results indicate that seed dormancy and germination were not affected efficiently either by mechanical scarification treatments for 3 min, nor by chemical scarification using H_2SO_4 for 5 and 15 min. Although, scarification for 5 min demonstrated some efficacy in enhancing germination percentage, the observed increase did not surpass 30%. This suggests that there is still a problem for seed germination. When scarified seeds absorb water adequately, but fail to show remarkable enhancement in germination percentage, the presence of physiological dormancy is suggested (Kildisheva et al. 2018a). Interestingly, the application of gibberellic acid treatment in the absence of scarification, at 300 and 600 mg L^{-1}, did not result in any significant outcome on seed dormancy alleviation or enhancement of germination percentage in *C. persicus* seeds. In contrast, both cold and warm stratification for 4 and 8 weeks notably increased germination percentage in both the Babolsar and the Sari populations. But the germination ability of seeds in warm stratification conditions was higher than that in cold stratification conditions after 4 and 8 weeks. This shows that cold and warm stratification treatments can release physical dormancy. Stratification enhances the embryo's growth capacity and then enables it to surpass the physical barrier to its development (Chen et al. 2022).

Building upon the progress made in overcoming the dormancy of *C. persicus* seeds and enhancing germination through cold and warm stratification methods, we decided to explore combined treatments with cold and warm stratification to further enhance the germination percentage. Previous studies have highlighted the efficacy of combined treatments in facilitating seed germination in various species. For instance, the combination of scarification and stratification treatments notably enhanced the germination of *Rubus* seeds. Especially, H_2SO_4 scarification with cold stratification was impressive for *Rubus parviflorus* Weston, *Rubus phoenicolasius* Maximand and *Rubus takesimensis* Nakai (Choi et al. 2016). Similarly, scarification with H_2SO_4 followed by warm stratification for 4-weeks was found to be highly effective in improving seed germination percentage for *Rosa multibracteata* Hemsl & E.H.Wilson, *Rosa hugonis* Hemsl. and *Rosa filipes* Rehder & E.H.Wilson (Zhou and Bao 2011). Our study demonstrates that utilizing a combination of mechanical scarification, H_2SO_4 and either cold or warm stratification considerably enhances the seed germination percentage of *C. persicus*. Although no statistically meaningful difference was found in the germination percentage between *C. persicus* seeds subjected to the combined treatment of mechanical scarification + H_2SO_4 and either cold or warm stratification, in both populations the results of germination rate and vigour index suggest that the combined treatment of mechanical scarification + H_2SO_4 and warm stratification may be more favourable to the breaking of seed dormancy and enhancing potential seedling survival than cold stratification. Mechanical scarification and H_2SO_4 treatment can simulate natural processes that enhance seed germination in situ. Factors such as waves, tidal movements, the burial and exhumation of seeds by shifting sands particularly in dune systems and biotic interactions such as ingestion by waterbirds can mimic the effects of natural abrasion on seed coats. The application of H_2SO_4 mimics natural processes such as microbial degradation or physical abrasion that occur in the seed's natural habitat, which can lead to the breaking of dormancy. Warm stratification can mimic natural warming of soils in spring, aligning with environmental cues for dormancy break and germination. The success of warm stratification over cold stratification may also reflect an adaptation to the specific climate and soil conditions of the area where the seeds originate (Baskin et al. 2002). Seeds from warmer climates or those that experience significant soil temperature fluctuations such as coastal ecosystems may be more responsive to warm stratification treatments.

Gibberellic acid is a highly effective hormone that stimulates germination and has been proposed as a solution for the problem of seed dormancy in various species. By activating the amylase enzyme, gibberellic acid facilitates the transfer of essential materials from storage sites to growth sites, ultimately enabling dormant seeds to germinate. Conversely, without gibberellin, the breakdown and transfer of materials do not occur, resulting in germination failure (Bewley and Black 1994). The effectiveness of gibberellic acid as a growth promoter is further enhanced when combined with cold or warm stratification treatments. Exogenous GA_3 application and cold stratification have proven to be particularly effective methods for releasing of physiological dormancy (Baskin and Baskin 2007). Recent research by Chen et al. (2022) demonstrated that the combined treatment of gibberellic acid and warm stratification successfully broke dormancy in *Cinnamomum migao* H. W. Li seeds and significantly increased their germination rate. Conforming to these findings, our own results also highlight the role of combining gibberellic acid treatment with both cold and warm stratification for overcoming dormancy and improving germination in *C. persicus* seeds. However, it is worth noting that compared to the combined treatments of mechanical scarification and H_2SO_4 during cold and warm stratification, the effect of the combined treatments of gibberellic acid and either cold or warm stratification was relatively low in terms of removing dormancy and increasing the seed germination percentage of *C. persicus*. Our findings provide evidence that dormancy in *C. persicus* seeds can be a combination of physical and physiological types, but the final answer to this issue requires more detailed research. To ensure successful germination, it is crucial to address both types of dormancies. Additionally, when working with rare plants, the quantity of available seeds is often limited. As a result, researchers typically rely on a single germination treatment (Crawford et al. 2007). Therefore, it becomes necessary to provide the most effective protocol for maximizing germination percentage. By doing so, seed banks can considerably enhance their efficiency and play a more significant role in conserving biodiversity (Godefroid et al. 2009).

Conclusion

Convolvulus persicus seeds exhibit a kind of combination of physical and physiological dormancy. Through comprehensive investigation, we have identified a highly effective method for overcoming dormancy in *C. persicus* seeds: a combined treatment involving mechanical scarification, H_2SO_4 application, and warm stratification. This particular treatment significantly enhances both germination percentage and rate, along with seed vigour. Importantly, our findings indicate that warm stratification serves as more favourable approach for breaking seed dormancy and promoting *C. persicus* seedling survival compared to cold stratification. Furthermore, while occasional variations in seed traits were observed between the Sari and Babolsar populations, the overall impact of population type on germination capacity was deemed insignificant. This underscores the robustness and adaptability of *C. persicus* seeds across different geographical locations. Overall, our study provides valuable insights into the dormancy mechanisms of *C. persicus* seeds and offers practical recommendations for enhancing germination and seedling survival in this species.

Acknowledgment

We thank Mr Abdolreza Yadollahpour for his valuable contribution to the field operations and University of Mazandaran for supporting this research.

Author contribution statement

The topic was conceived by SK and NJ. RB performed the experiments. RB and SK analysed all statistical data. The manuscript was written by SK. NJ revised the manuscript. All authors have read and approved the submitted version of the manuscript.

References

Abdul-Baki, A. A., Anderson, J. D., 1973: Vigour determination in soybean seed by multiple criteria. Crop Science 13(6), 630–633. https://doi.org/10.2135/cropsci1973.0011183X001300060013x.

Asheqian, F., Kelij, S., Jafari, N., 2021: Some Ecological and Biological Characteristics of *Convolvulus persicus* L., the endangered plant of Northern coast of Iran. Plant Ecosystem Conservation 9, 343–361.

Baskin, C. C., Baskin, J. M., 1998: Seeds: Ecology, biogeography and evolution of dormancy and germination. Academic Press, San Diego.

Baskin, C. C., Baskin, J. M., 2007: A revision of Martin's seed classification system, with particular reference to his dwarf-seed type. Seed Science Research 17(1), 11–20. https://doi.org/10.1017/S0960258507383189

Baskin, C. C., Baskin, J. M., 2014: Seeds: ecology, biogeography, and evolution of dormancy and germination, 150–162. Academic Press, San Diego.

Baskin, C. C., Zackrisson, O., Baskin, J. M., 2002: Role of warm stratification in promoting germination of seeds of *Empetrum hermaphroditum* (Empetracea), a circumboreal species with a stony endocarp. American Journal of Botany 89(3), 486–93. https://doi.org/10.3732/ajb.89.3.486.

Baskin, J. M., Baskin, C. C., 2004: A classification system for seed dormancy. Seed Science Research 14(1), 1–16. https://doi.org/10.1079/SSR2003150

Baskin, J. M., Baskin, C. C., 2021: The great diversity in kinds of seed dormancy: a revision of the Nikolaeva–Baskin classification system for primary seed dormancy. Seed Science Research 31(4), 249–277. http://doi.org/10.1017/S096025852100026X

Bewley, D. J., Black, M., 1994: Dormancy and the control of germination. In *Seeds:* Physiology of Development and Germination, 199–271. Plenum Press, New York.

Chen, J. Z., Huang, X. l., Xiao, X. F., Liu, J. M., Liao, X. F., Sun, Q. W., Liang, P., Zhang, L., 2022: Seed Dormancy Release and Germination Requirements of *Cinnamomum migao*, an Endangered and Rare Woody Plant in Southwest China. Frontiers in Plant Science 13, 1–14. https://doi.org/10.3389/fpls.2022.770940.

Choi, G. E., Ghimire, B., Lee, H., Jeong, M. J., Kim, H. J., Ku, J. J., Lee, K. M., Son, S. W., Lee, C. H., Park, J. I., Suh, G. U., 2016: Scarification and stratification protocols for breaking dormancy of *Rubus* (Rosaceae) species in Korea. Seed Science and Technology 44(2), 239–252. https://doi.org/10.15258/sst.2016.44.2.06.

Cochrane, A., Kelly, A., Brown, K., Cunneen, S., 2002: Relationships between seed germination requirements and ecophysiological characteristics aid the recovery of threatened native plant species in Western Australia. Ecological Management & Restoration 3(1), 47–60. https://doi.org/10.1046/j.1442-8903.2002.00089.x.

Cochrane, A., Yates, C. J., Hoyle, G. L., Nicotra, A. B., 2014: Will among-population variation in seed traits improves the chance of species persistence under climate change? Global Ecology and Biogeography 24(1), 12–24. https://doi.org/10.1111/geb.12234.

Crawford, A. D., Steadman, K. J., Plummer, J. A., Cochrane, A., Probert, R.J., 2007: Analysis of seed-bank data confirms suitability of international seed-storage standards for the Australian flora. Australian Journal of Botany 55(1), 18–29. https://doi.org/10.1071/BT06038.

Erickson, T. E., Barrett, R. L., Merritt, D. J., Dixon, K. W., 2016: Pilbara seed atlas and field guide: plant restoration in Australia's arid northwest. CSIRO Publishing, Australia.

Fernández, M., Tapias, R., 2022: Seed Dormancy and Seedling Ecophysiology Reveal the Ecological Amplitude of the Threatened Endemism *Picris willkommii* (Schultz Bip.) Nyman (Asteraceae). Plants 11(15), 1–27. https://doi.org/10.3390/plants11151981

Godefroid, S., Van deVyver, A., Vanderborght, T., 2009: Germination capacity and viability of threatened species collections in seed banks. Biodiversity and Conservation 19, 1365–1383. https://doi.org/10.1007/s10531-009-9767-3.

Güleryüz, G., Kırmızı, S., Arslan, H., Güleryüz, E., 2021: Breaking of dormancy in the narrow endemic *Jasione supina* Sieber subsp. supina (Campanulaceae) with small seeds that do not need light to germinate. Acta Botanica Croatica 80(1), 12–17. https://doi.org/10.37427/botcro-2021-009.

Hesp, P. A., 1991: Ecological processes and plant adaptations on coastal dunes. Journal of Arid Environments 21(2), 165–191. https://doi.org/10.1016/S0140-1963(18)30681-5.

Holobiuc, I., Voichita, C., Catana, R., 2015: In vitro conservation of the critically endangered taxon *Convolvulus persicus* L. and regenerants evaluation. Oltenia, Studii si Comunicari Seria Stiintele Naturii 31, 51–59.

ISTA., 2003: ISTA Working Sheets on Tetrazolium Testing. 1st ed. Bassersdorf, Switzerland.

Jayasuriya, K. M. G. G., Baskin, J. M., Baskin, C. C., 2008a: Dormancy, germination requirements and storage behaviour of seeds of Convolvulaceae (Solanales) and evolutionary considerations. Seed Science Research 18(4), 223–237. https://doi.org/10.1017/S0960258508094750.

Jayasuriya K. M. G. G., Baskin J. M., Baskin C. C., 2009: Sensitivity cycling and its ecological role in seeds with physical dormancy. Seed Science Research 19(1), 3–13. https://doi.org/10.1017/S096025850818730X.

Jayasuriya, K., Baskin, J., Geneve, R., Baskin, C., Chien, C. T., 2008b: Physical Dormancy in Seeds of the Holoparasitic Angiosperm *Cuscuta australis* (Convolvulaceae, Cuscuteae): Dormancy-breaking Requirements, Anatomy of the Water Gap and Sensitivity Cycling. Annals of Botany 102(1), 39–48. https://doi.org/10.1093/aob/mcn064.

Kildisheva, O. A., Dixon, K. W., Silveira, F. A. O., Chapman, T., Sacco, A. D., Mondoni, A., Turner, S. R., Cross, A. T., 2020: Dormancy and germination: making every seed count in restoration. Restoration Ecology 28(S3), S256–S265. https://doi.org/10.1111/rec.13140.

Kildisheva, O. A., Erickson, T. E., Madsen, M. D., Dixon, K. W., Merritt, D. J., 2018: Seed germination and dormancy traits of forbs and shrubs important for restoration of North American dryland ecosystems. Plant Biology 21(3), 458–469. https://doi.org/10.1111/plb.12892.

Kittock, D. L., Law, A. G., 1968: Relationship of seedling vigour to respiration and tetrazolium reduction in germinating wheat seeds. Agronomy Journal 60, 268–288.

Li, R., Chen, L., Wu, Y., Zhang, R., Baskin, C. C., Baskin, J. M., Hu, X., 2017: Effects of Cultivar and Maternal Environment on Seed Quality in *Vicia sativa*. Frontiers in Plant Science 8, 1–9. https://doi.org/10.3389/fpls.2017.01411.

Nautiyal, P. C., Sivasubramaniam, K., Dadlani, M., 2023: Seed Dormancy and Regulation of Germination. In: M. Dadlani, D. K. Yadava (eds), Seed Science and Technology, Biology, Production, Quality, 39-66. https://doi.org/10.1007/978-981-19-5888-5_3.

Newbold, T., Hudson, L. N., Contu, S., Hill, S. L. L., Beck, J., Liu, Y., Meyer, C., Philips, H. R. P., Scharlemann, J. P. W., Purvis, A., 2018: Widespread winners and narrow-ranged losers: Land use homogenizes biodiversity in local assemblages worldwide. PLoS Biology 16(12): e2006841, 1–24. https://doi.org/10.1371/journal.pbio.2006841.

Sayadi, S., Mehrabian, A., 2017: Distribution patterns of Convolvulaceae in Iran: priorities for conservation. Rostaniha 18(2), 181–197. https://doi.org/10.22092/BOTANY.2018.115955.

Silveira, F. A. O., 2013: Sowing seeds for the future: the need for establishing protocols for the study of seed dormancy. Acta Botanica Brasilica 27(2), 264–269. https://doi.org/10.1590/S0102-33062013000200003.

Strat, D., Holobiuc, I. M., 2018: The occurrence and conservation status of *Convolvulus persicus* L. (Solanales: Convolvulaceae) on the western Black Sea coast–Romania. Acta Zoologica Bulgarica 11, 125–132.

Tumpa, K., Vidakovi´c, A., Drvodeli´c, D., Šango, M., Idžojti´c, M., Perkovi´c, I., Poljak, I., 2021: The Effect of Seed Size on Germination and Seedling Growth in Sweet Chestnut (*Castanea sativa* Mill.). Forests 12(7), 858. https://doi.org/10.3390/f12070858.

Zhang, K. L., Baskin, J. M., Baskin, C. C., Yang, X. J., Huang, Z. Y., 2015: Lack of divergence in seed ecology of two Amphicarpaea (Fabaceae) species disjunct between eastern Asia and eastern North America. American Journal of Botany 102(6), 860–869. https://doi.org/10.3732/ajb.1500069.

Zhou, Z., Bao, W., 2011: Levels of physiological dormancy and methods for improving seed germination of four rose species. Scientia Horticulture 129(4), 818–824. http://doi.org/10.1016/j.scienta.2011.04.024.

Acta Bot. Croat. 84 (1), 54–62, 2025
DOI: 10.37427/botcro-2025-003

CODEN: ABCRA 25
ISSN 0365-0588
eISSN 1847-8476

Reproductive biology of *Centaurea kilaea* (Asteraceae, Cardueae) – an endemic species from Türkiye

Ciler Kartal

Trakya University, Faculty of Science, Department of Biology, 22030 Edirne, Türkiye

Abstract – In this study, the embryology of *Centaurea kilaea* Boiss., a species endemic to Türkiye, was examined using light microscopy. The anthers of *C. kilaea* are tetrasporangiate; the anther wall development is dicotyledonous; and the tapetum is amoeboid. The meiotic division of the microspore mother cells is regular, and when the pollen grains are thrown from the anthers, they are three-celled. The ovary of *C. kilaea* is inferior, bicarpellary, syncarpous, and unilocular, which is characteristic of the Asteraceae family. It carries only a single ovule with basal placentation. The ovule is anatropous, unitegmic, and tenuinucellate. The megaspore mother cell undergoes meiotic division, giving rise to a linear tetrad of megaspores. The chalazal megaspore remains functional, and the other three megaspores degenerate rapidly. The functional megaspore undergoes three mitotic divisions in succession. As a result, a Polygonum-type embryo sac, with eight nuclei and seven cells, is formed. The antipodal cells persist until the first divisions of the zygote. In the mature embryo sac stage, the integument consists of the endothelium, peri-endothelial region, parenchymatous cells, and outer epidermis, from the inside out. Endosperm development is initially free nuclear, becoming cellular in the globular embryo stage. Embryo development is of the asterad type. The mature seed does not contain endosperm, but the endothelium persists.

Keywords: Asteraceae, *Centaurea kilaea*, endemic, female gametophyte, male gametophyte

Introduction

The genus *Centaurea* L., comprising more than 300 species, is one of the largest genera in the Asteraceae and is widespread across the world (Bremer 1994). Most species of the genus are distributed in the Balkan Peninsula and Türkiye (Siljak-Yakovlev et al. 2005). Türkiye is one of the main diversity centers of *Centaurea*, where it is represented by 204 species, 59% of which are endemic (Sirin et al. 2020). *Centaurea kilaea* Boiss. is a plant endemic to Türkiye that spreads only in the provinces of Kirklareli, Istanbul, Sakarya, and Bolu (Wagenitz 1975). The species is classified as endangered (EN) according to the Red Data Book of Turkish Plants (Ekim et al. 2000). The chromosome number of the species has been reported as 2n = 4x = 36, and the amount of 2C nuclear DNA as 3.68 pg (Meric et al. 2010).

Embryological studies on members of the Asteraceae family date back to earlier years (Desole 1954, Davis 1962, 1964, Renzoni 1970). Recently, the embryology of some species belonging to the Asteraceae family has been studied; some examples are *Centaurea achtarovii, Arnica montana*, *Pilosella brzovecensis*, *Ageratum conyzoides*, and *Ageratum fastigiatum* (Franca et al. 2015, Yankova-Tsvetkova et al. 2016, 2018, Bonifacio et al. 2018, Janas et al. 2021). Members of the Asteraceae family have an inferior, bicarpellate, and unilocular ovary. The ovary contains an anatropous, unitegmic, and tenuinusellate ovule with basal placentation (Davis 1966). Although most species contain Polygonum-type embryo sacs, some also include Allium-type, Drusa-type, Adoxa-type, and Fritallaria-type embryo sacs (Davis 1966, Musial et al. 2012). In members of the Asteraceae family, the anthers are tetrasporangiate. Although there is generally a plasmodial type of tapetum, the existence of a secretory tapetum has been proven in some species (Bonifacio et al. 2018, Franca et al. 2015). Following the simultaneous type of meiosis, tetrahedral, decussate, or isobilateral type tetrads are seen. Pollen is thrown from the anther as three-celled (Davis 1966).

Scientific data on *C. kilaea* are also very limited. The chromosome number and nuclear DNA content of the species were determined by Meric et al. (2010). In addition, anti-proliferative compounds of the species were isolated and

Corresponding author e-mail: cilermeric@trakya.edu.tr

tested against human tumor cell lines (Sen et al. 2015). A literature review shows that there are no studies on the embryology of this species. The aim of this study is to reveal the reproductive biology of *C. kilaea*, which is distributed in a limited area and included in the endangered category according to the Red Data Book of Turkish Plants (Ekim et al. 2000).

Materials and methods

Materials

Capitula containing the buds, blooms, and fruits of *C. kilaea* were collected from the coast of Igneada (Kirklareli, Türkiye; 41°52'53'' N, 27°59'32'' E) in July. The samples were fixed in an ethyl alcohol/acetic acid mixture (v/v, 3:1) for 24 h, then transferred to 70% ethanol and kept at 4 °C. Likewise, pollen grains were collected from florets blooming in the same habitat.

Histological method

For histological observations, various sizes of anthers and ovaries were embedded in historesin according to the manufacturer's instructions (Leica historesin-embedding kit). Longitudinal and transverse serial sections (4 µm thick) of the embedded blocks were obtained using a rotary microtome with a tungsten carbide blade. The sections were stained in 0.5% (w/v) toluidine blue O solution (in 0.1 M phosphate buffer at pH 6.8) at 60 °C for 2 min. They were washed in distilled water for 30 seconds and then dried in air (O'Brien et al. 1964, modified). Finally, they were mounted with Entellan™ (Merck) for microscopy.

Histochemical method

Periodic acid–Schiff reaction (PAS) was applied for the determination of insoluble polysaccharides. The 4 µm-thick sections were kept in 1% (w/v) periodic acid solution (in 90% ethyl alcohol) for 30 min and rinsed with distilled water at the end of the period. After staining with Schiff's reagent (Fisher Chemicals) for 30 min, the slides were placed for 5 min each in 0.5% (w/v) sodium metabisulfite solution. They were washed for 5 min with running water and rinsed with distilled water. Then, the slides were dried in the air and mounted with Entellan™ (Merck). For determination of proteins, the slides were stained with 0.025% (w/v) Coomassie Brilliant Blue G-250 (CBB) in distilled water/acetic acid/methanol (v/v/v, 87:10:3) solution for 10 min in an oven (60 °C). They were then washed for 2 min in distilled water. Then the slides were dried in air and mounted with Entellan™ (Merck) (Heslop-Harrison et al. 1973).

Pollen viability

Acetocarmine dye was used to investigate pollen viability. Ripe pollen grains from newly opened anthers were transferred onto a clean slide, and a few drops of aceto-carmine were added to the slide. After 20 min, stained pollen grains were considered fertile (viable), and the unstained pollen grains sterile (non-living). A total of 4000 pollen grains were counted, and the percentage of viability was calculated.

All observations and photography were carried out using an Olympus CX21 light microscope and the KAMERAM software program (Argenit, Türkiye).

Results

Anther wall and male gametophyte development

In *C. kilaea*, the anthers are tetrasporangiate, and the anther wall development is of the dicotyledonous type. The anther wall is thin and consists of four layers, each in a single layer of cells from the outside to the inside, as follows: the epidermis, endothecium, middle layer, and tapetum. In the early stages, the anther consists of meristematic tissue surrounded by the epidermis. The archesporial cells differentiate beneath the epidermis of the microsporangium and divide periclinally, forming the primary parietal cells and the sporogenous cells (Fig. 1A). The primary parietal layer undergoes a periclinal division, giving rise to two secondary parietal layers (Fig. 1B). The cells of the outer secondary parietal layer undergo periclinal divisions, forming the endothecial layer (outer) and middle layer (inner). The cells of the inner secondary parietal layer differentiate directly into the tapetum (Fig. 1C). At the microspore mother cell stage, the volume of tapetum cells increases, and they begin to divide before the microspore mother cells (Fig. 1D). At the tetrad stage, the middle layer is flattened, and dark-colored materials appear in the cytoplasm of tapetal cells. However, the transverse inner and side walls of the tapetal cells are still intact (Fig. 1E). At the young microspore stage and the vacuolated microspore stage, the inner tangential and radial walls of the tapetum cells are broken down. The tapetal protoplasmic arms extend into the interior of the locule (Fig. 1F and Fig. 1G, arrowheads). At those stages, the middle layer is flattened or not observed. At the pollen mitosis stage, the tapetal protoplasts move into the locule and fuse to form the multinucleate tapetal periplasmodium. This mass surrounds the pollen grains (Fig. 1H). At the mature pollen stage, the endothecial cells radially elongate and develop fibrous thickenings, which arise from their inner tangential walls. The tapetal periplasmodium disappears. The mature anther wall consists of the epidermis and endothecium with fibrous thickenings (Fig. 1I).

The sporogenous cells develop directly into the microspore mother cells in *C. kilaea*. They are observed with large nuclei and obvious nucleoli (Fig. 1D). Microsporocytes undergo simultaneous meiotic division, generating tetrahedral tetrads (Fig. 1E).

Microspores released from the tetrad have a prominent nucleus in the middle of the cell (Fig. 2A). Then, the nucleus is pushed to the side due to the vacuole formed inside the cell (Fig. 2B), and it undergoes the first pollen mitosis, resulting in the formation of two unequal cells, a large vegeta-

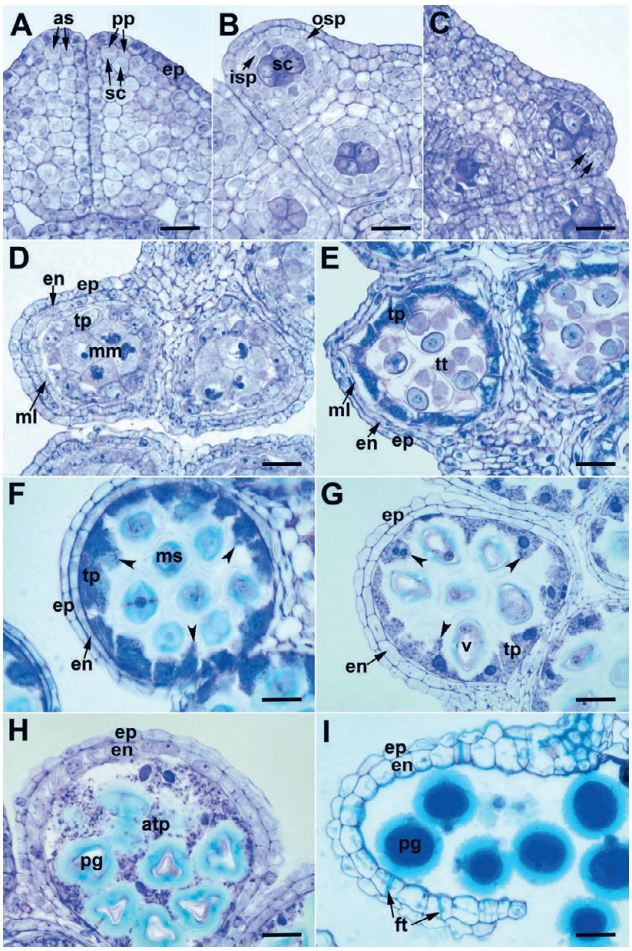

Fig. 1. Anther wall development in *Centaurea kilaea*: A) archespore cells and their divisions, B) outer and inner secondary parietal layers, C) division of the outer secondary parietal layer (arrows), D) microspore mother cell stage, E) tetrad stage, F) free microspore stage, G) vacuolated microspore stage (arrowheads indicate tapetal extensions), H) pollen mitosis stage, I) anthesis stage. as – archespore cell, atp – amoeboid tapetum, en – endothecium, ep – epidermis, ft – fibrous thickenings, isp – inner secondary parietal layer, ml – middle layer, mm – microspore mother cell, ms – microspore, osp – outer secondary parietal layer, pg – pollen grain, pp – primary parietal cells, sc – sporogenous cells, tp – tapetum, tt – tetrad, v – vacuole. Scale bars = 20 μm.

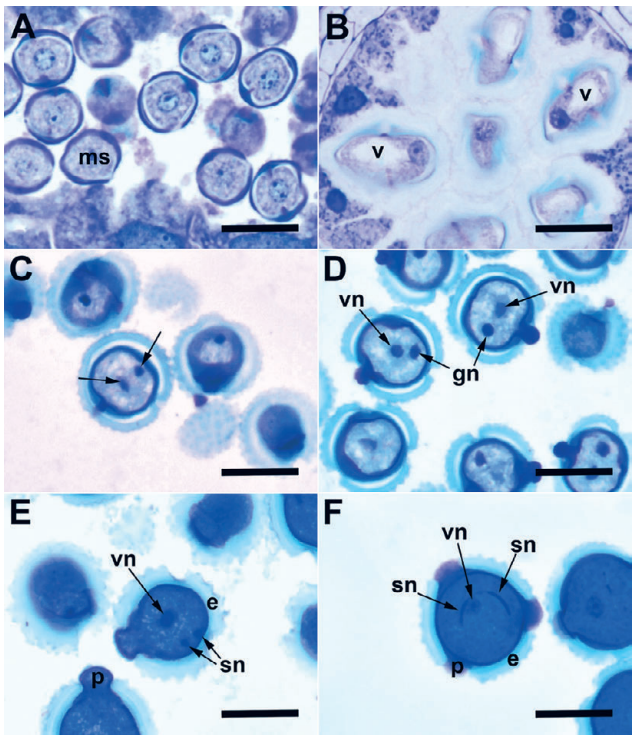

Fig. 2. Male gametophyte development in *Centaurea kilaea*: A) free-microspore stage, B) vacuolated microspore stage, C) telophase stage at the first pollen mitosis (arrows indicate chromosome groups at poles), D) vegetative and generative nuclei, E) second pollen mitosis, F) mature three-celled pollen grain. e – exine, gn – generative nucleus, ms – microspore, p – pore, sn – sperm nucleus, v – vacuole, vn – vegetative nucleus. Scale bars = 20 μm.

tive cell and a small generative cell (Fig. 2C and Fig. 2D). After the first mitotic division, the vacuole becomes invisible, and the generative cell divides to form two sperm cells (the second pollen mitosis) (Fig. 2E). Sperm cells are initially round in shape, then take the form of threads (Fig. 2F). Mature pollen grains are yellow, prolate-spheroidal, tricolporate and echinate, characteristic of the Asteraceae family.

In the PAS reaction employed for staining insoluble polysaccharides in the anther wall layers and pollen, all the anther wall layers and sporogenous cells give a negative reaction in terms of polysaccharide content at the beginning of development (Fig. 3A). In the tetrad stage, tapetum cells react weakly to PAS. At this stage, the epidermis and endothecium cells contain insoluble polysaccharides. Callose gives a positive PAS reaction at this stage (Fig. 3C). Insoluble polysaccharides are seen in the cytoplasm of the mature pollen grain (Fig. 3E). In protein staining with CBB, there is no considerable difference between the protein contents of the anther wall layers and sporogenous cells at the beginning of development (Fig. 3B). However, contrary to the other wall layers, the cytoplasm of tapetum cells becomes rich in protein content starting from the tetrad stage (Fig. 3D). The tapetum layer, which gives a strong positive reaction in the young pollen stage, begins to break down and transfers the protein-structured substances to the maturing pollen grains. Other anther wall layers are poor in protein content at the mature pollen stage (Fig. 3F).

Pollen viability

After the acetocarmine staining, the pollen viability rate was calculated as 87%, the dyed, large, and properly shaped mature pollen grains being considered fertile, and the unstained pollen sterile.

Ovule and female gametophyte development

C. kilaea has an inferior ovary, characteristic of the Asteraceae family. The ovary is syncarpous, unilocular, and carries a single ovule with basal placentation. The ovule is anatropous, tenuinucellate, and unitegmic (Fig. 4A). A single archespore cell develops under the epidermis, and this archespore cell differentiates directly into a megaspore mother cell (Fig. 4B). The megaspore mother cell undergoes

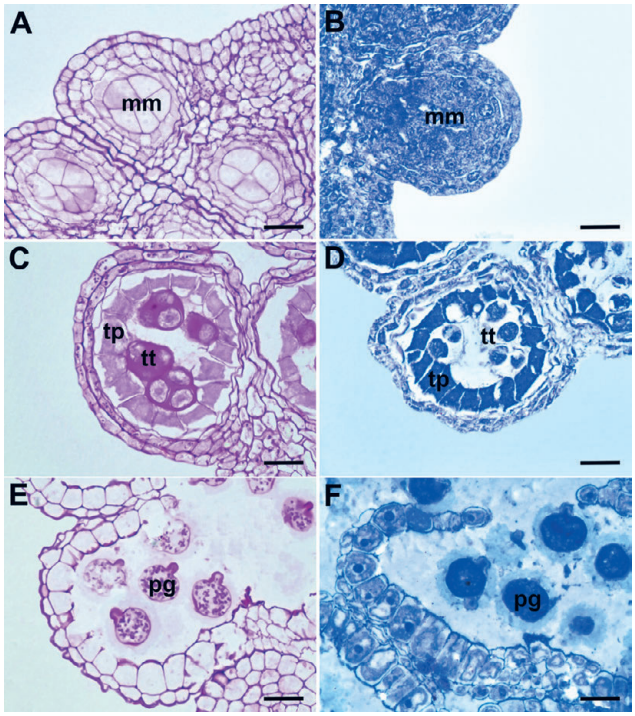

Fig. 3. Histochemical aspects of the anther wall and pollen development in *Centaurea kilaea*: A) insoluble polysaccharide content in the microspore mother cell stage, B) protein content in the microspore mother cell stage, C) insoluble polysaccharide content in the tetrad stage, D) protein content in the tetrad stage, E) insoluble polysaccharide content in the mature pollen grains, F) protein content in the mature pollen grains. mm – microspore mother cells, pg – pollen grain, tp – tapetum, tt – tetrad. Scale bars = 20 μm.

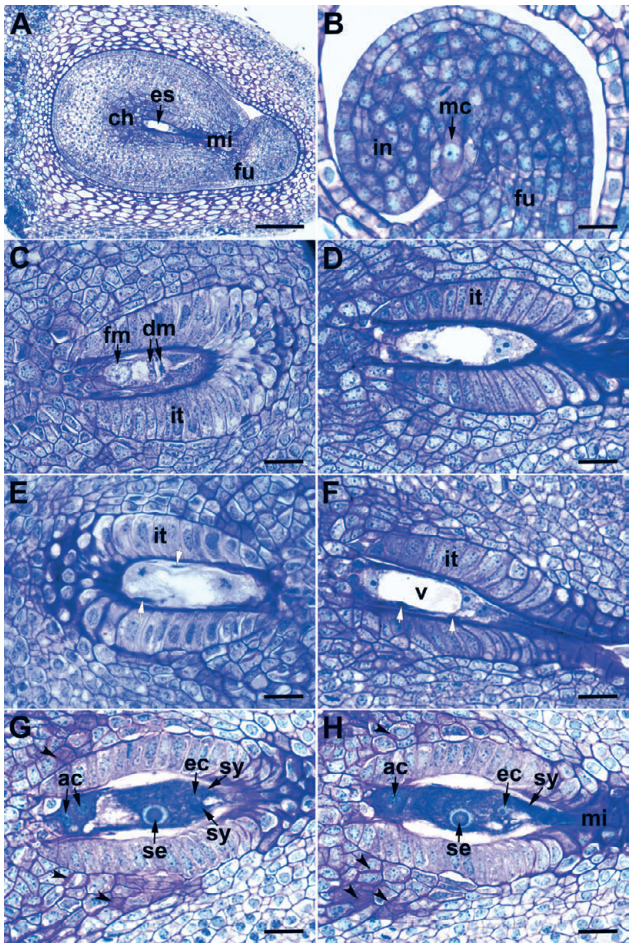

Fig. 4. Ovule and female gametophyte development in *Centaurea kilaea*: A) ovule, B) megaspore mother cell, C) functional megaspore and degenerated microspores, D) two-nucleate stage of megagametogenesis, E) metaphase stage of the second mitotic division, F) four-nucleate stage of megagametogenesis (white arrows indicate nucellar cell remnants), G) and H) mature embryo sac (the photos are taken from two consecutive sections of the same embryo sac; arrowheads indicate mucilage accumulation). ac – antipodal cell, ch – chalaza, dm – degenerated megaspores, ec – egg cell, es – embryo sac, fm – functional megaspore, fu – funiculus, in – integument, it – integumentary tapetum, mc – megaspore mother cell, mi – micropyle, sy – synergid cell, se – secondary nucleus, v – vacuole. Scale bars = A, 100 μm; B–H, 20 μm.

meiosis to produce a linear megaspore tetrad. The megaspore at the chalaza side is the functional megaspore; the other three megaspores rapidly degenerate (Fig. 4C). The functional megaspore undergoes three successive mitotic divisions to produce a two-, four-, and then eight-nucleate megagametophyte (Figs. 4D–H).

The embryo sac development is of the Polygonum type. The mature embryo sac consists of a three-celled egg apparatus, (an egg cell and two synergids) at the micropyle side, three antipodal cells at the chalazal end, and two polar nuclei in the central part of the sac. Before fertilization, the polar nuclei fuse to form the secondary nucleus (Fig. 4G and Fig. 4H). The synergids degenerate after fertilization. The antipodal cells persist until the first division of the zygote. Obturator cells originating from the funiculus are long, tubular shaped, and show prominent nuclei. They are elongated toward the synergids. The micropylar canal is completely filled with the obturator cells and the secretion produced by these cells (Fig. 5E and Fig. 5F).

In the ovules of *C. kilaea*, the megaspore mother cell, nucellus, and integument cells react poorly, in terms of insoluble polysaccharides, with the PAS reaction at the beginning of development (Fig. 5A). In the mature embryo sac stage, the part of the integument tapetum facing the embryo sac and the integument cells forming the micropylar opening show an intense PAS-positive reaction (Fig. 5C). In addition, at this stage, the obturator cells and their secretion give an intense PAS-positive reaction (Fig. 5E). In the ovules of *C. kilaea*, the megaspore mother cell, nucellus, and integument cells react moderately in terms of protein content with CBB at the beginning of development (Fig. 5B). In the mature embryo sac stage, the integumentary tapetum cells give an intense positive reaction to CBB (Fig. 5D). At this stage, it is observed that the obturator cells also give a positive reaction, but the protein is not secreted (Fig. 5F).

Endosperm and embryo development

During fertilization, one of the male gametes fuses with the egg cell, while the other male gamete fuses with the secondary nucleus and forms the primary endosperm nucleus.

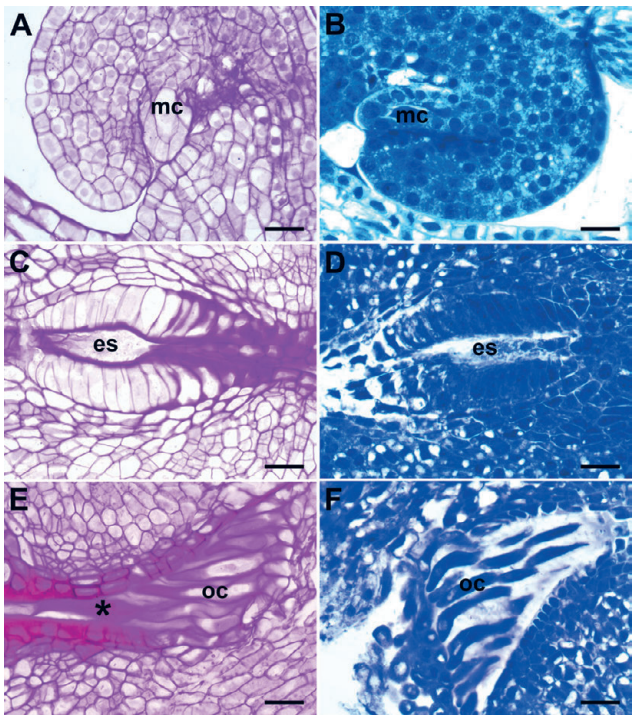

Fig. 5. Histochemical aspects of ovule and embryo sac development in *Centaurea kilaea*: A) insoluble polysaccharide content at the megaspore mother cell (mc) stage, B) protein content at mc stage, C) insoluble polysaccharide content in the mature embryo sac (es) stage, D) protein content at the mature es stage, E) insoluble polysaccharide content of the obturator cells (oc) and secretion (asterisk), F) protein content of the obturator cells. Scale bars = 20 μm.

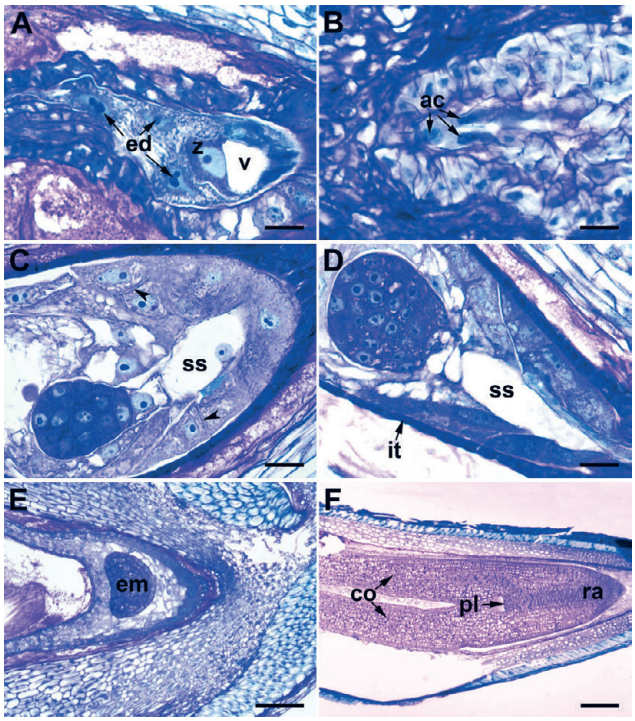

Fig. 6. Endosperm and embryo development in *Centaurea kilaea*: A) zygote and nuclear endosperm, B) persistent antipodal cells, C) and D) globular embryo with suspensor (arrows indicate the walls of endosperm cells), E) heart-shaped embryo, F) mature embryo. ac – antipodal cell, co – cotyledon, ed – endosperm, em – embryo, it – integumentary tapetum, pl – plumule, ra – radicle, ss – suspensor, v – vacuole, z – zygote. Scale bars = A–D, 20 μm; E, 100 μm; F, 200 μm.

The primary endosperm nucleus begins to divide before the zygote (Fig. 6A). The endosperm initially develops as free nuclei. The antipodal cells are still intact in this stage (Fig. 6B), and break down after the first zygote division. In the globular embryo stage, wall formation is observed between the endosperm nuclei, starting from the micropylar side (Fig. 6C). The mature seed does not contain endosperm (Fig. 7F).

The zygote has a pronounced polarity; the cytoplasm and nucleus are located at the apical end; there is a large vacuole in the basal portion (Fig. 6A). The zygote develops into an embryo by mitotic divisions. The first division is transverse and produces a basal cell toward the micropyle side and an apical cell toward the chalazal side. Embryo development is of the asterad type. The basal cell undergoes transverse divisions to give the suspensor, comprising 4–6 cells (Figs. 6C–E). The globular embryo is formed by the transverse and longitudinal divisions of cells in the proembryo (Fig. 6D). With further development, cells rapidly divide and the globular embryo becomes heart-shaped (Fig. 6E). After successive divisions, a mature dicotyledonous embryo forms with an obvious plumule (Fig. 6F).

Integument differentiation

In *C. kilaea*, the integument is initially homogeneous in structure (Fig. 4B). In the zygotene stage of meiotic prophase I, the innermost layer cells of the integument begin to elongate radially to differentiate into the endothelium (integumentary tapetum). The nucellar cells are still intact in this stage. At the end of megasporogenesis, the nucellar cells begin to deteriorate (Fig. 4C). During mitotic divisions (megagametogenesis), the nucellar cells break down and the remnants occur around the embryo sac (Figs. 4D-F). The mature embryo sac is surrounded by single-layered and radially elongated integumentary tapetum (Fig. 4G and Fig. 4H). In this stage, mucilage begins to accumulate rapidly on the walls of the integumentary cells close to the endothelium (Fig. 4G and Fig. 4H, arrowheads). After fertilization, the deposition of mucilage material continues between the primary wall and the plasma membrane on all sides of the cells, and the mucilage pushes the protoplast to the center of the cell (Fig. 7A). Afterwards, the protoplast of the mucilage cells degenerates, and the cell wall breaks down (Fig. 7B). In the globular embryo stage, the peri-endothelial region is completely filled with mucilage (Fig. 7C). Meanwhile, the endothelial cells elongate longitudinally to adapt to the growth of the embryo sac (Fig. 7B and Fig. 7D). In the torpedo-shaped embryo stage, the mucilage material appears homogeneous (Fig. 7D). As the embryo grows, the mucilage material is rapidly consumed, disappearing completely in the mature seed. Endothelium persists in the mature seed (Fig. 7F).

The integument has thin-walled parenchyma cells between the peri-endothelial zone and the outer epidermis

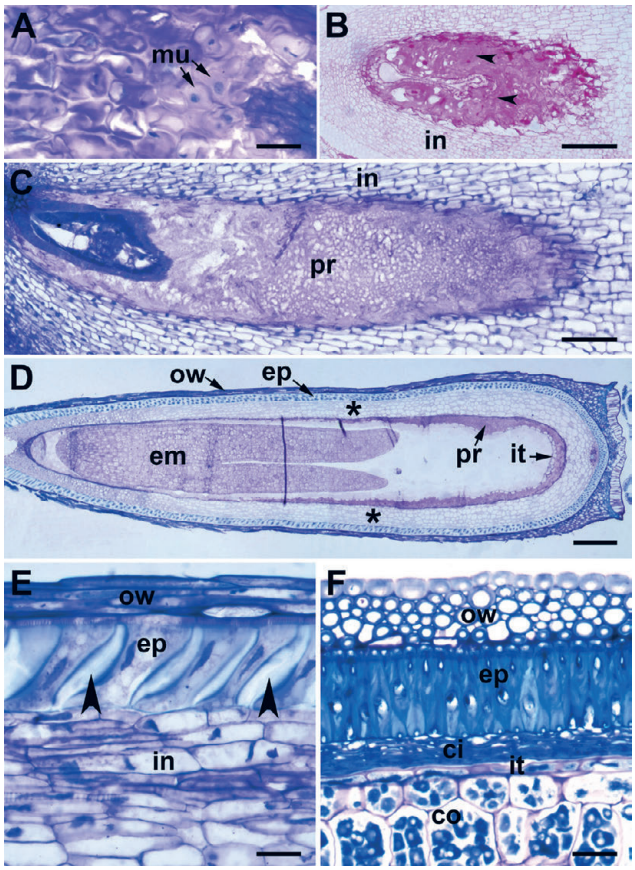

Fig. 7. Integument differentiation in *Centaurea kilaea*: A) deposition of mucilage (mu) in the integument (in) cells, B) degenerated mucilage cells stained with PAS (arrows), C) peri-endothelial region filled with mucilage, D) peri-endothelial region (pr) and integumentary tapetum (it) in the torpedo-shaped embryo (em) stage (asterisks indicate integumentary cells between the peri-endothelial zone and the outer epidermis), E) outer epidermis cells in the zygote resting stage (arrows indicate wall thickening), F) outer epidermis cells in the heart-shaped embryo stage. cl – cell lumen, co – cotyledon, ci – crushed integument cells, ep – epidermis, ow – ovary wall. Scale bars = A, E, F, 20 μm; B, C, 100 μm; D, 200 μm.

(Figs. 7B–D). There is no specific material accumulation in, or in the walls of, these cells. After fertilization, in the resting phase of the zygote, the outer epidermis cells of the integument begin to elongate radially starting from the micropylar pole. In the heart-shaped embryo stage, the outer epidermis cells elongate, and thickening develops on their radial walls (Fig. 7E). In the mature seed, the outer epidermis cells form the seed coat. The testa is represented by a single row of radially elongated, lignified cells (macrosclereids) (Fig. 7F).

Discussion

In this study, the embryology of *C. kilaea* (subfamily: Carduoideae, tribe: Cardueae), a tetraploid endemic species in Türkiye, was investigated histologically. *C. kilaea* shows the characteristics of the Asteraceae family in terms of anther structure (tetrasporangiate) and development (dicotyledonous anther wall). The anther wall consists of four layers (epidermis, endothecium, middle layer, tapetum). The outer secondary parietal layer develops an endothecium and a middle layer by periclinal division. The tapetum layer differentiates from the inner secondary parietal layer directly. These results agree with the pattern previously known for Asteraceae (Davis 1966, Yankova-Tsvetkova et al. 2016, 2018).

C. kilaea has an amoeboid type tapetum, which is the most representative of Asteraceae. It has also been observed in other tribes such as the Anthemideae (Li et al. 2010), Astereae (Davis 1968), Calenduleae (Ao 2007), Gnaphalieae (Davis 1962), Heliantheae (Gotelli et al. 2008), Inuleae (Pullaiah 1979), and Senecioneae (Pullaiah 1983). Secretory tapetum occurs in Eupatorieae (Franca et al. 2015), Stifftieae and Wunderlichieae (Bonifacio et al. 2018). Yankova-Tsvetkova et al. (2016, 2018) reported that initially, the tapetum of *Arnica montana* (Madieae) and *Centaurea achtarovii* (Cardueae) is secretory, and then it transforms into amoeboid. The persistent epidermis, fibrous endothecium, and ephemeral middle layers observed in *C. kilaea* are common in Asteraceae (Davis 1966).

Microspore mother cells of *C. kilaea* show simultaneous cytokinesis, resulting in tetrahedral type tetrads. These findings have also been reported in previous studies (Franca et al. 2015, Bonifacio et al. 2018); the cytokinesis of *Ambrosia artemisiifolia* is of the successive type (Liu et al. 2011). In *C. achtarovii* (Yankova-Tsvetkova et al. 2018), the tetrads are generally tetrahedral and isobilateral. *A. montana* has usually tetrahedral, occasionally isobilateral, rarely T-shaped, and linear tetrads (Yankova-Tsvetkova et al. 2016). The pollen grains of *C. kilaea* are shed with three cells (a vegetative cell and two sperm cells) from the mature anther, as in many Asteraceae members (Davis 1966). In *Stifftia chrysantha, Stifftia fruticose, Wunderlichia mirabilis,* and *Wunderlichia senae*, the pollen grains are shed with two cells (a vegetative cell and a generative cell) from the anther (Bonifacio et al. 2018). Mature pollen grains of *C. kilaea* contain insoluble polysaccharides and proteins. Similar observations have been also reported in *Galinsoga quadriradiata* (Kolczyk et al. 2015). Although *C. kilaea* is a tetraploid species (2n = 4x = 36) (Meric et al. 2010), meiosis is quite regular and the pollen fertility percentage is high (87%).

The ovary of *C. kilaea,* characteristically for the Asteraceae family, is single-chambered with two carpels and contains a single ovule with basal placentation. This feature has been reported for many Asteraceae family members (Davis 1966, Ao 2007, Chen et al. 2014, Franca et al. 2015, Bonifacio et al. 2018). The single archespore cell forms just below the nucellus epidermis and differentiates directly into the megaspore mother cell. The megaspore mother cell produces a linear type megaspore tetrad as a result of meiosis. The megaspore on the chalazal side is the functional megaspore, and the other three megaspores degenerate rapidly. This is characteristic of many Asteraceae family members (Davis 1966). Embryo sac development in *C. kilaea* is Polygonum-type, as it is in 70% of angiosperms. Monosporic Polygo-

num-type embryo sac development is mostly seen in Asteraceae family species, but monosporic Oenothera-, bisporic Allium-, tetrasporic Fritillaria-, Adoxa- and Drusa-type embryo sac developments are also seen (Davis 1966, Li et al. 2009, Musial et al. 2012). Thus, the embryo sac development of plants in the Asteraceae family is highly diverse.

The antipodal cells of *C. kilaea* persist until the first division of the zygote. They are similarly persistent in *Crepis bithynica, C. achtarovii, Wunderlichia* spp., *Ambrosia* spp., and *Taraxacum udum* (Yurukova-Grancharova and Dimitrova 2006, Musial et al. 2013, Chen et al. 2014, Bonifacio et al. 2018, Yankova-Tsvetkova et al. 2018). However, the antipodal cells in *Calendula officinalis* degenerate prematurely, so they are not found in the mature embryo sac of *C. officinalis* (Ao 2007). Before fertilization, the polar nuclei fuse to form the secondary nucleus of the embryo sac. Similar observations have been reported in previous studies (Chen et al. 2014, Yankova-Tsvetkova et al. 2016, 2018, Bonifacio et al. 2018).

Obturator cells with prominent nuclei and their secretions completely filled the micropylar canal in *C. kilaea*. These cells contain insoluble polysaccharides and proteins. The secretion produced by obturator cells gives an intense PAS-positive reaction; however, there is no protein in the secretion. Similarly, in sunflower and *Taraxacum* spp., the secretion (extracellular matrix) consists of only insoluble polysaccharides (Yan et al. 1991, Plachno et al. 2015). In *C. kilaea,* the obturator cells and their secretions play a key role in the growth of pollen tubes toward the micropyle, and further, their nutrition. It is similarly reported that the obturator plays roles in both the feeding of pollen tubes and their directing toward the micropyle in the sunflower (Yan et al. 1991).

In *C. kilaea*, the polar nuclei fuse before fertilization to form the secondary nucleus. This feature is common for Asteraceae (Davis 1966). Endosperm development is initially of nuclear type in *C. kilaea.* In the globular embryo stage, cytokinesis occurs between the free nuclei, starting from the micropylar side, and the endosperm transforms into a cellular type. Similar observations have been also reported in *Hieracium* spp.*, A. montana*, *C. bithynica,* and *C. achtarovii* (Yurukova-Grancharova and Dimitrova 2006, Yurukova-Grancharova et al. 2006, Yankova-Tsvetkova et al. 2016, 2018). The cellular endosperm is observed in *Ageratum, Ambrosia, Stifftia*, and *Wunderlichia* (Chen et al. 2014, Franca et al. 2015, Bonifacio et al. 2018). The embryogenesis of *C. kilaea* is of the asterad type, in which basal and apical cells participate in the formation of the embryo, as previously described for Asteraceae (Davis 1966).

The presence of integumentary tapetum (endothelium) has been reported in 65 dicotyledonous families with thin ovules (tenuinucellate and weakly crassinucellate) (Kapil and Tiwari 1978). The integumentary tapetum is a common feature in Asteraceae and forms in different developmental stages in the different representatives of the family (Davis 1966). The integument cells are initially homogeneously structured in *C. kilaea*. In the zygotene stage, the innermost layer cells of the integument elongate radially, and the endothelium forms. Endothelium begins to form in *C. achtarovii* at the one-nucleate stage, in *Hieracium pilosella* at the end of meiosis, in *Taraxacum udum* at the diad stage, and in *Ambrosia* spp. at the leptotene stage (Koltunow et al. 1998, Musial et al. 2013, Chen et al. 2014, Yankova-Tsvetkova et al. 2018).

In the mature female gametophyte stage, mucilage begins to accumulate rapidly on the walls of the integument cells close to the endothelium. The mucilage deposited between the primary wall and the plasma membrane pushes the protoplast toward the center of the cell. This region is called the peri-endothelial region (Pandey et al. 1978, Kolczyk et al. 2016, Plachno et al. 2016, 2017). In *Taraxacum*, the cells of the peri-endothelial region begin to differentiate at the young ovule stage, while in *Hieracium*, the wall changes of the peri-endothelial zone cells start during the four-nucleate embryo sac stage (Koltunow et al. 1998, Plachno et al. 2016). After fertilization, during the resting period of the zygote, the protoplast of the mucilage cell degenerates and the cell wall breaks down. Lysigenous cavities filled with mucilage are formed in the peri-endothelial region of *C. kilaea*. In *Hieracium* and *Pilosella*, the formation of lysigenous cavities occurs at the mature female gametophyte stage, while in *Taraxacum*, the peri-endothelial cells retain their individuality in the mature female gametophyte stage, and the formation of these cavities occurs during embryogenesis (Plachno et al. 2016, 2017, Gawecki et al. 2017). In the globular embryo stage, the peri-endothelial region is completely filled with mucilage. Meanwhile, endothelial cells elongate longitudinally to adapt to the growth of the ovule. In the torpedo-shaped embryo stage, the mucilage material appears homogeneous, and it disappears completely in the mature seed. Endothelium persists in mature seeds in *C. kilaea*. In *A. artemisiifolia*, endothelial cells begin to deteriorate during the multicellular proembryo stage. Meanwhile, integument cells adjacent to the endothelium also undergo hydrolysis. In the mature embryo period, the endothelium completely disappears (Chen et al. 2014). It is suggested by the present paper that mucilage might be a carbohydrate source for the developing embryo. Moreover, disruption of peri-endothelial cells creates the necessary space for the growing embryo. In the heart-shaped embryo stage of *C. kilaea*, the outer epidermis cells of the integument elongate radially, and their radial walls thicken. Like other members of the Asteraceae, the outer epidermis cells form the seed coat in the mature seed (Pandey et al. 1978; Kolczyk et al. 2016).

Conclusion

This study details the embryological characteristics and the fruit development of *C. kilaea*, a member of Asteraceae, a threatened coastal dune species that is facing a very high risk of extinction in the wild due to human activities. This is the first study on the reproductive biology and chemical

composition of the reproductive structures of the species. The revealed features of consisting structures of anthers, ovules, embryo and seeds show the characteristics of the Asteraceae family: tetrasporangiate anthers, dicotyledonous type of anther wall development, amoeboid tapetum, tetrahedral microspore tetrads, three-celled mature pollen grains containing insoluble polysaccharides and proteins, anatropous, unitegmic, and tenuinucellate ovule, Polygonum-type of embryo sac development, antipodal cells persisting until the first divisions of the zygote, obturator cells and their secretions (extracellular matrix) completely filling the micropylar canal, PAS-positive extracellular matrix without protein contains, mature embryo sac surrounded by an integumentary tapetum (endothelium), integument consisting of the integumentary tapetum (endothelium), peri-endothelial region, parenchymatous cells, and outer epidermis, from the inside out, with mucilage accumulation on the walls of the integument cells (peri-endothelial region) close to the endothelium in the mature female gametophyte stage, mature seed without mucilage, Asterad type of embryo development, endosperm of cellular type, mature seed without endosperm and with endothelium. The established normal unfolding of processes in the male and female generative sphere of *C. kilaea* and the high percent of viable pollen ensure a successful reproduction of populations of the species.

Acknowledgment

This study was supported by the Trakya University Scientific Research Projects Coordination Unit. Project Number: TUBAP-2014/72.

References

Ao, C., 2007: Comparative anatomy of bisexual and female florets, embryology in *Calendula officinalis* (Asteraceae), a naturalized horticultural plant. Scientia Horticulturae 114(3), 214–219. https://doi.org/10.1016/j.scienta.2007.06.019

Bonifacio, S.K.V., Moura, L.L., Marzinek, J., De-Paula, O.C., 2018: Comparative embryology of *Stifftia* and *Wunderlichia* and implications of its evolution in Asteraceae. Botanical Journal of the Linnean Society 189(2), 169–185. https://doi.org/10.1093/botlinnean/boy044

Bremer, K., 1994: Asteraceae: cladistics and classification. Timber Press, Portland.

Chen, B.X., Shi, C.Y., Huang, J.M., Wang, M., Liu, J.X., 2014: Megasporogenesis, female gametophyte development and embryonic development of *Ambrosia* L. in China. Plant Systematics and Evolution 300, 197–208. https://doi.org/10.1007/s00606-013-0872-0

Davis, G.L., 1962: Embryological studies in the Compositae, II. Sporogenesis, gametogenesis, and embryogeny in *Ammobium alatum* R. Br. Australian Journal of Botany 10, 65–75.

Davis, G.L., 1964: Embryological studies in the Compositae. IV. Sporogenesis, gametogenesis and embryogeny in *Brachycome ciliaris* (Labill.) Less. Australian Journal of Botany 12, 142–151.

Davis, G.L., 1966: Systematic embryology of the angiosperms. Wiley, New York.

Davis, G.L., 1968: Apomixis and abnormal anther development in *Calotis lappulacea* Benth. Australian Journal of Botany 16, 1–17.

Desole, L., 1954. Secondo contributo alla conoscenza dello sviluppo embriologico del genere *Centaurea* L. (Asteraceae). *Centaurea horrida* Bad. Giornale Botanico Italiano 61(2–3), 256–273. https://doi.org/10.1080/11263505409431572

Ekim, T., Koyuncu, M., Vural, M., Duman, H., Aytaç, Z., Adiguzel, N., 2000: Red data book of Turkish plants (Pteridophyta and Spermatophyta). Turkish Association for the Conservation of Nature, Ankara (In Turkish).

Franca, R.O., De-Paula, O.C., Carmo-Oliveira, R., Marzinek, J., 2015: Embryology of *Ageratum conyzoides* L. and *A. fastigiatum* R. M. King & H. Rob. (Asteraceae). Acta Botanica Brasilica 29(1), 8–15. https://doi.org/10.1590/0102-33062014abb3609

Gawecki, R., Sala, K., Kurczynska, E.U., Swiatek, P., Plachno, B.J., 2017: Immunodetection of some pectic, arabinogalactan proteins and hemicelluloses epitopes in the micropylar transmitting tissue of apomictic dandelions (*Taraxacum*, Asteraceae, Lactuceae). Protoplasma 254, 657–668. https://doi.org/10.1007/s00709-016-0980-0

Gotelli, M., Galati, B., Medan, D., 2008: Embryology of *Helianthus annuus* (Asteraceae). Annales Botanici Fennici 45(2), 81–96. https://doi.org/10.5735/085.045.0201

Heslop-Harrison, J., Heslop-Harrison, Y., Knox, R.B., Howlett, B., 1973: Pollen wall proteins: gametophytic and sporophytic fractions in the pollen walls of the Malvaceae. Annals of Botany 37(3), 403–412. https://doi.org/10.1093/oxfordjournals.aob.a084706

Janas, A.B., Szelag, Z., Musial, K., 2021: In search of female sterility causes in the tetraploid and pentaploid cytotype of *Pilosella brzovecensis* (Asteraceae). Journal of Plant Research 134, 803–810. https://doi.org/10.1007/s10265-021-01290-8

Kapil, R.N., Tiwari, S.C., 1978: The integumentary tapetum. Botanical Review 44, 457–490. https://doi.org/10.1007/BF02860847

Kolczyk, J., Stolarczyk, P., Plachno, B.J., 2016: Ovule structure of scotchthistle *Onopordum acanthium* L. (Cynareae, Asteraceae). Acta Biologica Cracoviensia Series Botanica 58(1), 19–28. https://doi.org/10.1515/abcsb-2016-0001

Kolczyk, J., Tuleja, M., Płachno, B.J., 2015: Histological and cytological analysis of microsporogenesis and microgametogenesis of the invasive species *Galinsoga quadriradiata* Ruiz & Pav. (Asteraceae). Acta Biologica Cracoviensia Series Botanica 57(2), 89–97. https://doi.org/10.1515/abcsb-2015-0018

Koltunow, A.M., Johnson, S.D., Bicknell, R.A., 1998: Sexual and apomictic development in *Hieracium*. Sexual Plant Reproduction 11, 213–230. https://doi.org/10.1007/s004970050144

Li, F., Chen, S., Chen, F., Teng, N., Fang, W., Zhang, F., Deng, Y., 2010: Anther wall development, microsporogenesis and microgametogenesis in male fertile and sterile chrysanthemum (*Chrysanthemum morifolium* Ramat., Asteraceae). Scientia Horticulturae 126(2), 261–267. https://doi.org/10.1016/j.scienta.2010.06.013

Li, J., Teng, N.J., Chen, F.D., Chen, S.M., Sun, C.Q., Fang, W.M. 2009: Reproductive characteristics of *Opisthopappus taihangensis* (Ling) Shih, an endangered Asteraceae species endemic to China. Scientia Horticulturae 121(4), 474–479. https://doi.org/10.1016/j.scienta.2009.02.025

Liu, J.X., Wang, M., Chen, B.X., Jin, P., Li, J.Y., Zeng, K., 2011: Microsporogenesis, microgametogenesis, and pollen morphology of *Ambrosia artemisiifolia* L. in China. Plant Systematic and Evolution 298, 1–8. https://doi.org/10.1007/s00606-011-0521-4

Meric, C., Arda, H., Güler, N., Dayan, S., 2010: Chromosome number and nuclear DNA content of *Centaurea kilaea* (Asteraceae), an endemic species from Turkey. Phytologia Balcanica 16, 79–84.

Musial, K., Gorka, P., Koscinska-Pajak, M., Marciniuk, P., 2013: Embryological studies in *Taraxacum udum* Jordan (sect. Palustria). Botany 91(9), 614–620. https://doi.org/10.1139/cjb-2013-0022

Musial, K., Koscinska-Pajak, M., Sliwinska, E., Joachimiak, A.J., 2012: Developmental events in ovules of the ornamental plant *Rudbeckia bicolor* Nutt. Flora 207(1), 3–9. https://doi.org/10.1016/j.flora.2011.07.015

O'Brien, T.P., Feder, N., McCully, M.E., 1964: Polychromatic staining of plant cell walls by Toluidine Blue O. Protoplasma 59, 368–373. https://doi.org/10.1007/BF01248568

Pandey, A.K., Singh, R.P., Chopra, S., 1978: Development and structure of seeds and fruits in Compositae: Cichorieae. Phytomorphology 28, 198–206.

Plachno, B.J., Kurczynska, E., Swiatek, P., 2016: Integument cell differentiation in dandelions (*Taraxacum*, Asteraceae, Lactuceae) with special attention paid to plasmodesmata. Protoplasma 253,1365–1372. https://doi.org/10.1007/s00709-015-0894-2

Plachno, B.J., Swiatek, P., Kozierdzka-Kiszkurno, M., Majesky, L., Marciniuk, J., Stolarczyk, P., 2015: Are obligatory apomicts invested in the pollen tube transmitting tissue? Comparison of the micropyle ultrastructure between sexual and apomictic dandelions (Asteraceae, Lactuceae). Protoplasma 252, 1325–1333. https://doi.org/10.1007/s00709-015-0765-x

Plachno, B.J., Swiatek, P., Kozierdzka-Kiszkurno, M., Szelag, Z., Stolarczyk, P., 2017: Integument cell gelatinization–The fate of the integumentary cells in *Hieracium* and *Pilosella* (Asteraceae). Protoplasma 254, 2287–2294. https://doi.org/10.1007/s00709-017-1120-1

Pullaiah, T., 1979: Studies in the embryology of Compositae. IV. The tribe Inuleae. American Journal of Botany 66(10), 1119–1127. https://doi.org/10.2307/2442210

Pullaiah, T., 1983: Studies in the embryology of Senecioneae (Compositae). Plant Systematics and Evolution 142, 61–70. https://doi.org/10.1007/BF00989604

Renzoni, G.C., 1970: Studi Sul Genere *Centaurea* L. (Asteraceae): I. Analisi Embriologica di *Centaurea cineraria* L. var. *veneris* Sommier. Giornale Botanico Italiano 104(6), 457–468. https://doi.org/10.1080/11263507009426518

Sen, A., Ozbas Turan, S., Akbuga, J., Bitis, L., 2015: *In vitro* antiproliferative activity of endemic *Centaurea kilaea* Boiss. against human tumor cell lines. Clinical and Experimental Health Sciences 5, 149–153.

Siljak-Yakovlev, S., Solic, M.E., Catrice, O., Brown, S.C., Papes, D., 2005: Nuclear DNA content and chromosome number in some diploid and tetraploid *Centaurea* (Asteraceae: Cardueae) from the Dalmatia region. Plant Biology 7(4), 397–404. https://doi.org/10.1055/s-2005-865693

Sirin, E., Uysal, T., Bozkurt, M., Ertugrul, K., 2020: *Centaurea akcadaghensis* and *C. ermenekensis* (Asteracaeae), two new species from Turkey. Mediterranean Botany 41(2), 173–179. https://doi.org/10.5209/mbot.68628

Wagenitz, G., 1975: *Centaurea* L. In: Davis, P.H. (ed.), Flora of Turkey and the East Aegean Islands, vol. 5, 465-585. Edinburgh University Press, Edinburgh.

Yan, H., Yang, H., Jensen, W., 1991: Ultrastructure of the micropyle and its relationship to pollen tube growth and synergid degeneration in sunflower. Sexual Plant Reproduction 4, 166–175. https://doi.org/10.1007/BF00190000

Yankova-Tsvetkova, E., Ilieva, I., Stanilova, M., Stoyanov, S., Sidjimova, B., 2018: Reproductive biology of the endangered Bulgarian endemic *Centaurea achtarovii* (Asteraceae) Biologia 73, 1163–1175. https://doi.org/10.2478/s11756-018-0126-2

Yankova-Tsvetkova, E., Yurukova-Grancharova, P., Baldjiev, G., Vitkova, A., 2016: Embryological features, pollen and seed viability of *Arnica montana* (Asteraceae) – a threatened endemic species in Europe. Acta Botanica Croatica 75(1), 39–44. https://doi.org/10.1515/botcro-2016-0014

Yurukova-Grancharova, P., Dimitrova, D., 2006: Cytoembryological study of *Crepis bithynica* (Asteraceae) from Bulgaria. Flora Mediterranea 16, 33–43.

Yurukova-Grancharova, P., Robeva-Davidova, P., Vladimirov, V., 2006: On the embryology and mode of reproduction of selected diploid species of *Hieracium* s.l. (Asteraceae) from Bulgaria. Flora 201(8), 668–675. https://doi.org/10.1016/j.flora.2006.01.003

Acta Bot. Croat. 84 (1), 63–69, 2025
DOI: 10.37427/botcro-2025-010

CODEN: ABCRA 25
ISSN 0365-0588
eISSN 1847-8476

Cymbella stomachsis sp. nov. (Bacillariophyta; Cymbellaceae), a new species from Guangdong Province, China

Yi-Han Zhao[1], Ji-Shu Guo[1], Zheng-Bin Tang[1], Yun Zhang[2], Shao-Feng Huang[3]*, John Patrick Kociolek[4], Yan-Ling Li[1]*

[1] Yunnan University, School of Ecology and Environmental Science, Institute for Ecological, Research and Pollution Control of Plateau Lakes, Kunming 650500, P. R. China

[2] Hubei Normal University, College of Life Sciences, Huangshi 435002, P. R. China

[3] Center for Ecology and Environment Monitoring and Research, Administration for Pearl River, Basin-South China Sea Ecology and Environment, Ministry of Ecology and Environment, Guangzhou 510611, P. R. China

[4] University of Colorado, Museum of Natural History and Department of Ecology and Evolutionary Biology, Boulder, Colorado-80309, USA

Abstract – A new diatom species from the genus *Cymbella* C. Agardh is described from samples collected during a survey of freshwater diatoms from Modaomen Channel, Guangdong Province, China. With the aid of light microscopy (LM) and scanning electron microscopy (SEM), we give a detailed morphological description of *Cymbella stomachsis* sp. nov., which is placed in the genus *Cymbella* according to the shared features of asymmetry about the apical axis, deflection of the external terminal raphe fissures towards the dorsal margin, and the presence of apical pore fields and stigmata. Although it shares some similar structural features with *C. tumida*, *C. stuxbergii*, *C. stuxbergioides*, *C. pesudostuxbergii*, *C. mexicana* and *C. australica*, *C. stomachsis* sp. nov. is easily distinguished by the valve outline, the shape and density of areola, and the appearance of a lack of an intermissio at the central nodule. Especially, the structure of the intermissio is absent in similar taxa. This work is important for its enrichment of our understanding of the genus *Cymbella* and improvement of the database of diatom biodiversity and distribution in China.

Keywords: China, Cymbellaceae, diatom, morphology, Pearl River, taxonomy

Introduction

The diatom genus *Cymbella* C. Agardh was established almost 200 years ago (Agardh 1830), with *C. cymbiformis* C. Agardh (1830) chosen later as the type species of the genus (Håkansson and Ross 1984). With advances in observation tools and increased understanding, 19 genera have been separated from *Cymbella* (Liu et al. 2021, Kulikovskiy et al. 2022). After several taxonomic revisions, Krammer (2002) revised and summarized the characteristics of this genus as follows: the shape of the valve with cymbelloid symmetry, the terminal raphe fissures bent towards the dorsal margin, at each apex the presence of one apical pore field, and one or more stigmata positioned on the ventral side of the valves. Subsequently, a series of papers reported many new species in this genus (Cantonati et al. 2010, Le Cohu et al. 2015, Bahls 2019, Solak et al. 2021). At present, AlgaeBase notes more than three hundred described taxa in the genus (Guiry and Guiry 2023). In China, our research over the last 20 years also found many new species. (Li et al. 2003a, 2005, 2019, Gong and Li 2011, Gong et al. 2013, Hu et al. 2013, Liu et al. 2021, Zhang et al. 2021).

New species of *Cymbella* have been described worldwide: from Europe, South America, Asia, North America, Africa, Australasia and Antarctica (Krammer 2002, Cantonati et al. 2010, Le Cohu et al. 2015, Wengrat et al. 2015, Bahls 2019, Li et al. 2019, Liu et al. 2021, Solak et al. 2021, Zhang et al. 2021). In China, research has been conducted in Fujian Province, Heilongjiang Province, Sichuan Province, Guizhou Province, Yunnan Province, Liaoning Province, Gansu Province, Qinghai Province, Hubei Province, Inner Mongolia, Xinjiang and Tibet (Li et al. 2003b, 2004,

* Corresponding authors e-mail: yanlingli@ynu.edu.cn, hsf@zjnhjg.mee.gov.cn

2005, 2007a,b, 2012, You et al. 2005, Liu et al. 2006, Wu et al. 2008, Liu et al. 2012, Fu et al. 2013, Sun and Zhi 2015). There have been no systematic diatom surveys in the Pearl River basin.

In this paper, we describe a new species of *Cymbella* from a tributary of the Pearl River: the Modaomen Channel of Guangdong Province, China. We present light and scanning electron microscopy observations on the valve of a new species and provide information on its ecology. *Cymbella stomachsis* sp. nov. is also compared with six most similar species: *C. tumida* (Brébisson) Van Heurck (1880: 64), *C. stuxbergii* (Cleve) Cleve (1894: 173), *C. stuxbergioides* Kulikovskiy, Metzeltin & Lange-Bertalot (2012: 81), *C. pseudostuxbergii* Kulikovskiy, Metzeltin & Lange-Bertalot (2012: 80), *C. mexicana* (Ehrenberg) Cleve (1894: 177) and *C. australica* (A.W.F. Schmidt) Cleve (1894: 176).

Material and methods

The Modaomen Channel is located in Zhuhai city, Guangdong Province, China. It is one of the tributaries of the Xijiang River, which in turn is a major tributary of the Pearl River (Hu 2010). The region is characteristic by a subtropical monsoon climate with distinct dry and wet seasons (Hu 2010, Han et al. 2022). According to Zhang et al. (2022), the water quality in this area may be considered mesotrophic. In July 2021, the sample containing the species of *Cymbella* studied here was collected from rock scrapings from the Modaomen Channel (22°24.523' N, 113°36.976' E) (Fig. 1).

pH and specific conductance of the river water were measured *in situ* using a YSI 650 multi-parameter display system (650 MDS, YSI Incorporated 1700/1725 Brannum Lane, Yellow Springs, OH 45387 USA) with a 600XL probe. The results are shown in Tab. 1.

Tab. 1. Physical and chemical parameters in Modaomen Channel on 29th July 2021.

	Modaomen Channel
Latitude (°N)	22°24.523'
Longitude (°E)	113°36.976'
Altitude (m)	78
Water temperature (°C)	29.8
pH	7.81
Dissolved Oxygen (mg L^{-1})	7.46
Conductivity (μs cm^{-1})	262

Algae was removed from the rocks with a toothbrush. 10% HCl and 30% H_2O_2 were used to dissolve and remove the calcium carbonate and organic matter, respectively (Battarbee 1986). After being washed several times in distilled water, a part of the cleaned diatom material was air-dried onto cover slips and mounted on glass slides using Naphrax. The sample and slides were deposited in the Herbarium of the Institute for Ecological Research and Pollution Control of Plateau Lakes, Yunnan University, Kunming, P.R. China (YUK). The isotype slides are stored in the Key Laboratory of Biodiversity of Aquatic Organisms, Harbin Normal University.

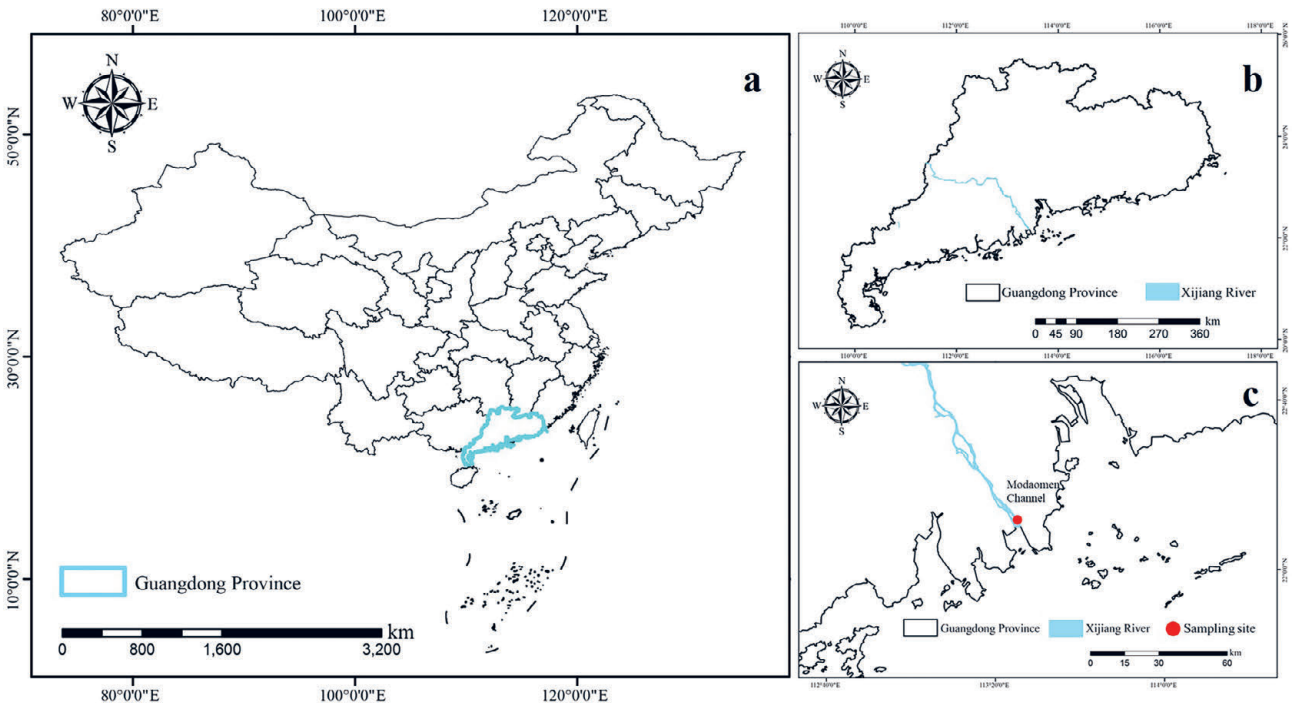

Fig. 1. Study areas and the sampling sites: a – Map of China and Guangdong Province, b – Guangdong Province and Xijiang River, c – Xijiang River and sampling point.

Morphological features of diatoms were observed under light microscopy (LM) using a ZEISS Axioscope 5 (DIC, ×1000, oil immersion lens) research microscope with a Canon EOS 6D Mark II digital camera. At least 500 valves of the associated diatom community were identified and counted. Cleaned material for scanning electron microscopy (SEM) was air-dried onto cover glasses, mounted onto stubs, and coated with 20 nm of Au (EMSCOP SC 500 sputter coater). The resulting stubs were examined and photographed in a LEO 1530 SEM with an acceleration voltage of 5–10 kV. The image analysis and plate arrangement were processed with the program Adobe Photoshop (CS5) (V. 12.1, Adobe Systems, San Jose, CA, USA). Description of the new species follows the terminology provided by Krammer (2002).

Results

Taxonomy

Class Bacillariophyceae Haeckel 1878: 95

Subclass Bacillariophycidae D.G. Mann in Round et al. 1990: 125

Order Cymbellales D.G Mann in Round et al. 1990: 653

Family Cymbellaceae D. Siliva and W. José 2016

Genus *Cymbella* C. Agardh 1830: 10

Cymbella stomachsis Li, sp. nov. (Figs. 2–4)

LM (Fig. 2): Valves semielliptic, strongly dorsiventral. Dorsal margin strongly convex. Ventral margin slightly convex, straight and with slightly tumid central portion. Valve ends distinctly constricted on both the dorsal and ventral sides, protracted, with truncate and bluntly square apices. Length 40.0 – 52.0 µm, width 14.0 – 17.0 µm. Maximum length/width ratio about 3.0 (N = 30). Axial area narrow, arched. Central area, orbicular-rhomboidal, occupying 2/5 – 2/3 the width of the valve. Raphe lateral, becoming filiform near the distal and proximal ends. External central raphe ends with distinct central pores. External distal raphe fissures hooked towards dorsal margin. Striae radiate more strongly towards the central portion, punctate-lineate, slightly wavy at the valve center dorsally, density 11 – 13/10 µm in the central valve portion becoming 13 – 14/10 µm near the ends. Individual areolae visible, 21 – 25/10 µm. 1 – 2 (mostly one) stigmata present at the ventral side of the central nodule.

In SEM external valve view (Fig. 3): Raphe with central ends dilated, drop-shaped pores and curved to the ventral side (Fig. 3A, 3C). The external distal raphe ends hooked, bent towards the dorsal side, and terminating on the mantle (Fig. 3A, 3B). Apical pore fields (APFs) are composed of vertically aligned porelli, not bisected, evidently present at the valve mantle of both apices (Fig. 3A, 3B). One small round stigma located on the ventral side of the central nodule (Fig. 3A, 3C). Transapical striae formed by slit-like areolae with apically oriented foramina, although there are small, rounded partly T-shaped, V-shaped or irregularly shaped areolae adjacent to the axial and central areas (Fig. 3A – 3C). The number of puncta per stria varies between 25 and 30 in 10 µm.

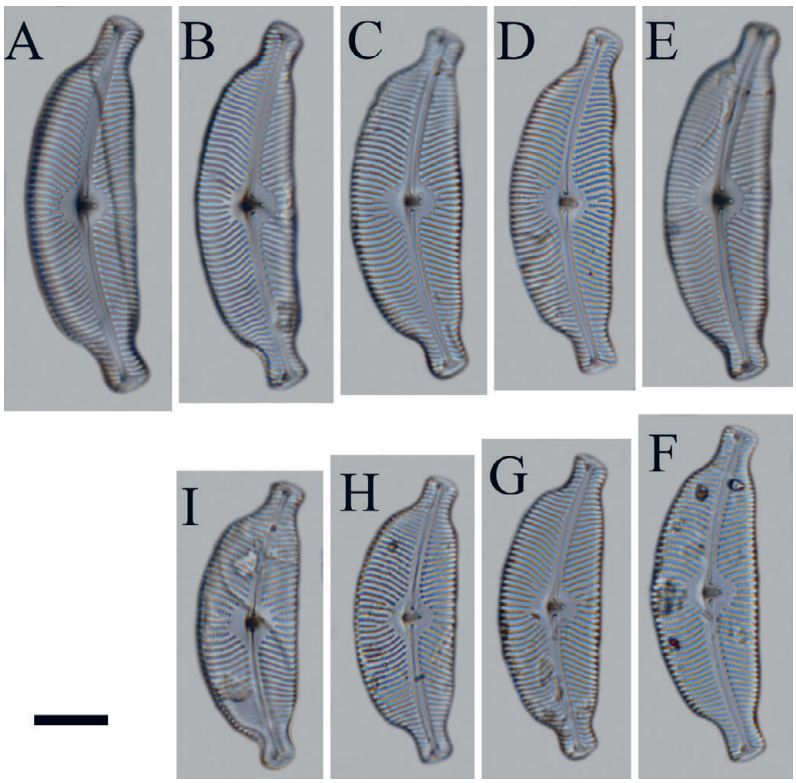

Fig. 2. *Cymbella stomachsis* sp. nov. under differential interference contrast microscopy. A-I – valve views, showing size range and variability of the holotype population. B – is of the holotype. Scale bar = 10 µm

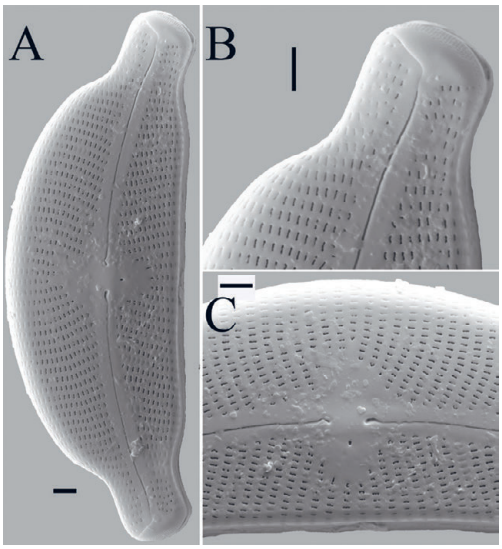

Fig. 3. *Cymbella stomachsis* sp. nov. under scanning electron microscope. A – external view of an entire valve. B – valve apices, striae with areolae mostly slit-like, the distal raphe ends dorsally bent and APFs composed of vertically aligned porelli, not bisected. C – external view of valve center, the central ends dilated with drop-shaped pores deflected ventrally and one small round stigma located on the ventral side. Scale bar = 2 μm.

In SEM internal valve view (Fig. 4): Stria opening in depressions between virgae elliptical in shape (Fig. 4A – 4C). The internal central raphe ends undulate, discontinuous, revealed with the absence of a hooded structure over the central nodule (Fig. 4A, 4C). The internal distal proximal raphe ends terminate in helictoglossae which are raised prominently from the internal valve surface (Fig. 4A, 4B). APFs composed of small, parallel arranged porelli (Fig. 4A, 4B). The large, slit-like stigma opening has irregular projections (Fig. 4A, 4C). The proximal ends of 11–13 striae form a semi-circular central area.

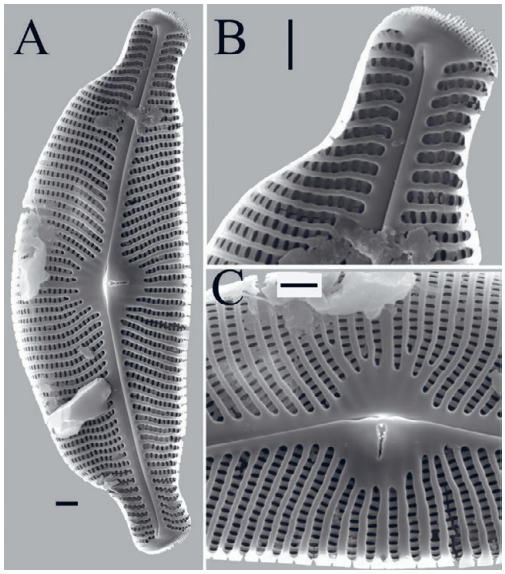

Fig. 4. *Cymbella stomachsis* sp. nov. under scanning electron microscope. A – internal view of entire valve. B – internal view of valve apices, the internal distal raphe ends terminate in helictoglossae, APFs composed of small, parallel arranged alveoli. C – showing the valve central area. One large, slit-like stigma opening with irregular structures. In this specimen the hooded structure over the central area is not present, revealing the raphe is not continuous. Scale bar = 2 μm.

Type: China. Guangdong Province: Modaomen waterway, freshwater, 22°24.523' N, 113°36.976' E, elevation 78 m a.s.l., 29th July 2021, rock scraping samples collected by Hong-Qu Tang (Holotype MDM202172902 in Coll. Hong-Qu Tang, Jinan University, Guangzhou, China = Fig. 2B; Isotype YUNGL20220320, Harbin Normal University, Harbin, China)

Etymology: *stomachsis*, referring to the stomach-like shape of new species.

Ecology: *Cymbella stomachsis* is found in the Modaomen Channel, Zhuhai city, Guangdong Province, on stone surfaces. Environmental measurements from the site at the time of collection include moderately alkaline pH (7.81), dissolved oxygen of 7.46 mg L^{-1}, conductivity of 262 μs cm^{-1}, and water temperature of 29.8 °C. At the type locality, the related species in decreasing order of abundance were *Amphora linearis* F. Meister (1935: 97), *Seminavis strigosa* (Hustedt) Danieledis & Economou-Amilli (2003: 30), *Nitzschia clausii* Hantzsch (1860: 40), *Navicula viridula* var. *rostellata* (Kützing) Cleve (1895: 15), *Navicula schroeteri* F. Meister (1932: 38), *Gomphonema parvulum* (Kützing) Kützing (1849: 65), *Aulacoseira granulata* (Ehrenberg) Simonsen (1979: 58).

Discussion

Cymbella stomachsis sp. nov. is assigned to the genus *Cymbella* by its cymbelloid valve shape, dorsally deflected external distal raphe fissures and by the presence of APFs and stigmata. *C. stomachsis* has some unique features, such as valve ends that are distinctly tapered on the dorsal and ventral sides, with truncate and bluntly square apices, with undulate striae near the ends on the dorsal side and with intermissio separating the proximal raphe ends. In particular, the intermissio structure is not typical of other species of *Cymbella*. However, the intermissio in *C. stomachsis* and *Didymosphenia* are nearly identical, and this may prove close phylogenetic relationships between these taxa (Kociolek and Stoermer 1988, Kulikovskiy et al. 2012, Metzeltin and Lange-Bertalot 2014). Comparing the outline of the valve and striae pattern, *C. stomachsis* is more similar to six species *C. tumida*, *C. stuxbergii*, *C. stuxbergioides*, *C. pseudostuxbergii*, *C. mexicana* and *C. australica*, the morphological characteristics of which are compared in Tab. 2.

Although there are some similarities among the six similar species, the new species can be easily distinguished from *Cymbella tumida*, *C. stuxbergii*, *C. stuxbergioides*, *C. pseudostuxburgii*, *C. mexicana* and *C. australica* by the shape of the valve end and the central area. According to the characteristics mentioned above, *C. stomachsis* most

Tab. 2. Morphological characteristics of *Cymbella stomachsis* sp. nov. compared with other similar taxa.

Species/Feature	Valve length (µm)	Valve width (µm)	Length/ width ratio	Number of areolae in 10 µm	Stigmata	Central area	Valve end	Distribution	Reference
C. stomachsis	40–52	14–17	Max 3.0	21–25	Small 1	orbicular-rhomboidal, 2/5–2/3 the width of the valve	truncate, bluntly square and extending	mesotrophic	Present study
C. tumida	35–95	16–22	Max 4.0	14–19	Very large 1	orbicular-rhomboidal, 1/2–1/3 the width of the valve	mostly rostrate	oligotrophic and mesotrophic	Krammer 2002
C. stuxbergii	48–94	20–29	Max 3.2	16–21	7–13 frequently about 10	orbicular to irregular, 1/4–1/2 the width of the valve	rostrate to truncate protracted and bluntly rounded	oligotrophic	Krammer 2002
C. mexicana	80–170	20–33	Max 6	8–12	Small 1	orbicular, rhomboidal to irregular, 1/5–1/4 the width of the valve	not or slightly truncate and obtusely rounded	none	Krammer 2002
C. australica	100–142	24–30	Max 5.1	12–15	Very large 1	orbicular-rhomboidal, 1/2 the width of the valve	not or slightly truncate and obtusely rounded	none	Krammer 2002
C. stuxbergioides	42.7–72.7	18.7–23.3	Max 3.3	21–23	none	none	less abruptly prostrated	none	Kulikovskiy et al. 2012
C. pesudostuxbergii	45–97	18–29	none	20–22	none	none	most indistinctly short-protracted	none	Kulikovskiy et al. 2012

Fig. 5. *Cymbella tumida* under scanning electron microscope. A – internal view of entire valve. B – internal view of valve apices, the internal distal raphe ends terminate in helictoglossae. APFs composed of small, parallel arranged alveoli. C – showing the valve central area. One water-drop shape stigma alveoli and filled with silica located on ventral side. Scale bar = 3 µm. *C. tumida* was collected from North River, in the sample NR 27 (113°30'26'' E, 24°38'11'' N), in July 2021.

closely resembles *C. tumida* (Fig. 5), but there are also some features that can be used to separate *C. stomachsis*.

For example, when the shape of the end is compared, the new species has more obvious constrictions near the ends. In terms of the internally proximal raphe ends, the proximal raphe ends of the new species are discontinuous with the intermissio while they are continuous in *C. tumida*. Taking into consideration the areola shape, the areolae of *C. tumida* are more oblong than those of *C. stomachsis*. With respect to the internal shape of stigmata, the stigmata of the new species are slit-like, while the stigmata of *C. tumida* are water-drop shaped. Besides, the size range of *C. stomachsis* is smaller than that of *C. tumida*. Finally, the areola density is very high compared to *C. tumida*. In summary of the above, these differences are sufficient to justify the description of *C. stomachsis* as an independent species.

Regarding the ecological distribution of *Cymbella*, the genus *Cymbella* tends to be distributed in lakes (Gong and Li 2011, Hu et al. 2013, Liu et al. 2021), reservoirs (Çelekli and Arslanargun 2019, Hansika and Yatigammana 2019), and rivers (Li et al. 2019, Long et al. 2022). For example, of the six species similar to our new species, *C. stuxbergii* is found not only in ancient lakes, but also in rivers (Cleve-Euler 1955, Foged 1993). In addition, some of these taxa are reported from ancient lakes. For example, *C. stuxbergioides* and *C. pesudostuxbergii* were reported in Lake Baikal (Kulikovskiy et al. 2012), while *C. australica* was found in Lake Tanganyika (Krammer 2002). Finally, others may live in lotic environments. For example, *C. tumida* and *C. mexicana* were found in river systems (Terao et al. 1993, Gou et al. 2015), which is same environment in which we found *C. stomachsis* sp. nov.

With global climate change and human activities, freshwater ecosystems are facing multiple crises (Dudgeon et al. 2006). As a member of the Generic Index (the sum of the ratio of the relative abundance of *Achnanthes*, *Cocconeis* and *Cymbella* to the relative abundance of *Cyclotella*, *Aulacoseira* and *Nitzschia* was calculated) (Wu 1999), *Cymbella* plays an important role in the indicators of water quality. In freshwater, *Cymbella* species can survive in oligotrophic, mesotrophic and eutrophic environments (Krammer 2002, Hu et al. 2013). For example, for similar species mentioned above, *C. stuxbergii* lives in freshwater with oligotrophic environmental conditions (Krammer 2002). *Cymbella tumida* has been found both in epiphyton and phytoplankton, within oligotrophic or mesotrophic water quality conditions (Gou et al. 2015, Cespedes-Vargas et al. 2016). In this study, *C. stomachsis* sp. nov. was found from rock scraping samples in the Modaomen Channel which is a mesotrophic environment according to Zhang et al. (2022). In short, the new species found in this genus it is helpful in increasing our understanding of *Cymbella* taxa and their ecological preferences and tolerances, and thus in providing more accurate diatom indices used in water quality evaluation.

Acknowledgments

This work was supported by the project of National Sciences and Foundation of China (Grant No. 42172206) and Yunnan Fundamental Research Project Q6 (202301AS070056). We are grateful to Ms. Yulan Luo for help in the scanning electron microscope observations.

References

Agardh, C. A. 1830: Conspectus criticus diatomacearum. Literis Berlingianus, Lundae.

Bahls, L. 2019: *Cymbella fontinalis* sp. nov. (Bacillariophyta, Cymbellaceae) from springs in the Rocky Mountains of North America. Nova Hedwigia 108(1–2), 1–15. https://doi.org/10.1127/nova_hedwigia/2018/0501

Battarbee, R. W., 1986: Diatom analysis. In: Berglund, B. E. (ed.), Handbook of holocene palaeoecology & palaeohydrology, 527–570. John Wiley and Sons Ltd., Chichester, UK.

Cantonati, M., Lange-Bertalot, H., Scalfi, A., Angeli, N., 2010: *Cymbella tridentina* sp. nov. (Bacillariophyta), a crenophilous diatom from carbonate springs of the Alps. Journal of the North American Benthological Society 29(3), 775–788. https://doi.org/10.1899/09-077.1

Çelekli, A., Arslanargun, H., 2019: Bio-assessment of surface waters in the south-east of Gaziantep (Turkey) using diatom metrics. Annales de Limnologie-International Journal of Limnology 55, 11. https://doi.org/10.1051/limn/2019010

Cespedes-Vargas, E., Umana-Villalobos, G., Silva-Benavides, A. M., 2016: The tolerance of ten diatom species (Bacillariophyceae) to water's physico-chemical factors in the Sarapiqui River, Costa Rica. Revista De Biologia Tropical 64(1), 105–115. https://doi.org/10.15517/rbt.v64i1.18295

Cleve-Euler, A. 1955: Die Diatomeen von Schweden und Finnland. Kungliga Svenska Vetenskapsakademiens Handlingar, Fjärde Serian 5, 1–232.

Cleve, P.T. 1894: Synopsis of the naviculoid diatoms. Part I. Kongliga Svenska Vetenskapsakademiens Handlingar Series 426, 1–194.

Cleve, P. T. 1895: Synopsis of the naviculoid diatoms. Part II. Kongliga Svenska Vetenskapsak Akademiens Handlingar, 27, 1–219.

Dudgeon, D., Arthington, A. H., Gessner, M. O., Kawabata, Z. I., Knowler, D. J., Leveque, C., Naiman, R. J., Prieur-Richard, A. H., Soto, D., Stiassny, M. L. J., Sullivan, C.A., 2006: Freshwater biodiversity: importance, threats, status and conservation challenges. Biological Reviews 81(2), 163–182. https://doi.org/10.1017/S1464793105006950

Foged, N., 1993: Some diatoms from Siberia, especially Lake Baikal. Diatom Research 8, 231–279.

Fu, B. R., Zhang, R. J., Li, X., Hui, X. J., Zhang, N., Fu, H., Zhang, Z., Xie, Y., 2013: Differences of periphytic algal community structure in different sections of Fanhe River, Liaoning Province of Northeast China. Chinese Journal of Ecology 32, 407–411 (in Chinese with English abstract).

Gong, Z. J., Li, Y. L., 2011: *Cymbella fuxianensis* Li and Gong sp. nov. (Bacillariophyta) from Yunnan Plateau, China. NOVA HEDWIGIA 92(3–4), 551–556. http://159.226.73.51/handle/332005/11011

Gong, Z. J., Li, Y. L., Metzeltin, D., Lange-Bertalot, H., 2013: New species of *Cymbella* and *Placoneis* (Bacillariophyta) from late Pleistocene Fossil, China. Phytotaxa 150(1), 29–40. https://doi.org/10.11646/phytotaxa.150.1.2

Gou, T., Ma, Q. L., Xu, Z. C., Wang, L., Li, J., Zhao, X. M., 2015: Phytoplankton community structure and eutrophication risk assessment of Beijiang River. Environmental Science 36, 946–954. [In Chinese with English abstract] https://link.cnki.net/doi/10.13227/j.hjkx.2015.03.025

Guiry, M. D., Guiry, G. M., 2023: Algaebase. Retrieved December 3, 2023 from https://www.algaebase.org/

Håkansson, H., Ross, R., 1984: Proposals to designate conserved types for *Cymbella* C. Agardh and *Cyclotella* (Kützing) Brébisson, and to conserve *Rhopalodia* O. Müller against *Pyxidicula* Ehrenberg (all Bacillariophyceae). Taxon 33(3), 525–531. https://doi.org/10.2307/1221005

Han, Z. Y., Li, H. Y., Xie, H. L., Zuo, S. H., Xu, T., 2022: Study of the long-term morphological evolution of the Modaomen Channel in the Pearl River delta, China. Water 14(9), 1331. https://doi.org/10.3390/w14091331

Hansika, R. V. H., Yatigammana, S. K., 2019: Distribution of diatom assemblages in the surface sediments in Sri Lankan reservoirs located in the main climatic regions and potential of using them as environmental predictors. Tropical Ecology 60, 415–425. https://doi.org/10.1007/s42965-019-00045-w

Hantzsch, C. A., 1860: Neue Bacillarien: *Nitzschia vivax* var. *elongata*, *Cymatopleura nobilis*. Hedwigia 2, 1–40.

Hu X. 2010: Numerical study of saltwater intrusion in Modaomen of Pearl Estuary. Doctoral dissertation, Tsinghua University (in Chinese with English abstract).

Hu, Z. J., Li, Y. L., Metzeltin, D., 2013: Three new species of *Cymbella* (Bacillariophyta) from high altitude lakes, China. Acta Botanica Croatica 72(2), 359–374. https://doi.org/10.2478/botcro-2013-0005

Kociolek, J. P., Stoermer, E. F. 1988: A preliminary investigation of the phylogenetic relationships of the freshwater, apical pore field-bearing cymbelloid and gomphonemoid diatoms (Bacillariophyceae). Journal of Phycology 24: 377–385.

Krammer, K. 2002: Diatoms of Europe, 3, Cymbella. A. R. G. Gantner Verlag K. G., Ruggell.

Kulikovskiy, M., Kociolek, J. P., Liu, Y., Kuznetsova1, I., Glushchenko1, A., 2022: *Vladinikolaevia*, gen. nov. – a new enigmatic freshwater diatom genus (Cymbellaceae; Bacillariophyceae)

from Mongolia. Fottea, Olomouc 22(2), 204–210. https://doi.org/10.5507/fot.2021.022

Kulikovskiy, M. S., Lange-Bertalot, H., Metzeltin, D., Witkowski, A., 2012: Lake Baikal: Hotspot of endemic diatoms I. Iconographia Diatomologica 23, 1–607.

Kützing, F. T., 1849: Species algarum. Friedrich Arnold Brockhaus, Leipzig.

Le Cohu, R., Azemar, F., Tudesque, L., 2015: *Cymbella marvanii* sp. nov., a new *Cymbella* species from the French Pyrenees. Diatom Research 30(3), 257–262. https://doi.org/10.1080/0269249X.2015.1071284

Li, B., Feng, J., Xie S.,L., 2012: Distribution and Floristic Characteristics of Algae in the Gongbu Nature Reserve, Tibet. Acta Botanica Boreali-Occidentalia Sinica 32, 807–814. [In Chinese with English abstract]

Li, Y. L., Bao, M. Y., Liu, W., Kociolek, J.,P., Zhang, W., 2019: *Cymbella hechiensis* sp. nov., a new cymbelloid diatom species (Bacillariophyceae) from the upper tributary of Liujiang River, Guangxi Province, China. Phytotaxa 425, 49–56. https://doi.org/10.11646/phytotaxa.425.1.4, Shen, J., 2007a: Freshwater diatoms of eight lakes in the Yunnan Plateau, China. Journal of Freshwater Ecology 22, 169–171. https://doi.org/1080/02705060.2007.9664161

Li, Y. L., Gong, Z. J., Xie, P., Shen, J., 2007b: Floral survey of the diatom genera *Cymbella* and *Gomphonema* (Cymbellales, Bacillariophyta) from the Jolmolungma mountain region of China. Cryptogamie Algologie 28, 209–244.

Li, Y. L., Gong, Z. J., Xie, P., Shen, J., 2005: New species and new records of fossil diatoms from the Late Pleistocene of the Jianghan Plain, Hubei Province. Acta Micropalaeontologica Sinica 22, 304–310 (in Chinese with English abstract).

Li, Y. L., Shi, Z. X., Xie, P., Rong, K. W., 2003a: New varieties of *Gomphonema* and *Cymbella* (Bacillariophyta) from Qinghai Province. Acta Hydrobiologica Sinica 27, 147–148 (in Chinese with English abstract).

Li, Y. L., Xie, P., Gong, Z. J., Shi, Z. X., 2003b: Cymbellaceae and Gomphonemataceae (Bacillariophyta) from the Hengduan Mountains region (southwestern China). Nova Hedwigia 76, 507–536. https://doi.org/10.1127/0029-5035/2003/0076-0507

Li, Y. L., Xie, P., Gong, Z. J., Shi, Z. X., 2004: A survey of the Gomphonemaceae and Cymbellaceae (Bacillariophyta) from the Jolmolungma Mountain (Everest) region of China. Journal of Freshwater Ecology 19, 189–194. https://doi.org/10.1080/02705060.2004.9664531

Liu, Y., You, Q. M., Wang, Q. X., 2006: Freshwater diatoms from Kinmen Island in Fujian, China. Plant Science Journal 24, 38–46. [In Chinese with English abstract]

Liu, Y., Fan, Y. W., Wang, Q. X., 2012: Newly recorded species in Cymbellaceae and Gomphonemataceae from Great Xingan Mountains, China. Acta Hydrobiologica Sinica 36, 496–508 (in Chinese with English abstract).

Liu, Q., Wu, H., Li, Y.L, Kociolek, J.P., 2021: One new species of *Cymbella* C.A. Agardh (Bacillariophyta) from high altitude lakes in the Hengduan Mountains of Southwest China. Acta Botanica Croatica 80(2), 184–190. https://doi.org/10.37427/botcro-2021-021

Long, J. Y., Liu, B., Zhou, Y. Y., Xu, S., Chen, J. H., 2022: *Cymbella pavanaensis* A. Vigneshwaran et al., a diatom reported for the first time in China. Guihaia 42, 1791–1796.

Meister, F., 1932: Kieselalgen aus Asien. Gebrüder Borntraeger, Berlin.

Meister, F., 1935: Seltene und neue Kieselalgen I. Bericht der Schweizerischen Botanischen Gesellschaft, 44, 88–108.

Metzeltin, D., Lange-Bertalot, H., 2014: The genus *Didymosphenia* M. Schmidt. A critical evaluation of established and description of 11 new taxa. Iconographia Diatomologica, 25, 1–293.

Simonsen, R., 1979: The diatom system: ideas on phylogeny. Bacillaria 2, 9–71.

Solak, C. N., Balkis-Ozdelice, N., Yilmaz, E., Durmus, T., Blanco, S., 2021: Description of two new *Cymbella* (Bacillariophyta) species from Sakarbasi spring, Turkey. Phytotaxa 484, 195–206. https://doi.org/10.11646/phytotaxa.484.2.4

Sun, D., Zhi, C. Y., 2015: Study on diatom communities and correlation analysis between diatom communities and water quality of karst cave groundwater. Environmental Science and Technology 38 (12), 36–40 (in Chinese with English abstract).

Terao, K., Mayama, S., Kobayasi, H., 1993: Observations on *Cymbella mexicana* (Ehrenb.) Cleve var. *Mexicana* (Bacillariophyceae) with special reference to the band structure. Hydrobiologia 269, 75–80. https://doi.org/10.1007/BF00028006

Van Heurck, H., 1880: Synopsis des Diatomées de Belgique Atlas. Ducaju et Cie, Anvers.

Wengrat, S., Marquardt, G. C., Bicudo, D. C., Bicudo, C. E. D., Wetzel, C. E., 2015: Type analysis of *Cymbella schubartii* and two new *Encyonopsis* species (Bacillariophyceae) from southeastern Brazil. Phytotaxa 221, 247–264. https://doi.org/10.11646/phytotaxa.221.3.3

Wu, J. T. 1999: A generic index of diatom assemblages as bioindicator of pollution in the Keelung River of Taiwan. Hydrobiologia 397, 79–87. https://doi.org/10.1023/A:1003694414751

Wu, F. S., Ge, L., Cai, Z. P., Feng, H. Y., 2008: Phytoplankton diversity of algae in Suganhu Lake in Gansu Province. Acta Botanica Boreali-Occidentalla Sinica 28, 2521–2526 (in Chinese with English abstract).

You, Q. M., Li, H. L., Wang Q. X., 2005: Preliminary studies on diatoms from Kanasi in Xinjiang Uighur Autonomous. Plant Science Journal 23, 247–256 (in Chinese with English abstract).

Zhang, M. L., Wang, E. R., Chang, S., Wang, S. J., Jin, D. C., Fan, Y. T., Zhang, K. F., Xie, Q., Fu, Q., 2022: Structural characteristics of phytoplankton communities and its relationship with environmental factors in a group of drinking water reservoirs by water transmission from Modaomen Waterway in Zhuhai. Environmental Science 43, 4489–4501 (in Chinese with English abstract). https://doi.org/10.13227/j.hjkx.202112285

Zhang, Y., Liao, M. N., Li, Y. L., Chang, F. Q., Kociolek, J. P., 2021: *Cymbella xiaojinensis* sp. nov., a new cymbelloid diatom species (Bacillariophyceae) from high altitude lakes, China. Phytotaxa 482, 55–64. https://doi.org/10.11646/phytotaxa.482.1.6

Acta Bot. Croat. 84 (1), 70–80, 2025
DOI: 10.37427/botcro-2025-015

CODEN: ABCRA 25
ISSN 0365-0588
eISSN 1847-8476

Combined application of rutin and silicon sustains maize seedlings osmotic stress tolerance by improving photosynthetic capacity and chlorophyll metabolism

Asiye Sezgin Muslu[1]*, Cansu Altuntaş[2], Namuun Altansambar[1,3], Mehmet Demiralay[4], Asim Kadıoğlu[1]

[1] Karadeniz Technical University, Faculty of Science, Department of Biology, 61080 Trabzon, Türkiye

[2] Medical-Aromatic Plants Application and Research Center, Artvin Coruh University, 08100 Artvin, Türkiye

[3] National University of Mongolia, School of Art and Sciences, Department of Biology, 14201 Ulaanbaatar, Mongolia

[4] Artvin Coruh University, Faculty of Forestry, Department of Forestry Engineering, 08000 Artvin, Türkiye

Abstract – In the current study, the role of external applications of rutin (Rut) and silicon (Si) in stress tolerance was investigated. Although it is known that Si has a role in improving plant defense against a variety of stresses, the role of Rut application in stress response remains unclear. Therefore, the current study was designed to evaluate the function of the synergistic effect of combined Rut and Si applications on the photosynthetic capacity of maize seedlings under osmotic stress. Twenty-one-day-old seedlings were treated with Rut (60 mg L^{-1}) and Si (1 mM), and exposed to osmotic stress (induced by 10% and 15% (w/v) polyethylene glycol) for 48 h. The individual application of Rut and Si and especially the simultaneous treatment of Rut+Si improved the gas exchange parameters, chlorophyll content, photosystem II (PSII) activity, Rubisco enzyme activity, and the expression levels of magnesium chelatase and Rubisco genes, but decreased the expression of chlorophyllase gene under osmotic stress in comparison to osmotic stress alone. These findings suggest that exogenous Rut and Si can improve photosynthetic capacity in maize seedlings exposed to osmotic stress by increasing PSII activity and the expression of genes involved in photosynthesis and chlorophyll metabolism, as well as reducing chlorophyll degradation. The simultaneous treatment of Rut+Si may be useful in developing osmotic stress tolerance of plants.

Keywords: chlorophyllase, chlorophyll fluorescence parameters, gas exchange parameters, gene expression, magnesium chelatase, Rubisco

Introduction

Water deficit, without a doubt one of the most critical stress situations, having a significant impact on crop growth and development and thus affecting crop productivity, and as a result, food security, is becoming a major concern around the world. It causes changes in fundamental plant morphophysiology and biochemistry and water loss, which reduces stomatal opening, chlorophyll content, and photosynthesis rate, potentially reducing plant growth and productivity (Xiang et al. 2013, Iqbal et al. 2020). Photosynthesis is a multi-step process that turns light energy into chemical energy, including photosynthetic electron transport and the carbon reduction cycle (Berry et al. 2013). In many plants, water-deficit stress causes stomatal closure, a decrease in transpiration rate and carbon dioxide assimilation capacity, and reduces the activities of photosynthetic carbon reduction cycle enzymes, including 1,5-bisphosphate carboxylase/oxygenase (Rubisco) and phosphoenolpyruvate carboxylase (PEPC) (Chaitanya et al. 2003), as well as the efficiency of photosynthetic electron transport and photosystem II (Xiang et al. 2013). In plants, Rubisco is composed of eight large subunits (LSUs) encoded by chloroplast *rbcL* gene and eight small subunits (SSUs) encoded by a family of nuclear *rbcS* genes (Lin et al. 2020).

Water-deficit stress considerably reduces the amount of chlorophyll. Chlorophyll metabolism may significantly affect the assembly of photosynthetic machineries as well as

* Corresponding author e-mail: asiyeszgn@outlook.com

communication between chloroplasts and nuclei (Flexas et al. 2006, Tanaka and Tanaka 2006). The incorporation of Mg^{2+} into protoporphyrin IX, catalyzed by magnesium protoporphyrin IX-chelatase (Mg-Ch), a three-subunit (ChlI, ChlD, and ChlH) enzyme, is the first unique step in chlorophyll biosynthesis. Chlorophyllase (Chlase), which catalyzes ester bond hydrolysis to produce protochlorophyllide and phytol, is the first enzyme thought to be involved in chlorophyll degradation (Santos 2004). Water- deficit stress-induced increase in Chlase activity and gene expression may result in a loss of chlorophyll accumulation (Banaś et al. 2011). Low Mg-Ch activity was also linked to a lack of chlorophyll. Under magnesium deficiency, reduced expression levels of Mg-Ch and chlorophyll synthase, inhibited chlorophyll synthesis (Zhou et al. 2011).

Silicon (Si) has attracted a lot of attention because it has been shown to improve plant tolerance to a wide range of abiotic stress factors (Coskun et al. 2019). Several studies have shown that Si can increase a plant's ability to withstand drought by either speeding up photosynthetic activity or slowing down transpiration. Si enhances crop growth, production, and quality by affecting photosynthetic activity, nitrogen uptake, and resilience to stress factors (Cooke and Leishman 2011, Liang et al. 2015, Ahanger et al. 2020). It was reported that Si mitigates low phosphorus stress by improving photosynthetic capacity, antioxidant potential, and nutrient homeostasis (Zhang et al. 2019). Due to improved water retention, Si reduces drought stress in a variety of plants (Gong and Chen 2012, Liu et al. 2014, Khan et al. 2020, Desoky et al. 2020, Verma et al. 2020).

Rutin (Rut), a flavonoid phenolic compound found in plants such as asparagus (Wang et al. 2003), has antioxidant properties and has been shown to reduce lipid peroxidation (Yang et al. 2008). In comparison to other antioxidant compounds, little research has been conducted to determine the effects of rutin on stressed plants (Ferdinando et al. 2012, Ismail et al. 2015, Singh et al. 2017). In recent studies, it was revealed that rutin improved salt stress tolerance in maize seedlings by modulating osmolyte accumulation and antioxidant capacity (Sezgin Muslu 2024).

The roles of exogenous rutin in protecting plants from abiotic stress factors remain to be fully determined. Moreover, reports showing the effects of rutin and silicon application alone and/or in combination on osmotic stress are limited. In a previous study, the combined application of rutin and silicon alleviated osmotic stress in maize seedlings by triggering the accumulation of osmolytes and antioxidants' defense mechanisms (Altansambar et al. 2024). However, no attempt has been undertaken to determine how combined application of silicon and rutin affects photosynthesis in plants subjected to osmotic stress. There is also insufficient evidence to explain the effects of rutin and silicon applications on the activities and gene expressions of some key enzymes involved in chlorophyll metabolism and photosynthetic processes. Therefore, in the current study, it was hypothesized that (1) Rut and Si might sustain maize seedlings' osmotic stress tolerance by improving photosynthetic capacity and chlorophyll metabolism, and (2) Rut might play an important role in the prominent effects of combined applications of Rut and Si in relieving osmotic stress. Our study will provide new information on the changes in photosynthetic capacity and chlorophyll metabolism of Rut and Si at the biochemical and molecular level.

Material and methods

Plant material, experimental conditions and treatments

Zea mays L. seedlings were grown hydroponically in Hoagland's solution (Hoagland and Arnon 1950) in a growth chamber (day/night temperatures of 25/22 °C, 60 ± 2% relative humidity, and photosynthetic photon flux density of 400 μmol m^{-2} s^{-1} with a 16-h photoperiod). After 21 days of growth, rutin (Rut, 60 mg L^{-1}) and silicon (Si, 1 mM) were applied to the seedlings. In our previous study, with concentrations of rutin (30, 60, and 90 mg L^{-1}) and silicon (0,5, 1, and 2 mM), plants under osmotic stress (10% and 15% (w/v) polyethylene glycol) pretreated with 60 mg L^{-1} Rut and 1 mM Si were found to better maintain water status and had lower membrane damage (Altansambar et al. 2024). Si treatment was added using calcium silicate ($CaSiO_3$) (Sigma Aldrich, USA). For Rut treatment, rutin hydrate was obtained from Sigma Aldrich, USA. After 24 h, seedlings were exposed to osmotic stress induced by adding 10 and 15% (w/v) polyethylene glycol (PEG_{6000}) to Hoagland's solution for 48 h. Seedlings treated with Hoagland's solution without PEG were used as the control group. Therefore, we designed nine different treatments: (1) mock; (2) moderate stress: 10% PEG; (3) severe stress: 15% PEG; (4) Rut application before moderate osmotic stress (Rut + 10% PEG); (5) Si application before moderate osmotic stress (Si + 10% PEG), (6) Rut and Si application before moderate osmotic stress (Rut + Si + 10% PEG); (7) Rut application before severe osmotic stress (Rut + 15% PEG); (8) Si application before severe osmotic stress (Si + 15% PEG); (9) Rut and Si application before severe osmotic stress (Rut + Si + 15% PEG). The experimental plan was arranged in a completely randomized design with five replicates, providing a total of five containers with a total of five plants per treatment. After treatments, 24-day-old seedlings were harvested and subjected to biochemical and molecular analysis.

Determination of total chlorophyll content

The total chlorophyll content was determined using Arnon's method (1949). At 0-4 °C, fresh leaf samples (0.1 g) were extracted with 80% acetone. The extracts were centrifuged for 10 min at 15000 g. A spectrophotometer was used to measure absorbance of the supernatant at 645 and 663 nm. The amount of total chlorophyll (mg chlorophyll per fresh tissue) was calculated using the following equation:

$$\text{mg chlorophyll } g^{-1}_{FW} = (20.2 \times (A_{645}) + 8.02 \times (A_{663}) \times \frac{V}{1000 \times W}$$

where, A is the absorbance at specific wavelengths; V is the final volume of chlorophyll extract in 80% acetone and W is the fresh weight.

Determination of gas exchange parameters

The LI-6800 Portable Photosynthesis System (LI-COR Biosciences, Inc., Lincoln, NE, USA) was used to quantify the net photosynthetic rate (Pn), transpiration (E), stomatal conductance (gsw), and intercellular CO_2 concentration (Ci) of *Zea mays*. Five plants were included in each group, and ten measurements were taken manually from the upper most fully developed third leaf of each plant at 5-second intervals. The following circumstances were used for the measurements: light intensity of 250 µmol m^{-2} s^{-1} (Demiralay 2022), block and leaf temperatures of 25 °C, and relative humidity of 60%. The integrated CO_2 mixer in the portable photosynthetic system allowed for independent adjustment of the CO_2 concentration. After the leaf was clamped, it was held for at least 30 min until the values of reference CO_2 and sample CO_2 reached equilibrium at 400 µmol mol^{-1} CO_2.

Determination of chlorophyll fluorescence parameters

A Multi-Mode Chlorophyll Fluorometer (OS5p, Opti-Sciences, Inc., Hudson, NJ, USA) was used to measure chlorophyll fluorescence (CF). Three seedlings were chosen at random for each group and used to measure CF parameters. The leaves were maintained in the dark for 20 min before the Chl fluorescence was measured. A modest red light (0.1 µmol m^{-2} s^{-1}) was used to determine the minimal fluorescence (F_0) after 20 min of acclimation to darkness using the dark leaf clip. The maximum fluorescence (F_m) was then measured using an 8 sec saturating pulse (8000 µmol m^{-2} s^{-1}) (Nar et al. 2009). Then, in plants exposed to actinic light (500 µmol m^{-2} s^{-1}) (Chen et al. 2019) F_m', the maximum fluorescence observed in a light-adapted state when all PSII reaction centers are closed and F_s, the fluorescence level measured under steady-state photosynthesis conditions (Krause and Weis 1991), were also determined. The fluorescence parameters were calculated using the following formulas (van Kooten and Snel 1990): the maximum quantum yield of PSII photochemistry, $F_v/F_m = (F_m - F_0)/F_m$; photochemical quenching of variable chlorophyll fluorescence, $qP = (F'_m - F_s)/(F'_m - F'_0)$; and nonphotochemical chlorophyll fluorescence quenching, $NPQ = (F_m - F'_m)/F_m$. The effective quantum yield of ΦPSII = $(F_m' - F_s)/F_m'$) of Genty et al. (1989), and electron transfer rate (ETR) of Nar et al. (2009) were also determined.

Determination of Rubisco activity

Extraction buffer (50 mM Tris-HCl, 0.1% (w/v) mercaptoethanol, 12% (v/v) glycerol, 10 mM magnesium chloride ($MgCl_2$), 1 mM EDTA, and 1% (w/v) polyvinylpolypyrrolidone (PVPP-40) was used to prepare extracts from the samples (Parry et al. 1997). The protein contents of the extracts were measured as described by Bradford (1976), with bovine serum albumin as a standard. Rubisco activity was measured according to Sawada et al. (2003) method. The activity was measured at 25°C for 5 min by adding 100 µl of supernatant into 900 µl of assay buffer containing 50 mM of HEPES-KOH (pH 8.0), 1 mM of EDTA, 20 mM of $MgCl_2$, 25 mM of dithioerythritol, 10 mM of $NaHCO_3$, 5 mM of ATP, 0.15 mM of nicotinamide adenine dinucleotide (NADH), 5 mM of creatine phosphate, 0.6 mM of ribulose-1,5-bisphosphate (RuBP), 10 units of phosphocreatine kinase, 10 units of glyceraldehyde-3-phosphate dehydrogenase and 10 units of phosphoglycerate kinase. The enzymatic activity was determined via the decrease in absorbance at 340 nm using extinction coefficient of 6.22 mM^{-1} cm^{-1}. Total Rubisco activity was expressed in units per milligram of proteins.

Determination of chlorophyllase activity

To determine the activity of chlorophyllase (Chlase), extraction was performed by a slight modification of the method described by Yang et al. (2004). The leaf samples (0.1 g) were homogenized with extraction buffer (5 mM potassium phosphate buffer (pH 7), 50 mM KCl, and 0.24% Triton X-100). After extraction, to remove chlorophyll, the samples were treated with cold acetone, followed by incubation at 30 °C for 30 min in the dark. The samples were then centrifuged at 15000 g for 15 min. Chlase activity was determined by adapting the method of McFeeters et al. (1971). A standard reaction mixture was prepared containing the reaction buffer (100 mM sodium phosphate buffer (pH 7), 0.24% Triton X-100) (2 mL), 1 µmol mL^{-1} chlorophyll *a* (0.2 mL) as a substrate and supernatant (0.3 mL), and the reaction was stopped using 0.5 mL of 10 mM KOH with incubation at 30 °C for 30 min. After that, 5 mL of hexane/acetone (3:2, v/v) was added to 1 mL of reaction medium. The content of chlorophyllide *a* in the acetone phase was determined spectrophotometrically at 667 nm using extinction coefficient of 74.9 mM^{-1} cm^{-1}. Chlase activity was expressed as production of chlorophyllide *a*. Proteins were determined by the method of Bradford (1976). The activity was expressed in units per milligram of proteins.

Determination of the expression levels of the *rbcL*, *rbcS*, *Mg-ChlI,* and *Chlase* genes

Fresh samples (0.1 g) were used for total RNA isolation. After the samples were broken down in a tissue homogenizer, total RNA isolation was performed using a total RNA isolation kit (Favorgen FavorPrep Plant Total RNA Mini Kit) following the kit's protocol. A NanoDrop spectrophotometer was used to determine the quantity and purity of the RNA samples. The RNA samples were assessed for purity before being stored at -80 °C for cDNA extraction. From the isolated total RNA samples, 2000 ng of cDNA was obtained per group using the High Capacity cDNA Reverse Transcription Kit from Applied Biosystems USA. The synthesized cDNAs were stored at -20 °C until real time PCR analyses were performed.

The resulting cDNAs were used to identify gene expression using real-time PCR. 5 HOT FIREPol EvaGreen qPCR Supermix and the CFX Connect Real-Time PCR System were used for analysis. The real-time PCR protocol was modified from the Solis BioDyne instructions: 12 min at

Tab. 1. The sequences of specific primers of genes, used for qRT-PCR analysis. Ribulose-1,5-bisphosphate carboxylase/oxygenase large subunit (*rbcL*), ribulose-1,5-bisphosphate carboxylase/oxygenase small subunit (*rbcS*), magnesium chelatase subunit I (*Mg-ChlI*), chlorophyllase (*Chlase*).

Primers	Sequences
Actin (*ACT*), forward	5'-GAAGATCACCCTGTGCTGCT-3'
Actin (*ACT*), reverse	5'-ACCAGTTGTTCGCCCACTAG-3'
rbcL, forward	5'-AAAGCCTTACGCGCTCTACGT-3'
rbcL, reverse	5'-CGGACCTTGGAAAGTTTTTGAA-3'
rbcS, forward	5'-ATGTGGAAGCTGCCCATGTT-3'
rbcS, reverse	5'-GCCTCCTGCAGCTCCTTGTA-3'
Mg-ChlI, forward	5'-TGTATGCTGCTCGAGTTGCA-3'
Mg-ChlI, reverse	5'-CTTGCTGCTGATCCTGTGGA-3'
Chlase, forward	5'-ACACCACCGAGGAGATCAAC -3'
Chlase, reverse	5'-GTCCAGCTCGTCGTAGAAGG -3'

95 °C, 45 cycles of 15 sec at 95 °C, 30 sec at 60 °C, 30 sec at 72 °C, and 0.5 °C increments from 65 °C to 95 °C for the melt curve. Each biological repeat was examined as three technical replications, with the average technical error accepted as 0.5 (± 1) Cq values. Furthermore, gene-specific primers were used to investigate the levels of expression of the genes (Tab. 1). The data obtained as a result of the analysis were normalized to the *β-actin* reference gene and presented as relative gene expression using the $2^{-\Delta\Delta CT}$ method, following the protocol outlined by Bookout and Mangelsdorf (2003).

Statistical analysis

All experiments were performed five times with five biological replicates in total. The Shapiro-Wilk normality test was used to test the normal distribution of variables. A two-way ANOVA and Tukey's multiple range test was performed at the 0.05 (5%) level using IBM SPSS 23.0 Statistics Package (SPPS Corp., Chicago, IL, USA).

Results

Total chlorophyll content

According to the results of two-way ANOVA (Tab. 2), the total chlorophyll content was significantly ($P < 0.001$) affected by osmotic stress conditions (OS) and treatments with Rut, Si or both (T). Moreover, the interaction between OS and T factors was also highly significant for the total chlorophyll content, suggesting that the effect of one factor depends on the level of the other factor.

As shown in Fig. 1, the differences in the concentration of the osmotic stress (10 or 15% PEG) had a significant ($P < 0.05$) effect on the total chlorophyll content of maize leaves. The stressed seedlings showed 47.25 and 162.02% lower total chlorophyll levels, respectively, in comparison with the

Tab. 2. Results of two-way ANOVA (P-Values, F ratios) for the independent osmotic stress conditions (OS), treatment (T) and osmotic stress × treatment interactions (OS x T). Pn – net photosynthesis, E – transpiration, gsw – stomatal conductance, Ci – intercellular CO_2 concentration, F_v/F_m – maximum quantum yield of PSII photochemistry, ΦPSII – the effective quantum yield of PSII, qP – photochemical quenching, NPQ – non-photochemical quenching, *rbcL* – Rubisco large subunit, *rbcS* – Rubisco small subunit, *Mg-ChlI* – magnesium chelatase subunit I, *Chlase* – chlorophyllase. * indicate significant difference at $P < 0.05$; ** indicate significant difference at $P < 0.01$; *** indicate significant difference at $P < 0.001$.

Experimental parameters	Varience sources of two – way ANOVA					
	OS (3 levels)		T (3 levels)		OS × T	
	F	P-Value	F	P-Value	F	P-Value
Total chlorophyll content	2218.166***	<0.001	356.934***	<0.001	41.695***	<0.001
Pn	716.197***	<0.001	81.093***	<0.001	8.901***	<0.001
E	620.588***	<0.001	32.367***	<0.001	8.276**	0.001
gsw	98.33***	<0.001	114.129***	<0.001	91.277***	<0.001
Ci	127.886***	<0.001	78.912***	<0.001	10.515***	<0.001
F_v/F_m	205.39***	<0.001	101.56***	<0.001	61.83***	<0.001
ΦPSII	9.86**	0.006	58.69***	<0.001	8.77***	<0.001
ETR	26.45**	0.006	32.99***	<0.001	19.88***	<0.001
qP	45.144***	<0.001	63.64***	<0.001	5.47**	0.007
NPQ	36.78**	0.007	47.66***	<0.001	27.184***	<0.001
Rubisco activity	1132.542***	<0.001	226.229***	<0.001	33.179***	<0.001
Chlase activity	3201.211***	<0.001	97.006***	<0.001	26.456***	<0.001
rbcL gene expression	12358.673***	<0.001	1712.888***	<0.001	113.346***	<0.001
rbcS gene expression	10641.439***	<0.001	613.537***	<0.001	65.199***	<0.001
Mg-ChlI gene expression	269.346***	<0.001	7.005**	0.003	0.399	0.755
Chlase gene expression	1652.202***	<0.001	35.847***	<0.001	13.655***	<0.001

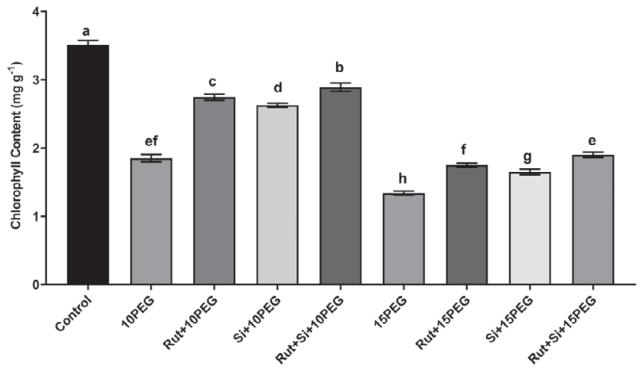

Fig. 1. Effect of the treatments (T) with rutin (Rut), silicon (Si), and their combination (Rut+Si) on total chlorophyll content of maize seedlings under osmotic stress (OS) conditions (10% or 15% polyethylene glycol - PEG). Vertical bars represent standard deviations of the means, N = 5. Data were subjected to two-way ANOVA while Tukey's multiple range test was used for determinating the differences among means for interaction OS × T. Values marked with the different letters denote significant difference (P < 0.05).

control group. However, the total chlorophyll content was significantly enhanced (P < 0.05) by the application of Rut or Si alone and in combination under both osmotic stress treatments, especially moderate stress. Additionally, compared to Rut or Si alone, the combination of Rut and Si was found to further increase the total chlorophyll content (Fig. 1).

Gas exchange parameters

According to results of two-way ANOVA (Tab. 2), both OS and T had highly significant effects (P < 0.001) on net photosynthesis (Pn) and the transpiration rate (E). Similarly, OS and T both significantly affected (P < 0.001) stomatal conductance (gsw) and intercellular CO_2 concentration (Ci). The interaction between OS × T was also significant for Pn, E, gsw and Ci, though the F-value for the interaction was small compared to the OS and T factors, indicating a less strong but still significant interaction (P ≤ 0.001).

The Pn, E, gsw and Ci values were significantly decreased (P < 0.05) with 10% and 15% PEG treatments compared to the non-stress group. The decrease in these values was highest in the 15% PEG treated group. However, exogenous Rut, Si and Rut+Si treatments significantly increased (P < 0.05) Pn, E, gsw, and Ci under both osmotic stress conditions. However, the highest values of Pn and E were observed in Rut, Si and Rut+Si treatments under 10% PEG. Furthermore, the highest value of gsw was observed in Si and Rut+Si treatments and the highest value of Ci were detected in Rut+Si treatment under 10% PEG, which were significantly (P < 0.05) different from 15% PEG conditions (Tab. 3).

Chlorophyll fluorescence parameters

Two-way ANOVA analysis (Tab. 2) showed that the content of all chlorophyll fluorescence parameters (F_v/F_m, ΦPSII, ETR, qP, and NPQ) was significantly different in respect of osmotic stress conditions (OS), treatments (T) and their interactions (OS × T).

As shown in Tab. 4, the values of F_v/F_m, ΦPSII, ETR, qP were significantly (P < 0.05) reduced under both 10% and 15% PEG treatments compared to the non-stressed group.

In contrast, values of NPQ were significantly (P < 0.05) increased under both osmotic stresses compared to the non-stress group. Application of Rut or Si, and especially their combination significantly increased values of F_v/F_m, ΦPSII and qP under both osmotic stresses, although values were still not as high as in control. In contrast, NPQ values were lower after application of Rut or Si, and especially of a combination of the two, than under osmotic stress alone.

Rubisco activity

According to results of two-way ANOVA (Tab. 2) the Rubisco activity was significantly affected (P < 0.001) by OS and T as well as their interaction (OS × T) indicating strong effects.

Compared to non-stressed plants, osmotic stress significantly reduced the activity of Rubisco, with severe stress

Tab. 3. Effect of the treatments (T) with rutin (Rut), silicon (Si), and their combination (Rut+Si) on net photosynthesis (Pn), transpiration (E), stomatal conductance (gs) and intercellular CO_2 concentration (Ci) of maize seedlings under osmotic stress (OS) conditions (10% or 15% polyethylene glycol - PEG). All values are presented as means ± standard deviation, N = 5. Data were subjected to a two-way ANOVA and Tukey's multiple range test was used to determine the differences among means for interaction OS × T. Values marked with the different letters denote significant difference (P < 0.05).

Applications	Net photosynthesis ($\mu mol\ CO_2\ m^{-2}\ s^{-1}$)	Transpiration ($mmol\ H_2O\ m^{-2}\ s^{-1}$)	Stomatal conductance ($mmol\ H_2O\ m^{-2}\ s^{-1}$)	Intercellular CO_2 concentration ($\mu mol\ mol^{-1}$)
Control	19.53 ± 0.18^{a}	0.0013 ± 0.0008^{a}	0.092 ± 0.001^{a}	47.52 ± 1.23^{a}
10 % PEG	11.00 ± 0.36^{c}	0.0008 ± 0.00005^{c}	0.041 ± 0.002^{f}	38.06 ± 1.21^{e}
Rut + 10 % PEG	12.58 ± 0.12^{b}	0.0009 ± 0.00001^{b}	0.046 ± 0.0001^{d}	43.45 ± 0.15^{c}
Si + 10% PEG	12.56 ± 0.36^{b}	0.0008 ± 0.00002^{bc}	0.06 ± 0.001^{b}	43.07 ± 0.2^{c}
Rut + Si + 10% PEG	12.72 ± 0.23^{b}	0.0009 ± 0.00002^{b}	0.059 ± 0.001^{b}	45.24 ± 1.23^{b}
15% PEG	8.46 ± 0.08^{f}	0.0003 ± 0.00004^{h}	0.036 ± 0.0021^{g}	33.46 ± 1.22^{g}
Rut + 15% PEG	9.2 ± 0.23^{e}	0.0006 ± 0.00002^{e}	0.057 ± 0.001^{c}	35.73 ± 0.21^{f}
Si + 15% PEG	10.36 ± 0.14^{cd}	0.0004 ± 0.00001^{g}	0.045 ± 0.0002^{e}	41.23 ± 1.12^{d}
Rut + Si + 15% PEG	10.58 ± 0.23^{c}	0.0005 ± 0.00001^{h}	0.044 ± 0.001^{e}	41.93 ± 0.82^{d}

Tab. 4. Effect of the treatments (T) with rutin (Rut), silicon (Si), and their combination (Rut+Si) on maximum efficiency of PSII (F_v/F_m), the effective quantum yield of PSII (ΦPSII), photochemical quenching (qP), non-photochemical quenching (NPQ) of maize seedlings under osmotic stress conditions (OS) (10% or 15% polyethylene glycol – PEG). All values are presented as means ± standard deviation, N = 5. Data were subjected to a two-way ANOVA and Tukey's multiple range test was used to determine the differences among means for interaction OS × T. Values marked with the different letters denote significant difference (P < 0.05).

Applications	F_v/F_m	ΦPSII	ETR	qP	NPQ
Control	0.754 ± 0.004^{a}	0.598 ± 0.037^{a}	24.03 ± 1.01^{a}	0.852 ± 0.01^{a}	0.145 ± 0.015^{e}
10 % PEG	0.455 ± 0.01^{e}	0.32 ± 0.03^{e}	13.55 ± 1.6^{g}	0.710 ± 0.02^{f}	0.345 ± 0.008^{a}
Rut + 10 % PEG	0.536 ± 0.002^{d}	0.477 ± 0.006^{b}	19.3 ± 0.9^{bc}	0.822 ± 0.01^{c}	0.285 ± 0.007^{bc}
Si + 10% PEG	0.672 ± 0.02^{c}	0.425 ± 0.002^{c}	17.8 ± 0.1^{de}	0.821 ± 0.01^{c}	0.225 ± 0.006^{d}
Rut + Si + 10% PEG	0.71 ± 0.002^{b}	0.476 ± 0.004^{b}	20.4 ± 0.1^{b}	0.842 ± 0.01^{b}	0.285 ± 0.01^{bc}
15% PEG	0.452 ± 0.01^{e}	0.404 ± 0.002^{d}	16.7 ± 0.4^{f}	0.713 ± 0.007^{f}	0.33 ± 0.009^{a}
Rut + 15% PEG	0.529 ± 0.03^{d}	0.469 ± 0.006^{b}	18.1 ± 00.4^{cd}	0.759 ± 0.007^{e}	0.243 ± 0.01^{d}
Si + 15% PEG	0.471 ± 0.02^{e}	0.431 ± 0.005^{c}	17.9 ± 0.1^{de}	0.802 ± 0.04^{d}	0.303 ± 0.01^{b}
Rut + Si + 15% PEG	0.526 ± 0.01^{d}	0.482 ± 0.01^{b}	17.05 ± 0.35^{de}	0.817 ± 0.004^{c}	0.265 ± 0.02^{c}

(15% PEG) having a more prominent effect. Exogenous applications of Rut, Si, and Rut+Si significantly (P < 0.05) increased Rubisco activity under both osmotic stress conditions, especially moderate stress (10% PEG), compared to the same level of stress alone. Moreover, compared to Rut or Si alone, the combination of Rut and Si was found to further increase Rubisco activity (Fig. 2).

Chlorophyllase activity

Two-way ANOVA analysis showed that the chlorophyllase activity was significantly affected by OS and T factors as well as OS × T (P < 0.001) indicating strong effects (Tab. 2).

Both levels of osmotic stress, but especially severe stress (15% PEG) significantly (P < 0.05) increased chlorophyllase activity, compared to the control. Exogenous treatments with Rut and Si decreased the chlorophyllase activity under osmotic stress, compared to the seedlings exposed to the same level of osmotic stress alone but more efficiently at moderate stress. Also, compared to Si alone, seedlings treated with Rut+Si exhibited an even more significant (P < 0.05) decrease in chlorophyllase activity under stress conditions (Fig. 2).

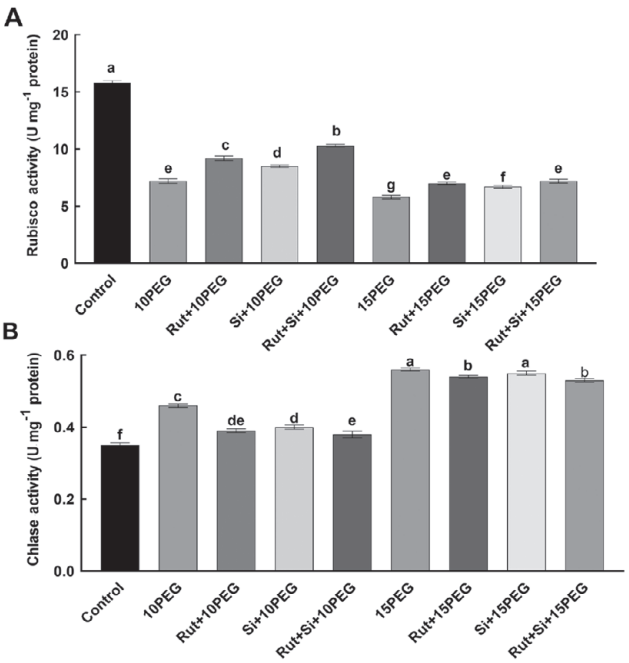

Fig. 2. Effect of the treatments (T) with rutin (Rut), silicon (Si), and their combination (Rut+Si) on Rubisco activity (A) and chlorophyllase (Chlase) activity (B) of maize seedlings under osmotic stress (OS) conditions (10% or 15% polyethylene glycol – PEG). Vertical bars represent standard deviations of the means, N = 5. Data were subjected to a two-way ANOVA and Tukey's multiple range test was used to determine the differences among means for interaction OS × T. Values marked with the different letters denote significant differences (P < 0.05).

The expression levels of *rbcL*, *rbcS*, *Mg-ChlI* and *Chlase* genes

According to results of two-way ANOVA, the expression levels of the *rbcL* and *rbcS*, endcoding large and small Rubisco subunits, respectively, were significantly different (P < 0.001) in respect of osmotic stress conditions (OS), treatments (T) and their interactions (OS × T) (Tab. 2). As compared to the control, the expression levels of *rbcL* and *rbcS* were significantly down-regulated by 10 and 15% PEG. Exogenous applications of Rut, Si, and especially Rut+Si significantly up-regulated the expression levels of *rbcL* and *rbcS* under moderate and severe osmotic stress as compared to the same level of stress alone (Fig. 3).

Two-way ANOVA analysis showed that the effect of OS factor on the expression levels of the *Mg-ChlI* was significant with P < 0.001 as well as the effects of T with P = 0.003 (Tab. 2). The expression levels of the *Mg-ChlI* in maize seedlings treated with 10 and 15% PEG were significantly lower than in the control. In addition, under moderate and severe osmotic stress conditions, the expression levels of *Mg-ChlI* in seedlings pretreated with Rut, Si, and Rut+Si were higher than under moderate and severe osmotic stress (Fig. 3).

According to results of two-way ANOVA, the expression level *Chlase* was significantly different (P < 0.001) in respect of osmotic stress conditions (OS), treatments (T) and their interactions (OS × T) (Tab. 2). Both levels of osmotic stress caused a significant increase in the expression level of

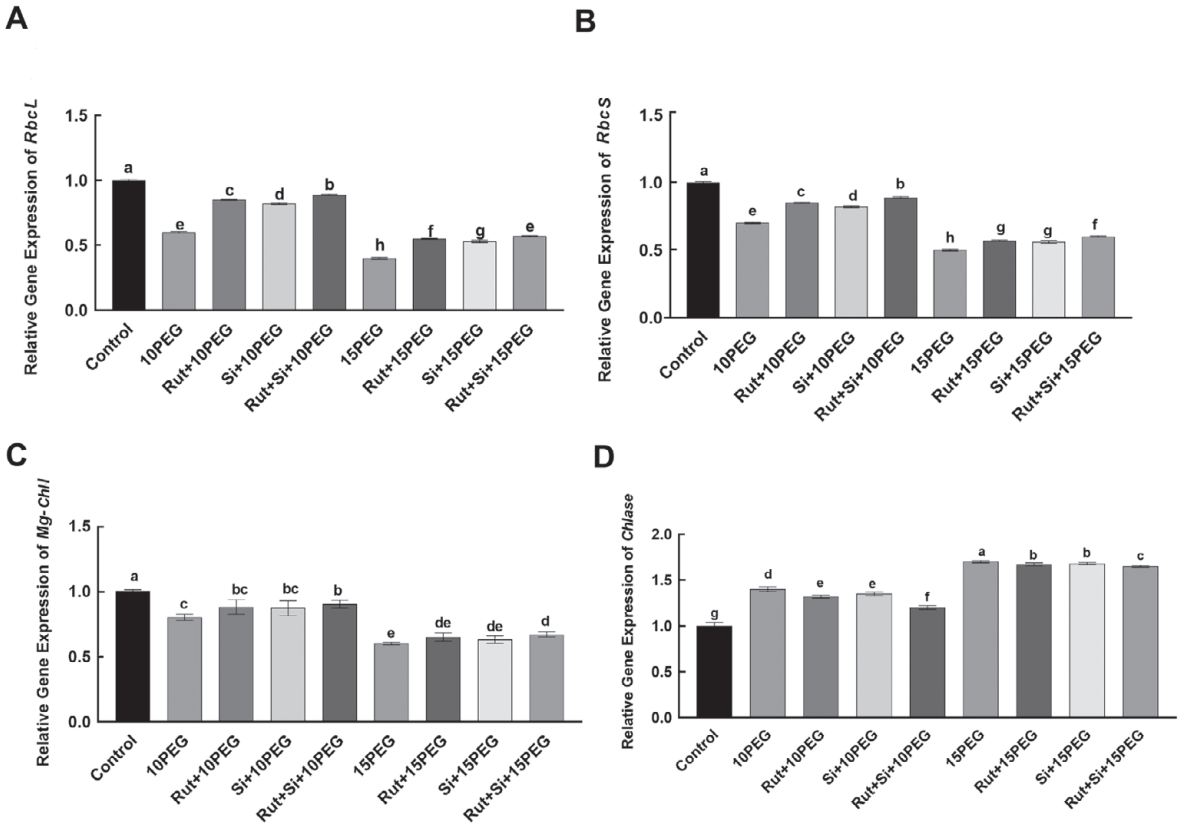

Fig. 3. Effect of the treatments (T) with rutin (Rut), silicon (Si), and their combination (Rut+Si) on the expression levels of of the *rbcL* (A) *and rbcS* (B), *Mg-ChlI* (C) and *Chlase* (D) genes of maize seedlings under osmotic stress (OS) conditions (10% or 15% polyethylene glycol - PEG). Vertical bars represent standard deviations of the means, N = 5. Data were subjected to two-way ANOVA and Tukey's multiple range test was used for determinating the differences among means for interaction OS × T. Values marked with the different letters denote significant differences ($P < 0.05$).

Chlase, compared to the control. Under moderate and severe osmotic stress, exogenous application of Rut, Si, and especially Rut+Si significantly down-regulated the expression level of *Chlase* (Fig. 3).

Discussion

Chlorophyll is required to convert light energy to chemical energy, and its depletion limits the photosynthetic process in plants (Kalaji et al. 2017). In current study, two-way ANOVA analysis of variance revealed that both independent variables (OS and T) had significant effects on the total chlorophyll content. Total chlorophyll content decreased in seedlings exposed to osmotic stress, while Rut, Si, and especially Rut+Si applications reduced the negative effects of osmotic stress on chlorophyll content. Consistently with our findings, Si- treated wheat and *Eruca sativa* L. plants showed a significant increase in chlorophyll content (Maghsoudi et al. 2015, Bukhari et al. 2021). Moreover, Si application improved the chlorophyll content in *Fagopyrum esculentum* M. plants under aluminium stress (Dar et al. 2022). In another study, total content of chlorophyll in *Oryza sativa* L., leaves increased during treatment with rutin (Singh et al. 2017). The chlorophyll content could decline due to increased Chlase activity under abiotic stressors (Dawood et al. 2014). Increased Chlase activity has been correlated with chlorophyll degradation in plants under osmotic stress conditions (Altuntaş et al. 2020), which is agreement with our results in maize seedlings where osmotic stress conditions induced significant enhancement of Chlase activity. However, Chlase activity significantly decreased in seedlings pretreated with Rut, Si, and especially Rut+Si under osmotic stress thus contributing to the higher content of chlorophyll content observed. In mustard seedlings exposed to salinity and drought stress, it was found that Chlase activity and chlorophyll degradation were decreased by Si (Alamri et al. 2020). Moreover, we also observed a correlation of Chlase activity with gene expression of *Chlase* i.e. Chlase activity decreased and the *Chlase* gene expression was considerably down-regulated in seeedlings under osmotic stress pretreated with Rut, Si, and Rut+Si. Therefore, we can hypothesize that Rut, Si and Rut+Si may have adjusted the transcript levels of genes encoding the Chlase that degrades chlorophyll, which can prevent the bleaching of chlorophyll and preserve photosynthetic activity. In the production of chlorophyll, a crucial regulation and enzymatic step is catalyzed by the heterotrimeric enzyme complex known as Mg-Chl (Rissler et al. 2002). Overexpression of the Mg-chelator H subunit in guard cells has been shown to increase drought tolerance in *Arabidopsis thaliana* (Tsuzuki et al. 2013). Another study also showed that Si application upreg-

ulated the expression of genes encoding enzymes in chlorophyll synthesis, Mg-Chl and chlorophyll oxygenase in cucumber seedlings under excess nitrate stress. In our study, the expression of the *Mg-ChlI* gene was significantly upregulated in Rut, Si, and Rut+Si applied maize seedlings under osmotic stress. As a result, we can conclude that increased *Mg-ChlI* gene expression and decreased *Chlase* expression can confer stress tolerance to maize seedlings.

Damage to photosynthesis can reduce chlorophyll content, causing the chloroplast bilayer membrane to rupture and disrupting coordination between the two photosystems, ultimately decreasing the photosynthesis rate (Lawlor and Cornic 2002, Chaves and Oliveira 2004). Lower Pn could be due to the fact that osmotic stress can lead to a decrease in gsw, Ci, and E as a result of stomatal closure (Chaves et al. 2003). Similarly, in our study, osmotic stress conditions (10% and 15% PEG) significantly decreased values of gas exchange parameters. The decreases were found to be higher at 15% PEG compared to 10% PEG application because severe drought stress can lead to structural and biochemical impairments in light-dependent reactions and carboxylation processes (Ghotbi-Ravandi et al. 2014). Many researchers have reported that exogenous applications of Si can enhance photosynthesis performance under osmotic stress (Maghsoudi et al. 2016, Li et al. 2018, Li et al. 2022, Mavondo-She et al. 2024). Like those studies, our results showed that Rut, Si and Rut+Si significantly increased all of the gas exchange parameters in maize seedlings. The results suggest that exogenous treatments of Rut, Si and Rut+Si can mitigate the adverse effects of osmotic stress on gas exchange due to more efficient light use and improved chlorophyll metabolism through the regulation of the *Mg-ChlI* and *Chlase* gene. Hence, those applications can maintain higher chlorophyll content, preserve the photosynthetic machinery and enhance overall photosynthetic performance.

Osmotic stress can have a significant impact on plant photosynthesis resulting in changed chlorophyll fluorescence (Chen et al. 2021). However, exogenous applications of various compounds have been shown to mitigate the negative effects of osmotic stress and enhance chlorophyll fluorescence parameters due to improved photosynthetic performance and overall plant resilience (Hayat and Ahmad 2007, Ashraf and Foolad 2007, Ahmed et al. 2019, Hussain et al. 2023). Many researchers have reported that chlorophyll fluorescence parameters are valuable for assessing PSII activity and functioning of the photosynthetic apparatus in plants under osmotic stress. The maximum quantum efficiency of PSII is linked to photosynthetic efficiency in leaves (Baker and Rosenqvist 2004, Baker 2008) and the F_v/F_m ratio serves as an indicator of photoinhibition or stress damage. In the present study, 10% and 15% PEG reduced F_v/F_m, ΦPSII, and qP values, indicating a potential decline in photosynthetic activity. The reduction in F_v/F_m is likely linked to decreased activity of PSII reaction centers and/or decreased energy transfer efficiency within reaction centers as well as reduced gsw and CO_2 availability, suggesting photoinhibition. An increase in NPQ indicating enhanced energy dissipation, as a mechanism to avoid photodamage, observed in stressed plants confirms these results. Additionally, the reductions in ΦPSII and qP may be associated with the changes in F_v/F_m (Maxwell and Johnson 2000). These declines are probably due to altered chlorophyll content, leading to the conclusion that osmotic stress inhibits PSII activity as previously established for maize (Altuntaş et al. 2020). However, applications of Rut, Si, and the combination of Rut+Si mitigated the impairment of photosynthetic parameters, as evidenced by enhanced electron transport under osmotic stress, and improved PSII efficiency.

Abiotic stressors can also reduce photosynthesis by reducing the activity of Rubisco which is the enzyme that fixes CO_2 and catalyzes photo-respiratory carbon oxidation (Abdulbaki et al. 2022). We determined that osmotic stress in maize seedlings negatively affected the activity of Rubisco while application of Rut, Si, and Rut+Si alleviated this negative effect. Especially effective was the combination of Rut and Si under moderate osmotic stress. Similarly, Si application increased Rubisco activity in cucumber seedlings under cinnamic-acid-induced stress (Lyu et al. 2022). Rubisco biosynthesis requires a high number of chaperones and involves eight large (Rubisco LSU) and eight small subunits (Rubisco SSU) (Lin et al. 2020). The abundances of transcripts of *rbcL* encoding LSU and *rbcS* encoding SSU could enhance photosynthetic properties, photosynthetic efficiency or capacity (Chen et al. 2015). In the current study, it was found that the expression levels of *rbcL* and *rbcS* were downregulated in the maize seedlings under osmotic stress conditions which correlates with decreased activity of Rubisco. Rut, Si, and Rut+Si applications significantly upregulated the expression of *rbcL* and *rbcS* genes in seedlings exposed to osmotic stress, consequently also increasing Rubisco activity. Consistently with our study, Si application significantly upregulated the expression of genes encoding Rubisco subunits in tomato seedlings under low-calcium stress (Li et al. 2022). No study has been found in the literature on the way in which Rut application affects the activities of photosynthetic enzymes and the expression of genes encoding these enzymes. In our study, it was revealed that the alleviating effect of Si was further stimulated by Rut. We found that increased expression of genes involved in the regulation of the activity of major photosynthetic enzymes and genes encoding Rubisco following combined application of Rut+Si could be one of the primary causes of enhanced photosynthesis under osmotic stress, suggesting that the synergistic effect of Rut and Si may positively modulate CO_2 assimilation.

In conclusion, the results of this study show that the application of Rut, Si, or Rut+Si to maize plants under osmotic stress can suppress chlorophyll degradation and stimulate chlorophyll synthesis and Rubisco activity, thereby preserving photosynthetic activity. Rut, Si, and especially Rut+Si applications have the potential to maintain photosynthesis or alleviate photosynthetic damage in plants under osmotic stress. Our research was aimed at a better understanding of the key mechanisms underlying Rut+Si-mediated osmot-

ic stress tolerance. Furthermore, the study may help to address gaps in knowledge regarding the effects of Rut on stress tolerance. By using the benefits of Rut and Si, researchers may be able to plan more sustainable agriculture. Based on the findings of the current study, we can conclude that the application of Rut and Si or their combination to plants subjected to osmotic stress can improve plant growth and provide the plants with an advantage under stress conditions.

Acknowledgments

The study was supported by the project at Karadeniz Technical University Research Projects Unit (Project No: FDK-2022-10061)

References

Abdulbaki, A. S., Alsamadany, H., Alzahrani, Y., Olayinka, B. U., 2022: Rubisco and abiotic stresses in plants: Current assessment. Turkish Journal of Botany 46(6), 541–552. https://doi.org/10.55730/1300-008X.2730

Ahanger, M.A., Bhat, J.A., Siddiqui, M.H., Rinklebe, J., Ahmad, P., 2020: Integration of silicon and secondary metabolites in plants: a significant association in stress tolerance. Journal of Experimental Botany 71(21), 6758–6774. https://doi.org/10.1093/jxb/eraa291

Ahmed, N., Zhang, Y., Li, K., Zhou, Y., Zhang, M.,Li, Z., 2019: Exogenous application of glycine betaine improved water use efficiency in winter wheat (*Triticum aestivum* L.) via modulating photosynthetic efficiency and antioxidative capacity under conventional and limited irrigation conditions. The Crop Journal 7(5), 635–650. https://doi.org/10.1016/j.cj.2019.03.004

Alamri, S., Hu, Y., Mukherjee, S., Aftab, T., Fahad, S., Raza, A., Siddiqui, M. H., 2020: Silicon-induced postponement of leaf senescence is accompanied by modulation of antioxidative defense and ion homeostasis in mustard (*Brassica juncea*) seedlings exposed to salinity and drought stress. Plant Physiology and Biochemistry 157, 47–59. https://doi.org/10.1016/j.plaphy.2020.09.038

Altansambar, N., Sezgin Muslu, A., Kadıoglu, A., 2024. The combined application of rutin and silicon alleviates osmotic stress in maize seedlings by triggering accumulation of osmolytes and antioxidants' defense mechanisms. Physiology and Molecular Biology of Plants 30, 513–525. https://doi.org/10.1007/s12298-024-01430-z

Altuntaş, C., Demiralay, M., Sezgin Muslu, A., Terzi, R., 2020: Proline-stimulated signaling primarily targets the chlorophyll degradation pathway and photosynthesis associated processes to cope with short-term water deficit in maize. Photosynthesis Research 144, 35–48. https://doi.org/10.1007/s11120-020-00727-w

Arnon, P. I., 1949: Copper enzymes in isolated chloroplasts. Polyphenoloxidase in *Beta vulgaris*. Plant Physiology 24, 1–15. https://doi.org/10.1104/pp.24.1.1

Ashraf, M., Foolad, M. R. (2007): Roles of glycine betaine and proline in improving plant abiotic stress resistance. Environmental and Experimental Botany 59(2), 206–216. https://doi.org/10.1016/j.envexpbot.2005.12.006

Baker, N. R., Rosenqvist, E., 2004:Applications of chlorophyll fluorescence can improve crop production strategies: an examination of future possibilities. Journal of Experimental Botany 55(403), 1607–1621. https://doi.org/10.1093/jxb/erh196

Baker N. R., 2008: Chlorophyll fluorescence: a probe of photosynthesis in vivo. Annual Review of Plant Biology 59, 89–113. https://doi.org/10.1146/annurev.arplant.59.032607.092759

Banaś, A. K., Łabuz, J., Sztatelman, O., Gabryś, H., Fiedor, L., 2011: Expression of enzymes involved in chlorophyll catabolism in *Arabidopsis* is light controlled. Plant Physiology 157(3), 1497–1504. https://doi.org/10.1104/pp.111.185504

Berry, J. O., Yerramsetty, P., Zielinski, A. M., Mure, C. M., 2013: Photosynthetic gene expression in higher plants. Photosynthesis Research 117(1-3), 91–120. https://doi.org/10.1007/s11120-013-9880-8

Bookout, A. L., Mangelsdorf, D. J., 2003: Quantitative real-time PCR protocol for analysis of nuclear receptor signaling pathways. Nuclear Receptor Signal 1(1):e012. https://doi.org/10.1621/nrs.01012

Bradford, M. M., 1976: A rapid and sensitive method for the quantitation of microgram quantities of protein utilizing the principle of protein–dye binding. Analytical Biochemistry 72(1-2), 248–254. https://doi.org/10.1016/0003-2697(76)90527-3

Bukhari, M. A., Ahmad, Z., Ashraf, M. Y., Afzal, M., Nawaz, F., Nafees, M., Jatoi, W. N., Malghani, N. A., Shah, A. N., Manan, A., 2021: Silicon mitigates drought stress in wheat (*Triticum aestivum* L.) through improving photosynthetic pigments, biochemical and yield characters. Silicon 13, 4757–4772. https://doi.org/10.1007/s12633-020-00797-4

Chaitanya, K. V., Jutur, P. P., Sundar, D., Reddy, A. R., 2003: Water stress effects on photosynthesis in different mulberry cultivars. Plant Growth Regulation 40(1), 75–80. https://doi.org/10.1023/A:1023064328384

Chaves, M. M., Maroco, J. P., Pereira, J. S., 2003: Understanding plant responses to drought-from genes to the whole plant. Functional Plant Biology 30(3), 239–264. https://doi.org/10.1071/FP02076

Chaves, M. M., Oliveira, M. M., 2004: Mechanisms underlying plant resilience to water deficits: prospects for water-saving agriculture. Journal of Experimental Botany 55(407), 2365–2384. https://doi.org/10.1093/jxb/erh269

Chen, J., Liu, X., Du, S., Ma, Y., Liu, L., 2021: Effects of drought on the relationship between photosynthesis and chlorophyll fluorescence for maize. IEEE Journal of Selected Topics in Applied Earth Observations and Remote Sensing 14, 11148–11161. https://doi.org/10.1109/JSTARS.2021.3123111

Chen, X., Mo, X., Hu, S., Liu, S., 2019: Relationship between fluorescence yield and photochemical yield under water stress and intermediate light conditions, Journal of Experimental Botany 70(1), 301–313. https://doi.org/10.1093/jxb/ery341

Chen, Y., Wang, B., Chen, J., Wang, X., Wang, R., 2015: Identification of Rubisco rbcL and rbcS in *Camellia oleifera* and their potential as molecular markers for selection of high tea oil cultivars. Frontiers in Plant Science 6, 131993–132004. https://doi.org/10.3389/fpls.2015.00189

Cooke, J., Leishman, M. R., 2011: Silicon concentration and leaf longevity: is silicon a player in the leaf dry mass spectrum? Functional Ecology 25(6), 1181–1188. https://doi.org/10.1111/j.1365-2435.2011.01880.x

Coskun, D., Deshmukh, R., Sonah, H., Menzies, J. G., Reynolds, O., 2019: The controversies of silicon's role in plant biology. New Phytologist 221(1), 67–85. https://doi.org/10.1111/nph.15343

Dar, F. A., Tahir, I., Hakeem, K. R., Rehman, R. U., 2022: Silicon application enhances the photosynthetic pigments and phenolic/flavonoid content by modulating the phenylpropanoid pathway in common buckwheat under aluminium stress. Silicon 14(1), 323–334. https://doi.org/10.1007/s12633-021-01501-w

Dawood, M. G., Taie, H. A. A., Nassar, R. M. A., Abdelhamid, M. T., Schmidhalter, U., 2014: The changes induced in the physiological, biochemical and anatomical characteristics of *Vicia faba* by the exogenous application of proline under seawater stress. The South African Journal of Botany 93, 54–63. https://doi.org/10.1016/j.sajb.2014.03.002

Demiralay, M., 2022: Exogenous acetone O-(4-chlorophenylsulfonyl) oxime alleviates Cd stress-induced photosynthetic damage and oxidative stress by regulating the antioxidant defense mechanism in *Zea mays*. Physiology and Molecular Biology of Plants (PMBP) 28, 2069–2083. https://doi.org/10.1007/s12298-022-01258-5

Desoky, E. S. M., Mansour, E., Yasin, M. A., El Sobky, E. S. E., Rady, M. M., 2020: Improvement of drought tolerance in five different cultivars of *Vicia faba* with foliar application of ascorbic acid or silicon. Spanish Journal of Agricultural Research 18(2), 16–36. https://doi.org/10.5424/sjar/2020182-16122

Ferdinando, M. D., Brunetti, C., Fini, A., Tattini, M., 2012: Flavonoids as antioxidants in plants under abiotic stresses. Abiotic Stress Responses Plants 159–179. https://doi.org/10.1007/978-1-4614-0634-1_9

Flexas, J., Ribas-Carbó, M., Bota, J., Galmés, J., Henkle, M., Martínez-Cañellas, S., Medrano, H., 2006: Decreased Rubisco activity during water stress is not induced by decreased relative water content but related to conditions of low stomatal conductance and chloroplast CO_2 cncentration. New Phytologist 172(1), 73–82. https://doi.org/10.1111/j.1469-8137.2006.01794.x

Genty, B., Jean-Marie B., Neil, R. B., 1989: The relationship between the quantum yield of photosynthetic electron transport and quenching of chlorophyll fluorescence. Biochimica et Biophysica Acta (BBA)-General Subjects 990(1), 87–92. https://doi.org/10.1016/S0304-4165(89)80016-9

Ghotbi-Ravandi, A. A., Shahbazi, M., Shariati, M., Mulo, P., 2014: Effects of mild and severe drought stress on photosynthetic efficiency in tolerant and susceptible barley (*Hordeum vulgare* L.) genotypes. Journal of Agronomy and Crop Science 200(6), 403–415. https://doi.org/10.1111/jac.12062

Gong, H., Chen, K., 2012: The regulatory role of silicon on water relations, photosynthetic gas exchange, and carboxylation activities of wheat leaves in field drought conditions. Acta Physiologiae Plantarum 34(4), 1589–1594. https://doi.org/10.1007/s11738-012-0954-6

Hayat, S., Ahmad, A. (eds.), 2007: Salicylic acid: a plant hormone. Springer. https://doi.org/10.1007/978-1-4020-5184-7

Hoagland, D. R., Arnon, D. I., 1950: The water-culture method for growing plants without soil. Circular California Agriculture Experiment Station.

Hussain, I., Ayub, A., Nayab, A., Ashraf, M. A., Ashraf, M. A., Hussain, S., Siddiqui, M. H., Sabie M. E., Zulfiqar, U., Khan, T. H., 2023: Exogenous application of silicon and zinc attenuates drought tolerance in *Eruca sativa* L. through increasing chlorophyll pigments, osmoprotectants, and modulating defense mechanisms. Journal of Plant Growth Regulation 43, 3221–3237. https://doi.org/10.1007/s00344-023-11116-7

Iqbal, M. S., Singh, A. K., Ansari, M. I., 2020: Effect of drought stress on crop production. In: Rakshit, A., Singh, H. B., Singh, A. K., Singh, U. S., Fraceto, L. (eds.), New frontiers in stress management for durable agriculture, 35–47. Springer, Singapore.

Ismail, H., Maksimovic, J. D., Maksimovic, V., Shabala, L., Zivanovic, B. D., Tian, Y., Jacobsen, S. E., Shabala, S., 2015: Rutin, a flavonoid with antioxidant activity, improves plant salinity tolerance by regulating K^+ retention and Na^+ exclusion from leaf mesophyll in quinoa and broad beans. Functional Plant Biology 43(1), 75–86. https://doi.org/10.1071/FP15312

Kalaji, H. M., Dąbrowski, P., Cetner, M. D., Samborska, I. A., Łukasik, I., Brestic, M., Zivcak, M., Tomasz, H., Mojski, J., Kociel, H., Panchal, B. M., 2017: A comparison between different chlorophyll content meters under nutrient deficiency conditions. Journal of Plant Nutrition 40(7), 1024–1034. https://doi.org/10.1080/01904167.2016.1263323

Khan, Z. S., Rizwan, M., Hafeez, M., Ali, S., Adrees, M., Qayyum, M. F., Sarwar, M. A. 2020: Effects of silicon nanoparticles on growth and physiology of wheat in cadmium contaminated soil under different soil moisture levels. Environmental Science and Pollution Research 27(5), 4958–4968. https://doi.org/10.1007/s11356-019-06673-y

Krause, H., Weis, W., 1991: Chlorophyll fluorescence and photosynthesis: The Basics. Annual Review of Plant Physiology and Plant Molecular Biology 42, 313–349. http://dx.doi.org/10.1146/annurev.pp.42.060191.001525

Lawlor, D. W., Cornic, G., 2002: Photosynthetic carbon assimilation and associated metabolism in relation to water deficits in higher plants. Plant, Cell and Environment 25(2), 275–294. https://doi.org/10.1046/j.0016-8025.2001.00814.x

Li, L., Ai, S., Li, Y., Wang, Y., Tang, M., 2018: Exogenous silicon mediates alleviation of cadmium stress by promoting photosynthetic activity and activities of antioxidative enzymes in rice. Journal of Plant Growth Regulation 37, 602–611. https://doi.org/10.1007/s00344-017-9758-7

Li, Z., Liu, Z., Yue, Z., Wang, J., Jin, L., Xu, Z., Yu, J., 2022: Application of exogenous silicon for alleviating photosynthetic inhibition in tomato seedlings under low– calcium stress. International Journal of Molecular Sciences 23(21), 13526–13549. https://doi.org/10.3390/ijms232113526

Liang, Y., Nikolic, M., Bélanger, R., Gong, H., Song, A., 2015: Silicon in agriculture. Silicon-mediated tolerance to salt stress. Silicon in Agriculture, 123–142. Springer, Dordrecht. https://doi.org/10.1007/978-94-017-9978-2_6

Lin, M. T., Stone, W. D., Chaudhari, V., Hanson, M. R., 2020: Small subunits can determine enzyme kinetics of tobacco Rubisco expressed in *Escherichia coli*. Nature Plants 6, 1289–1299. https://doi.org/10.1038/s41477-020-00761-5

Liu, P., Yin, L., Deng, X., Wang, S., Tanaka, K., Zhang, S., 2014: Aquaporin-mediated increase in root hydraulic conductance is involved in silicon-induced improved root water uptake under osmotic stress in *Sorghum bicolor* L. Journal of Experimental Botany 65(17), 4747–4756. https://doi.org/10.1093/jxb/eru220

Lyu, J., Jin, L., Meng, X., Jin, N., Wang, S., Hu, L., Yu, J. 2022: Exogenous Si mitigates the effects of cinnamic-acid-induced stress by regulating carbon metabolism and photosynthetic pigments in cucumber seedlings. Agronomy 12(7), 1569–1583.

Maghsoudi, K., Emam, Y., Ashraf, M., 2015: Influence of foliar application of silicon on chlorophyll fluorescence, photosynthetic pigments, and growth in water-stressed wheat cultivars differing in drought tolerance. Turkish Journal of Botany 39(4), 625–634. https://doi.org/10.3390/agronomy12071569

Maghsoudi, K., Emam, Y., Pessarakli, M., 2016: Effect of silicon on photosynthetic gas exchange, photosynthetic pigments, cell membrane stability and relative water content of different wheat cultivars under drought stress conditions. Journal of Plant Nutrition 39(7), 1001–1015. https://doi.org/10.1080/01904167.2015.1109108

McFeeters, R. F., Chichester, C. O., Whitaker, J. R., 1971: Purification and properties of chlorophyllase from *Ailanthus altissima* (tree-ofheaven). Plant Physiology 47(5) 609–618. https://doi.org/10.1104/pp.47.5.609

Mavondo-She, M. A., Mashilo, J., Gatabazi, A., Ndhlala, A. R., Laing, M. D. 2024: Exogenous silicon application improves chilling injury tolerance and photosynthetic performance of cit-

rus. Agronomy 14(1), 139–153. https://doi.org/10.3390/agronomy14010139

Maxwell, K., Johnson, G. N., 2000: Chlorophyll fuorescence-A practical guide. Journal Experimental Botany 51(345), 659–668. https://doi.org/10.1093/jexbot/51.345.659

Nar, H., Saglam, A., Terzi, R. Várkonyi, Z., Kadıoglu, A., 2009: Leaf rolling and photosystem II efficiency in *Ctenanthe setosa* exposed to drought stress. Photosynthetica 47(3), 429–436. https://doi.org/10.1007/s11099-009-0066-8

Parry, M. A. J., Andralojc, P. J., Parmar, S., Keys, A. J., Habash, D. Z., Paul, M. J., Alred, R., Quick, W. P., Servaites, J. C., 1997: Regulation of Rubisco by inhibitors in the light. Plant Cell Environment 20(4), 528–534. https://doi.org/10.1046/j.1365-3040.1997.d01-85.x

Rissler, H. M., Collakova, E., DellaPenna, D., Whelan, J., Pogson, B. J., 2002: Chlorophyll biosynthesis. Expression of a second *chl I* gene of magnesium chelatase in Arabidopsis supports only limited chlorophyll synthesis. Plant Physiology 128(2), 770–779. https://doi.org/10.1104/pp.010625

Santos, C. V., 2004: Regulation of chlorophyll biosynthesis and degradation by salt stress in sunflower leaves. Scientia Horticulturae 103(1), 93–99. https://doi.org/10.1016/j.scienta.2004.04.009

Sawada, S., Sato, M., Kasai, A., Yaochi, D., Kameya, Y., Matsumoto, I., Kasai, M., 2003: Analysis of the feed-forward effects of sink activity on the photosynthetic source-sink balance in single-rooted sweet potato leaves. I. Activation of RuBPcase through the development of sinks. Plant Cell Physiology 44(2), 190–197. https://doi.org/10.1093/pcp/pcg024

Sezgin Muslu, A., 2024: Improving salt stress tolerance in *Zea mays* L. by modulating osmolytes accumulation and antioxidant capacity with Rutin. Anatolian Journal of Botany 8(1), 21–29. https://doi.org/10.30616/ajb.1387695

Singh, A., Gupta, R., Pandey, R., 2017: Exogenous application of rutin and gallic acid regulate antioxidants and alleviate reactive oxygen generation in *Oryza sativa* L. Physiology and Molecular Biology of Plants 23, 301–309. https://doi.org/10.1007/s12298-017-0430-2.

Tanaka, A., Tanaka, R., 2006: Chlorophyll metabolism. Current Opinion Plant Biology 9(3), 248–255. https://doi.org/10.1016/j.pbi.2006.03.011

Tsuzuki, T., Takahashi, K., Tomiyama, M., Inoue, S. I., Kinoshita, T., 2013: Overexpression of the Mg-chelatase H subunit in guard cells confers drought tolerance via promotion of stomatal closure in *Arabidopsis thaliana*. Frontiers in Plant Science 4, 440–448. https://doi.org/10.3389/fpls.2013.00440

van Kooten, O., Snel, J. F. H., 1990: The use of chlorophyll fluorescence nomenclature in plant stress physiology. Photosynthesis Research 25, 147–150. https://doi.org/10.1007/BF00033156

Verma, K. K., Singh, P., Song, X. P., Malviya, M. K., Singh, R. K., Chen, G. L., Solomon, S., Li, Y. R., 2020: Mitigating climate change for sugarcane improvement: role of silicon in alleviating abiotic stresses. Sugar Technology 22(5), 741–749. https://doi.org/10.1007/s12355-020-00831-0

Wang, M., Tadmor, Y., Wu, Q. L., Chin, C., Garrison, S. A., Simon, J. E., 2003: Quantification of protodioscin and rutin in asparagus shoots by LC/MS and HPLC methods. Journal of Agricultural and Food Chemistry 51(21), 6132–6136. https://doi.org/10.1021/jf0344587

Xiang, D. B., Peng, L. X., Zhao, J. L., Zou, L., Zhao, G., Song, C., 2013: Effect of drought stress on yield, chlorophyll contents and photosynthesis in tartary buckwheat (*Fagopyrum tataricum*). Journal of Food, Agriculture and Environment 11(3-4), 1358–1363.

Yang, C. M., Chang, I. F., Lin, S. J., Chou, C. H., 2004: Effects of three allelopathic phenolics on chlorophyll accumulation of rice (*Oryza sativa*) seedlings: II. Stimulation of consumption-orientation. Botanical Bulletin of Academia Sinica 45, 119–125.

Yang, J., Guo, J., Yuan, J., 2008: In vitro antioxidant properties of rutin. Lebensmittel Wissenschaft Technologie 41(6), 1060–1066. https://doi.org/10.1016/j.lwt.2007.06.010

Zhang, Y., Liang, Y., Zhao, X., Jin, X., Hou, L., Shi, Y., Ahammed, G. J., 2019: Silicon compensates phosphorus deficit-induced growth inhibition by improving photosynthetic capacity, antioxidant potential, and nutrient homeostasis in tomato. Agronomy 9(11), 733–749. https://doi.org/10.3390/agronomy9110733

Zhou, M., Gong, X., Ying, W., Chao, L., Hong, M., Wang, L., Fashui, H., 2011: Cerium relieves the inhibition of chlorophyll biosynthesis of maize caused by magnesium deficiency. Biological Trace Element Research 143(1), 468–477. https://doi.org/10.1007/s12011-010-8830-y

Acta Bot. Croat. 84 (1), 81–90, 2025
DOI: 10.37427/botcro-2025-020

CODEN: ABCRA 25
ISSN 0365-0588
eISSN 1847-8476

Sulfur deficiency reduces the thermotolerance of *Heliotropium thermophilum* to high temperatures

Ece Nisa İmamoğlu[1], Aykut Sağlam[1]*, Asim Kadıoğlu[2]

[1] Karadeniz Technical University, Faculty of Science, Department of Molecular Biology and Genetics, 61080 Trabzon, Türkiye

[2] Karadeniz Technical University, Faculty of Science, Department of Biology, 61080 Trabzon, Türkiye

Abstract – *Heliotropium thermophilum*, a thermotolerant plant, was subjected to low sulfate treatments to examine the effects of sulfur deficiency on the plant's thermotolerance. For this aim, two different concentrations (0.15 mM and 0.30 mM) of low-sulfate media as well as full nutrition (FN) medium were prepared and the plants were cultured at 25 °C for 60 days, then divided into 2 groups for temperature applications and kept at either 25 or 40 °C for 7 days. *H. thermophilum* could survive in low-sulfate media at 40 °C, but high temperature damages such as chlorosis, and green color retention were observed. In addition, heat treatment reduced plant fresh weight, relative water content, and total sugar contents in both low-sulfate media. Moreover, proline and hydrogen peroxide levels were the highest in plants grown in 0.15 mM sulfate at 40 °C. Peroxidase activities were increased in plants grown in low-sulfate media at high temperature, compared to values at 25 °C. In plants grown in 0.30 mM sulfate medium, catalase activity was elevated, whereas it was reduced in 0.15 mM sulfate-grown plants at 40 °C compared to the values at 25 °C. Glutathione reductase (GR) activity at 40 °C was downregulated in 0.30 mM sulfate-grown plants while in those grown in FN and 0.15 mM-sulfate media it did not change. *Heat Shock Factor 4* (*HSF4*) and *HSFA4A* genes were also upregulated by low sulfate and high temperature although *HSFA4A* gene activation was lower under sulfur deficiency. Moreover, *HSFA3* gene expression at 40 °C decreased upon the application of 0.30 mM sulfate. We hypothesize that sulfur deficiency makes *H. thermophilum* susceptible to high temperatures by decreasing chlorophyll and sugar contents, and reducing the activities of the antioxidant enzymes and thus plant growth. Moreover, the down-regulation of the *HSFA3* and *HSFA4A* gene, caused by sulfur deficiency, confirms the negative effects of sulfur deficiency on plant response to high temperatures.

Keywords: antioxidants, gene expression, heat shock factors, nutrition deficiency, thermophile

Introduction

Abiotic stress factors affect the development, survival, biomass production, and yield of plants. Among the abiotic stress factors, heat disrupts plants by damaging their metabolism, in various ways. However, plants have developed different mechanisms to tolerate or avoid high temperatures. High-temperature tolerance is defined as the capacity of the plant to grow under high temperatures and still be economically productive (Sezgin Muslu and Kadıoğlu 2021). *Heliotropium thermophilum* (Boraginaceae), a heat-tolerant plant species, is an endemic and thermophilic flowering plant. The natural distribution area of the plant is a geothermal region in Buharkent, Aydın, Türkiye with an optimum soil temperature range, between 55 and 65 °C. In addition, there is a high concentration of sulfate anion (772 mg L^{-1}) in the soil environment where the plant grows, which is caused by the oxidation of H_2S gas escaping from magma (Tan et al. 2008). It is widely acknowledged that in these conditions the plants attain their ideal nutrient status for optimal productivity and tolerance to environmental constraints.

The sulfur content in plant cells varies with plant growth and developmental stage and the length and intensity of exposure to stress conditions (Ihsan et al. 2019). Sulfur is found in the composition of important biomolecules, including specific vitamins like thiamine and biotin, amino acids such as cysteine and methionine, antioxidants like glutathione (GSH), thioredoxin, fatty acid, i.e., lipoic acid, and glucosinolate (Ali et al. 2019). It has been established that all these sulfur-containing biomolecules have a role in detoxifying reactive oxygen species (ROS) and redox control of proteins under stress conditions (Hill et al. 2022), but are also important signal compounds in plants (Narayan et. al 2023).

* Corresponding author e-mail: saglama@ktu.edu.tr

During the stress conditions, such as heat and drought, GSH undergoes oxidation to glutathione disulfide (GSSG), which is essential for maintaining the optimal functioning of cellular and biochemical redox systems within plant cells (Hasanuzzaman et al. 2017). In addition, GSH is involved in the cellular redox buffer system and acts as an electron donor to remove ROS which may appear in plant metabolic pathways as a result of oxidative stress due to elevated temperatures (Dard et al. 2023). Methionine plays an important role in the nutrition of plants and the translation of mRNAs (Hesse et al. 2004), but is also involved in ROS detoxification in the response to high temperatures (Ihsan et al. 2019). For example, a chloroplast low molecular weight heat shock protein (HSP), which is rich in methionine, plays a crucial role in safeguarding the transportation of electrons from photosystem II when a plant is subjected to thermal stress (Heckathorn et al. 1998). Additionally, chloroplastic HSPs rich in methionine play a direct role in the thermotolerance of the photosynthetic machinery in plants (Sehar et al. 2022).

Heat shock transcription factors (HSF) also play important roles in regulating plant thermotolerance. The rapid synthesis and accumulation of HSPs, which are molecular chaperones that prevent protein aggregation and maintain cellular protein homeostasis, are regulated by HSFs (Kang et al. 2022). For example, an enhanced ability to withstand high temperatures has been observed in wheat plants that overexpress the *TaHSFA6f* gene that regulates a suite of heat stress protection genes in wheat, including *TaHsps* (*TaHSP16*.8, *TaHSP17*, *TaHSP17*.3, and *TaHSP90.1-A1*), *TaRof1*, galactinol synthase, and glutathione-S-transferase (Xue et al. 2015) Moreover, when soil temperature rose from 20 to 80 °C, the expression levels of *HSFA4A*, *HSFA3* and *HSF4* were significantly upregulated in *H. thermophilum* (Sezgin Muslu and Kadıoğlu, 2021). However, there is no information in the relevant literature cited about how HSFs are affected by sulfur content in plants at high temperatures.

In our study, we hypothesized that there may be a link between the high sulfate concentration in the environment where *H. thermophilum* grows and its resilience to high soil temperatures. To test the hypothesis and clarify the possible role of sulfur in high temperature tolerance, *H. thermophilum* plants were grown in sulfur-deficient growth media with two different sulfate levels. Then, the changes in osmotic balance, antioxidant system, and HSF expressions during high temperature as a result of sulfur deficiency were studied.

Material and methods

Plant growth, sulfur deficiency, and temperature applications

Seeds of *H. thermophilum*, were exposed to surface sterilization with 0.1% hypochloric acid for 5 min in a laminar flow cabinet, then 50 μM GA_3 was applied at +4 °C for two days to break seed dormancy. The seeds were sown in vermiculite containing two low-sulfate media (0.15 and 0.30 mM SO_4^{2-}) or full nutrition (FN) medium (control), prepared based on the Hoagland solution recipe (On-line Suppl. Tab. 1) (Bielecka, 2007). $MgCl_2$ was used instead of $MgSO_4$ to create sulfur deficiency. Seeds were sown in plastic trays including vermiculite (8 seeds/pot, 5 replicates for each treatments) in a water bath located in a growth chamber and grown while being watered with the solution twice a week in the following conditions for 60 days: 25 °C, 16/8-hour light/dark photoperiod, 350 μmol m^{-2} s^{-1} light intensity and 60% relative humidity. Water baths were used to keep the temperature of the media constant. The temperature of the media in which the plants grew was measured daily with a thermometer to verify whether the temperature was 25 °C. Afterward, half of these 60-day-old plants were kept growing at 25 °C and the other half were exposed to heat stress at 40 °C for another 7 days (On-line Suppl. Fig. 1). Although *H. thermophilum* plants grow in soil at temperatures between 55-65 °C in their natural habitat, our preliminary experiment showed that in a liquid media the best growth performance was obtained at 40 °C. At higher temperatures liquid media is lost due to evaporation, and pH is unstable causing retardation of growth. In order to determine the presence of sulfur deficiency, attention was paid to the parameters of chlorosis in plants (pale green chlorosis), lack of green color in the veins or in many cases paler than the interveinal tissue, and earlier or more severe yellowing of young leaves than of mature leaves. At the end of the applications, measurements were made with the leaves of the plants.

Plant fresh weight

The fresh weights of the whole plants grown in the above-mentioned conditions were determined with precision scales at the end of the applications.

Relative water, proline and total soluble sugar contents

Relative water, proline and total soluble sugar contents were determined based on Saglam et al (2008). After measuring the fresh weight of leaves, plants were kept in deionized water at 4 °C for 24 h and the turgid weights were weighed. Afterward, the samples were kept in the oven set at 65 °C for 48 h, their dry weights were recorded, and their relative water content (RWC) was determined according to the formula:

$$\mathrm{RWC}(\%) = \frac{\text{fresh weight} - \text{dry weight}}{\text{turgid weight} - \text{dry weight}} \times 100$$

For determination of proline content, 0.1 g of fresh plant samples were homogenized in 40% ethanol, incubated overnight in a micromixer at 300 rpm at 4 °C and then filtered. One mL of the filtrate was taken and mixed with 2 mL of reaction mixture containing 1 mL of 60% acetic acid, 20% ethanol, and 1% (w/v) ninhydrin. The samples were placed in tubes and kept in a water bath at 95 °C for 20 min, and the reaction was terminated on ice. The cooled samples were read in the spectrophotometer at 520 nm. The amount of proline was determined from a standard curve in the range of 20–100 μg.

To determine total soluble sugars, oven-dried leaves (0.1 g) were homogenized with 5 mL of 70% ethanol. The homogenate was boiled at 80 °C for 3 min and then cooled to room temperature and centrifuged at 10000 g for 5 min. For spectrophotometric determination, 100 µL of the supernatant was diluted by adding 900 µL of distilled water. One mL of 5% phenol was added to 1 mL of the sample and vortexed. After that, 5 mL of 96% sulfuric acid was added to the mix and then vortexed. The tubes containing the mixture were cooled to room temperature and their absorbance was measured at 490 nm by a spectrophotometer. The standard curve was made from 0, 20, 40, 60, 80, and 100 µg mL^{-1} glucose.

Hydrogen peroxide content and antioxidant enzyme activities

The content of hydrogen peroxide (H_2O_2) and antioxidant enzyme activities were determined according to Sağlam et al (2011).

To assess H_2O_2 content, 0.25 g of leaf samples was ground in 5 mL of 0.1% (w/v) trichloroacetic acid. The homogenate was centrifuged at 15000 g at 4 °C for 15 min. After the removal of 1 mL of the supernatant, 10 mM potassium phosphate buffer and 1 M potassium iodide were added, and the absorption of the mixture was measured at 390 nm. The hydrogen peroxide was determined from the standard curve of known concentration of hydrogen peroxide ranging from 0-100 nM.

For measurements of antioxidant enzymes activity, leaf samples (0.1 g) were powdered with liquid nitrogen and then extracted in 5 mL of extraction buffer (50 mM dipotassium hydrogen phosphate (K_2HPO_4), 1 mM ethylenediaminetetraacetic acid (EDTA) pH 7.0, 1% (w/v) polyvinylpyrrolidone (PVPP). The extracts were centrifuged at 20000 g at 4 °C for 20 min. The antioxidant enzyme activities were measured in the obtained supernatant, except for ascorbate peroxidase (APX) where 5 mM ascorbic acid was added to the extraction buffer.

Peroxidase (POD, EC 1.11.1.7) activity was assessed in 1 mL of the reaction mixture, which consisted of 100 mM potassium phosphate buffer (pH 7.0), 0.1 mM EDTA, 5 mM guaiacol, 15 mM H_2O_2, and 50 µL of enzyme extract, at a wavelength of 470 nm for a duration of 1 min. The POD activity was calculated by employing the extinction coefficient of 26.6 mM^{-1} cm^{-1} for tetraguaiacol, a colored product of enzymatic reaction.

Catalase (CAT, EC 1.11.1.6) activity was determined by measuring 1 mL of the reaction mixture containing 50 mM potassium phosphate buffer (pH 7.0), 30 mM H_2O_2, and 100 µL enzyme extract at 240 nm for 3 min. The CAT activity was calculated using the extinction coefficient of 39.4 $mM^{-1}cm^{-1}$ for H_2O_2.

To determine the activity of glutathione reductase (GR, EC 1.6.4.2), 50 µL of enzyme extract was added to a mixture consisting of 50 mM tris(hydroxymethyl)aminomethane hydrochloride (pH 7.8), 250 µL of 1 mM L-glutathione oxidized (GSSG), and 500 µL of 0.25 mM NADPH, which was prepared in 200 µL of 0.5 mM EDTA. The reduction of NADPH was measured by following the oxidation for a duration of 5 min at a wavelength of 340 nm. The enzyme activity was calculated using the extinction coefficient of NADPH, which is 6.22 mM^{-1} cm^{-1}.

Ascorbate peroxidase (APX, EC 1.11.1.11) activity was determined based on the decrease in absorbance at 290 nm. The determination of enzyme activity involved the measurement of a 1 mL reaction mixture composed of 50 mM potassium phosphate buffer (with a pH of 7.0), 250 µM ascorbate (ASC), 5 mM H_2O_2, and 100 µL enzyme extract. The activity of APX was calculated by employing the extinction coefficient of 2.8 mM^{-1} cm^{-1} for ASC.

Protein determination

Determination of protein concentration was made spectrophotometrically (Thermo Scientific, Evolution 201 UV-VIS Spectrophotometer) according to Bradford (1976). By preparing bovine serum albumin standards (20-140 µg protein), the complex formed by proteins was measured at 595 nm with Coomassie Brilliant Blue G250 dye. Protein concentration was calculated in mg per liter and used to express enzyme activities.

RNA extraction and cDNA synthesis

Fresh leaf samples (0.1 g) were frozen with liquid nitrogen and thoroughly lysed with a tissue shredder. Afterwards, the protocol of the FavorPrep Plant Total RNA Purification Mini Kit (Favorgen Biotech Corp) was applied to obtain total RNA. The amount and purity of RNA in the samples were determined spectrophotometrically by Nanodrop (Thermo Scientific, NanoDrop 2000). Using a High Capacity Cdna Reverse Transcription Kit (Applied Biosystems) from isolated total RNA samples, cDNA was obtained at 2000 ng.

Quantitative PCR (qPCR)

Analyses were completed on the CFX Connect Real Time PCR System (BioRad) device using EvaGreen qPCR Supermix (Solis Biodyne) solution with cDNA to determine the gene expressions. The analysis was carried out by modifying the Solis Biodyne instructions and following the steps: The qPCR reaction program was set as follows: initial activation at 95 °C for 12 s; then denaturation at 95 °C for 15 s, annealing at 60 °C for 30 s, and extension at 72 °C for 30 s, repeated for 44 cycles; and a melting curve protocol (65–95 °C with fluorescence measured every 0.5 °C). Three biological replications were adopted for each sample. Gene-specific primers for qPCR analysis were created using the primer 3.0 online tool (http://bioinfo.ut.ee/primer3). The primers were used to examine the expression levels of actin 7 (reference gene) and *HSFA4A, HSF4, and HSFA3* genes. Actin 7 was used to normalize the data obtained from the analysis and present it as the relative gene expression. The $2^{-\Delta\Delta Cq}$ method was used to calculate gene expression (Bookout and Mangelsdorf, 2003). The primer sequences (5'–3') are as listed below:

ACT 7: Reference gene (ACT 7-F: TACGAGCAGGAGCTTGACAC, ACT 7-R: CCGATCATGGAAGGCTGGAA),

HSFA4A: Heat shock factor a4a (HSFA4A-F: TTCACCGACGCAAGCCAATA, HSFA4A-R: TTATGCCTCTCAAGCTCCGC),

HSF4: Heat shock factor 4 (HSF4-F: GCTTCGTTCGCCAGCTTAAC, HSF4-R: GCTTCGTTCGCCAGCTTAAC),

HSFA3: Heat shock factor a3 (HSFA3-F: CCTCCTAATAGTACGCCGCC, HSFA3-R: CAAGGGGAGAGGCCATTGTT).

Sulfur analysis

Plant samples were dried at 105 °C and ground using a mill (Sinbo SCM-2934). An elemental analyzer (LECO 628) burned 1.0 g of sample at a 300 mL min^{-1} flow rate at 1050 °C. The resulting SO_2 was measured in the infrared cell of the elemental analyzer (Maj et al. 2020).

Statistical analysis

The statistical software SPSS version 23.0 was used to conduct two-way analysis of variance (ANOVA) on all the data. All the traits were examined in order to determine how high temperature, sulfur deficiency, and their interactions affect them. With the use of post hoc Tukey's multiple range test, the significance of differences between mean values ($P < 0.05$) was confirmed. The mean values for five replicates ± standard deviation (SD) were presented.

Results

When plants were given low amounts of sulfate and were exposed to high temperature, as opposed to complete nutrient delivery at 40 °C, the indications of sulfur deficiency, such as chlorosis, green color retention in the veins, and yellowing of young leaves were clearly visible (Fig. 1).

Measurement of sulfur content confirmed that plants grown in both low-sulfate media experienced a decrease in sulfur content; the percentages of sulfur in plants growing at 25 °C in FN medium and in media containing 0.30 and 0.15 mM SO_4^{2-} (later in the text 0.30 and 0.15 mM sulfate media) were 0.73%, 0.67%, and 0.63%, respectively. Compared to the plants at 25 °C, the S content was greater in plants at 40 °C; it was 0.77% and 0.79% in plants grown in the 0.30 and 0.15 mM sulfate media, while an even higher S level (0.82%) was measured in plants in the FN media.

Fig. 1. Plants grown in full nutrition (FN) medium at (A) 25 °C and (B) 40 °C; 0.30 mM sulfate medium at (C) 25 °C and (D) 40 °C, and 0.15 mM sulfate medium at (E) 25 °C and (F) 40 °C. Plants were grown 60 days at 25 °C in FN, 0.30 mM or 0.15 mM sulfate media and then subjected to a temperature of 40 °C for 7 days.

The two-way ANOVA indicated highly significant ($P < 0.01$) effects of temperature, sulfur and the temperature × sulfur interaction on the plant fresh weight (Tab. 1).

The fresh weight of the plants grown at 25 °C in 0.15 mM sulfate medium was lower than that of those grown in FN

Tab. 1. Two-way ANOVA (F values and statistical significance) considering the effect of treatment, variety, and interactions on the measured variables, as indicated. ns, **, *** indicate non-significant or significant at $P < 0.05$ and $P < 0.01$, respectively. Values in parentheses are degrees of freedom.

Parameter	Temperature	Sulfur	Temperature × sulfur
Plant fresh weight	78.492*** (1)	678.349*** (2)	141.195*** (2)
Relative water content	14.459*** (1)	91.488*** (2)	32.584*** (2)
Hydrogen peroxide level	627.022*** (1)	3071.088*** (2)	733.367*** (2)
Proline level	7903.739*** (1)	5992.479*** (2)	4960.552*** (2)
Total soluble sugar content	105.314*** (1)	21.328*** (2)	11.060*** (2)
APX activity	2.137ns (1)	138.860*** (2)	12.087*** (2)
GR activity	157.809*** (1)	121.541*** (2)	135.859*** (2)
CAT activity	8.641** (1)	162.605*** (2)	24.683*** (2)
POD activity	670.775*** (1)	85.656*** (2)	50.987*** (2)
HSF4 gene expression	4085.341*** (1)	808.344*** (2)	866.233*** (2)
HSFA4A gene expression	258.000*** (1)	232.045*** (2)	135.295*** (2)
HSFA3 gene expression	93.656*** (1)	91.028*** (2)	74.911*** (2)

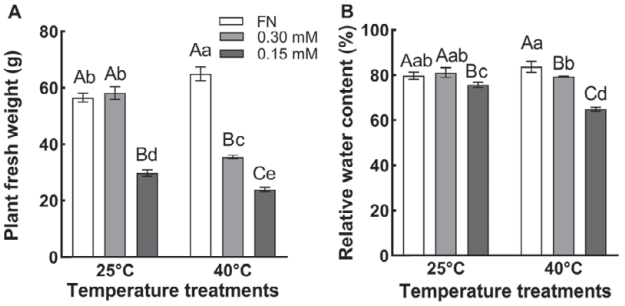

Fig. 2. The fresh weight (A) and the relative water content (B) of the plants grown at 25 °C and 40 °C in full nutrition (FN), 0.30 mM and 0.15 mM sulfate media. Data show the means ± the standard deviation of five independent samples. Different small letters indicate that means were statistically different ($P < 0.05$). Different capital letters indicate differences in different sulfate treatments at same temperature group ($P < 0.05$). Tukey's multiple testing method was used to compare the means. Plants were grown 60 days at 25 °C in FN, 0.30 mM or 0.15 mM sulfate media and then subjected to 40 °C for 7 days.

or 0.30 mM sulfate media. In addition, the plants in 0.15 mM sulfate medium were smaller than the plants in 0.30 mM sulfate and FN media. When high temperatures were applied, the fresh weights of plants grown in 0.30 and 0.15 mM sulfate media decreased compared with those grown in FN media (Fig. 2A). The high temperature treatment resulted in an increase in the fresh weight of plants in FN medium, while in 0.30 and 0.15 mM sulfate grown plants it was reduced by 39% and 20%, respectively, compared to respective values obtained at 25 °C.

The RWC was significantly affected by temperature, sulfur, and the temperature × sulfur interaction ($P < 0.01$) as demonstrated by the two-way ANOVA (Tab. 1). At both temperature, 25 and 40 °C, the RWC of the plants grown in 0.15 mM sulfate was lower than in plants grown in FN and 0.30 mM sulfate media (Fig. 2B). RWC of 0.15 mM sulfate-grown plants at 40 °C was reduced by 4.3% compared to the RWC of the plants at 25 °C. RWC values of FN and 0.30 mM-sulfate grown plants at 40 °C were not different from respective values at 25 °C.

Two-way ANOVA indicated highly significant ($P < 0.01$) effects of temperature, sulfur and the temperature × sulfur interaction on H_2O_2 content (Tab. 1). At 25 °C, the H_2O_2 level was found to be equal in plants grown in FN and 0.30 mM sulfate media, but significantly higher than in plants grown in 0.15 mM sulfate medium. The highest level of H_2O_2 was observed in plants grown in 0.15 mM sulfate medium at 40 °C (Fig. 3A). H_2O_2 level of plants grown in FN was reduced by 43% by heat treatment compared to the value of FN at 25 °C, while the H_2O_2 contents of the plants grown in 0.30 and 0.15 mM sulfate media at 40 °C were 39% and 105% higher than in those grown in 0.30 and 0.15 mM sulfate media at 25 °C.

The proline content was significantly ($P < 0.01$) affected by temperature, sulfur, and the temperature × sulfur interaction in two-way ANOVA (Tab. 1). The proline levels of plants grown in 0.15 and 0.30 mM sulfate media at 25 °C did not differ, but it was higher than in the plants grown in FN media. An increase in the proline content was evident in plants exposed to high temperature since the values in plants grown in FN, 0.30 mM, or 0.15 mM sulfate media increased by 10%, 26%, and 220%, respectively, compared to the respective values from the plants in FN, 0.30 and 0.15 mM sulfate media at 25 °C. Besides, the plants that were grown in 0.15 mM sulfate medium at 40 °C had a higher proline content than those grown in FN or 0.30 mM sulfate media (Fig. 3B).

In the two-way ANOVA (Tab. 1), temperature, sulfur, and the temperature × sulfur interaction all affected the soluble sugar content significantly ($P < 0.01$). The total soluble sugar content of plants grown in FN, 0.30 and 0.15 mM sulfate media did not differ at 25 °C. At high temperature (40 °C), the sugar content of plants grown in FN medium was similar to that in plants at 25 °C, while in plants grown in 0.30 and 0.15 mM sulfate media it was reduced by 27% and 36% compared to the plants grown in 0.30 and 0.15 mM sulfate media. Also, at 40 °C sugar content in plants grown in 0.30 and 0.15 mM sulfate media was lower than in FN medium grown plants at 40 °C (Fig. 3C).

Two-way ANOVA showed significant effects of sulfur deficiency and the temperature × sulfur interaction on APX

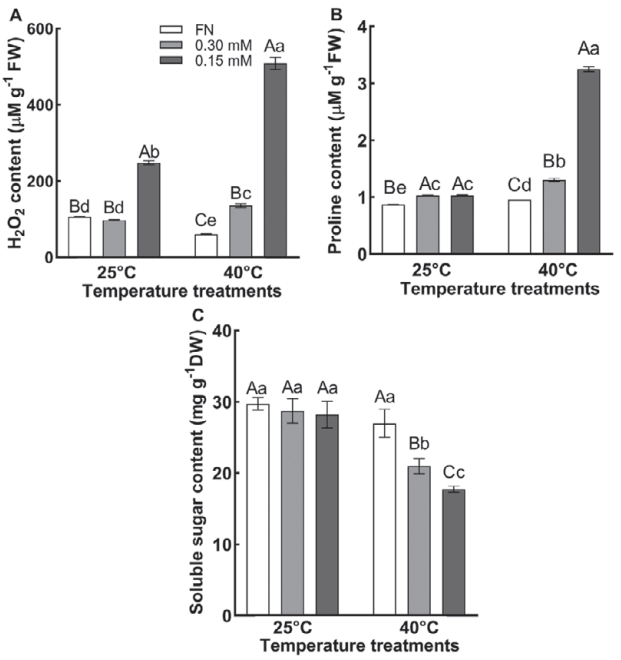

Fig. 3. The level of hydrogen peroxide (H_2O_2) (A), proline (B), and total soluble sugar (C) of the plants grown at 25 °C and 40 °C in full nutrition (FN), 0.30 mM and 0.15 mM sulfate media Data show the means ± the standard deviation of five independent samples. Different small letters indicate that means were statistically different ($P < 0.05$). Different capital letters indicate differences in different sulfate treatments at same temperature group ($P < 0.05$). Tukey's multiple testing method was used to compare the means. Plants were grown 60 days at 25 °C in FN, 0.30 mM and 0.15 mM sulfate media then subjected to a temperature of 40 °C for 7 days.

activity (P < 0.01) while no significant effect was observed for high temperature on the enzyme activity (Tab. 1). The APX activity of the plants grown in FN medium was higher than that of those grown in 0.30 and 0.15 mM sulfate media at 25 °C. (Fig. 4A). The APX activities in FN medium-grown plants at 25 °C and 40 °C were not different. However, APX activity was induced by low sulfur and high temperature treatments. The APX activity of plants grown in 0.30 and 0.15 mM sulfate media at 40 °C was increased by 25 and 83%, respectively, compared to values of the plants grown in 0.30 and 0.15 mM sulfate media at 25 °C. In addition, the activity in the plants grown in 0.15 mM sulfate medium was lower than in the plants grown in 0.30 mM sulfate medium at 40 °C (Fig. 4A).

Temperature, sulfur, and the temperature × sulfur interaction affected the GR activity significantly (P < 0.01) according to two-way ANOVA (Tab. 1). The GR activity of plants grown in 0.30 mM sulfate at 25 °C was found to be significantly higher than that of plants grown in FN and 0.15 mM sulfate media at 25 °C (Fig. 4B). GR activity decreased by 56% in plants grown in 0.30 mM sulfate medium at 40 °C compared to value of the plants grown in 0.30 mM sulfate medium at 25 °C. At 40 °C, GR activity was found to be higher in plants grown in FN medium compared to the plants grown in 0.30 and 0.15 mM sulfate media (Fig. 4B).

Two-way ANOVA showed highly significant effects of sulfur deficiency and the temperature × sulfur interaction on CAT activity (P < 0.01) and a significant effect of temperature (P < 0.05). While CAT activity was similar in the plants grown in FN and 0.15 mM sulfate media at 25 °C, it was higher in the plants grown in 0.30 mM sulfate medium. Under high-temperature conditions, CAT activity significantly increased in plants grown in 0.30 mM sulfate medium compared to plants grown in 0.30 mM sulfate medium at 25 °C. In addition, the CAT activity of the plants in 0.30 mM sulfate medium at 40 °C was higher than that of the plants in FN and 0.15 mM sulfate medium (Fig. 4C). At 40 °C, the CAT activity in 0.30 mM-sulfate grown plants increased by 16% while in 0.15 mM-sulfate grown plants it decreased by 46% compared to the plants grown in the same media (0.30 mM and 0.15 mM) at 25 °C, respectively.

The POD activity was significantly (P < 0.01) affected by temperature, sulfur, and the temperature × sulfur interaction in two-way ANOVA (Tab. 1). At 25 °C, the POD activity did not differ between plants grown in 0.30 mM and 0.15 mM sulfate media. However, they showed higher activities than plants grown in FN medium at 25 °C (Fig. 4D). Plants with high-temperature conditions showed a significant increase in POD activity compared to plants with 25 °C conditions. POD activity in the plants grown in FN, 0.30 and 0.15 mM sulfate media at 40 °C increased by 234%, 442%, and 348% respectively, compared to the corresponding values obtained from the plants grown in FN, 0.30 and 0.15 mM sulfate media at 25 °C. At 40 °C, there was no significant difference in POD activity between plants grown in 0.30 and 0.15 mM sulfate media. However, these groups had higher POD activity than plants grown in FN medium (Fig. 4D).

HSF4 expression was affected significantly (P < 0.01) by temperature, sulfur, and the temperature × sulfur interaction according to the two-way ANOVA (Tab. 1). The expression level of the *HSF4* gene in the plants grown in 0.30 mM sulfate medium was lower at 25 °C than plants grown in FN medium and 0.15 mM-sulfate grown plants. Moreover, it was the highest in 0.15 mM-sulfate grown plants. In addition, the *HSF4* gene expression level increased with increasing temperature in all sulfate concentrations (Fig. 5A); the plants grown in FN, 0.30 and 0.15 mM sulfate media experienced a 9.9, 194, and 20-fold increase in *HSF4* gene expression, respectively compared to corresponding values of the plants grown in FN, 0.30 mM and 0.15 mM sulfate media at 25 °C. At 40 °C, the expression level was highest in plants grown in 0.30 mM sulfate medium and the lowest in FN medium-grown plants (Fig. 5A).

Two-way ANOVA (Tab. 1) demonstrated a very significant (P < 0.01) effect on *HSFA4A* expression due to temperature, sulfur, and the temperature × sulfur interaction. At 25 °C, the *HSFA4A* gene expression level of FN-medium grown plants was higher than that of plants grown in 0.30 mM and 0.15 mM sulfate media. Under all sulfate conditions, gene expression increased when plants were exposed to a temperature at 40 °C i.e. plants grown in FN, 0.30 mM, and 0.15 mM sulfate media experienced a 6.6, 3.2, and 7.3-fold increase in *HSFA4A* gene expression, respec-

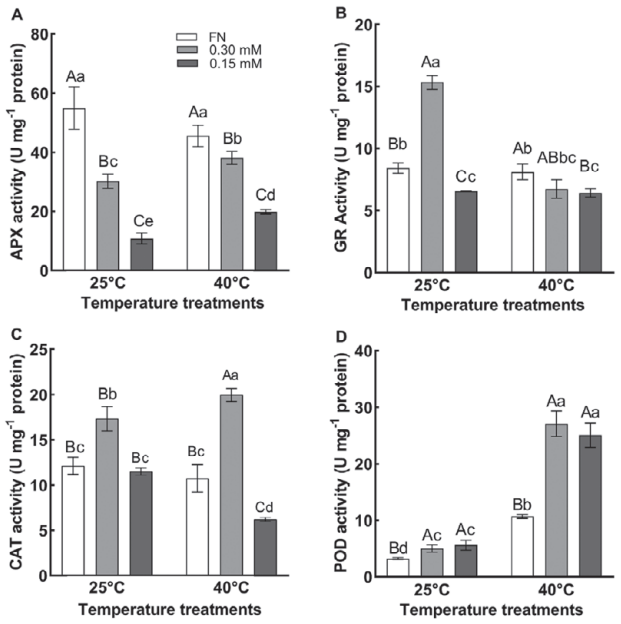

Fig. 4. Activities of ascorbate peroxidase (APX) (A), glutathione reductase (GR) (B), catalase (CAT) (C) and peroxidase (POD) of the plants grown at 25 °C and 40 °C in full nutrition (FN), 0.30 mM and 0.15 mM sulfate media. Data show the means ± the standard deviation of five independent samples. Different small letters indicate that means were statistically different (P < 0.05). Different capital letters indicate differences in different sulfate treatments at same temperature group (P < 0.05). Tukey's multiple testing method was used to compare the means. Plants were grown 60 days at 25 °C in FN, 0.30 mM and 0.15 mM sulfate media then subjected to a temperature of 40 °C for 7 days.

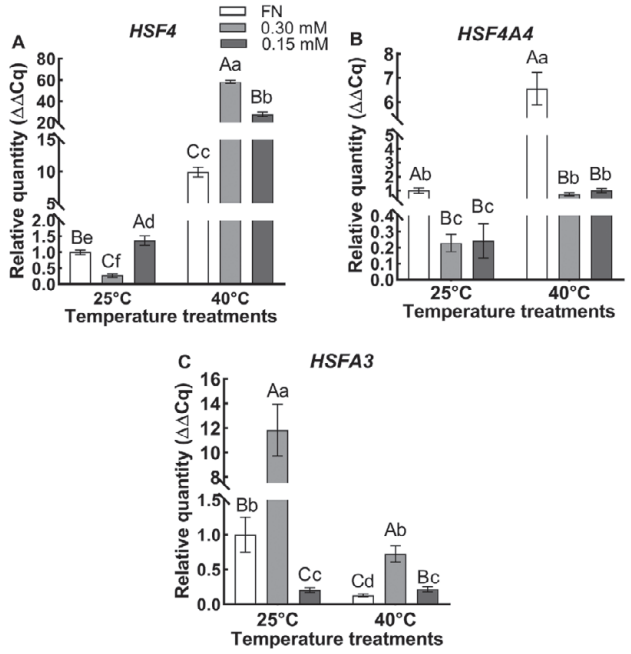

Fig. 5. The expression level of the *HSF4* (A), *HSF4A4* (B) and *HSFA3* (C) genes of the plants grown at 25 °C and 40 °C in full nutrition (FN), 0.30 mM and 0.15 mM sulfate media. Data show the means ± the standard deviation of five independent samples. Different small letters indicate that means were statistically different ($P < 0.05$). Different capital letters indicate differences in different sulfate treatments in the same temperature group ($P < 0.05$). Tukey's multiple testing method was used to compare the means. Plants were grown 60 days at 25 °C in FN, 0.30 mM and 0.15 mM sulfate media then subjected to a temperature of 40 °C for 7 days.

tively, compared to respective values obtained at 25 °C. *HSFA4A* gene expression levels were similar in plants grown in 0.30 and 0.15 mM sulfate media at 40 °C (Fig. 5B). Moreover, sulfur-deficient plants had lower expression levels than FN-medium grown plants.

The two-way ANOVA (Tab. 1) demonstrated that *HSFA3* expression was significantly ($P < 0.01$) influenced by temperature, sulfur, and the interaction between temperature and sulfur. When the temperature increased, the expression level of *HSFA3* in plants grown in FN and 0.30 mM-sulfate media decreased by 7.7- and 16.2-fold, respectively, compared to the respective values of the plants grown in FN and 0.30 mM-sulfate media at 25 °C. Furthermore, the gene expression level in 0.15 mM-sulfate medium grown plants was similar and the lowest at both 25 °C and 40 °C (Fig. 5C).

Discussion

Plant growth parameters such as fresh weight are affected negatively by high temperature (Ihsan et al. 2019). Sezgin Muslu and Kadıoğlu (2021) found a decrease in *H. thermophilum*'s shoot fresh weight at soil temperatures exceeding 80 °C. In our study, *H. thermophilum* plants were exposed to two distinct sulfate concentrations to evaluate the impact of sulfur deficiency on their response to high temperatures in vermiculite media with Hoagland nutrient solution. At 40 °C, the plants treated with low sulfate concentrations experienced a greater decrease in fresh weight than the plants at 25 °C. Sulfur deficiency has been found to have an impact on plant biomass, overall morphology, yield, and nutritional value. For instance, in *Eruca sativa*, sulfur deficiency resulted in a reduction in biomass production and chlorophyll synthesis (Narayan et al. 2023). Sulfur deficiency may also cause a decrease in the synthesis of sulfur-containing protein and amino acids (Ali et al. 2019), which may affect the growth of *H. thermophilum* in our study especially during stress caused by higher temperature.

The water content was shown to decrease in plants at high temperatures (Gupta et al. 2018). The RWC at various sulfate concentrations and temperatures was determined in *Heliotropium* plants. FN and 0.30 mM sulfate did not affect RWC, but 0.15 mM sulfate at 25 °C decreased it. Sulfur deficit has been found to impede stomatal closure in plants (Ren et al. 2022). Besides stomatal closure being hindered by the increase in sulfur deficiency it is also possible that the water content could have decreased due to tissue damage in the leaves. As in our findings, tissue damage and consequent water loss occurred in pyrethrum flowers subjected to drought and high temperature of 40 °C (Carins-Murphy et al. 2023). Since in our study there was no change in water content when there was enough sulfur, we may conclude that the decrease in water content under conditions of 0.15 mM sulfate concentration may be attributable to a shortage of sulfur rather than high temperature.

In our study, we found morphological alterations such as chlorosis, immature leaves being paler than adult leaves, and an inability to keep the green color in leaf veins in plants treated with low sulfate concentrations at high temperatures. These changes revealed that the leaves' stress level increased when the temperature was applied together with low sulfate concentration. Tian et al (2009) observed that *Agrostis scarba* was not damaged by high temperature when applied for 12 days at 35 °C in the absence of sulfur deficiency. Similarly, Sezgin Muslu and Kadıoğlu (2021) did not report morphological damage in *H. thermophilum* caused by high soil temperature at temperatures of 40, 60, and 80 °C compared to the control (20 °C) when adequate sulfate concentration was present. According to Chung et al. (2022), structural problems in the iron-sulfur protein, which is involved in the formation of chlorophyll, could be involved in the sulfur deficiency-induced chlorosis in our study. When plants are subjected to high temperatures, they not only lose chlorophyll but also experience an increase in H_2O_2 content (Sezgin Muslu and Kadıoğlu, 2021). Additionally, it was noted that mulberry and maize undergo an increase in H_2O_2 due to sulfur deficiency (Tewari et al. 2010). In our investigation, we discovered an increase in H_2O_2 concentration in response to increased sulfur deficiency and high temperature. The maximum concentration of H_2O_2 was found in plants grown at 0.15 mM sulfate and exposed to 40 °C. This result showed that the balance between H_2O_2 production and breakdown was disturbed. Moreover, the

application of 0.15 mM sulfate on plants resulted in low activity of antioxidant enzymes APX, CAT, and GR compared to FN in which enough sulfate was supplied. The insufficiency of sulfur induces the oxidation of biomolecules as a result of the excessive buildup of ROS and diminished production of compounds containing sulfur, such as GSH, thioredoxin, and glutaredoxin, which can efficiently form a line of defense against reactive oxygen and nitrogen species (Hill et al. 2022). In line with that, we observed higher GR and CAT activities in the plants subjected to 0.30 mM sulfate at 25 °C. The GR activity, which converts GSSH, may be increased to replace the decreased GSH due to sulfur deficiency and CAT activity may be triggered to remove H_2O_2. Therefore, the plants tried to keep levels of the metabolites related to sulfur metabolism, such as cysteine and methionine, at a constant level under stress conditions. In addition, at 40 °C in plants grown at 0.30 mM sulfate, APX and CAT activities increased compared to plants grown at 25 °C. However, there was a visible downward trend for GR when high temperature was applied. Bashir et al. (2015) reported that *Brassica juncea* plants that were subjected to low sulfate (30 μM SO_4^{2-}) become sensitive to cadmium toxicity. Besides, Wang et al. (2021) discovered that when *Brassica rapa* plants were grown in low sulfur environments, there were notable reductions in GSH content and GR activity when compared to the control group. In summary, sulfur shortage negatively affected the antioxidant system which is necessary for the thermotolerance of *H. thermophilum*.

In addition to antioxidant enzymes, plants also build up substances known as osmolytes such as proline and soluble sugars to lessen the impacts of stresses. Proline has been shown to have functions beyond osmotic regulation, including protecting membrane integrity, stabilizing proteins, and regulating cytosol pH (Mehta and Vyas, 2023). The highest amount of proline was found in plants that were treated with 0.15 mM sulfate at 40 °C temperature during our study. The accumulation of proline was increased in order to reduce temperature sensitivity due to the decrease in sulfate concentration. Various species, such as *Vigna unguiculata*, *Cicer arietinum*, *Solanum lycopersicum*, and *Gossypium hirsutum*, have been documented to exhibit proline accumulation in response to elevated temperatures (Du et al. 2011). However, the severity of high temperature was a significant factor in the extent of proline accumulation. An elevated proline level caused by a sulfur shortage and high temperature in our study was a sign of mounting stress. In addition, a rise in proline levels may support the preservation of the cytoplasmic osmotic potential of cells, a critical process for plant survival in stressful environments.

Sugar builds up in plant tissues in a manner similar to that of proline to protect biomolecules and membranes by regulating the intrinsic osmotic potential (Mehta and Vyas, 2023). Sugar accumulation under stress has been documented in numerous species and is believed to exert a significant influence on thermal tolerance (Zhao et al. 2022). Zheng et al. (2022) found that the soluble sugar contents of tomato plants subject to high temperature (41 °C) diminished due to the inhibition of sucrose synthase. In our study, we observed a decrease in the soluble sugar content in sulfur deficiency media under heat stress which could be a result of either inhibition of sugar biosynthesis enzymes or a shift in metabolism to the synthesis of antioxidant compounds or proline instead of sugar synthesis. Yu et al. (2022) reported that sulfur deprivation leads to a decrease in glucose content in *Arabidopsis thaliana*. Furthermore, Wawrzyńska et al. (2022) discovered that when a sulfur deficiency occurred, the production of anthocyanin was triggered while the photosynthesis rate and sugar production were slowed down.

HSFs are the primary factor responsible for activating *HSP* genes in response to heat stress. The activation of HSFA2, a transcriptional activator of *HSP* expression, and *HSP17-CII* has been documented in the anther of the tomato plant during its growth in elevated temperatures (Giorno et al. 2010). The thermotolerance of transgenic soybeans may be amplified by the over-expression of *GmHSFA1* in soybeans, potentially by activating downstream genes like *GmHsp70*, *GmHsp22*, and other *GmHsps* in response to heat stress (Zhu et al. 2006). In Arabidopsis, HsfB1 (also known as HSF4 or TBF1) suppresses the overall heat shock response in the absence of high heat but promotes the development of acquired thermotolerance during heat stress (Pick et al. 2012). In the current study, *HSF4* and *HSFA4A* genes were up-regulated at 40 °C in all sulfate treatments (FN, 0.30 mM sulfate and 0.15 mM sulfate) compared to the values at 25 °C. At 0.30 mM sulfate, the rate of *HSF4* gene expression was the highest after high-temperature treatment which probably changed the expression levels of various genes to resist heat and sulfur deficiency stress. Lin et al. (2018) reported that HSFA2 and HSFA4a control the transcription of HSPs to establish the heat shock response in *A. thaliana* seedlings subjected to 39 °C. Induction of *HSFA4* genes in *H. thermophilum* under heat stress was the greatest in FN plants but much lower under sulfur deficiency which may have negatively affected plant resistance to high temperatures. The expression level of the *HSFA3,* which is a pivotal heat shock factor that interacts with HSFA2 to effectively enhance transcriptional memory in response to heat stress (Friedrich et al. 2021), was lower in the FN plants and plants at 0.15 mM sulfate compared to those supplied with 0.30 mM sulfate at 25 °C. The induction of *HSFA3* in the plants subjected to 0.30 mM sulfate at 25 °C may be a result of sulfur deficiency while application of 0.15 mM sulfate may have disrupted the functioning of systems that control *HSFA3* expression. However, the expression of HSFA3 genes in plants at 40 °C was lower than that in plants at 25 °C at all sulphate treatments which should be further investigated.

In summary, while plants growing in a full nutrition medium were tolerant to increasing temperatures, they became sensitive as the sulfate content decreased. As the dose level of sulfur deficiency increased, chlorophyll loss, injuries, and increased oxidative stress damage were observed in the leaves. The antioxidant system was negatively affected by sulfur deficiency. While plants preferred proline for osmoregulation, sugar production decreased. In addition,

plants attempted to resist high-temperature damage caused by sulfur deficiency through the activation of the *HSF4* and *HSF4A4* genes, as well as the downregulation of *HSFA3*. However, more detailed studies on this subject are necessary.

Acknowledgments

The authors would like to thank lecturer Kamil OZTURK, who collected the plant seeds in the natural conditions where the plant lived. The authors also want to thank Ardahan ESKI and Bilecik Şeyh Edebali University Central Research Laboratory for performing the sulfur measurements.

This study was supported by TUBITAK 2209-A – Research Project Support Programme for Undergraduate Students under Grant number 1919B012000384 and TUBITAK ARDEB 1001- Support Program for Scientific and Technological Research Projects under Grand number 114Z336.

Author contribution statement

A.S and AK. designed the work. E.N.I performed the experiments. A.S., A.K. and E.N.I analyzed the data. A.S. and E.N.I wrote the manuscript. A.S. and A.K. revised the manuscript. The manuscript has been read and approved by all authors.

References

Ali, Q., Athar, H. R., Haider, M. Z., Shahid, S., Aslam, N., Shehzad, F., Naseem, J., Ashraf, R., Ali, A., Hussain, S. M., 2019: Role of amino acids in improving abiotic stress tolerance to plants. In: Hasanuzzaman, M., Fujita M., Oku, H., Islam, M. T. (eds.), Plant tolerance to environmental stress: Role of phytoprotectants, 175-203. CRC Press, Boca Raton.

Bashir, H., Ibrahim, M. M., Bagheri, R., Ahmadi J., Arif, I. A., Baig, M. A., Qureshi, M. I., 2015: Influence of sulfur and cadmium on antioxidants, phytochelatins and growth in Indian mustard. AoB Plants 7, plv001. https://doi.org/10.1093/aobpla/plv001

Bielecka, M., 2007: Analysis of transcription factors under sulphur deficiency stress, PhD Dissertation. University of Postdam, Germany.

Bookout, A. L., Mangelsdorf, D. J., 2003: Quantitative real-time PCR protocol for analysis of nuclear receptor signaling pathways. Nuclear Receptor Signaling 1, e012. https://doi.org/10.1621/nrs.01012

Bradford, M. M., 1976: Rapid and sensitive method for the quantitation of microgram quantities of protein utilizing the principle of protein-dye binding. Analytical Biochemistry 72(1–2), 248–254. https://doi.org/10.1016/0003-2697(76)90527-3

Carins-Murphy, M. R., Cochard, H., Deans, R. M., Gracie, A. J., Brodribb, T. J., 2023: Combined heat and water stress leads to local xylem failure and tissue damage in pyrethrum flowers, Plant Physiology, 193(1), 356–370. https://doi.org/10.1093/plphys/kiad349

Chung, J. S., Kim, H. C., Yun, S. M., Kim, H. J., Kim, C. S., Lee, J. J., 2022: Metabolite analysis of lettuce in response to sulfur nutrition. Horticulturae, 8(8), 734. https://doi.org/10.3390/horticulturae8080734

Dard, A., Weiss, A., Bariat, L., Auverlot, J., Fontaine, V., Picault, N., Pontvianne, F., Riondet, C., Reichheld, J. P., 2023: Glutathione-mediated thermomorphogenesis and heat stress responses in *Arabidopsis thaliana*. Journal of Experimental Botany 74(8), 2707–2725. https://doi.org/10.1093/jxb/erad042

Du, H., Wang, Z., Yu, W., Liu, Y., Huang, B., 2011: Differential metabolic responses of perennial grass *Cynodon transvaalensis*× *Cynodon dactylon* (C4) and *Poa pratensis* (C3) to heat stress. Physiologia Plantarum, 141(3), 251–264. https://doi.org/10.1111/j.1399-3054.2010.01432.x

Friedrich, T., Oberkofler, V., Trindade, I., Altmann, S., Brzezinka, K., Lämke, J., Gorka, M., Kappel, C., Sokolowska, E., Skirycz, A., Graf, A., Bäurle, I., 2021: Heteromeric HSFA2/HSFA3 complexes drive transcriptional memory after heat stress in Arabidopsis. Nature Communications 12, 3426. https://doi.org/10.1038/s41467-021-23786-6

Giorno, F., Wolters-Arts, M., Grillo, S., Scharf, K. D., Vriezen, W. H., Mariani, C., 2010: Developmental and heat stress-regulated expression of HsfA2 and small heat shock proteins in tomato anthers. Journal of Experimental Botany 61(2), 453–462. https://doi.org/10.1093/jxb/erp316

Gupta, S., Ram, J., Singh, H., 2018: Comparative study of transpiration in cooling effect of tree species in the atmosphere. Journal of Geoscience and Environment Protection 6(8), 151–166. https://doi.org/10.4236/gep.2018.68011

Hasanuzzaman, M., Nahar, K., Anee, T. I., Fujita, M., 2017: Glutathione in plants: biosynthesis and physiological role in environmental stress tolerance. Physiology and Molecular Biology of Plants 23, 249–268. https://doi.org/10.1007/s12298-017-0422-2

Heckathorn, S. A., Downs, C. A., Sharkey, T. D., Coleman, J. S., 1998: The small, methionine-rich chloroplast heat-shock protein protects photosystem II electron transport during heat stress. Plant Physiology, 116(1), 439–444. https://doi.org/10.1104/pp.116.1.439

Hesse, H., Kreft, O., Maimann, S., Zeh, M., Hoefgen, R., 2004: Current understanding of the regulation of methionine biosynthesis in plants. Journal of Experimental Botany 55(404), 1799–1808. https://doi.org/10.1093/jxb/erh139

Hill, C. R., Shafaei, A., Balmer, L., Lewis, J. R., Hodgson, J. M., Millar, A. H., Blekkenhorst, L. C., 2022: Sulfur compounds: From plants to humans and their role in chronic disease prevention. Critical Reviews in Food Science and Nutrition 63(27), 8616–8638. https://doi.org/10.1080/10408398.2022.2057915

Ihsan, M. Z., Daur, I., Alghabari, F., Alzamanan, S., Rizwan, S., Ahmad, M., Waqas, M. Shafqat, W., 2019: Heat stress and plant development: role of sulphur metabolites and management strategies. Acta Agriculturae Scandinavica Section B, Soil and Plant Science 69(4), 332–342. https://doi.org/10.1080/09064710.2019.1569715

Kang, Y., Lee, K., Hoshikawa, K., Kang, M., Jang, S., 2022: Molecular bases of heat stress responses in vegetable crops with focusing on heat shock factors and heat shock proteins. Frontiers in Plant Science 13, 837152. https://doi.org/10.3389/fpls.2022.837152

Lin, K. F., Tsai, M. Y., Lu, C. A., Wu, S. J., Yeh, C. H., 2018: The roles of Arabidopsis HSFA2, HSFA4a, and HSFA7a in the heat shock response and cytosolic protein response. Botanical Studies 59, 15. https://doi.org/10.1186/s40529-018-0231-0

Maj, G., Najda, A., Klimek, K., Balant, S., 2020: Estimation of energy and emissions properties of waste from various species of mint in the herbal products industry. Energies 13(1), 55. https://doi.org/10.3390/en13010055

Mehta, D., Vyas, S., 2023: Comparative bio-accumulation of osmoprotectants in saline stress tolerating plants: a review. Plant Stress 9, 100177. https://doi.org/10.1016/j.stress.2023.100177

Narayan, O. P., Kumar, P., Yadav, B., Dua, M., Johri, A. K., 2023: Sulfur nutrition and its role in plant growth and development. Plant Signaling and Behavior 18(1), e2030082. https://doi.org/10.1080/15592324.2022.2030082

Pick, T., Jaskiewicz, M., Peterhaensel, C., Conrath, U., 2012: Heat shock factor HSFB1 primes gene transcription and systemic acquired resistance in Arabidopsis. Plant Physiology 159(1), 52–55. https://doi.org/10.1104/pp.111.191841

Ren, Z., Wang, R. Y., Huang, X. Y., Wang, Y., 2022: Sulfur compounds in regulation of stomatal movement. Frontiers in Plant Science 13, 846518. https://doi.org/10.3389/fpls.2022.846518

Saglam, A., Kadioglu, A., Terzi, R., Saruhan, N., 2008: Physiological changes in them in post-stress emerging *Ctenanthe setosa* plants under drought conditions. Russian Journal of Plant Physiology, 55, 48–53. https://doi.org/10.1134/S1021443708010056

Sağlam, A., Saruhan, N., Terzi, R., Kadıoğlu, A., 2011: The relations between antioxidant enzymes and chlorophyll fluorescence parameters in common bean cultivars differing in sensitivity to drought stress. Russian Journal of Plant Physiology, 58(1), 60–68. https://doi.org/10.1134/S102144371101016X

Sehar, Z., Gautam, H., Iqbal, N., Alvi, A. F., Jahan, B., Fatma, M., Albaqami, M., Khan, N. A., 2022: The functional interplay between ethylene, hydrogen sulfide, and sulfur in plant heat stress tolerance. Biomolecules 12(5), 678. https://doi.org/10.3390/biom12050678

Sezgin Muslu, A., Kadıoğlu, A., 2021: Role of abscisic acid, osmolytes and heat shock factors in high temperature thermotolerance of *Heliotropium thermophilum*. Physiology and Molecular Biology of Plants 27(4), 861–871. https://doi.org/10.1007/s12298-021-00975-7

Tan, K., Çelik, A., Gemici, Y., Gemici, M., Yildirim, H., 2008: *Heliotropium thermophilum* (Boraginaceae), a new taxon from SW Anatolia, Turkey. Advanced Science Letters 1(1), 132–139. https://doi.org/10.1166/asl.2008.003

Tewari, R. K., Kumar, P., Sharma, P. N., 2010: Morphology and oxidative physiology of sulphur-deficient mulberry plants. Environmental and Experimental Botany 68(3), 301–308. https://doi.org/10.1016/j.envexpbot.2010.01.004

Tian, J., Belanger, F. C., Huang, B., 2009: Identification of heat stress-response genes in heat-adapted thermal *Agrostis scabra* by suppression subtractive hybridization. Journal of Plant Physiology 166(6), 588–601. https://doi.org/10.1016/j.jplph.2008.09.003

Wang, D., Wang, K. H., Yang, J., Zhu, Z. J., Zhu, B., 2021: Effects of exogenous glutathione on glutathione metabolism in pakchoi under sulfur deficiency. Journal of Plant Nutrition and Fertilizers 27(3), 511–519. https://doi.org/10.11674/zwyf.20355

Wawrzyńska, A., Piotrowska, J., Apodiakou, A., Brückner, F., Hoefgen, R., Sirko, A., 2022: The SLIM1 transcription factor affects sugar signaling during sulfur deficiency in Arabidopsis. Journal of Experimental Botany 73(22), 7362–7379. https://doi.org/10.1093/jxb/erac371

Xue, G. P., Drenth, J., Mcintyre, C. L., 2015: TaHsfA6f is a transcriptional activator that regulates a suite of heat stress protection genes in wheat (*Triticum aestivum* L.) including previously unknown Hsf targets. Journal of Experimental Botany 66(3), 1025–39. https://doi.org/10.1093/jxb/eru462

Yu, Y., Zhong, Z., Ma, L., Xiang, C., Chen, J., Huang, X. Y., Xu, P., Xiong, Y., 2022: Sulfate-TOR signaling controls transcriptional reprogramming for shoot apex activation. New Phytologist 236(4), 1326–1338. https://doi.org/10.1111/nph.18441

Zhao, X., Huang, L. J., Sun, X. F., Zhao, L. L., Wang, P. C., 2022: Differential physiological, transcriptomic, and metabolomic responses of *Paspalum wettsteinii* under high-temperature stress. Frontiers in Plant Science 13, 865608. https://doi.org/10.3389/fpls.2022.865608

Zheng, Y. J., Yang, Z. Q., Wei, T. T., Zhao, H. L., 2022: Response of tomato sugar and acid metabolism and fruit quality under different high temperature and relative humidity conditions. Phyton-International Journal of Experimental Botany 91(9), 2033–2054. https://doi.org/10.32604/phyton.2022.019468

Zhu, B., Ye, C., Lu, H., Chen, X., Chai, G., Chen, J., Wang, C., 2006: Identification and characterization of a novel heat shock transcription factor gene, *GmHsfA1*, in soybeans (*Glycine max*). Journal of Plant Research 119, 247–256. https://doi.org/10.1007/s10265-006-0267-1

Acta Bot. Croat. 84 (1), 91–100, 2025
DOI: 10.37427/botcro-2025-008

CODEN: ABCRA 25
ISSN 0365-0588
eISSN 1847-8476

Indications of programmed cell death in wheat roots upon exposure to silver nanoparticles

Fatma Yanık, Filiz Vardar*

Marmara University, Science Faculty, Department of Biology, Göztepe Campus, 34722 Istanbul, Türkiye

Abstract- Programmed cell death (PCD) can occur at every developmental stage as a plant's response to various biotic and abiotic environmental factors. Silver nanoparticles (AgNPs) are widely used in consumer products and possess antimicrobial properties, making them important in assessing nanoparticle effects on plants. In the present study, we examined the impact of AgNPs (0, 0.5, 1, 5, 10, and 20 mg L^{-1}) on wheat root PCD by evaluating parameters such as the mitotic index, chromosomal behaviors, nuclear deformation, cytochrome c release, caspase-1-like activity, and the expression of cysteine protease genes (*TaVPE4*, *TaMCA1* and *TaMCA4*). Our findings revealed a dose-dependent decrease in the mitotic index ratio and increased chromosomal abnormalities induced by AgNPs. Additionally, we observed various hallmarks of PCD, including chromatin condensation, slight DNA smear, reduction in mitochondrial inner membrane potential, and cytochrome c release to the cytoplasm as well as increased caspase-1-like activity and *TaVPE4* gene expression. Notably, the gene expressions of *TaMCA1* and *TaMCA4* were found to be antagonistically regulated by AgNPs, further indicating the induction of PCD by AgNP treatment. Overall, our study provides evidence of AgNP-induced PCD in wheat roots, elucidating the involvement of cysteine protease genes in this process.

Keywords: AgNP, cytochrome c, metacaspase, mitotic index, vacuolar processing enzyme

Introduction

Programmed cell death (PCD) is generally described as a genetically controlled mechanism that eliminates specific cells under developmental and environmental stimuli. In recent years, due to the complexity of classification based on morphological and biochemical characteristics, plant PCD has been divided into two main categories: developmentally regulated PCD (dPCD) and environmentally induced PCD (ePCD), depending on the type of activation. dPCD is activated by internal stimuli, whereas ePCD is triggered by various biotic and abiotic stress factors such as pathogens, fungi, salinity, UV radiation, drought, heat, flooding, heavy metals, etc. (Li et al. 2007, Yanık et al. 2017, Minina et al. 2021, Paes de Melo et al. 2022).

Probably the most thoroughly understood form of PCD in animals is apoptosis, which is associated with caspase activity and initiated and regulated by these proteases. Although plants lack caspases, PCD is regulated by various proteases such as metacaspases, vacuolar processing enzymes (VPEs), and phytaspases which are suggested as the main regulators of PCD in plants. Moreover, VPEs are also proposed as the primary regulators of vacuolar cell death in plants. Vacuolar cell death is a crucial process in plant development accompanied by striking expansion of lytic vacuole digesting cytoplasmic content, which leads to the self-clearance of dying cells (Emanuele et al. 2018). In many plants, PCD generally shows characteristic features such as cell and cytoplasm shrinkage, chromatin condensation, DNA laddering, decreased mitochondrial membrane potential, disruption of microtubule organization, and cytochrome c (cyt-c) release from mitochondria to the cytoplasm (Huang et al. 2014, Paes de Melo et al. 2022).

In recent years, the increasing presence of consumer products containing nanoparticles (NPs) has raised concerns about nano-waste as a potential environmental threat. Silver nanoparticles (AgNPs) are among the NPs most used in consumer products, posing a potential risk as pollutants. AgNPs are extensively used in many fields due to their antimicrobial features, e.g., in the healthcare

* Corresponding author e-mail: filiz.vardar@gmail.com

industry, food packaging, water treatment, textile coating, cosmetics, etc. (Alshameri and Owais 2022). With the development of nanotechnology, they have also attracted attention as nano-pesticides for controlling bacterial and fungal diseases in agriculture (Chhipa and Joshi 2016). The increasing prevalence of nanotechnology in consumer products inevitably leads to the release of AgNPs into the ecosystem during synthesis, consumption, and disposal processes. This has prompted researchers to assess the ecotoxicological impact of AgNPs on organisms such as human cells, algae, and plants (McGillicuddy et al. 2017). In plants, exposure to AgNPs can induce oxidative stress, genotoxicity, up-regulation of stress-related genes, and cell death, depending on the size and concentration of AgNPs and the plant species (Mirzajani et al. 2014, Huang et al. 2022). Investigations based on NP size have shown that 10 nm-sized AgNPs induce various effects in different plant species. In *Triticum aestivum*, they inhibit root and shoot length, induce metallothionein gene expression, and cause oxidative stress (Dimkpa et al., 2013). In *Arabidopsis thaliana*, 10 nm-sized AgNPs disrupt chloroplastic membrane structure, reduce chlorophyll content, and alter the expression of antioxidant and aquaporin-related genes (Qian et al., 2013). Additionally, *Wolffia globosa* exposed to these AgNPs show higher malondialdehyde (MDA) content indicative of oxidative stress, along with an increase in superoxide dismutase (SOD) activity (Dimkpa et al. 2013). Our previous study also revealed the phytotoxicity of 10 nm-sized AgNPs, with observed adverse effects on root and shoot length, increased H_2O_2 and MDA content, antioxidant activity, lignin accumulation, and callose deposition (Yanık and Vardar 2019). Moreover, a recent study has demonstrated that AgNP treatment induces autophagy-type PCD in grapevine suspension cells, characterized by reactive oxygen species (ROS) generation, caspase-3-like activity, an increase in poly-ubiquitin conjugated proteins, and degradation of the proteasome 20S subunit PBA1 (Filippi et al. 2019). Despite their toxic behavior, the potential of AgNPs to induce cell death in plant cells remains unclear. The present study aims to evaluate PCD hallmarks induced by 10 nm-sized AgNPs in wheat roots. We investigated various cell death features, including mitotic division, chromosomal behaviors, nucleus morphology, DNA fragmentation, cyt-c release, and caspase-1-like activity, along with the expression of cysteine proteases genes (*TaVPE4*, *TaMCA1,* and *TaMCA4*). Our goal is to understand the potential impacts of AgNPs on agricultural processes.

Material and methods

Plant material and light microscopic observations

Wheat (*T. aestivum* L. cv Demir 2000) seeds were obtained from the Central Research Institute for Field Crops (Ankara, Türkiye). The seeds were germinated with distilled water and then exposed to different aqueous concentrations (0, 0.5, 1, 5, 10, and 20 mg L^{-1}) of 10 nm-sized AgNPs (Sigma-Aldrich 730785) for 15 days, following the method described by Yanık and Vardar (2019). For screening anatomical alterations, roots were fixed in 6% glutaraldehyde (v/v) in 0.1 M phosphate-saline buffer (PBS, pH 7.8) for 16 h. Semi-thin cross-sections (1 µm) were stained with toluidine blue. To determine the mitotic index (MI) and chromosomal abnormalities (CA), roots were fixed for 24 h with acetic acid: alcohol (1:3) and hydrolyzed with 1 M HCl for 10 min at 60 °C. The roots were then kept in the dark for 30 min with Schiff's reagent and squashed with 2% aceto-orcein (w/v). Approximately, 1500 cells were scored from each group, and the MI and CA were expressed as the number of the cells in mitosis per 100 cells and expressed as a percentage.

Nuclear morphology and DNA fragmentation

The roots were fixed with 4% paraformaldehyde (w/v) and stained with 1 µg mL^{-1} 4',6-diamidino-2-phenylindole (DAPI) for 30 min in the dark (Schweizer 1976). Fifty nuclei were counted and expressed as the number of nuclear deformations per 100 cells for all treated groups and expressed as a percentage. DNA fragmentation was analyzed using the TUNEL (terminal deoxynucleotidyl transferase dUTP nick end labeling) reaction and DNA gel electrophoresis (Hameed et al. 2004). TUNEL reaction was obtained with the Sigma-Aldrich ApopTagR Plus Fluorescein *In situ* Apoptosis Detection kit (Merck KGaA, Darmstadt, Germany). Light and fluorescence microscopic results were obtained using KAMERAM software, assisted by a KAMERAM camera and an Olympus BX-51 integrated microscope (Argenit, Istanbul, Türkiye). For DNA gel electrophoresis, genomic DNA was isolated according to Hameed et al. (2004). DNA isolates (100 ng μL^{-1}) were run on a 0.8% (w/v) agarose gel at 100 V for 2 h. Gel was analyzed using the Isogen ProXima (2850) transilluminator and photographed using ProXima AQ-4 software (LabExchange, Germany).

Isolation of mitochondria and measurement of mitochondria inner membrane potential (ΔΨm)

Fresh roots weighing 1 g were ground in 2 mL of cold homogenization buffer (0.4 M sucrose, 50 mM Tris-HCl pH 7.4, 1 mM ethylenediaminetetraacetic acid (EDTA)). Filtered homogenates were then centrifuged at 1500 × g for 15 min at 4 °C. The supernatants were used as cytosolic fractions, while pellets were resuspended in mitochondrial suspension buffer (0.4 M sucrose, 50 mM Tris-HCl pH 7.4), centrifuged at 14000 × g for 15 min, and used as a mitochondrial fraction (Panda et al. 2008). Isolated mitochondria were diluted in a buffer (220 mM sucrose, 68 mM mannitol, 10 mM KCl, 5 mM KH_2PO_4, 2 mM $MgCl_2$, 500 µM ethylene glycol-bis(β-aminoethyl ether)-N,N,N',N'-tetraacetic acid (EGTA), 5 mM succinate, 2 µM rotenone, 10 mM 4-(2-Hydroxyethyl)-1-piperazine ethanesulfonic acid (HEPES), pH 7.2) to a concentration of 0.1 mg mL^{-1}, then rhodamine-123 was added (10 µg mL^{-1}) and incubation in the dark followed for 5 minutes. The BiotekCytation micro-

plate reader (Agilent, US) was used to measure ΔΨm-dependent quenching of Rh-123 fluorescence at excitation 490 nm and emission 535 nm (Huang et al. 2014).

Detection of cytochrome c release

Proteins (20 μg mL^{-1}) from cytoplasmic and mitochondrial fractions were separated with 12% SDS-PAGE and transferred onto polyvinylidene difluoride (PVDF) membranes using transfer buffer (0.29 g glycine, 0.58 g Tris, 0.037 g sodium dodecyl sulfate (SDS), 20 mL methanol). The membrane was then blocked with 5% (w/v) skim milk solubilized in buffer (8 g NaCl, 0.2 g KCl, 3 g SDS, pH 7.4) at 4 °C overnight. Subsequently, the membrane was cut into two parts between 35 and 25 kDa according to the protein marker. The upper part of the membrane was probed with the monoclonal antibody against mouse ATP5A (1:1000 dilution with 5% Tween 20 in PBS, Novusbio NBP2-15512) as mitochondrial marker protein (housekeeping protein). The lower part of the membrane was incubated with the monoclonal antibody against mouse cyt-c (1:1000 dilution with 5% Tween 20 in PBS, Novusbio NB100-56503). Goat anti-mouse IgG horseradish peroxidase (HRP)-conjugated secondary antibody was added at a dilution of 1:10000 with 5% Tween 20 in PBS. Membranes were stained with 0.06% (w/v) 3,3'-diaminobenzidine (DAB). Membranes were analyzed using the Isogen ProXima (2850) transilluminator and photographed using ProXima AQ-4 software (LabExchange, Germany), and the relative density of the bands was determined with the Image J program. The protein bands of cyt-c (in both cytoplasmic and mitochondrial fractions) were normalized by the ATP5A protein marker bands (housekeeping protein) using the formula:

$$\text{Relative band density} = \frac{\text{density of cyt} - \text{c of sample}}{\text{density of ATP5A}}$$

Determination of caspase-1-like activity

Caspase-1-like activity was measured according to the Caspase 1/ICE Colorimetric Assay Kit (ENZO Life Sciences, Switzerland). The roots (0.5 g) were ground in 1 mL cold extraction buffer (50 mM HEPES-KOH pH 7, 10% sucrose, 0.01% Chaps (3-((3-cholamidopropyl) dimethylammonio)-1-propanesulfonate), 5 mM dithiothreitol, 1 mM EDTA) (Lombardi et al. 2007). The homogenate was centrifuged at 14000 × g for 10 min at 4 °C. Supernatants were assayed for caspase-1-like activity, using YVAD *p*NA (N-acetyl-L-tyrosyl-L-valyl-L-alanyl-N-(4-nitrophenyl)-L-α -asparagine) as substrate. After incubation at 37 °C for 1 h, the absorbance was measured at 405 nm. Caspase-1-like activity was calculated according to the standard curve (y = 0.0435×), and expressed as nmol L^{-1}.

RNA isolation, cDNA synthesis, and expression analysis of *TaVPE4*

Fresh roots weighing 100 mg were collected into RNase-free tubes and homogenized in liquid nitrogen. Total RNA was extracted using the Qiagen RNeasy Plant Mini Kit (Catalog No./ID: 74904), following the manufacturer's instructions. Next, cDNA was synthesized from the total RNA using QuantiTect Reverse Transcription Kit (Catalog No./ID: 205311). The expression of *TaVPE4* was analyzed by semi-quantitative RT-PCR using Applied Biosystems Real-Time PCR (USA). The specific primers for semi-quantitative RT-PCR experiments were obtained from Kang et al. (2013). The actin gene was used as an internal control. PCR was performed using the cDNA templates and a Sigma-Aldrich PCR core kit with Taq DNA polymerase (CORET-1KT). The PCR products were loaded onto 1% agarose gels stained with 2 μL RedSafe nucleic acid staining solution (20.000×, Intron 21141) in Tris/Borat/EDTA buffer.

Quantitative PCR expression analysis of *TaMCA1* and *TaMCA4*

The expressions of *TaMCA1* and *TaMCA4* genes were analyzed using quantitative real-time PCR (qPCR) using synthesized cDNA templates and specific primers [*TaMC1-F* GCGGATACTTCAGCCTTGTC (NCBI accession no KU958719.1); *TaMC1-R* CTTCCCGTGTTCCGTATTGT; *TaMC4-F* CCTCAAAGAGACCGTTCGTG (NCBI accession no JN807891.1); *TaMC4-R* ATCCTTCCCAGTTTGCTCCT]. The qPCR was performed on Applied Biosystems StepOne™ Real-Time PCR (USA) using Thermo Fisher reagents. Relative gene expression levels were calculated using the $2^{-\Delta\Delta Ct}$ formula, with the *TEF1* gene serving as an internal control (Livak and Schmittgen 2001).

Statistical analyses

All analyses were conducted with three biological and three technical replicates. Statistical analysis was performed using SPSS statistics 21.0. Significant differences were determined using one-way analysis of variance (ANOVA) followed by Tukey's posthoc HSD test ($P < 0.05$).

Results

The mitotic index (MI) was 11.78% in control, 9.01% in 0.5 mg L^{-1}, 8.13% in 1 mg L^{-1}, 7.04% in 5 mg L^{-1}, 6.88% in 10 mg L^{-1}, and 5.51% in 20 mg L^{-1} of AgNP. The dose-dependent reduction of MI was observed after AgNP treatments, statistically significant, however, only at 20 mg L^{-1} (Fig. 1a). The percentage of chromosomal abnormalities (CA) induced by AgNPs in wheat roots was found to increase by 3.6, 4.5, 5.2, 5.3, and 5.5 fold with 0.5, 1, 5, 10, and 20 mg L^{-1} of AgNP, respectively (Fig. 1b).

The frequency of cells with CAs (c-mitosis, anaphase bridges, multiple chromosome bridges, sticky chromosome, unoriented metaphase) increased in a dose-dependent manner in comparison to control. Semi-thin sections of control and treated wheat roots revealed that AgNPs affected the root diameter (On-line Suppl. Fig. 1.). Roots treated with AgNPs exhibited anatomical changes, including shrinkage

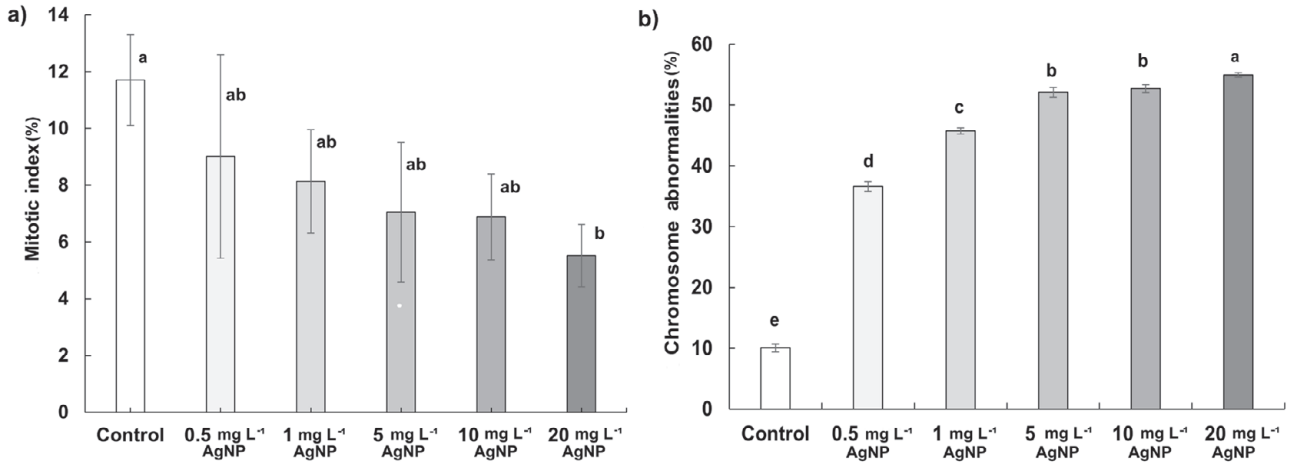

Fig. 1. Effects of 0.5, 1, 5, 10, and 20 mg L^{-1} of AgNPs on the mitotic index (**a**) and chromosome abnormalities (**b**) in wheat roots after 15 days of exposure. Data with different letters are statistically significant ($P < 0.05$) based on Tukey's HSD test. Bars on columns represent means ± standard deviation.

of epidermal and cortical cells and a decrease in cell diameter. In roots treated with 0.5, 1, and 5 mg L^{-1} of AgNPs, deformation was observed in the epidermal and cortical cells, while no deformation was observed in the endodermis and central cylinder. Relatively high degeneration in root anatomy was observed in samples treated with 10 and 20 mg L^{-1} of AgNP.

The samples were stained with DNA-specific fluorescent dye DAPI to detect alterations in nuclear morphology. DAPI staining showed loss of nucleus spherical shape and exhibited chromatin condensation in wheat roots exposed to 0.5 mg L^{-1} of AgNPs. Similarly, nuclear deformation gradually increased with the increase of AgNP dose; it was 2% in control, 10% in 0.5 mg L^{-1}, 12% in 1 mg L^{-1}, 14% in 5 mg L^{-1}, 20% in 10 mg L^{-1}, and 24% in 20 mg L^{-1} of AgNP (Fig. 2).

The TUNEL reaction was used to detect the presence of free 3' OH in DNA strand breaks. No TUNEL-positive nucleus was observed in the control, while a low number of TUNEL-positive nuclei was visible in all AgNP-treated roots (Fig. 3).

Our gel electrophoresis results revealed a slight induction of DNA smearing with no sign of DNA laddering, which was observed only in samples treated with 10 and 20 mg L^{-1} of AgNP concentrations (Fig. 4).

The early indications of PCD include alterations in mitochondrial morphology, loss of internal membrane potential, and cytochrome c (cyt-c) release from mitochondria to cytosol. According to our results, mitochondrial inner

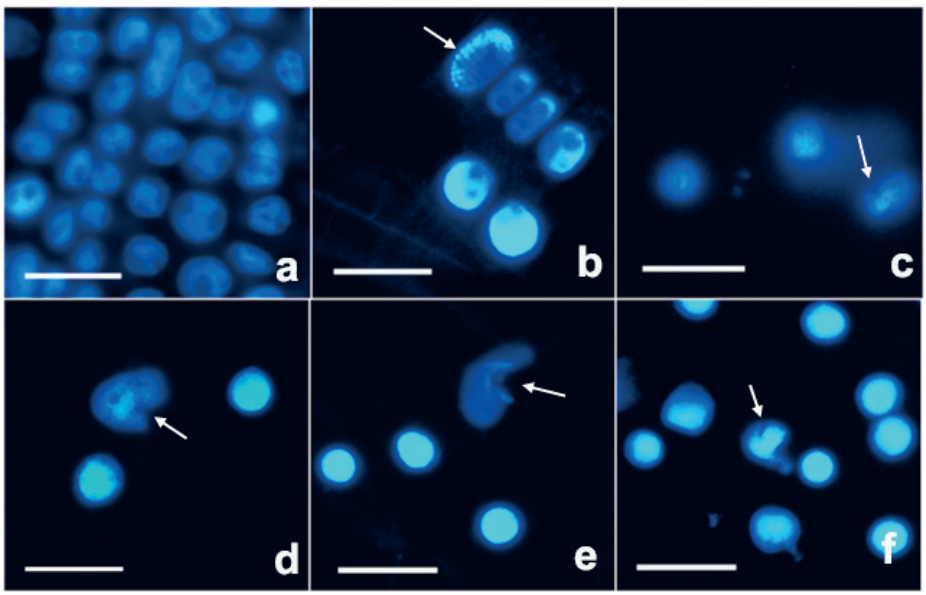

Fig. 2. Nucleus morphology in control wheat root cells (**a**) and after 15 days of exposure to 0.5 (**b**), 1 (**c**), 5 (**d**), 10 (**e**), and 20 mg L^{-1} of AgNPs (**f**). Arrows indicate nuclear deformation. Nuclei were stained with DAPI (4',6-diamidino-2-phenylindole). Scale bar = 50 µm.

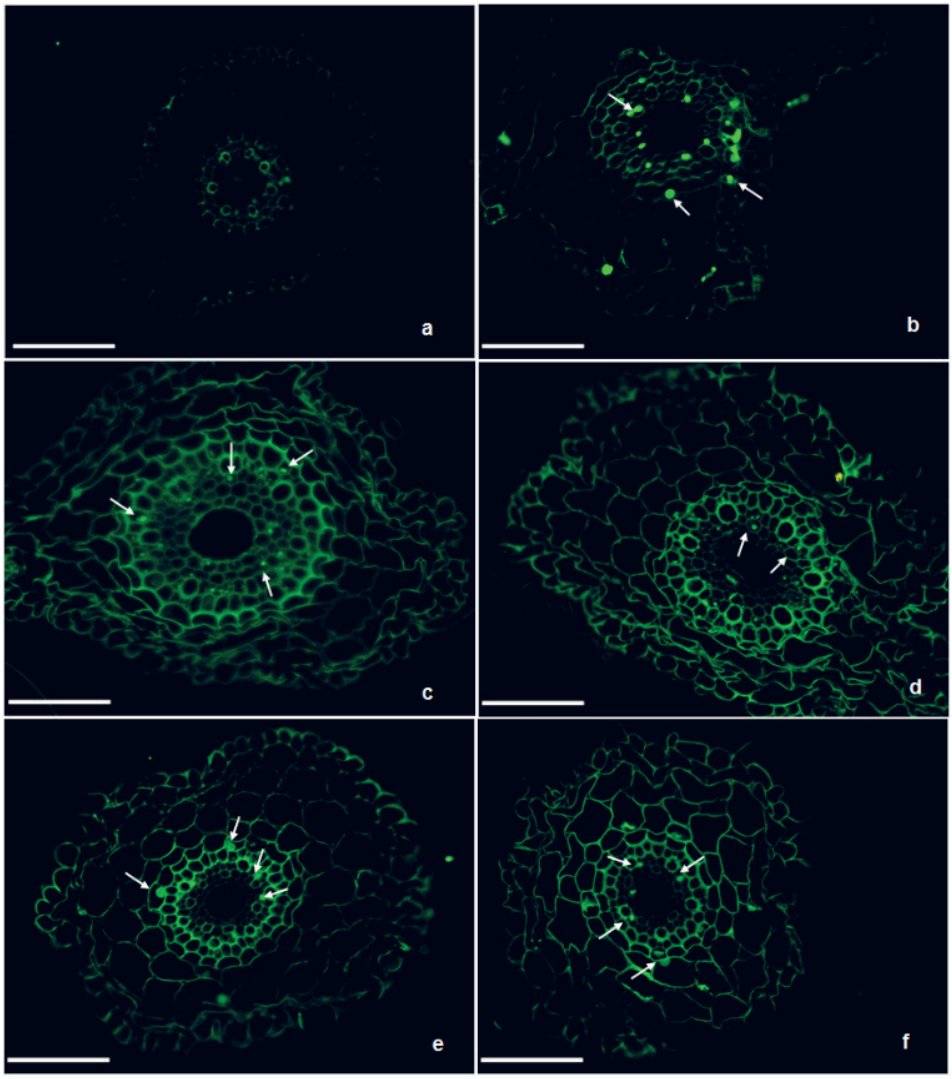

Fig. 3. TUNEL reaction in control wheat root cells (**a**) and after 15 days of exposure to 0.5 (**b**), 1 (**c**), 5 (**d**), 10 (**e**), and 20 mg L^{-1} of AgNPs (**f**). Images were obtained by TUNEL staining. Arrows indicate TUNEL-positive nuclei. Scale bars = 100 μm.

membrane potentials decreased significantly below the value obtained for control in a dose-dependent manner (Fig. 5a). The reduction was 7% at 0.5 mg L^{-1}, 11% at 1 mg L^{-1}, 15% at 5 mg L^{-1}, 22% at 10 mg L^{-1}, and 30% at 20 mg L^{-1} of AgNP in comparison to control. Furthermore, western blot analysis revealed the release of cyt-c to cytosol in all AgNP-treated roots (Fig 5c). However, we observed no significant differences in the cyt-c release between treatments and control based on the relative density of bands (Fig. 5b).

We observed a significant increase in caspase 1-like activity, by 9%, 33%, 13%, 43%, and 49% at concentrations of 0.5, 1, 5, 10, and 20 mg L^{-1} concentrations of AgNP treatments, respectively (Fig. 6).

Furthermore, according to PCR results, *TaVPE4* gene expression increased significantly at all applied concentrations of AgNP compared to the control (Fig. 7). The relative band density increased by 45% at 0.5 mg L^{-1}, 139% at 1 mg L^{-1}, 81% at 5 mg L^{-1}, 80% at 10 mg L^{-1}, and 145% at 20 mg L^{-1} of AgNP treatments compared to control. The increase in expression was particularly notable at concentrations of 1 and 20 mg L^{-1} of AgNP.

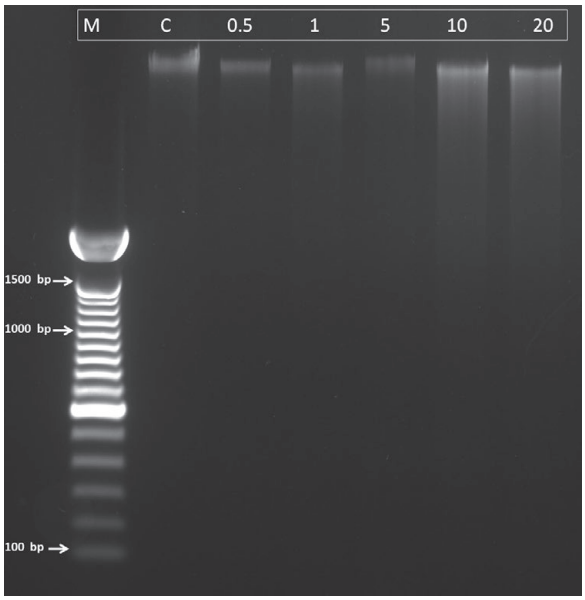

Fig. 4. DNA gel electrophoresis of control wheat root cells (C) and after 15 days of exposure to 0.5 mg L^{-1}, 1 mg L^{-1}, 5 mg L^{-1}, 10 mg L^{-1}, and 20 mg L^{-1} of AgNPs. M = 1 kb DNA marker.

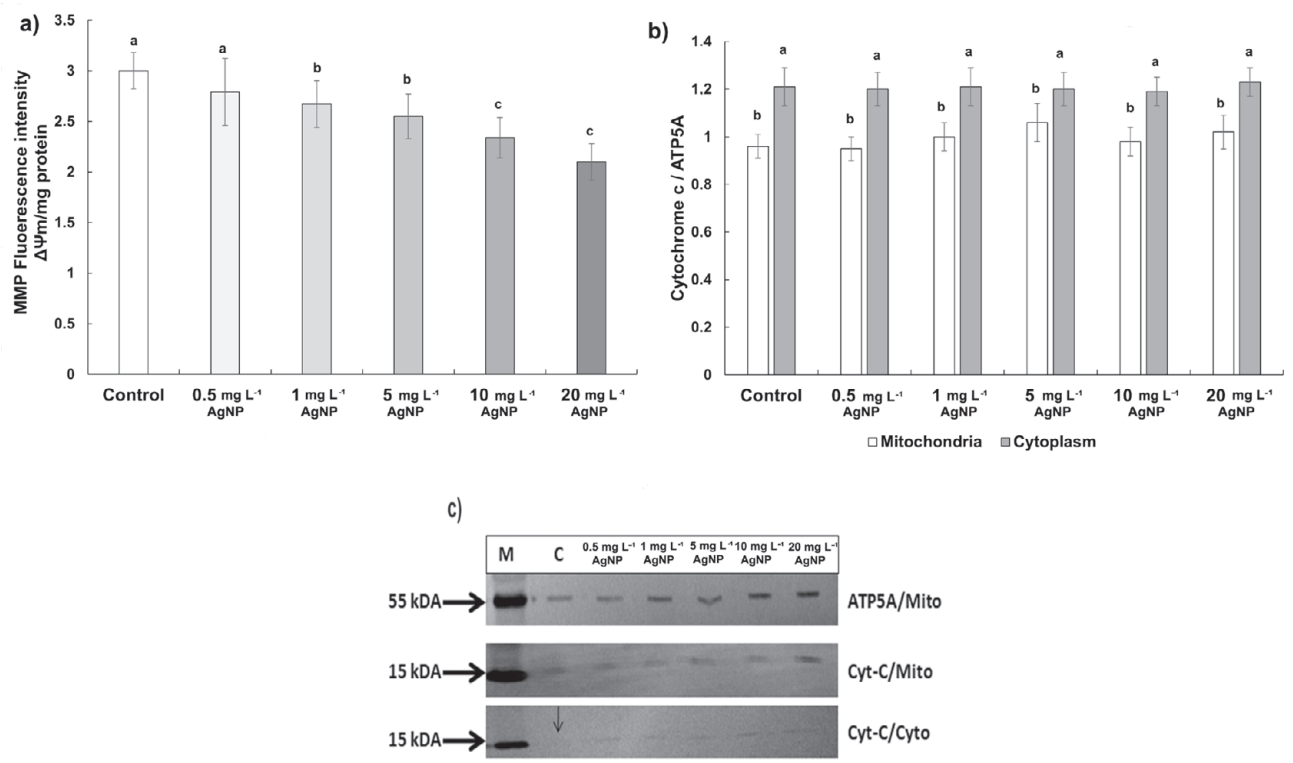

Fig. 5. Mitochondria inner membrane potential and cytochrome c expression in control wheat root cells and after 15 days of exposure to 0.5, 1, 5, 10, and 20 mg L^{-1} of AgNPs. Mitochondrial membrane potential (MMP, ΔΨm) (**a**), comparison of relative density of cytochrome c (cyt-c) in mitochondrial and cytosolic fractions (**b**), western blot analysis of cyt-c in mitochondrial and cytosolic fractions (**c**). Data with different letters are statistically significant ($P < 0.05$) based on Tukey's HSD test. Bars on columns represent means ± standard deviation. Immunodetection was performed on three biological replicates, and one representative membrane was selected for display. ATP5A – marker protein, Cyto – Cytoplasmic fraction, C – Control, M – Marker, Mito – Mitochondrial fraction.

According to qPCR results, *TaMCA1* and *TaMCA4* exhibited differential expression patterns across AgNP concentrations. *TaMCA1* was significantly up-regulated at 10 and 20 mg L^{-1} of AgNP, while no statistically significant difference was observed in the 0.5, 1, and 5 mg L^{-1} of AgNP treatments. In contrast, *TaMCA4* was up-regulated at 1 and 5 mg L^{-1} of AgNP, whereas no statistically significant change was observed at 0.5, 10, and 20 mg L^{-1} of AgNP (Fig. 8).

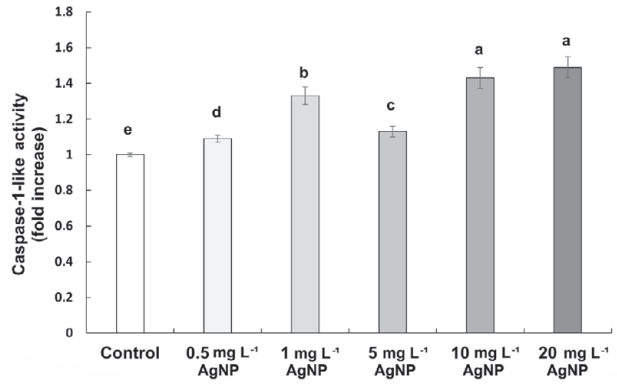

Fig. 6. Caspase-1-like activity in control wheat root cells and after 15 days of exposure to 0.5, 1, 5, 10, and 20 mg L^{-1} of AgNPs. Data with different letters are statistically significant ($P < 0.05$) based on Tukey's HSD test. Bars on columns represent means ± SD.

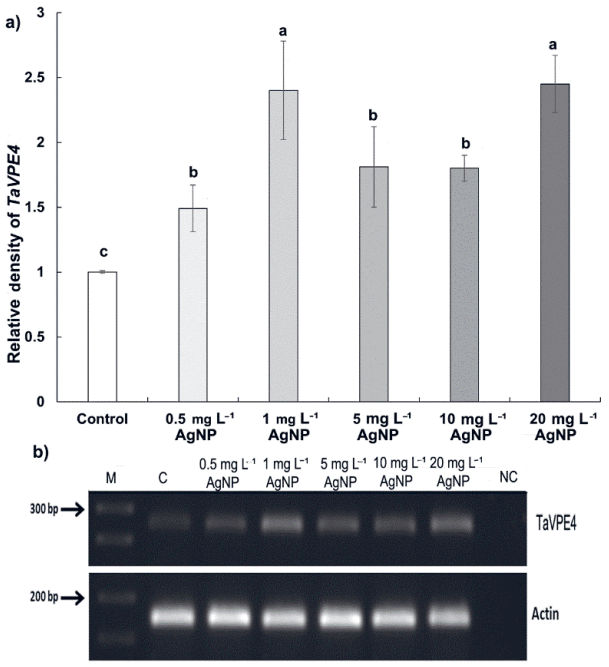

Fig. 7. Expression of *TaVPE4* gene in control wheat root cells and after 15 days of exposure to 0.5, 1, 5, 10, and 20 mg L^{-1} AgNPs. Relative density of *TaVPE4* (**a**), band intensities acquired by semi-quantitative PCR (arrows indicate 300 bp and 200 bp marker DNA) (**b**). Data with different letters are statistically significant ($P < 0.05$) based on Tukey's HSD test. Bars on columns represent means ± standard deviation. Expression analyses were performed on three biological replicates, and one representative gel was selected for display.

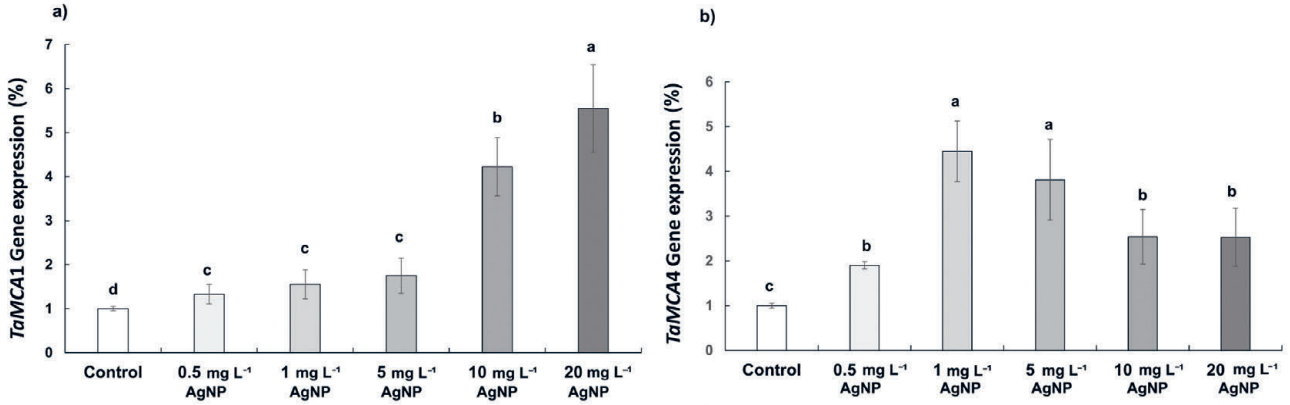

Fig. 8. The expression of *TaMCA1* (**a**) and *TaMCA4* (**b**) genes in control wheat root cells and after 15 days of exposure to 0.5, 1, 5, 10, and 20 mg L^{-1} of AgNPs. Data with different letters are statistically significant ($P < 0.05$) based on Tukey's HSD test. Bars on columns represent means ± SD.

Discussion

AgNPs are widely utilized daily and across various industries. It is estimated that European countries produce 5.5 tons of AgNP annually, increasing their content in the soil by 4 mg L^{-1} at a rate of 1.2 μg L^{-1}. The US produces between 2.8 and 20 tons of AgNPs yearly, leading to an annual soil content increase of 6.6 μg L^{-1} to 2.3 mg L^{-1}. On a global scale, the yearly input of AgNPs into soil ranges from 15 to 77 tons, with production expected to reach 400–800 tons by 2025 (Pulit-Prociak and Banach 2016, Kulikova 2021). Current estimations suggest that AgNP content in sewage sludge varies from 1.31–4.44 mg L^{-1} in Europe and 1.29–5.86 mg L^{-1} in the US. Some studies indicate that the highest safe AgNP concentration in soil is 0.05 mg L^{-1}, and other estimates predict this concentration could be reached within 50 years in some European countries (Schlich et al. 2013, Kampe et al. 2018). Considering these accumulation values and estimations, we investigated cell death features after AgNP treatments which correspond to 0.5, 1, 5, 10, and 20 mg L^{-1} AgNP.

The percentage of cells in mitosis reveals the rate of cell division and low MI can be correlated with growth regression, genotoxicity, and cell death (Yanık et al. 2017). Consistently with the reduced MI and elevated CA results in our study, several researchers have reported an AgNP-induced increase in the frequency of CA and a decrease in MI in various species, including *Allium cepa* (Fouad and Hafez 2018), *Drima polyantha* (Daphedar and Taranath 2018), and *T. aestivum* (Abdelsalam et al. 2018). Furthermore, AgNP treatments adversely affect the root anatomy of wheat (Abdelsalam et al. 2018). Mirzajani et al. (2014) stated that AgNPs permeated the cell wall and damaged the cell morphology and structure of *Oryza sativa* roots. Similarly, Tripathi et al. (2017) observed irregularities in the shape of cortical cells on cucumber roots following AgNP exposure. Cvjetko et al. (2018) revealed that tobacco root cells are highly vacuolated and absorb AgNPs in the meristem cells, indicating vacuolization where AgNPs are stored. Likewise, our previous study confirmed the uptake of AgNPs by roots, their accumulation in the cytoplasm of cortical cells, and significant inhibition of root elongation in higher concentrations (10 and 20 mg L^{-1}) (Yanık and Vardar 2019). When our previous (Yanık and Vardar 2019) and present results are evaluated together, it can be concluded that regression in root elongation may be related to the decrease in MI and increase in CA due to AgNP accumulation and toxicity.

Chromatin condensation, its passage through the nucleus periphery, and degradation of nuclear DNA are among the most prominent characteristics observed in cells undergoing PCD. During chromatin condensation, DNA is firstly cleaved into high molecular weight fragments (50–300 kb), followed by low molecular weight fragments (Minina et al. 2021). We observed alterations in nuclear morphology, chromatin condensation, and slight DNA smear, particularly in response to higher AgNP concentrations (10 and 20 mg L^{-1}). Several researches have shown that aluminum (Al) nanoparticles (AlNPs) induce chromatin condensation and DNA fragmentation in *T. aestivum* roots, as evidenced by DAPI staining, TUNEL assay, and gel electrophoresis (Yanık and Vardar 2015, Yanık et al. 2017). Additionally, Thiruvengadam et al. (2015) found that different concentrations of AgNPs (1, 5, and 10 mg L^{-1}) cause DNA damage in *Brassica rapa* roots, as confirmed by DNA laddering, comet assay, and TUNEL staining. These results show that both NPs and AgNPs can induce chromatin and/or DNA damage in a concentration-dependent manner, which is consistent with the observations in our experiments.

The earliest characteristic indications of PCD in plants include alterations in mitochondrial morphology, loss of inner mitochondrial membrane potential, and cyt-c release to the cytosol (Paes de Melo et al. 2022). Cyt-c is localized in the mitochondrial intermembrane space and is linked to the inner mitochondrial membrane. Under stress conditions, ROS regulates cardiolipin oxidation, resulting in cyt-c diffusion into the intramembrane region. Additionally, ROS triggers the mobilization of Ca^{2+} ions from the endoplasmic reticulum (ER) lumen to the mitochondria. These Ca^{2+} ions can induce a decrease in mitochondrial transmembrane po-

tential and the opening of mitochondrial permeability transition pores (MPTP) in the outer mitochondrial membrane, facilitating the cyt-c release to the cytoplasm (Huang et al. 2014, Paes de Melo et al. 2022). The release of cyt-c further stimulates ROS generation within the mitochondria, creating a positive feedback loop to enhance the initial signal. ROS production and cyt-c release may be prerequisites for the PCD execution rather than directly activating it (Reape and McCabe 2008). Previous studies have observed cyt-c release in plants under various stress conditions, such as heavy metal exposure, temperature, fusarium toxin, salt, and flooding (Li et al. 2007, Sarkar and Gladish 2012, Huang et al. 2014). For example, Huang et al. (2014) investigated Al toxicity in the roots of *Arachis hypogaea* and found that it induces DNA fragmentation, chromatin condensation, caspase-3-like activity, and reduction in mitochondrial inner membrane potential and membrane permeability, resulting in the cyt-c release from the mitochondria to the cytoplasm. More recently, Qi et al. (2018) showed that waterlogging stress led to the degradation of mitochondrial structure, increase of the mitochondrial permeability transition, and decrease of mitochondrial transmembrane potential and cyt-c release in the endosperm of wheat as evidence of PCD process. In the presented study similarly, a significant decrease of mitochondrial inner membrane potentials and release of cyt-c to cytosol in all AgNP-treated wheat roots were observed, for the first time as far as we know.

PCD is regulated by proteases belonging to five distinct categories: serine, aspartate, cysteine, threonine, and metalloproteases (Rawlings et al. 2018). While the most well-known proteases involved in the initiation and execution of animal apoptosis are caspases, which cleave their substrates after an aspartate residue using a catalytic dyad consisting of cysteine and histidine amino acids (Klemenčič and Funk 2018), plants lack true caspase. Instead, plant PCD is thought to be mediated by caspase-like or other protease enzymes (Salguero-Linares and Coll 2019). Among the main cysteine proteases in plants are vacuolar processing enzymes (VPEs), metacaspases (MCs), and papain-like cysteine proteases (PLCPs). These proteases play crucial roles in various physiological processes, including PCD (Salguero-Linares and Coll 2019). Hatsugai et al. (2015) showed that VPEs have structural and enzymatic properties similar to mammalian caspase-1, displaying YVADase/caspase-1-like cleavage activity despite limited sequence identity to caspase. It has also been revealed that the synthetic caspase-1 inhibitor Ac-YVAD-CHO inhibits the activation of VPE (Hatsugai et al. 2015). Various studies focusing on PCD have examined *VPE* gene expression and caspase-like activity. For example, Kariya et al. (2013) reported that the VPE activity increases with the loss of plasma membrane integrity in cell lines exposed to 100 μM Al, and caspase-1 inhibitor suppresses PCD in *Nicotiana tabacum* cell line BY-2. It was stated that the expression of *VPE* genes was significantly enhanced by Al treatment. Moreover, many studies have demonstrated that various abiotic stressors, such as ethylene, salicylic acid, gibberellic acid, nitric oxide, H_2O_2, and salt, upregulate *VPE* genes across different plant species (Kang et al. 2013, Wang et al. 2018). Kang et al. (2013) reported temporal and spatial expression patterns of *TaVPEs* in different tissues of wheat under various stress conditions. After treatment with NaCl and H_2O_2, *TaVPEs* were upregulated in roots, particularly *TaVPE4*, which showed extensive expression. After treatment with NaCl, the expression of *TaVPE4* was remarkably high for 24 hours, but then it decreased. On the other hand, the expression of *TaVPE4* was significantly high in roots after H_2O_2 treatment, and it remained consistent over time. NaCl treatment slightly induced *TaVPE1* and *TaVPE2* in roots. After 48 hours of treatment, visible transcripts of *TaVPE1* and *TaVPE2* were detected in leaves (Kang et al., 2013). Based on this study, we observed that *TaVPE4*, which is expressed in roots, especially under stress conditions, was significantly upregulated compared to the control and reached the highest value, especially at 1 and 20 mg L^{-1}. To the best of our knowledge, our study is the first to demonstrate the induction of *TaVPE4* gene expression and caspase 1-like activity by AgNP treatment.

Metacaspases represent the largest subfamily of cysteine proteases and are found in plants, fungi, and protists based on their caspase homology. They are classified into three categories – type I, type II, and type III, based on the architecture of their p10 and p20 domains. Unlike caspases, metacaspases exhibit substrate specificity to arginine or lysine instead of aspartate. Several reviews have compiled studies suggesting that plant metacaspases are involved in dPCD and ePCD (Minina et al. 2017, 2021). *TaMCA1* is a type I metacaspase and it has been reported that while the *TaMCA1* gene does not exhibit caspase-1-like activity, it could suppress PCD in tobacco and wheat leaves induced by the mouse *Bax* gene in interaction with pathogen *Puccinia striiformis* (Pst) (Hao et al. 2016). Hao et al. (2016) also indicated that the knockdown of the *TaMCA1* gene increases plant resistance to Pst. They reported that the expression level of *TaMCA1* increased significantly at 48 and 72 hours post inoculation (hpi) with Pst, indicating that *TaMCA1* may play an important role in the interaction between wheat and Pst. Their research suggests that *TaMCA1* regulates cell death only after generating sufficient signals, such as mammalian Bax, Pst, or H_2O_2. Our results showed that *TaMCA1* up-regulated significantly only in 10 and 20 mg L^{-1} of AgNP treatment. It may be increased to suppress PCD in these stages where only DNA fragmentation is observed.

Another wheat metacaspase, *TaMCA4*, is classified as a type II metacaspase and was identified by Wang et al. (2012). It was demonstrated that overexpression of *TaMCA4* enhances PCD induced by Pst, while knockdown of *TaMCA4* has the opposite effect, suggesting that *TaMCA4* acts as a positive regulator of PCD (Wang et al. 2012). To assess the involvement of metacaspase genes in AgNP-induced PCD, we examined the expression of *TaMCA1* and *TaMCA4* genes. While *TaMCA1* expression increased at 10 and 20 mg L^{-1}, *TaMCA4* expression up-regulated significantly only at 1 and 5 mg L^{-1} AgNP treatment. Based on these results, we speculate that *TaMCA1* and *TaMCA4* genes may work an-

tagonistically and they may suppress each other. Moreover, different concentrations of AgNPs may induce the activity of different types of metacaspases to regulate ePCD.

While numerous studies have investigated the accumulation, translocation, and toxicity of NPs in plants, the phytotoxicity mechanisms remain unclear. Additionally, the execution and regulation of NP-induced PCD are still not fully understood. This study is the first to examine AgNP-induced PCD in wheat root cells. Our results showed that AgNPs at different concentrations (0.5, 1, 5, 10, and 20 mg L^{-1}) induce PCD to varying degrees. This research contributes to our understanding of NPs' role in regulating and executing PCD, which is crucial for advancing knowledge on the long-term effects of NPs on ecosystems and crop yield stability in current and future investigations.

Acknowledgment

This study is part of a Ph.D. dissertation by Fatma Yanık at Marmara University and supported by the Research Foundation of Marmara University (BAPKO) project number FEN-C-DRP-130116-0011.

References

Abdelsalam, N. R., Abdel-Megeed, A., Ali, H. M., Salem, M. Z. M., Muwafaq, F.A. et al., 2018: Genotoxicity effects of silver nanoparticles on wheat (*Triticum aestivum* L.) root tip cells. Ecotoxicology and Environmental Safety 155, 76–85. https://doi.org/10.1016/j.ecoenv.2018.02.069

Alshameri, A.W., Owais, M., 2022: Antibacterial and cytotoxic potency of the plant-mediated synthesis of metallic nanoparticles AgNPs and ZnONPs: A review. OpenNano 8, 100077. https://doi.org/10.1016/j.onano.2022.100077

Chhipa, H., Joshi, P., 2016: Nanofertilisers, nanopesticides and nanosensors in agriculture. In: Ranjan, S., Dasgupta, N., Lichtfouse, E. (ed.), Nanoscience in Food and Agriculture 1, Sustainable Agriculture Reviews, Springer, Switzerland, pp 247–282.

Cvjetko, P., Milošić, A., Domijan, A. M., Vrček, I. V., Tolić, S. et al., 2018: Toxicity of silver ions and differently coated silver nanoparticles in *Allium cepa* roots. Ecotoxicology and Environmental Safety 137, 18–28. https://doi.org/10.1016/j.ecoenv.2016.11.009

Daphedar, A., Taranath, T. C., 2018: Characterization and cytotoxic effect of biogenic silver nanoparticles on mitotic chromosomes of *Drimia polyantha* (Blatt. & McCann) Stearn. Toxicology Reports 5, 910–918. https://doi.org/10.1016/j.toxrep.2018.08.018

Dimkpa, C. O., McLean, J. E., Martineau, N., Britt, D. W., Haverkamp, R. et al. 2013: Silver nanoparticles disrupt wheat (*Triticum aestivum* L.) growth in a sand matrix. Environmental Science and Technology 47(2), 1082–1090. https://doi.org/10.1021/es302973y

Emanuele, S., Oddo, E., D'Anneo, A., Notaro, A., Calvaruso, G. et al. 2018: Routes to cell death in animal and plant kingdoms: from classic apoptosis to alternative ways to die review. Rendiconti Lincei-Scienze Fisiche e Naturali 29(2), 397–409. https://doi.org/10.1007/s12210-018-0704-9

Filippi, A., Zancani, M., Petrussa, E., Braidot, E. 2019: Caspase-3-like activity and proteasome degradation in grapevine suspension cell cultures undergoing silver-induced programmed cell death. Plant Physiology 233, 42–51. https://doi.org/10.1016/j.jplph.2018.12.003

Fouad, A. S., Hafez, R. M. 2018: The effects of silver ions and silver nanoparticles on cell division and expression of cdc2 gene in *Allium cepa* root tips. Biologia Plantarum 62 (1), 166–172. https://doi.org/10.1007/s10535-017-0751-6

Hameed, A., Malik, S. A., İqbal, N., Arshad, R., Farooq, S. 2004: A Rapid (100 min) method for ısolating high yield and quality DNA from leaves, roots, and coleoptile of wheat (*Triticum aestivum* L.) suitable for apoptotic and other molecular studies. International Journal of Agricultural Biology 6(2), 383–387. http://doi.org/1560–8530/2004/06–2–383–387

Hao, Y., Wang, X., Wang, K., Li, H., Duan, X. et al. 2016: *TaMCA1*, a regulator of cell death, is important for the interaction between wheat and *Puccinia striiformis*. Science Reports 6, 26946. https://doi.org/10.1038/srep26946

Hatsugai, N., Yamada, K., Goto-Yamada, S., Hara-Nishimura, I. 2015: Vacuolar processing enzyme in plant programmed cell death. Frontiers in Plant Science 6, 234. https://doi.org/10.3389/fpls.2015.00234

Huang, W. J., Oo,T. L., He, H. Y., Wang, A. Q., Zhan, J. et al. 2014: Aluminum induces rapidly mitochondria-dependent programmed cell death in Al-sensitive peanut root tips. Botanical Studies 55, 67. https://doi.org/10.1186/s40529-014-0067-1

Huang, D., Dang, F., Huang, Y., Chen, N., Zhou, D. 2022: Uptake, translocation and transformation of silver nanoparticles in plants. Environmental Science: Nano Journal 9, 12–39. https://doi.org/10.1039/D1EN00870F

Kampe, S., Kaegi, R., Schlich, K., Wasmuth, C., Hollert, H., Schlechtriem, Ch. 2018. Silver nanoparticles in sewage sludge: bioavailability of sulfidized silver to the terrestrial isopod *Porcellio scaber*. Environmental Toxicology Chemistry 37(6), 1606–1613. https://doi.org/10.1002/etc.4102

Kang, T. H., Kim, D. Y., Seo, Y. W. 2013: Identification and expression analysis of wheat vacuolar processing enzymes (VPEs). Plant Breeding and Biotechnology 1(2), 148–161. https://doi.org/10.9787/PBB.2013.1.2.148

Kariya, K., Demiral, T., Sasaki, T., Tsuchiya, Y., Turkan, I. et al. 2013: A novel mechanism of aluminum-induced cell death involving vacuolar processing enzyme and vacuolar collapse in tobacco cell line BY-2. Journal of Inorganic Biochemistry 128, 196–201. https://doi.org/10.1016/j.jinorgbio.2013.07.001

Klemenčič, F., Funk, C. 2018: Structural and functional diversity of caspase homologs in non-metazoan organisms. Protoplasma 255(1), 387–397. https://doi.org/10.1007/s00709-017-1145-5

Kulikova, N.A. 2021. Silver nanoparticles in soil: input, transformation, and toxicity. Soil Chemistry 54, 352–365. https://doi.org/10.1134/S1064229321030091

Li, J. Y., Jiang, A. L., Zhang, W. 2007: Salt stress-induced programmed cell death in rice root tip cells. Journal of Integrative Plant Biology 49(4), 481–486. https://doi.org/10.1111/j.1744-7909.2007.00445.x

Livak, K. J., Schmittgen, T. D. 2001: Analysis of relative gene expression data using real-time quantitative PCR and the 2ΔΔC(T). Methods 25(4), 402–408. https://doi.org/10.1006/meth.2001.1262

Lombardi, L., Ceccarelli, N., Picciarelli, P., Lorenzi, R. 2007: Caspase-like proteases involvement in programmed cell death of *Phaseolus coccineus* suspensor. Plant Science 172(3), 573–578. https://doi.org/10.1016/j.plantsci.2006.11.002

McGillicuddy, E., Murray, I., Kavanagh, S., Morrison, L., Fogarty, A. et al. 2017: Silver nanoparticles in the environment: Sources, detection, and ecotoxicology. Science of the Total Environment 575, 231–246. https://doi.org/10.1016/j.scitotenv.2016.10.041

Minina, A. E., Coll, N. S., Tuominen, H., Bozhkov, P. V. 2017: Metacaspases versus caspases in development and cell fate regulation. Cell Death and Differentiation 24, 1314–1325. https://doi.org/10.1038/cdd.2017.18

Minina, A. E., Dauphinee, A. N., Ballhaus, F., Gogvadze, V., Smertenko, A. P. et al. 2021: Apoptosis is not conserved in plants as revealed by critical examination of a model for plant apoptosis-like cell death. BMC Biology 19, 100. https://doi.org/10.1186/s12915-021-01018-z

Mirzajani, F., Askari, H., Hamzelou, S., Schober, Y., Römpp, A. et al. 2014: Proteomics study of silver nanoparticles toxicity on *Oryza sativa* L. Ecotoxicology and Environmental Safety 108, 335–339. https://doi.org/10.1016/j.ecoenv.2014.07.013

Paes de Melo, B., Carpinetti, Pd. A., Fraga, O. T., Rodrigues-Silva, P. L., Fioresi, V. S. et al. 2022: Abiotic stresses in plants and their markers: A practice view of plant stress responses and programmed cell death mechanisms. Plants 11(9), 1100. https://doi.org/10.3390/plants11091100

Panda, S. K., Yamamoto, Y., Kondo, H., Matsumoto, H. 2008: Mitochondrial alterations related to programmed cell death in tobacco cells under aluminium stress. Comptes Rendus Biologies 331(8), 597–610. https://doi.org/10.1016/j.crvi.2008.04.008

Pulit-Prociak, J., Banach, M. 2016: "Silver nanoparticles-a material of the future…?" Open Chemistry 14(1), 76–91. https://doi.org/10.1515/chem-2016-0005

Qi, Y. H., Mao, F. F., Zhou, Z. Q., Liu, D. C., Yu, M. et al. 2018: The release of cytochrome c and the regulation of the programmed cell death progress in the endosperm of winter wheat (*Triticum aestivum* L.) under water logging. Protoplasma 255, 1651–1665. https://doi.org/10.1007/s00709-018-1256-7

Qian, H., Peng, X., Han, X., Ren, J., Sun, L. et al. 2013: Comparison of the toxicity of silver nanoparticles and silver ions on the growth of terrestrial plant model *Arabidopsis thaliana*. Journal of Environmental Sciences 25(9), 1947–1956. https://doi.org/10.1016/S1001-0742(12)60301-5

Rawlings, N. D., Alan, J., Thomas, P. D., Huang, X., Bateman, A. et al. 2018: The MEROPS database of proteolytic enzymes, their substrates and inhibitors in 2017 and a comparison with peptidases in the PANTHER database. Nucleic Acids Research 46(D1), D624-D632. https://doi.org/10.1093/nar/gkx1134

Reape, T. J., McCabe, P. F. 2008: Apoptotic-like programmed cell death in plants. New Phytologist 180 (1), 13–26. https://doi.org/10.1111/j.1469-8137.2008.02549.x

Salguero-Linares, J., Coll, N. S. 2019: Plant proteases in the control of the hypersensitive response. Journal of Experimental Botany 70(7), 2087–2095. https://doi.org/10.1093/jxb/erz030

Sarkar, P., Gladish, D. K. 2012. Hypoxic stress triggers a programmed cell death pathway to induce vascular cavity formation in *Pisum sativum* roots. Physiologia Plantarum 146(4), 413–426. https://doi.org/10.1111/j.1399-3054.2012.01632.x

Schlich, K., Klawonn, T., Terytze, K., Hund-Rinke K. 2013. Hazard assessment of a silver nanoparticle in soil applied via sewage sludge. Environmental Sciences Science 25, 17. https://doi.org/10.1186/2190-4715-25-17

Schweizer, D. 1976: Reverse fluorescent chromosome banding with chromomycin and DAPI. Chromosoma 58, 307–324.

Thiruvengadam, M., Gurunathan, S., Chung, I. M. 2015: Physiological, metabolic, and transcriptional effects of biologically-synthesized silver nanoparticles in turnip (*Brassica rapa* ssp. *rapa* L.). Protoplasma 252, 1031–1046. https://doi.org/10.1007/s00709-014-0738-5

Tripathi, A., Liu, S., Singh, P. K., Kumar, N., Pandey, A. C. et al. 2017: Differential phytotoxic responses of silver nitrate ($AgNO_3$) and silver nanoparticle (Ag Nps) in *Cucumis sativus* L. Plant Gene 11(B), 255–264. https://doi.org/10.1016/j.plgene.2017.07.005

Wang, W., Zhou, X., Xiong, H., Mao, W. Y., Zhao, P. et al. 2018: Papain-like and legumain-like proteases in rice: genome-wide identification, comprehensive gene feature characterization and expression analysis. BMC Plant Biology 18, 87. https://doi.org/10.1186/s12870-018-1298-1

Wang, X., Kang, Z. S., Feng, H., Tang, C., Bai, P. et al. 2012: TaMCA4, a novel wheat metacaspase gene functions in programmed cell death induced by the fungal pathogen *Puccinia striiformis* f. sp. *tritici*. Molecular Plant Microbe Interaction 25 (6), 755–763. https://doi.org/10.1094/MPMI-11-11-0283-R

Yanık, F., Ayturk, O., Vardar, F. 2017: Programmed cell death evidence in wheat (*Triticum aestivum* L.) roots induced by aluminum oxide (Al_2O_3) nanoparticles. Caryologia 70(2), 112–119. https://doi.org/10.1080/00087114.2017.1286126

Yanık, F., Vardar, F. 2015: Toxic effects of aluminum oxide (Al_2O_3) nanoparticles on root growth and development in *Triticum aestivum*. Water Air and Soil Pollution 226, 296–308. https://doi.org/10.1007/s11270-015-2566-4

Yanık, F., Vardar, F. 2019: Assessment of silver nanoparticle-induced morphological, biochemical and physiological alterations in wheat roots. Annali di Botanica 9; 83–94. https://doi.org/10.13133/2239-3129/14633

Acta Bot. Croat. 84 (1), 101–104, 2025
DOI: 10.37427/botcro-2025-013

CODEN: ABCRA 25
ISSN 0365-0588
eISSN 1847-8476

Short communication

Carex distachya (Cyperaceae) with both subspecies in Europe

Jacob Koopman[1], Helena Więcław[2], Sandro Bogdanović[3]*, Teodor T. Denchev[4]

[1] ul. Kochanowskiego 27, 73-200 Choszczno, Poland

[2] University of Szczecin, Institute of Marine and Environmental Sciences, Adama Mickiewicza 18, 70-383 Szczecin, Poland

[3] University of Zagreb, Faculty of Agriculture, Department of Agricultural Botany, Svetošimunska cesta 25, HR-10000 Zagreb, Croatia

[4] Bulgarian Academy of Sciences, Institute of Biodiversity and Ecosystem Research, 2 Gagarin St., 1113 Sofia, Bulgaria

Abstract – *Carex distachya* Desf. is a circum-Mediterranean species. Since 1985 two varieties have been distinguished, *C. distachya* var. *distachya* and *C. distachya* var. *phyllostachioidea* Ö.Nilsson. The former is widespread, while the latter is considered to be restricted to West Türkiye and the East Aegean Islands, but our research has revealed that *C. distachya* var. *phyllostachioidea* is much more widespread in the south-east of Europe, in Croatia, Bulgaria, Montenegro, and mainland Greece. It seems to have been overlooked in these countries so far. As *C. distachya* var. *phyllostachioidea* occurs in the East Mediterranean region, we have therefore raised this taxon to subspecies level. Our research has also shown that the differences between the two subspecies are less clear than initially suggested. An upgraded key is therefore added.

Keywords: *Carex*, herbarium revision, identification key, Mediterranean, morphology

Introduction

The genus *Carex* L. (Cyperaceae) is species-rich, with more than 2000 species worldwide (POWO 2023). In Europe, Chater (1980) mentioned 180 species of *Carex*, while Koopman (2022) presents 235 species. The difference is partly due to the arbitrary use of the borders of Europe. Koopman (2022) included the three Caucasus countries, Armenia, Azerbaijan and Georgia, where several carices specific for the Caucasus or more Asian species which have their western border in the Caucasus can be found. On the other hand, since 1980 several new species have been described for Europe as well, e.g. *C. randalpina* B.Walln. (Wallnöfer 1993), *C. pallidula* Harmaja (Harmaja 2005), and *C. castroviejoi* Luceño & Jim.Mejías (Jiménez-Mejías & Luceño 2009). Molina et al. (2008a, 2008b) described another ten taxa within the section *Phaestoglochin* Dumort., including seven new species. Finally, some species have been discovered recently as new for Europe, e.g. *C. kurdica* Kük. ex Hand.-Mazz. (Jiménez-Mejías et al. 2013).

Chater (1980) put *C. distachya* Desf. into subgenus *Indocarex* Baillon, together with *C. phyllostachys* C.A.Mey. The former occurs in dry places in South Europe, in France, Spain, Portugal, Italy, Croatia, Bosnia and Herzegovina, Montenegro, North Macedonia, Albania, Greece, Bulgaria, and European Türkiye; the occurrence in Serbia and Romania needs confirmation (Koopman 2022; Fig. 1). It occurs also in North Africa (Algeria, Libya, Morocco, and Tunisia), as well as in Asian Türkiye. The last mentioned *C. phyllostachys*, a forest plant, was only known in Europe from W North Macedonia till 1980. More recently it has been found in several other (South) East European countries: Greece (Bergmeijer 1988, Authier 1997), Albania (Barina and Pifkó 2011), Italy (Wagensommer et al. 2014), and Croatia (Terlević et al. 2021). *Carex phyllostachys* is also known from Türkiye, Russia (Caucasus), Armenia, Azerbaijan, Georgia, and Iran (Koopman 2022).

Nilsson (1985) followed Chater (1980) by putting *C. phyllostachys* and *C. distachya* in subgenus *Indocarex* (Baillon) Kük., but added also *C. illegitima* Ces. to this subgenus. *Carex phyllostachys* and *C. illegitima* are both in

* Corresponding author e-mail: sbogdanovic@agr.hr

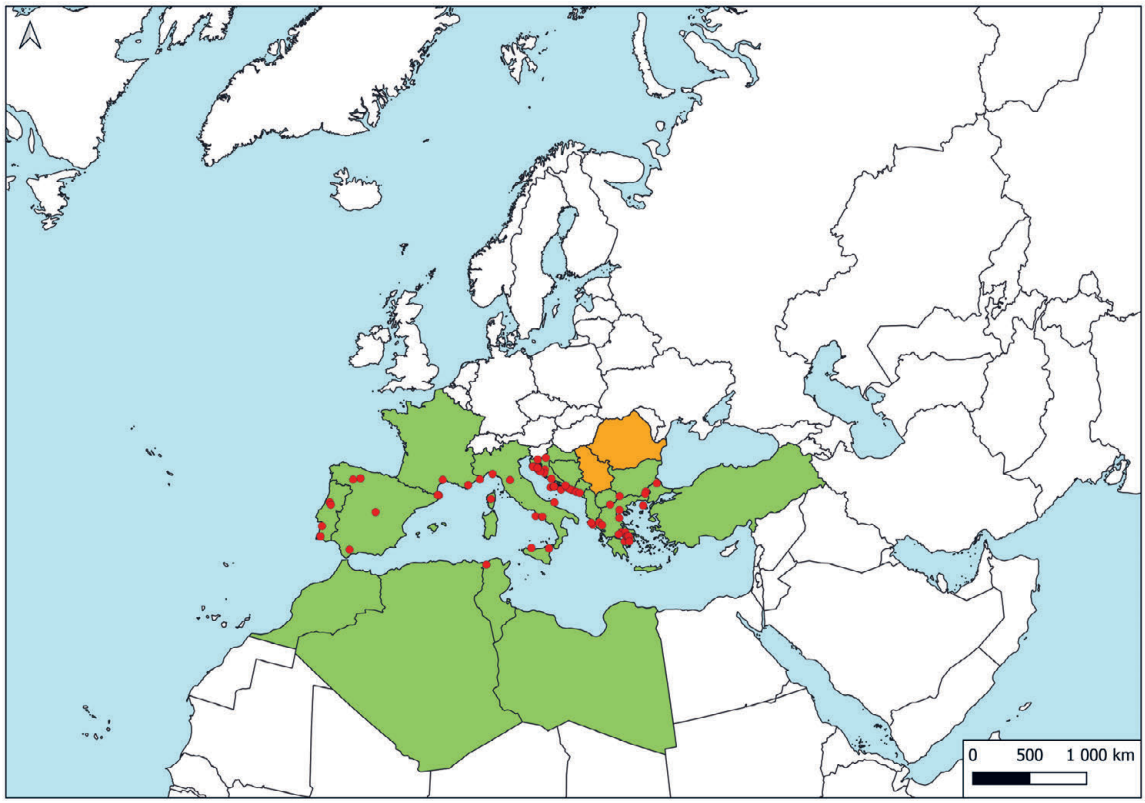

Fig. 1. Distribution of *Carex distachya* subsp. *distachya*. The map of the subspecies distribution (in green) follows Koopman (2022). It is also found on São Miguel, Azores. For the countries designated in orange, confirmation is needed. The red dots show the records indicated in the On-line Supplementary Material.

section *Phyllostachys* (Torrey & A.Gray ex J.Carey) Bailey by Nilsson (1985), *C. distachya* is housed in section *Schiedeanae* Kük., although Nilsson (1985) is said to have treated this section within the subgenus *Indocarex* tentatively, and maybe it would be better to treat this section in subgenus *Carex*, close to section *Hallerianae* Asch. & Graebn. More recently, Roalson et al. (2021) placed *C. phyllostachys* in subgenus *Psyllophora* (Degl.) Peterm., in section *Psyllophorae* Degl.

Nilsson (1985) distinguished two varieties in *C. distachya*: *C. distachya* var. *distachya* and *C. distachya* var. *phyllostachioidea* Ö.Nilsson, the former being widespread in the Mediterranean (Fig. 1), the latter endemic to West Türkiye and the East Aegean Islands (Greece).

For many botanists the latter is a rather unknown taxon, as few botanists have ever visited the East Aegean Islands and/or do not have access to The Flora of Türkiye vol. 9, in which Nilsson described *C. distachya* var. *phyllostachioidea* (Nilsson 1985: 622). Moreover, as far as we know, apart from the description by Nilsson (1985) there has never been anything else written about *C. distachya* var. *phyllostachioidea*. Therefore, this taxon has stayed almost unnoticed since its description in 1985. Nilsson (1985) distinguished the two varieties as follows: leaves 0.5–1.5 mm broad; utricles almost veinless, beak not scabrid – *C. distachya* var. *distachya*; leaves 0.9–2.5 mm broad; utricles with 2 distinct veins, beak somewhat scabrid – *C. distachya* var. *phyllostachioidea*. The two distinct veins on the utricles are often difficult to see, but the differences in leaf width as well as the tiny teeth on the beak of *C. distachya* var. *phyllostachioidea* are clearly visible. Besides, in our opinion, the inflorescences of *C. distachya* var. *phyllostachioidea* are often significantly larger than those of *C. distachya* var. *distachya*.

As, according to Nilsson (1985), *C. distachya* var. *phyllostachioidea* is restricted to West Türkiye and the East Aegean Islands near the West coast of Türkiye, we have reckoned so far "automatically" all the found and collected material in South Europe to *C. distachya* var. *distachya*. In this article, we present our current knowledge of the distribution of *C. distachya* var. *phyllostachioidea* in Eurasia, which is probably not complete yet.

Material and methods

In this article we have analysed material of *C. distachya* s.l., available in B, BG, CL, CNHM, SOM, ZA, ZAGR, and the first author's private herbarium, in total 95 collections (see On-line Supplementary material). In the Results below, collections with duplicates and exsiccates in several herbaria are counted only once. The herbarium acronyms follow Thiers (2024), the nomenclature Koopman (2022). All material has been checked against the characters of both *C. distachya* varieties given by Nilsson (1985), mentioned in the Introduction above.

Results and discussion

In May 2023 we found *C. distachya* on the Croatian island of Vis. The material had very narrow leaves and rather small inflorescences, so it was obviously *C. distachya* var. *distachya*, with smooth beaks. However, when we compared this material with all our previous collections, we came soon to the conclusion that several of these older collections are significantly different, with wider leaves, tiny teeth on the outside of the beak, and a larger inflorescence, hence belonging without any doubt to *C. distachya* var. *phyllostachioidea*, which is therefore proved to occur over a much larger area than so far known. Of the 95 herbarium collections studied in total, 83 belong to *C. distachya* var. *distachya* and 12 to *C. distachya* var. *phyllostachioidea*. The latter has been found and collected in Bulgaria, Croatia, Greece, and Montenegro, and was originally given for West Türkiye and the East Aegean Islands (Greece) by Nilsson (1985) (Fig. 2). *Carex distachya* var. *phyllostachioidea* is restricted to the East Mediterranean (Fig. 2).

We therefore raise this variety here to subspecies rank:

Carex distachya subsp. *phyllostachioidea* (Ö.Nilsson) Jac. Koopman, Więcław, Bogdanović & T.Denchev **stat. nov.**

≡ *Carex distachya* var. *phyllostachioidea* Ö.Nillson in P.H. Davis (ed.), Fl. Turkey 9: 622 (1985)

Holotype: [Islands] Samos, valley W. of Leka, 200–400 m, Runemark & Snogerup 18861 (LD!)

However, the differences between the subspecies need some refinement. According to Nilsson (1985) the beak of *C. distachya* var. *distachya* is not scabrid, but smooth. A drawing of the utricles of both taxa is given by Nilsson (1985: p. 83). But in the material we have studied we could see on several specimens a few tiny teeth on the beak of some utricles of further typical *C. distachya* var. *distachya*, i.e. with leaves (far) less than 1.5 mm wide. Often in one and the same spike or inflorescence there are utricles with a smooth beak and some have one or a few tiny teeth on the beak. On the other hand, material of typical *C. distachya* var. *phyllostachioidea*, i.e. with flat leaves mostly more than 2 mm wide, has several teeth on every utricle beak.

It is rather amazing that in the floristically best explored continent in the world, Europe, a new *Carex* taxon could be discovered, *C. distachya* subsp. *phyllostachioidea*. Of course, geographically, the East Aegean Islands, part of Greece, do belong to Europe. But Nilsson (1985) as well as Koopman (2022) count these islands as belonging botanically to West Asia. Anyway, our study has revealed that this taxon also occurs in several (other) South-eastern European countries, where it seems to have been overlooked so far. Further research is needed to find out the exact distribution of the two taxa, especially of *C. distachya* subsp. *phyllostachioidea*. The study of herbarium material in other countries may reveal the occurrence of *C. distachya* subsp. *phyllostachioida* there, too. Finally, its occurrence may not be restricted to Eurasia; it may occur also in North Africa, in the countries in which *C. distachya* subsp. *distachya* has been recorded (Fig. 1).

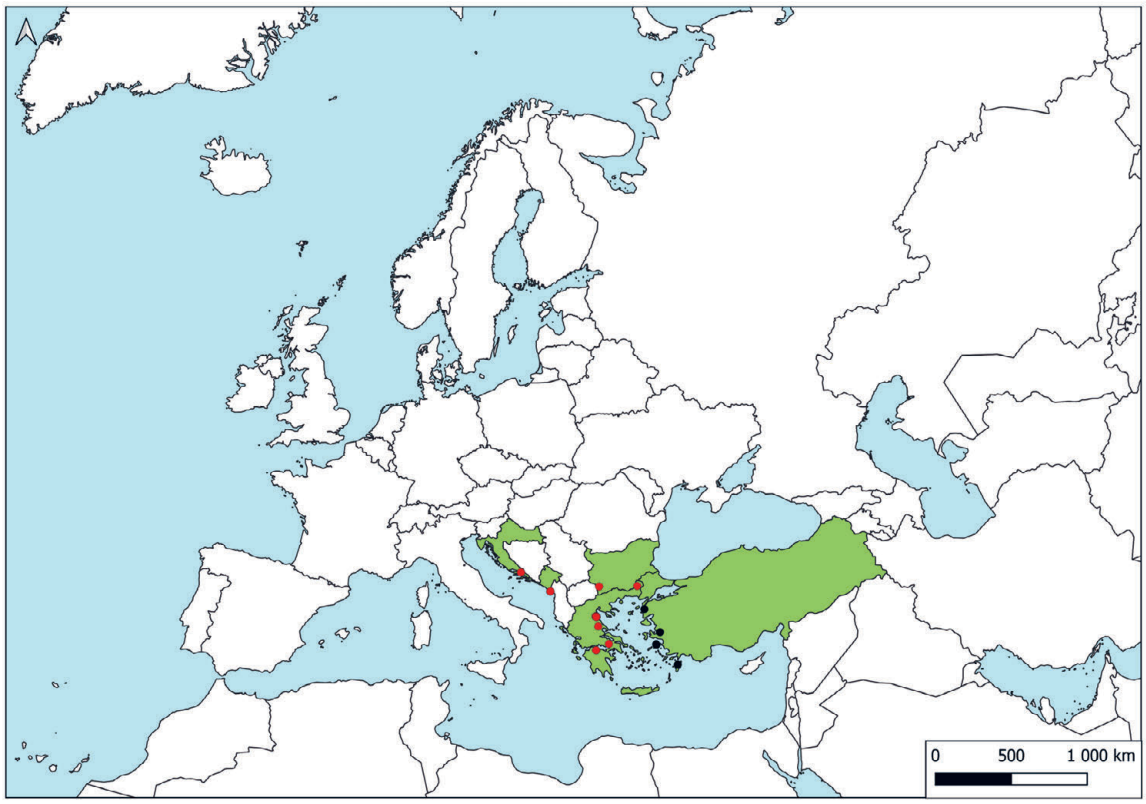

Fig. 2. Distribution of *Carex distachya* subsp. *phyllostachioidea*. Four black dots in Türkiye represent localities reported by Nilsson (1985). Red dots represent new localities found in this study, and they are reported in the On-line Supplementary Material.

Both taxa occur in all four countries where we could find *C. distachya* subsp. *phyllostachioidea*: Bulgaria, Croatia, Greece, and Montenegro, and also in Türkiye.

Key for identifying the two subspecies of *Carex distachya*

Leaves 0.5–1.5 mm broad; utricles almost veinless, beak smooth or some utricles with 1–4 tiny teeth at each beak side ..... ***C. distachya* subsp. *distachya***

Leaves 0.9–2.5 mm broad, flat; utricles with 2 distinct veins, all beaks scabrid, with more than 4 tiny teeth at each beak side ..... ***C. distachya* subsp. *phyllostachioidea***

Acknowledgments

We are grateful to the curators and staff of B, BG, CL, CNHM, SOM, ZA, and ZAGR for having access to their herbarium collections. Thanks also to Piotr Kobierski (Górzyn, PL) for compiling both the distribution maps, and to Zhivko Barzov (BG) for sending us some material of *C. distachya* subsp. *phyllostachioidea* from Bulgaria.

References

Authier, P., 1997: *Carex phyllostachys* C.A. Meyer, une rare et intéressante espèce de la flore de Grèce. Lagascalia 19(1–2), 927–936.

Barina, Z., Pifkó, D., 2011: Distribution of *Carex distachya* in Albania. Botanica Serbica 35(2), 125–130.

Bergmeijer, E., 1988: Floristic notes on the Kato Olimbos area (NE Thessaly, Greece). Willdenowia 17, 37–58.

Chater, A. O., 1980: *Carex* L., In: Tutin, T. G., Heywood, V. H., Burges, N. A., Moore, D. M., Valentine, D. H., Walters, S. M., Webb, D. A., (eds.), Flora Europaea, vol. 5, 290–323. Cambridge University Press, Cambridge.

Harmaja, H., 2005: *Carex pallidula*, nom. nov. Annales Botanici Fennici 42(3), 221–222.

Jiménez-Mejías, P., Luceño, M., 2009: *Carex castroviejoi* Luceño & Jiménez-Majías (Cyperaceae), a new species from North Greek mountains. Acta Botanica Malacitana 34, 231–233.

Jiménez-Mejías, P., Martín-Bravo, S., Amini-Rad, M., Luceño, M., 2013: Disentangling the taxonomy of *Carex acuta* s.l. in the Mediterranean basin and the Middle East: Reevaluation of *C. panormitana* Guss. and *C. kurdica* Kük. ex Hand.-Mazz. Plant Biosystems 148(1), 64–73. http://dx.doi.org/10.1080/11263504.2012.758675

Koopman, Jac., 2022: *Carex* Europaea, vol. 1 (3rd ed.). Margraf Publishers, Weikersheim.

Molina, A., Acedo, C., Llamas, F., 2008a: Taxonomy and new taxa in Eurasian *Carex* (Section *Phaestoglochin*, Cyperaceae). Systematic Botany 33(2), 237–250. https://doi.org/10.1600/036364408784571563

Molina, A., Acedo, C., Llamas, F., 2008b: Taxonomy and new taxa of the *Carex divulsa* aggregate in Eurasia (section *Phaestoglochin*, Cyperaceae). Botanical Journal of the Linnean Society 156(3), 385–409. https://doi.org/10.1111/j.1095-8339.2007.00760.x

Nilsson, Ö., 1985: *Carex* L. In: Davis, P. H. (ed.), Flora of Turkey and the East Aegean Islands, vol. 9. Edinburgh University Press, Edinburgh.

POWO, 2023: Plants of the World Online. Facilitated by the Royal Botanic Gardens, Kew. Retrieved September 17, 2023 from http://www.plantsoftheworldonline.org/.

Roalson, E. H., Jiménez-Mejías, P., Hipp, A. L., Benítez-Benítez, C., Bruederle, L., Chung, K.-S., Escudero, M., Ford, B. A., Ford, K., Gebauer, S., Gehrke, B., Hahn, M., Hayat, M. Q., Hoffmann, M. H., Jin, X.-F., Kim, S., Larridon, I., Léveillé-Bourret, É., Lu, Y.-F., Luceño, M, 2021: A framework infrageneric classification of *Carex* (Cyperaceae) and its organizing principles. Journal of Systematics and Evolution 59(4), 726–762. https://doi.org/10.1111/jse.12722

Terlević, A., Koopman, Jac., Więcław, H., Rešetnik, I., Bogdanović, S., 2021: *Carex phyllostachys* (Cyperaceae), a new species in Croatia. Acta Botanica Croatica 80(1), 106–111. https://doi.org/10.37427/botcro-2021-002

Thiers, B., 2024+ continuously updated. Index Herbariorum: A Global Directory of Public Herbaria and Associated Staff. New York Botanical Garden's Virtual Herbarium. Retrieved January 10, 2024 from http://sweetgum.nybg.org/science/ih/.

Wagensommer, R. P., Perrino. E. V., Silletti, G. N., 2014: *Carex phyllostachys* C.A. Mey. (Cyperaceae) new for Italy and phytogeographical considerations. Phyton (Horn, Austria) 54(2), 215–222. https://doi.org/10.12905/0380.phyton54(2)2014-0215

Wallnöfer, B., 1993: Die Entdeckungsgeschichte von *C. randalpina* B. Wallnöfer spec. nov. (="*C. oenensis*") und deren Hybriden. Linzer Biologische Beiträge 25(2), 709–744.

Acta Bot. Croat. 84 (1), 105–106, 2025
DOI: 10.37427/botcro-2025-007

CODEN: ABCRA 25
ISSN 0365-0588
eISSN 1847-8476

Short communication

First record of *Pisutiella phaeothamnos* in the western Mediterranean

Gregorio Aragón[1, 2]*, Valerie Negrón[1], Gil Fernando Giménez[3]

[1] Rey Juan Carlos University, ESCET, Physics and Inorganic Chemistry Department, Biodiversity and Conservation Area, Biology and Geology, 28933 Móstoles, Madrid, Spain

[2] Rey Juan Carlos University, Global Change Research Institute (IIGC), 28933 Móstoles, Madrid, Spain

[3] Cabañeros National Park (TRAGSA), Ctra. Torrijos s.n., 13194 Pueblonuevo del Bullaque, Spain

Abstract – We report the first record of *Pisutiella phaeothamnos* (Kalb & Poelt) S.Y. Kondr., Lőkös & Farkas in the western Mediterranean (Central Spain). The nearest previous records were from the Canary Islands and Greece. The species was discovered among mosses on volcanic rocks in the Spanish Central Volcanic Region. This finding represents a significant expansion of its distribution range.

Keywords: Iberian Peninsula, muscicolous lichen, volcanic rocks, new record

Introduction

Pisutiella phaeothamnos (Kalb & Poelt) S.Y. Kondr., Lőkös & Farkas (= *Caloplaca phaeothamnos* Kalb & Poelt) is a muscicolous species growing amongst moss (primarily *Grimmia* spp.) on base-rich volcanic rocks under arid or semiarid environmental conditions (Malíček et al. 2021). The known distribution range of the species extends to a few localities in Türkiye (Poelt and Kalb 1985, Vondrák et al. 2012), Greece (Malíček et al. 2021), Iran (Sohrabi and Sipman 2020) and the Canary Islands (Hafellner 1995). Herein, we document the first record of *Pisutiella phaeothamnos* in the Iberian Peninsula, thereby broadening its known range to encompass the southwestern region of Europe (Fig. 1).

Fig. 1. Global distribution of *Pisutiella phaeothamnos*. White cross: the new localities. Scale bar = 1000 km (derived and adapted from Google Earth).

* Corresponding author e-mail: gregorio.aragon@urjc.es

Material and methods

Specimens were collected in 2023 and 2024, in the volcanic area "Campo de Calatrava" in Mediterranean Spain. The samples were deposited in the MACB Herbarium (Faculty of Biology, Complutense University of Madrid). The nomenclature followed the Index Fungorum Partnership (2024).

Localities of sampling: Spain: Ciudad Real province, Ballesteros de Calatrava, la Conejera, 38°48'0.2''N, 3°56'20.5''W, 830 m a.s.l., among mosses on volcanic rocks, G. Aragón & G. F. Giménez, nº 1566, November 16, 2023, MACB. Ciudad Real province, Almagro, Granátula de Calatrava, Cerro Gordo, 38°49'51.8''N, 3°44'23''W, 785 m a.s.l., G. Aragón, G. F. Giménez & V. Negrón, nº 1610, January 29, 2024, MACB.

Results and discussion

Pisutiella phaeothamnos is distinguishable from other crustose species of *Caloplaca* s. l. by the brown, minutely fruticulose thallus composed of branched lobes (4–5 mm tall), K–, ochraceous brown to orange apothecia (Fig. 2), and its ellipsoid and polarilocular spores of (7) 9–10 (11) × (4) 5–6 µm, and septum 3 µm wide. A comprehensive description of the species is documented in Poelt and Kalb (1985).

The species grows among bryophytes (*Grimmia decipiens* (Schultz) Lindb.) on volcanic rocks, under dry and sunlit conditions, at elevations ranging from 750 to 850 meters (Fig. 2). It is found on moderately inclined surfaces together with *Caloplaca stillicidiorum* (Vahl) Lynge and small thalli of *Cladonia foliacea* (Huds.) Willd. and *Protoparmeliopsis bolcana* (Pollini) Lumbsch, which partially cover the bryophyte surface (Fig. 2).

The habitat was similar to that previously reported for *Pisutiella phaeothamnos*. The species appears solely amongst mosses in volcanic rocks at altitudes of 500–1700 m a.s.l. in Eastern Europe (Poelt and Kalb 1985, Vondrák et al. 2012, Malíček et al. 2021) and at elevations from 1500 to 1850 m a.s.l. in the Canary Islands (Hafellner 1995).

The new site is located within a vast volcanic region in central Spain, about 5,000 square kilometers in area (Becerra-Ramírez et al. 2020). The volcanic formations resulted from low-explosivity events dated to between 700,000 and 800,000 years ago and are primarily composed of alkaline rocks from the basalt series (Becerra-Ramírez et al. 2020). The predominant land use in this area is extensive agriculture of cereals, olive and almond trees, and sheep livestock management (Becerra-Ramírez et al. 2020).

Pisutiella phaeothamnos is reported here from SW Europe for the first time and its distribution area is now enlarged to include the Iberian Peninsula (Fig. 1). The nearest locality is situated in the Canary Islands (Hafellner1995).

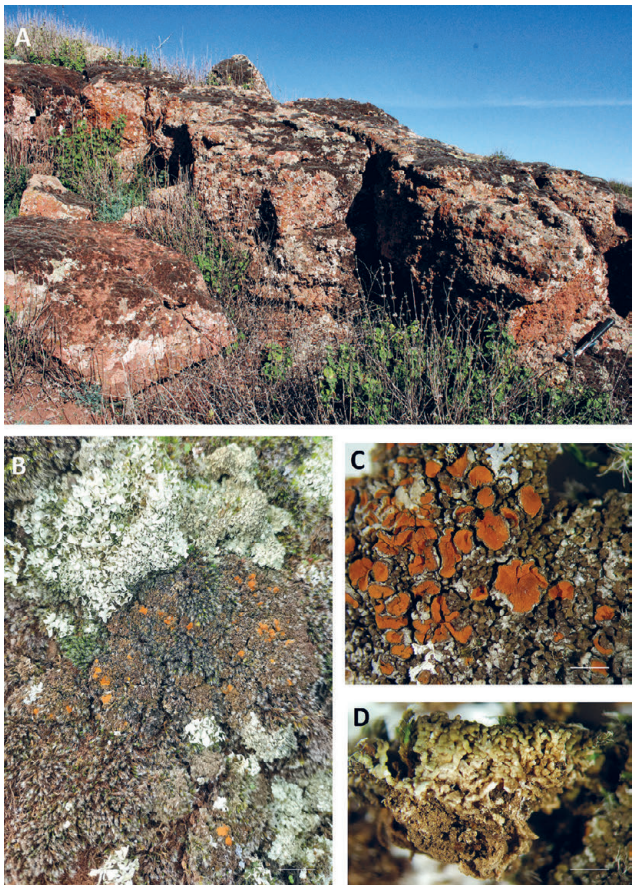

Fig. 2. *Pisutiella phaeothamnos*. A – volcanic rocks in "Cerro Gordo", B – *P. phaeothamnos* among mosses in volcanic rock (scale bar = 1 cm), C – ochraceous brown apothecia (scale bar = 2 mm), D – minutely fruticulose thallus (scale bar = 2 mm) (Photo: G. Aragón).

References

Becerra-Ramírez, R., Gosálvez, R. U., Escobar, E., González, E., Serrano-Patón, M., Guevara, D., 2020: Characterization and geotourist resources of the Campo de Calatrava Volcanic Region (Ciudad Real, Castilla-La Mancha, Spain) to develop a UNESCO global geopark project. Geosciences 10(11), 441. https://doi.org/10.3390/geosciences10110441

Hafellner, J., 1995: Bemerkenswerte Funde von Flechten und lichenicolen Pilzen auf makaronesischen Inseln III. Einige bisher auf den Kanarischen Inseln übersehene lecanorale Arten. Linzer Biologische Beiträge 27, 489–505.

Malíček, J., Bouda, F., Konečná, E., Sipman, H., Vondrák, J., 2021: New country records of lichenized and non-lichenized fungi from Southeastern Europe. Herzogia 34(1), 38–54. https://doi.org/10.13158/heia.34.1.2021.38

Poelt, J., Kalb, K., 1985: Die Flechte Caloplaca congrediens und ihre Verwandten: Taxonomie, Biologie und Verbreitung. Flora 176, 129–140.

Sohrabi, M., Sipman, H., 2020: An updated checklist of the lichenized and lichenicolous fungi of Arasbaran, UNESCO-Man and Biosphere Reserve, Northwest of Iran. Mycologia Iranica 7(1), 45–62. https://doi.org/10.22043/mi.2020.122654

Vondrák, J., Halici, M. G., Kocakaya, M., Vondráková, O., 2012: Teloschistaceae (lichenized Ascomycetes) in Turkey. 1. Some records from Turkey. Nova Hedwigia 94(3–4), 385–396. https://doi.org/10.1127/0029-5035/2012/0007

The 2024 anniversaries of the Botanical Garden, University of Zagreb, Faculty of Science

Several anniversaries of the Botanical Garden of University of Zagreb Faculty of Science and its former employees were celebrated in 2024. The Garden's 135th birthday coincided with the birthday jubilees of two retired Garden managers: the 90th of Assistant Professor Ljerka Regula, and the 70th of Biserka Juretić, MSc. Moreover, the founding fathers of the Garden, University Professor Antun Heinz and Head Gardener Vítězslav Durchánek, died 105 and 100 years ago, respectively. A combined celebration and commemoration were organized in October of 2024 with the unveiling the monument dedicated to Professor Heinz.

135 years of Zagreb University Botanical Garden

Zagreb University Botanical Garden was founded in 1889 on the same 4.5 hectares which occupies today. Back then intended for the approximately 47,000 citizens of a provincial town of the Austro-Hungarian monarchy, the Garden is nowadays situated in the very heart of the Croatian capital and is visited by more than 100,000 guests per year. For its educational, cultural and touristic values, as well as its overall Croatian historic significance, the Botanical Garden was statutorily protected in 1971 as a National Monument of Culture and Park architecture.

Originally, the Garden operated as a component of the Department of Botany and Physiology of the Faculty of Philosophy. From 1946, after the Faculty of Science was established, all natural disciplines were transferred to it, and the Division of Botany with the Botanical Garden was formed among others in the Department of Biology. The Garden was separated from the Division in 2013, becoming an independent subunit of the Department of Biology.

Most of the Botanical Garden area consists of the arboretum, designed in the informal English landscape style. A smaller part was designed in classic French style with a central *parterre*, above which an exhibition glasshouse was erected in 1892 (Fig. 1). Designed and produced in Vienna, it is unique in Croatia. Never thoroughly reconstructed, deteriorating slowly, the glasshouse has been inaccessible to

Fig. 1. The central *parterre* of the Botanical Garden around 1925, with newly appointed Head Gardener Franjo Kušenić. The exhibition glasshouse above the *parterre* was already closed to the public. (photo: Franjo Kušenić, from the Garden Archives).

the public since the First World War; today it is empty. Numerous attempts were made for a full restoration of this only public greenhouse in Zagreb and Croatia – so far, unsuccessfully.

The first inventory of the Garden plants, compiled by its founder Professor Antun Heinz and published in 1895/6, numbered ca 1500 species: today we grow about 7500, divided into collections that are being systematically revised. Since its foundation, the Botanical Garden has maintained its role in university teaching, scientific research and professional work in the field of botany, as well as educating the general public via the popularization of nature and plant life protection. It is the only Croatian certified member of the Botanic Garden Conservation International (BGCI), as well as a leading national botanical garden and representative in the European Botanic Gardens Consortium (EBGC).

105th anniversary of the death of Professor Antun Heinz (1861 – 1919)

Founder of the Royal Botanical Garden, as it was called at its birth in 1889 during the Austro-Hungarian Monarchy, was Professor of botany and bacteriology Dr Antun Heinz. In his career he held such posts as Head of the Department of Botany and Physiology, and Rector of the University of Zagreb. Although a well-known intellectual, Professor Heinz was constrained to retire in 1913, due to his anti-monarchical and anti-Yugoslavian but pro-Croatian views, in the historically extremely difficult times before the First World War. Though Professor Heinz had (a very short) street in Zagreb named after him, and we named a pergola-passage promenade along the Botanical Garden in his honour, it has been our long-lasting wish to erect a monument to his memory. Finally, it came true in October of 2024,

Fig. 2. Bust of Professor Antun Heinz, with its young author Ira Orešković, erected at the Alpinum rockery. (photo: Vanja Stamenković).

Fig. 3. Festive gathering in celebration of 135 years of the Garden, with the unveiling of the bust of Professor Heinz. In the front row, the guests of honour (left-right): Biserka Juretić MSc, retired Garden manager; Professor Mirko Planinić, Dean of the Faculty of Science; Dr Ljerka Regula-Bevilacqua, retired Garden manager; Ms Roberta Gazibarić, Professor Heinz's great-granddaughter. (photo: Mirna Kirin).

commemorating the 105th year since his death and the 135 years of the Garden he established. The bust representing Professor Heinz in his prime, for he was only 28 years old when he founded the Garden, was selected in a school competition from a dozen models made by pupils at the *School of Applied Arts and Design* in Zagreb. Young sculptors had a difficult task to create a likeness of Professor Heinz in the form of a bust, based on his only known photographic portrait. From three best models, the first prize was given to the work of Ira Orešković, a 3rd year school student, and that model was used for casting a bronze bust (Fig. 2).

The bust on a stone plinth was erected at the historic main entrance to the Botanical Garden, at the edge of the Alpinum (Fig. 3) – the oldest Garden rockery, designed by Professor Heinz.

It was unveiled by two retired Garden managers, and two members of the Heinz family, in a festive ceremony attended by the representatives of the Faculty, the School, the City Council, the Ministry of Culture and Media, as well as many students (Fig. 4).

100th anniversary of the death of Vítězslav Durchánek (1857 – 1924)

All the historical records make much of Czech gardener, teacher and garden architect Vítězslav Durchánek as co-founder of the Botanical Garden, alongside Professor Heinz. Educated in Czechia and Germany, additionally trained in Belgium and France, Durchánek moved to Croatia in 1890. Drawing on the concepts of Professor Heinz and his own practical skills, Durchánek drew the plans and

Fig. 4. Dean of the Faculty of Science, Professor Mirko Planinić, addressing the guests. Also shown is the 1905 photo of Professor Antun Heinz wearing his rectoral chain, upon which the young sculptors based their models, one of which is seen on the left. Original Garden Plans by Heinz and Durchánek are displayed for the guests. A photo of Vítězslav Durchánek is to be seen upon the wall. (photo: Mirna Kirin).

supervised the construction of the Garden, of which he was appointed Head Gardener until his retirement in 1923.

It is interesting to note, in the light of the Garden's anniversaries and its continuous maintenance, that the role of Head Gardener after Durchánek, exactly one hundred years ago, was taken over by his apprentice and 'right hand' Franjo Kušenić (Fig. 1). Of Kušenić's life very little is known: he was a keen photographer, born in the year of the Garden's establishment (1889), retired after the Second World War, and died 70 years ago (in 1954).

That year, again, coincides with the birth of another long-time Garden employee: retired manager MSc Biserka Juretić.

70th birthday of Biserka Juretić

Biserka Juretić MSc has spent all her professional life in the Garden. She was born on December 7, 1954, in Orahovica, but moved to Split soon after, where she graduated from the Classical Gymnasium. She graduated in 1980 from the Biology Department of the Faculty of Science, University of Zagreb, and got her master's degree at the same Faculty in 1987. She was employed in the Botanical Garden first as a senior technician (1979) in charge of seed collecting and exchanging via *Index Seminum* publications, then a (senior) collection curator (1980) supervising the collections of swamp, insectivorous, medicinal and tropical plants, as well as ornamental flowerbeds. In 1995 Ms Juretić become Garden manager, which she remained for almost 25 years. She supervised all administrative issues, overseeing the fundraising and spending, planning and implementing of investments, renovation and revitalization projects in the Garden, etc. She was also engaged in professional and popularization work, co-authored books and guides, as well as professional and popular articles, conference announcements, educational exhibitions and workshops. She participated in many radio and television educational programmes, gave public lectures, etc. Since 2007, Ms Juretić has been a representative of the Croatian botanical gardens in the European Botanic Gardens Consortium (EBGC), and a regular member of the organizing committee of the European Botanic Gardens Congresses. Together with her colleagues, Ms Juretić encouraged the association of Croatian botanical gardens and arboretums in the Section of Botanical and School Gardens, Arboretums and Botanical Collections, which operates as a part of the Croatian Botanical Society.

In 2009, Biserka Juretić received the University of Zagreb Award for her dedicated work on the restoration of the Botanical Garden and its promotion in the City of Zagreb and in the academic community.

90th birthday of Assistant Professor Ljerka Regula-Bevilacqua

After her retirement in 1999, Dr Regula had her career path depicted in *Acta Botanica Croatica* (64(2), 401–406, 2005) in honour of her 70th birthday. During the succeeding 20 years Dr Regula has never ceased to work and write: she published 10 scientific and professional papers, 15 biographical articles, 16 articles on protected plant species of the Republic of Croatia and ca 50 articles of other contents. She participated in symposiums, photo-exhibitions, TV and radio programmes, and also gave many public lectures. In 2004 she was invited by the Department of Biology of J.J. Strossmayer University in Osijek, to organize horticulture classes, which she taught in the summer semesters of 2004/5 and 2006/7. Since 2005 she has been a regular member of the Department of Natural Sciences and Mathematics of *Matrix Croatica* (Matica Hrvatska). In 2008 she was elected an honorary member of the Croatian *Camellia* Society, and in 2011 the Head of the Section for the Protection of Biological Diversity, Scientific Council for Nature Protection of the Croatian Academy of Sciences and Arts. In the period between 2004 and 2024, Dr Regula was co-founder and specialist expert of the Croatian *Iris* Garden and Mt Strahinjščica Wild Flora Garden.

The lifetime-achievement acknowledgement came in 2009, when Dr Regula received the 'Ivo Horvat Award' from the Ministry of Culture of the Republic of Croatia, for outstanding accomplishments in the field of nature protection.

Dr Regula still visits the Botanical Garden quite often. She always announces her arrival, giving the staff time to prepare any questions about a plant, book or photograph in the archives or database, to which there is always a swift an-

swer of what it is, where to look for it, or how it is to be found. The rich flower garden around Dr Regula's private cottage is still perfectly maintained: she divides her iris collection yearly, regularly bringing every duplicate to the Garden, along with many books, memorabilia and perfectly categorized photos. And she still drives her car.

While wishing Dr Regula much joy for her 90th birthday, and many happy years to come, we would also wish the same for all of us: to have her wit, her spirit and her good will as long as she has! Perhaps with a "slightly better back and knees", as that is the only thing that she ever complaints about, still "dreaming all night of botanizing across Croatian mountains and islands" …

Sanja Kovačić
Vanja Stamenković
Botanical Garden,
Department of Biology, Faculty of Science,
University of Zagreb, Zagreb, Croatia

Professor Emerita Marijana Krsnik Rasol – an appreciation on the occasion of her eightieth birthday

Professor Emerita Marijana Krsnik-Rasol is a distinguished Croatian biologist, known for her extensive research into plant molecular biology and proteomics. She was born on July 2, 1944, in Zagreb, Croatia. Prof. Krsnik-Rasol's academic journey began with her high school education in Zagreb, followed by her studies in experimental biology at the University of Zagreb's Faculty of Science, where she graduated in 1968. She obtained her master's degree in 1972, with a thesis entitled "Research on plant tumours induced by the bacterium *Agrobacterium tumefaciens*" under the supervision of Prof. Zvonimir Devidé. She earned her Ph.D. in 1983 with a thesis on "Proteins as indicators and regulators of plant cell differentiation" (supervisors Prof. Z. Devidé and Prof. D. Šerman).

After completing her studies, Prof. Krsnik-Rasol worked as a research assistant at the laboratory of electron microscopy of the Ruđer Bošković Institute. In 1971, she joined the Division of Botany within the Department of Biology at the University of Zagreb's Faculty of Science as an instructor, to be promoted to assistant professor in 1987. Her professional trajectory continued on its upward path as she moved to the newly founded Division of Molecular Biology in 1989, where she made significant contributions to the field. In 1995, she was appointed associate professor. In 1999, she became a full professor, and in 2004 a tenured professor. She is particularly to be credited with the founding of the laboratory for electrophoretic research on plant proteins. From 1998 to 2000 she was Head of the Department of Biology and from 2002 to 2005 Head of the Division of Molecular Biology. In this role, she was responsible for setting up new laboratories and practicums and organized the relocation of the Department of Molecular Biology to the new building of the Faculty of Science in Horvatovac. She retired in 2011 and was appointed *professor emerita* in 2012.

Marijana Krsnik-Rasol furthered her academic development through advanced studies at prestigious universities throughout Europe. She honed her expertise at the University of Leipzig in 1979, in Heidelberg in 1980, in Hamburg in 1991 and 1995, in Brest in 1993 and in Munich in 1994. As a visiting professor, she contributed to teaching and scientific research at the University of Orleans in 1997, 1998, 1999 and 2004 and at the Karl-Franzens University in Graz in 1998 and 1999. In 2009, she also spent time at the Ben-Gurion University of the Negev in Beer Sheva, Israel, as part of a bilateral research project.

Prof. Krsnik-Rasol's research focuses on cell biology, in particular the differentiation and tumour transformation of plant cells under controlled *in vitro* conditions. Through light and electron microscopic studies of cellular structures and ultrastructure, she discovered that differentiated plant cells undergoing tumour transformation with the Ti plasmid undergo a process of dedifferentiation that is clearly reflected in the conversion of the developed chloroplasts into a juvenile proplastid form (Acta Bot. Croat. 1974; Plant Physiol. Biochem. 1993; J. Plant. Physiol. 1994). One of her notable discoveries was the identification of changes in the activity and isoforms of the enzymes peroxidase and esterase as early biochemical markers of morphogenesis and tumour transformation in plant cells (J. Dev. Biol. 1991; Biologia Plantarum 1997; Chem. Biol. Interact. 1999). Her work also showed that horseradish tumour cells produce peroxidase in abundance, making them a potential source of this enzyme for biotechnological production (Period. Biol. 1992). In addition, transformed sugar beet cells were found to be a source of betalain pigments, which are used as natural, non-toxic colorants in the food industry (Food Technol. Biotechnol. 2011). Prof. Krsnik-Rasol has contributed to the further development of new laboratory techniques, especially in the field of plant proteomics (Proteomics, 2008). She was the principal investigator of scientific projects funded by the Ministry of Science and Sports, including "Differential protein expression in plant cells" (2006-2011), "Proteins and sugars in plant development" (2002-2005) and "Signalling molecules in plant development" (1996-2002). She also co-led a bilateral project with Professor Dudy Bar-Zvi from Israel on "Life Under Stress: Molecular Components and Mechanisms of Plant Response to Osmotic Stress" (2010-2011). As a member of the "International Association for Plant Biotechnology" and president of the "Croatian Society for Plant Physiology" she has been actively involved in advancing the study and understanding of plant biology both in Croatia and internationally.

Throughout her career, Marijana Krsnik-Rasol has been devoted to teaching and supervising students. While still an

instructor she led practical courses in Cell Biology and Genetics, and after her advancement in science and teaching positions, she began lecturing in cell biology. She also introduced a new course "Methods for Plant Protein Research", which focused on hands-on work and introduced students to scientific research and the presentation of results. Under her guidance, numerous students completed their bachelor's and master's theses and she supervised several doctoral dissertations. As a guest lecturer, she gave seminars on electrophoretic analysis of plant proteins at the Institute of Plant Physiology at the University of Graz. At the University of Orléans she taught courses in Plant Physiology and Genetics and led practical sessions. She played an active role in the development of new curricula and their adaptation to the recommendations of the Bologna Declaration. Together with Professor Daniel Hagegé, she initiated a joint Master's programme in Molecular Biotechnology (Bioindustrial Techniques) with the University of Orléans and was involved in its implementation. Her teaching was highly rated in student surveys and she was awarded the title "Chevalier dans l'Ordre des Palmes Académiques" by the Ministry of Education of the French Republic. The author of the high school textbook "From Molecule to Organism" (Školska knjiga, 1995–2001) and co-author of subsequent editions of the same textbook (2003–2013), she also collaborated on the high school textbook "Life 1" (Školska knjiga, 2014). She also jointly wrote the university textbook "Electrophoretic Techniques for Protein Research" (Hrvatska sveučilišna naklada, 2011).

The papers cited are listed here according to the order in which they appear in the text:

1. Krsnik-Rasol, M., 1974: Crown-Gall tumors on bean leaves induced by *Agrobacterium tumefacien*s. Acta Botanica Croatica 33, 63–67.
2. Lorković, Z., Muraja-Fras, J., Krsnik-Rasol, M., Wrischer, M., 1993: Ultrastructural and biochemical changes in potato tuber cells related to tumorigenesis. Plant Physiology and Biochemistry 31, 633–638.
3. Muraja-Fras, J., Krsnik-Rasol, M., Wrischer, M., 1994: Plastid transformation in greening potato tuber tissue. Journal of Plant Physiology, 144 (1), 58–63.
4. Krsnik-Rasol, M., 1991: Peroxidase as a developmental marker in plant tissue culture. The International Journal of Developmental Biology 35(3), 259–623.
5. Peškan, T., Pedreno, M.A., Krsnik-Rasol, M., Munoz R., 1997: Subcellular localization and polymorphism of peroxidase in horse-radish tumour and teratoma tissue. Biologia plantarum 39 (4), 575–582.
6. Krsnik Rasol, M., Čipčić, H., Hagège, D., 1999: Isoesterases related to cell differentiation in plant tissue culture. Chemico-Biological Interactions 119–120, 587–592.
7. Krsnik-Rasol, M., Jelaska, S., Derkos-Sojak, V., Delić, V., 1992: Regeneration and peroxidase activity in horse-radish transformants, Periodicum biologorum 94, 105–110.
8. Pavoković, D., Krsnik-Rasol, M., 2011: Complex biochemistry and biotechnological production of betalains. Food Technology and Biotechnology 49 (2), 145–155.
9. Supek, F., Peharec, P., Krsnik-Rasol, M., Šmuc, T., 2008: Enhanced analytical power of SDS-PAGE using machine learning algorithms. Proteomics 8(1), 28–31.

Professor Biljana Balen
University of Zagreb, Faculty of Science
Department of Biology
Division of Molecular Biology

Professor emerita Marijana Krsnik-Rasol duringa field trip to Žumberak – Samobor hills Nature Park, locality Sošice - cret Jarak, organised by the Croatian Plant Biology Society, 2024 (photo: B. Balen).

Ivo Trinajstić (1933–2024)

Ivo Trinajstić, Professor Emeritus at the University of Zagreb, passed away on August 2, 2024, after a long illness. A professor of botany at the Faculty of Forestry, University of Zagreb, for many years, he was one of the leading authorities on Croatian flora and vegetation.

Born on October 27, 1933, in Sisak, Professor Trinajstić completed his degree in agronomy at the Faculty of Agriculture and Forestry, University of Zagreb, in 1958. He earned his master's degree in 1964 from the Faculty of Science, Zagreb, with a thesis titled Vegetation of the Coastal Area of the Drava River in the Wider Vicinity of Varaždin. A year later, in 1965, he completed his PhD at the same faculty with a dissertation entitled The Vegetation of the Island of Krk.

Following his graduate studies, he worked at the Agricultural Cooperative in Varaždinske Toplice and at the Horticultural School in Vinica near the city of Varaždin. From October 1960 until his retirement in 1999, he was a faculty member at the University of Zagreb's Faculty of Forestry. He also taught several botanical courses at the University of Split and postgraduate courses at the Faculty of Science, University of Zagreb.

Professor Trinajstić was an enthusiastic and passionate educator. He not only sought to convey botanical knowledge to his students but also encouraged them to reflect deeply on the intricate relationships within ecosystems. He shared his vast life experience with his students, preparing them for future challenges. His vivid, dynamic lectures and memorable field trips to Medvednica, Samoborsko Gorje, and Velebit had a lasting impact on generations of students.

Professor Trinajstić's scientific career was characterized by meticulous work and unwavering dedication to every challenge he encountered. He authored over 700 articles and contributions across scientific journals, books, and popular science and professional magazines. His tireless efforts greatly enriched the understanding of Croatian flora, as he published numerous important contributions. His research spanned the flora of many Adriatic islands, including Krk, Korčula, Lastovo, Hvar, and Unije. He also made significant

Professor Ivo Trinajstić (1933–2024)

contributions by documenting new and rare plant species within Croatian flora.

As a legacy for future generations of botanists, Professor Trinajstić left behind a substantial herbarium collection, now preserved in the Croatian Natural History Museum in Zagreb. A portion of this collection has been digitized and is publicly available through the *Flora Croatica Database* web portal.

One of the hallmarks of his career was his extensive work in vegetation research. He described numerous new syntaxa and contributed significantly to the ecological and phytogeographical classification of the vegetation of Croatia. His book *Plant Communities of Croatia*, published in 2008, is a testament to his vast knowledge and extensive fieldwork. It provided the first comprehensive syntaxonomic overview of Croatian vegetation, complete with association descriptions and an extensive bibliography.

Professor Trinajstić was also deeply involved in the taxonomic study of plant species, particularly through his

contributions to the edition *Analytical Flora of Yugoslavia*. His work on resolving taxonomic issues, alongside his mentorship of younger colleagues for whom he suggested topics for master's and doctoral theses, left a profound impact on the trajectory of botanical research in Croatia.

His legacy in botanical science will forever be remembered, notably through the species *Viola ivonis*, named in his honour by German botanist Matthias Erben.

He was a member of the editorial boards of Hladnikia and Periodicum Biologorum, and was also affiliated with several prestigious organizations, including the Academy of Forestry Sciences, the Amicale Internationale de Phytosociologie, the Organization for the Phyto-Taxonomic Investigations of the Mediterranean Area (OPTIMA), the Croatian Ecological Society, and the Croatian Biological Society. His active involvement in the Eastern Alpine and Dinaric Society for Vegetation Ecology (EADSVE) was particularly notable; he served as president from 1993 to 1997 and was named an honorary member in 2015.

In addition to his scientific work, Professor Trinajstić was deeply committed to popularizing botany, contributing numerous articles to popular science publications.

Ivo Trinajstić was an outstanding scientist and a respected professor who generously shared his huge knowledge and experience. His unique understanding and appreciation of nature and plants brought a special, personal dimension to botany, one that will continue to inspire researchers for generations to come.

Professor Željko Škvorc
University of Zagreb
Faculty of Forestry and Wood Technology
Zagreb

INSTRUCTIONS FOR AUTHORS

The interest of the journal is field (terrestrial and aquatic) and experimental botany including plant viruses, bacteria, archaea, algae and fungi, from subcellular level to the ecosystem level with a geographic focus on karstic areas of the southern Europe and the Adriatic Sea (Mediterranean).

The journal welcomes manuscripts for publication in the following categories: original research papers, short communications, book reviews, social news and announcements. Review articles are accepted on editor invitation only.

Article submission and publishing are free of charge.

Manuscripts should be submitted using On-line Manuscript Submission at http://www.abc.botanic.hr. Registration and login are required to submit items on-line and to check the status of current submissions. For submission, after LOGIN find USER HOME then AUTHOR and go to NEW SUBMISSION.

Under SUBMISSION METADATA, fill in the names and e-mail addresses of **all authors**. Criteria for authorship are as set out by the ICMJE and as recommended by the Committee on Publication Ethics (COPE).

Cover letter

In the cover letter addressed to Editor-in-Chief, the authors should explain how the manuscript meets the scope of the journal and indicate why it will be of interest to the general readership of Acta Botanica Croatica. Authors should propose the names and e-mail addresses of at least **five potential reviewers who are experts in the topic of manuscript. Please avoid colleagues with joint publications, or from the same institutions. At least three of them have to be international recognized scientists outside of your home country**. Also, in the cover letter, confirm that the manuscript has not been published or submitted for publication elsewhere and that all authors have read the manuscript and approved it for submission. Include also Founding statement in which any sources of financial support should be specified.

Type of contribution

ORIGINAL RESEARCH PAPER

An original research paper is a fully documented report of original research. The manuscript should be divided into Introduction, Material and methods, Results, Discussion, Acknowledgements, References (**maximum 40**), Table and figure captions, Tables, Figures. There may be up to **12 single-spaced typewritten pages**, excluding figures and tables. There may be up to **8 tables and/or figures in total** per manuscript. Additional figures and/or tables can be published online only as supplementary materials. All tables and figures should be cited in the text properly (Fig. 1, 2, …, On-line Suppl. Tab. or Fig.). Exceptionally, in papers dealing with conceptual and theoretical bases, especially botanical and phytosociological nomenclature, Results and Discussion can be combined into one section.

SHORT COMMUNICATIONS

Short communications should consist of not more than **3 single-spaced typewritten pages** and a **maximum of two tables and/or figures**. The text should be divided into Abstract (containing no more than 100 words), Keywords (up to five; listed in alphabetical order), Introduction, Material and methods, Results and discussion, Acknowledgements, References (**maximum 10**), Table and figure captions, Tables and/or Figures.

We may consider longer short communication and research articles with a compelling rationale in the cover letter, contingent upon the content's justification for the extended length.

REVIEW ARTICLE

Review and mini-review articles are usually accepted for the reviewing process if invited by editor. Authors who wish to contribute a manuscript to this category are encouraged to contact the Editor-in-Chief. The manuscript should be organized according to Acta Botanica Croatica guidelines and there are no limitations on the number of references.

SOCIAL NEWS AND BOOK REVIEWS

We also welcome popular news describing interesting events, anniversaries, as well as short and concise reviews of newly published books in the field of plant sciences.

PREPARATION OF MANUSCRIPT

General

The manuscript should be submitted as a Word document. The writing needs to be clear, concise and in correct English. Unfortunately, we do not offer a language editing service as part of the submission process, so it is up to authors to ensure the highest quality of writing in their manuscript. If the language is deemed too inadequate for easy understanding, the manuscript will be returned to authors without review.

The text should be single-spaced and left-adjusted, using Times New Roman and 12 point letter size. The layout of the document should be A4 (21 × 29.5 cm). Adjust indentation to 1 cm (i.e., the first line of all paragraphs and hanging paragraphs of References). Input your text continuously, i.e. insert hard returns exclusively at the ends of paragraphs, headings etc. Do not use the space bar to create indents; the indent command should be used for this purpose. Leave a space between mathematical symbols and numbers (e.g. 2 + 3, 3 < 9). Always leave a space between a number and a Celsius degree symbol (e.g. 12 °C). Do not leave a space when using the multiplication and percentage symbols (e.g. 6×12%). Each page should be numbered.

The metric system should be used throughout the manuscript. If required, equivalent values in other systems may be placed in parentheses immediately after the metric value.

Italicize only the names of genes (e.g. *Arpl* gene), genera, species, subspecies and lower taxonomic units. Genetic information, such as DNA, RNA, or protein sequences, should

be submitted to public data bases (GenBank, EMBL, etc.), and accession numbers should be available in Material and methods. Voucher specimens must be made and deposited in a public herbarium. For endemic and protected taxa, permission has to be obtained from the competent authority. The nomenclature of taxa and syntaxa has to be in strict accordance with international rules (codes).

Title page

TITLE, should not exceed 120 characters (without spaces).

NAMES OF ALL AUTHORS (name and surname in full), their mailing and e-mail addresses, and institutional affiliations should be given. Include the corresponding author's e-mail address and telephone number.

RUNNING TITLE, should not exceed 50 characters (without spaces).

ABSTRACT of up to 250 words that highlights the objective, results, and conclusion of the paper.

KEY WORDS (up to eight, in alphabetical order), to identify the subjects under which the article may be indexed.

Content of manuscript

Keep the Introduction brief, stating clearly the purpose of the article and its relation to other papers on the same subject. Do not give an extensive review of literature. Provide enough information in the Material and methods section to enable other investigators to repeat the experiments. Report Results clearly. In the Discussion interpret the results, state their meaning and draw conclusions. Do not simply repeat the results. Proceed with Acknowledgments where any sources of financial support as well as any individuals who were of direct help to the authors should be acknowledged. At the end give Author contribution statement in which the contributions of all authors should be described.

References

Cite references in the text by name and year in parentheses. Some examples: Wrischer (1998), … Jones and Smith (1987), …. (Jones 1987a, b), ….. Jones et al. (1986), … (Facca et al. 2002, 2003, Socal et al. 2006).

Arrange names of authors chronologically in text, e.g: (Jones 1986, Allen 1987). The list of references should be typed in alphabetical order. The articles in English, Spanish, French, German and Italian are accepted in the Reference list. For any other language, please provide the English translation in parentheses. Unpublished materials should be cited in the text as personal observations or unpublished data. Identify authors of unpublished work. Check the text citations against the Reference list to make sure there are no gaps or inconsistencies. Names of journals should be given in full, followed by volume and (issue) numbers and pages. To mark a span of pages use en dash (–) instead of a hyphen(-). Please provide doi numbers wherever is possible.

Use the following formats for Reference list style:

Journal article:

Colangelo, E. P., Guerinot, M. L., 2006: Put the metal to the petal: metal uptake and transport throughout plants. Current Opinion in Plant Biology 9(3), 322–330. https://doi.org/10.1016/j.pbi.2006.03.015

Books:

Horvat, I., Glavaš, V., Ellenberg, H., 1974: Vegetation Sudosteuropas. Geobotanica selecta 4. Gustav Fischer Verlag, Stuttgart.

Chapter in a book:

Broadwater, S. T., Scott, J., 1994: Ultrastructure of unicellular red algae. In: Seckbach, J. (ed.), Evolutionary pathways and enigmatic algae: *Cyanidium caldarium* (Rhodophyta) and related cells, 215–230. Kluwer Academic Publishers, Amsterdam.

On-line sources: Author, year, title, source. Retrieved October 15, 2015 from http://www....

Table and figures

Table and figure legends should be added following references, on the next page.

Tables should be on separate pages. Tables should be prepared in Microsoft Office Word or Excel. Vertical lines should not be visible in tables. The maximum width of a printed table should be 150 characters in broadside. The preferred table organization format can be seen in articles published in previous issues of Acta Botanica Croatica, which are freely available on-line. Large tables and primary data can be published as supplementary materials on-line, but not in the printed version. All tables should be numbered consecutively with Arabic numerals. They should be cited in the text properly (Tab. 1, On-line Suppl. Tab. 1, etc.). Table title should be above the table, on the same page as the table to which it corresponds. The tables need to be self-explanatory: the authors should provide enough information in captions (explain all abbreviations, write full Latin names etc.) so that each table is understandable without reference to the text.

Figures should be submitted in appropriate electronic formats as Supplementary files as well as embedded within the manuscript after the tables. Every figure must be referenced in the text. Figures should be numbered in Arabic numerals (below the figure). Figures may be arranged in panels, in which individual images should be divided by white lines no more than 2 mm wide. Line art-works and half-tones or photographic images should be saved as Tagged Image Format (tif) with a resolution of at least 600 dpi or in pdf. The size of tif files can be decreased using Lossless Compression (LZW). Vector graphics (xls, cmx, eps, wmf) should be saved in pdf. All lettering on figures should be in Arial and legible after reduction. Y- and X-axis need to be black, tick marks on axes should be oriented inwards. Graph lines should be thicker than axes lines. Each figure and figure caption should contain all the information necessary for it to be self-explanatory (explain all abbreviations, write full Latin names etc.) so that each figure is understandable without reference to the text. Colour figures are acceptable only if necessary (photographs, not plots and curves) and they are free of charge.

Additional guidelines

All on-line supplementary materials have to be uploaded as a separate Word document and supplementary figures should be submitted in appropriate electronic formats (tif or pdf) as separate files.

Appendices (optional): Each appendix must be numbered as Appendices 1., 2. etc and must have a title.

Footnotes should not be used; information should be integrated into the text.

REVIEW PROCESS

Acta Botanica Croatica is committed to peer-review integrity and upholding the highest standards of review. Once your paper has been assessed for suitability by the Editor-in-Chief and Section Editor, it will then be single blind peer reviewed by independent, anonymous expert referees.

Manuscripts that meet the scientific and journal technical criteria will be sent to the review process. Please note that the journal uses software to screen for plagiarism. Acta Botanica Croatica participates in an initiative by CrossRef (http:// www.crossref.org) to prevent scholarly and professional plagiarism in scientific publications. This initiative is known as Crossref Similarity Check and provides its members a service to screen received content for originality against a vast database of relevant published material.

AHEAD OF PRINT

The accepted article, including supplementary files, that has been language edited and checked for references, will be published on-line as "Ahead of print" at https://hrcak.srce.hr/acta-botanica-croatica and citable with the DOI number.

PROOFS

The proof is sent to the corresponding author for a final check and approval. Corrected proofs must be returned within 72 hours to the Technical Editor-in-Chief. PDF of corrected proofs will be posted on-line and after release of the printed version (1st April, 1st October), the paper can also be cited by issue and page numbers.

Free unlimited electronic reprints (in pdf.) are available from http://hrcak.srce.hr/acta-botanica-croatica.

A printed copy of the journal volume is available for subscribed readers who have paid the annual fee.

COPYRIGHT